

Design and Synthesis and Testing of Conformationally Constrained Peptidomimetics

Joanna Duncan

A thesis submitted in total fulfilment of the requirements for
the degree of Doctor of Philosophy



2013

Department of Chemistry

The University of Adelaide

Abstract.....	IV
Declaration.....	VII
Acknowledgments.....	VIII
Abbreviations.....	IX
1 Introduction.....	1
1.1 Protein-protein interactions.....	2
1.2 Mediating protein-protein interactions.....	3
1.2.1 Peptides as drugs.....	3
1.2.2 Disadvantages of peptides.....	3
1.2.3 Peptidomimetics.....	5
1.3 Peptide secondary structure.....	6
1.4 Classes of peptidomimetic.....	9
1.4.1 Side chain modification.....	9
1.4.2 Strategies for restriction of φ , ψ and ω torsion angles.....	11
1.5 A ring closing metathesis route to peptidomimetics.....	18
1.5.1 A brief history of metathesis.....	18
1.5.2 Peptidomimetics by ring closing metathesis.....	19
1.6 Research described in this thesis.....	22
1.7 References.....	23
2 Synthesis of medium sized rings comprised of β -amino acids by ring closing metathesis.....	31
2.1 Peptidomimetics from β -amino acids.....	32
2.2 Synthesis and analysis of cyclic scaffolds.....	45
2.2.1 Synthesis of building blocks 2.31 – 2.36.....	45

2.2.2	Synthesis of cyclic scaffolds.....	53
2.2.3	Synthesis and NMR analysis of tripeptides containing cyclic scaffolds.....	55
2.3	Conclusions.....	64
2.4	References.....	66
3	Synthesis of macrocyclic protease inhibitors.....	70
3.1	Calpain and its inhibition.....	71
3.1.1	The role of calpain in pathological conditions.....	74
3.1.2	Calpain inhibitors.....	76
3.2	Synthesis of the N-terminal FBS macrocycle 3.02.....	84
3.3	Design, synthesis and testing of diol-containing macrocycles 3.03 and 3.04.....	92
3.3.1	Computational modelling of diols 3.03 and 3.04.....	94
3.3.2	Synthesis of diol-based inhibitors.....	100
3.4	Design and synthesis of novel macrocycle 3.05.....	106
3.4.1	Designing a macrocycle to investigate selectivity towards calpain II, α -chymotrypsin and 20S proteasome.....	106
3.4.2	Synthesis of macrocycle 3.05.....	109
3.5	Conclusions.....	112
	References.....	113
4	<i>In vitro</i> testing of macrocycles synthesised in Chapter 3.....	119
4.1	Introduction.....	120
4.2	Assay of compounds 3.02, 3.03 and 3.04 against ovine calpain II.....	121

4.3	Analysis of calpain II inhibition data.....	126
4.4	Biological testing of 3.05.....	137
4.5	Conclusions.....	144
4.6	References.....	146
5	<i>In vivo</i> testing of tritiated macrocycles.....	149
5.1	Introduction.....	150
5.1.1	Summary of <i>in vivo</i> trials of CAT0811.....	152
5.2	Results and discussion.....	155
5.2.1	Synthesis and formulation of radio-labelled analogues.....	155
5.2.2	<i>In Vivo</i> study methods.....	159
5.2.3	Liquid scintillation counting results.....	162
5.3	Conclusions.....	171
5.4	References for Chapter 5.....	172
6	Experimental.....	174
6.1	General methods and experimental procedures.....	175
6.2	Experimental for Chapter 2.....	178
6.3	Experimental for Chapter 3.....	223
6.4	Experimental for Chapter 5.....	255
A1	Liquid Scintillation Counting (LSC).....	261

Abstract

This thesis describes the design, synthesis and testing of peptidomimetics pre-organised into bioactive conformations. **Chapter One** introduces the concept of peptidomimetics, their importance as potential pharmaceuticals. The concept of constraining a compound into a bioactive conformation (α -helix, β -turn or β -strand) by incorporation of a ring or bridge is discussed. The technique of ring closing metathesis as a strategy for cyclisation of peptidomimetics is introduced.

Chapter Two surveys β -turn mimics comprised of β -amino acids. The synthesis of novel cyclic peptidomimetics comprised of β -amino acids (cyclised by ring closing metathesis) is presented. Three of the cyclic dipeptides were predicted (through *in silico* conformational searches) to adopt a β -turn motif. Cyclic scaffolds **2.62**, **2.65** and **2.66** were each incorporated into a tri-peptide to give **2.68**, **2.69** and **2.70**. The propensity of each tri-peptide to adopt a β -turn motif was investigated by ^1H NMR. There is strong evidence that **2.70** has a β -turn geometry based on the presence of an intra-molecular hydrogen bond between the *i* and *i*+3 residues.

Chapter Three introduces cysteine protease calpain II as the primary biological target for this thesis. Calpain is implicated in cataract formation and its inhibition is a logical approach to cataract prevention. Proteases are known to, almost universally, bind substrates and inhibitors in a β -strand conformation. Four macrocycles, designed to be preorganised in a β -strand geometry, were synthesised by ring closing metathesis (compounds **3.02** – **3.05**). Macrocycle **3.02** was made to investigate the suitability of an N-terminal 4-fluoro-benzyl-sulfonyl (FBS) in macrocyclic calpain

inhibitors. The synthesis of **3.02** was optimised to give the required compound in 33% yield compared to a reported 1% for analogue **CAT0811**. Diols **3.03** and **3.04** (as a mixture with **3.03** in an 85:15 ratio) were designed to explore possible hydrophilic interactions with the active site of calpain. Macrocycle **3.05** was designed to investigate the relative importance of having an aromatic residue at P₁ for inhibition of calpain, α -chymotrypsin and the 20S proteasome.

Chapter Four reports the *in vitro* testing of macrocycles **3.02**, **3.03** and **3.04** against calpain II and discusses these results in the context of the SAR study completed by the Abell group to identify the criteria for the most potent macrocyclic calpain inhibitor. **CAT0811** was confirmed as the most potent macrocyclic calpain II inhibitor to date with an IC₅₀ of 0.03 μ M. Macrocycle **3.02** had an IC₅₀ of 0.045 μ M against calpain II, confirming the suitability of FBS as an N-terminus in these macrocycles. Macrocycle **3.03** had an IC₅₀ of 3.7 μ M against calpain II, suggesting a diol substituent is not tolerated by the enzyme at P₁. Diol **3.04** (as a mixture with **3.03** in an 85:15 ratio) was essentially inactive against calpain II (IC₅₀ > 50 μ M), presumably as **3.04** has a low propensity to adopt a β -strand conformation. Macrocycle **3.05** had an IC₅₀ of 0.15 μ M against calpain II, a K_i of 686 μ M against α -chymotrypsin and an IC₅₀ of 1.46 μ M against the chymotrypsin-like sub-site of the 20S proteasome. **CAT0811** was inactive against α -chymotrypsin and had an IC₅₀ of 1.51 μ M against the chymotrypsin-like sub-site of the 20S proteasome. While modification to the P₁ and P₃ positions moderately influenced the selectivity of the macrocycles (comparing **3.05** with **CAT0811**), a much more dramatic affect was gain by modification of the P₂ residue (as in **4.02**).

Chapter Five reports the synthesis and *in vivo* testing of tritiated analogues of **CAT0811** and **4.04** by reduction of **CAT0811** with NaBT₄ to give macrocycle **5.02**, and subsequent oxidation of **5.02** to give **5.03**. Compounds **5.02** and **5.03** were separately formulated and administered to sheep from the cataract flock. Liquid scintillation counting was used to get a preliminary outlook on the absorption, distribution and excretion of the macrocycles and to investigate the phenomenon of lens crossover of the inhibitors. Previous *in vivo* trials of **CAT0811** have reported that when the formulated inhibitor is administered to the left lens, both lenses are equally observed to have slowing of cataract progression ($p < 0.05$). Levels of tritium in the treated and untreated lenses were measured. Equal amounts of **5.02** were found in both lenses 48 h after application. This supports our hypothesis that lens crossover of the macrocycles is occurring.

Declaration

I certify that this work contains no material which has been accepted for the award of any other degree or diploma in any university or other tertiary institution and, to the best of my knowledge and belief, contains no material previously published or written by another person, except where due reference has been made in the text. In addition, I certify that no part of this work will, in the future, be used in a submission for any other degree or diploma in any university or other tertiary institution without the prior approval of the University of Adelaide and where applicable, any partner institution responsible for the joint-award of this degree.

I give consent to this copy of my thesis, when deposited in the University Library, being made available for loan and photocopying, subject to the provisions of the Copyright Act 1968.

I also give permission for the digital version of my thesis to be made available on the web, via the University's digital research repository, the Library catalogue and also through web search engines, unless permission has been granted by the University to restrict access for a period of time.

Joanna Duncan

Date:

Acknowledgements

Primarily, thank you to Professor Andrew Abell for his support, guidance and supervision throughout this PhD. I am especially grateful for the time he has spent guiding me in the writing of this thesis.

I would like to thank the post doctoral fellows and senior PhD students who have provided invaluable assistance during my studies, especially Dr Matthew Jones, Dr Steve Aiken, Dr Stephen McNabb, Dr Markus Pietsch, Dr Seth Jones, Dr Scott Walker, Dr William Tieu and Dr Ashok Pehere.

I would also like to acknowledge the people who helped me in this research, especially, Dr Matthew Jones, Dr Markus Pietsch and Dr Ondrej Zvarec for performing the calpain assays, Dr Paul Nielson and Limei Sieu for performing the 20S proteasome assays, Dr Stephen McNabb and Dr Blair Stuart for performing the molecular modelling studies, Michelle Zhang for help with the chymotrypsin assay and Jade Cottam for helping with the HPLC. I would also like to say a big thank you to all the technical staff at the University of Canterbury and the University of Adelaide for their help over the years.

Finally I would like to thank my family and friends for their support and love over the course of these studies – I could not have done this without you.

Abbreviations

aq	aqueous
Boc	<i>tert</i> -butoxycarbonyl
br	broad (spectroscopic)
calc	calculated
Cbz	benzyloxycarbonyl
conc	concentrated
Cy	cyclohexyl
DCM	dichloromethane
d.e.	diastomeric excess
DIPEA	N,N-diisopropylethylamine
DMB	2,4-dimethoxy benzaldehyde
DMF	dimethylformamide
DMSO	dimethyl sulphoxide
EM	effective molarity
eq	equivalent
ESI	electrospray ionisation
Et	ethyl
FDA	Food and Drug Administration (US)
FTIR	Fourier transform infrared
GABA	gamma-aminobutyric acid
h	hour(s)
HATU	2-(7-aza-1 <i>H</i> -benzotriazol-1-yl)-1,1,3,3-tetramethyluronium hexafluorophosphate

HIV	Human Immunodeficiency Virus
HPLC	high-performance liquid chromatography
HRMS	high-resolution mass spectrometry
IR	infrared
LDA	lithium diisopropylamide
LiHMDS	lithium hexamethyl-disilyl-amide
lit.	literature value
Me	methyl
MS	mass spectrometry
<i>m/z</i>	mass-to-charge ratio
NaHMDS	Sodium-hexamethyl-disilyl-amide
NMR	nuclear magnetic resonance
PDB	Protein Data Bank
Ph	phenyl
ppm	part(s) per million
Py	pyridine
quant	quantitative
RCM	ring closing metathesis
rt	room temperature
SAR	structure activity relationship
spec	spectrometry
TCE	1,1,2-trichloroethane
temp	temperature
TFA	trifluoroacetic acid
THF	tetrahydrofuran

TLC	thin layer chromatography
UV	ultraviolet
v/v	volume per unit volume
w/w	weight per unit weight

CHAPTER ONE

INTRODUCTION

1 Introduction

1.1 Protein-protein interactions

Proteins control essentially all functions in living organisms, with enzyme catalysis, cell signaling, ligand binding and structural components of all cells and tissues across all animal, plant and micro-organism life forms reliant on the presence of proteins. The function of proteins is largely controlled by regulation of protein-protein interactions,¹ the disruption of which forms the basis of many diseases either through the loss of an essential interaction, through the formation of an undesirable interaction or through host-pathogen interactions. One example of the formation of an undesirable interaction is when an influx of calcium leads to the over activation of cysteine protease calpain which can lead to calpain mediated cleavage of the crystallins in the lens of the eye.²⁻⁴ This process is implicated in cataract formation as discussed in detail in **Chapter 3**. An often cited example of host-pathogen protein-protein interactions occurs in the HIV life cycle. HIV protease is an enzyme that catalyses the cleavage of polyproteins Gag and GagPol. This cleavage allows maturation of the virus and is crucial to infection of additional cells.⁵ As such the design of molecules that can bind to the relevant site of proteins to act as agonists or antagonists and remove undesirable physiological symptoms is an important area of drug design.⁶

1.2 Mediating protein-protein interactions

1.2.1 Peptides as drugs

The logical method for controlling protein-protein interactions is through the use of peptides. It is estimated that between 15% and 40% of all cellular interactions are mediated through protein-peptide interactions.⁷ Insulin was the first peptide to be isolated and has been administered therapeutically since 1922,⁸ however it was not until the pioneering work of du Vigneaud in the early 1950's, sequencing and synthesising oxytocin and vasopressin,^{9, 10} that the field of synthetic pharmaceutical peptides became truly viable. The use of naturally occurring or novel peptides to interact with proteins as therapeutics is now common place with approximately 60 peptide-based drugs currently approved for therapeutic use by the FDA.^{11, 12} Peptides, as a class of drugs, cover a broad range of pathologies, acting as treatments of diabetes, gastrointestinal disorders, osteoporosis, cancers, bacterial and fungal infections.^{13, 14} Most therapeutic peptides are receptor agonists, and generally, only small percentages of receptors (5 – 20 %) require peptide occupancy to elicit a desired effect.¹³

1.2.2 Disadvantages of peptides

Despite intense interest since the 1950's, therapeutic peptides generally do not make good drugs due to their unfavourable physiochemical properties.¹⁵ Such structures can have a number of disadvantages including poor bioavailability, low solubility, low stability towards hydrolysis and poor membrane permeability.¹⁶⁻¹⁹ The major barriers to the oral bioavailability of peptides are the intestinal lumen, the intestinal mucosa and the liver.^{13, 15} The gastrointestinal tract is designed to break proteins

down into smaller units, for example, amino acids, di- and tri-peptides. This is primarily achieved through exo- and endo- peptidases, enzymes that hydrolyse peptide bonds.²⁰ While this process is fundamental in producing essential building blocks obtained from food, unsurprisingly, these same enzymes are major contributors to the break down of peptide drugs.²⁰⁻²² Peptide degradation begins in the gastric juices by the pepsins and continues in the small intestine, where the primary digestive enzymes are trypsin, α -chymotrypsin, elastase and carboxypeptidase.¹⁵ Finally, the bulk of small peptides (di- and tri-peptides) are subject to digestion at the brush border or in the cytoplasm.²⁰ It should be noted that proteolytic enzymes are ubiquitous in the body, and enzymatic degradation of peptides also occurs in the blood, liver and kidney, which further limits the bioavailability of peptides when administered via a non-oral route (for example by injection).²¹⁻²³

Research into improving the bioavailability of peptides is ongoing. This is primarily focused on novel delivery methods such as adsorption enhancers and mucoadhesive delivery systems designed to increase mucosal adsorption in the GI tract, or polymeric particulate systems including nanoparticles as delivery agents to protect the peptide from proteolytic cleavage.²⁴ However, even if an efficient delivery system for peptides is developed which can overcome the problems described above; peptides are still limited in their effectiveness as pharmaceuticals due to their flexibility, as depicted in **Figure 1.1**.²⁵

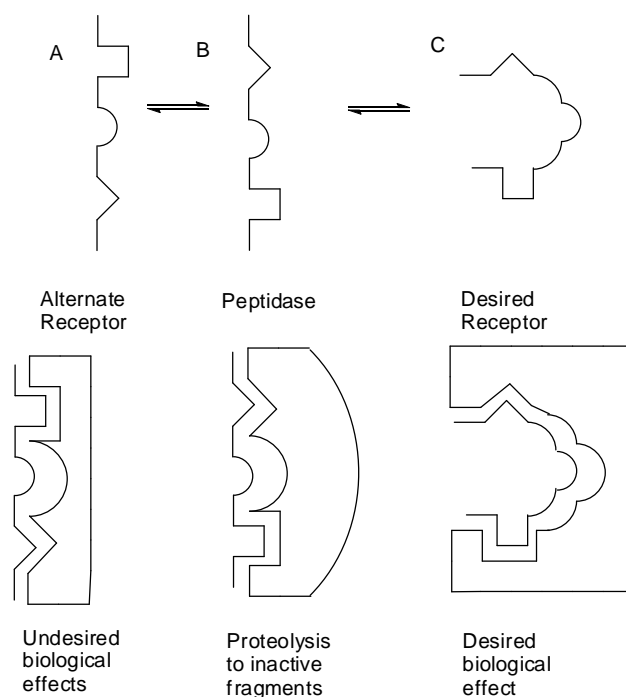


Figure 1.1. Peptide conformation equilibrium. Adapted from literature.²⁵

Adoption of the requisite conformation for binding to the desired receptor is crucial for obtaining the desired pharmacological effect (C in **Figure 1.1**). Peptides are limited in their effectiveness as drugs due to their propensity to adopt secondary structures capable of binding to alternate receptors (A and B in **Figure 1.1**). This may lead to undesirable side effects or to proteolysis as discussed above.²⁵

1.2.3 Peptidomimetics

A peptidomimetic is a substance having a secondary structure as well as other structural features analogous to that of the original peptide which allows it to displace the original peptide from receptors or enzymes. As a result the effects of the original peptide are inhibited (antagonist, inhibitor) or duplicated (agonist).²⁶ Since the early 1990's the goal of finding small, drug like molecules that mimic peptide function has emerged as a leading area of drug design.^{27, 28} The development of peptidomimetics is

based on knowledge of the electronic and conformational interactions between the native peptide and the target protein.¹ There are two key factors to consider when designing peptidomimetics: the first is that the functional groups, hydrophilic and hydrophobic regions of the mimic must be placed in defined positions to allow required interactions with the protein to occur, for example, hydrogen bonds, electrostatic or hydrophobic interactions. Secondly, the backbone of the mimic must be able to adopt (or be pre-organised in) the correct geometry to fit the binding site. Often the bioactivity of proteins stems from a small region of the protein surface which has a specific binding structure; the three most common are the α helix, β -turn and β -strand geometries.²⁸ Knowledge of the key secondary structures that proteins adopt at biologically important sites has driven the relatively recent search for peptidomimetics. Enhanced activity can be achieved through the mimicking of the bioactive conformation of a native substrate, with the incorporation of additional structural elements designed to stabilise and make rigid this desired bioactive conformation. These rigid structural features are designed to ensure the correct positioning of key functional groups in order to optimise hydrogen bonding, electrostatic, and hydrophobic interactions between the peptidomimetic ligand and the receptor.

1.3 Peptide secondary structure

An important goal in the development of rationally designed mimics is to restrict the backbone and side chain moieties into a bioactive conformation (e.g. α -helix, β -strand or β -turn), while reducing the affinity of the mimic to proteolytic enzymes described above.²⁹ Such protein secondary structures are defined by their ϕ (phi), ψ (psi) and ω (omega) angles, while side chain geometry is defined by χ (chi) space (**Figure 1.2**).

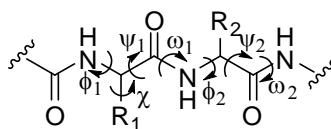


Figure 1.2. Dihedral angles that define peptide structure. The backbone is defined by ϕ , ψ , ω , while side chain geometry is defined by χ .

Amide bonds are planar and usually trans ($\omega = 180^\circ$). A survey of approximately 33 000 angles in 154 X-ray structures found only 0.3% of amide bonds were in a cis geometry ($\omega = 0^\circ$).³⁰ This leaves the secondary structure of peptides largely determined by the ϕ and ψ torsion angles as shown in **Table 1.1**.^{31, 32}

		ϕ_1	ψ_1	ϕ_2	ψ_2
α -helix		-58	-47	-58	-47
β -turn	I	-60	-30	-90	0
	I'	60	30	90	0
	II	-60	120	80	0
	II'	60	-120	-80	0
	IV	-61	10	-53	17
	VIa1	-60	120	-90	0
	VIa2	-120	120	-60	0
	VIb	-135	-135	-75	160
	VIII	-60	-30	-120	120
β -Strand		-139	135	-139	135

Table 1.1 Dihedral angles defining the secondary structure of peptides.^{31, 32}

The α -helix is the most common peptide secondary structure constituting >40% of the residues in proteins.³³ α -Helices are characterised by a hydrogen bond between the first (i) residue carbonyl oxygen and fifth ($i+4$) residue NH hydrogen as shown in **Figure 1.3**.

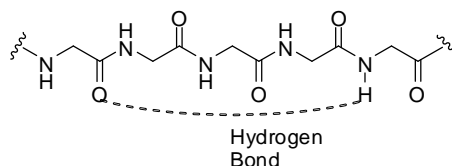


Figure 1.3. Hydrogen bonding in an α -helix

When found in the core of a protein, the α -helix is an important stabiliser of tertiary structure, when located at the exterior of a protein, the α -helix forms a key recognition element.³⁴ α -helices are a bioactive region in a number of human proteins, involved in hormone receptor, binding DNA and RNA binding and hemolytic activity.³⁵ Approximately 62% of protein-protein complexes in the Protein Data Bank have a helical interface;³⁶ mimics of this secondary structure are a powerful tool in the regulation of protein-protein interactions.

The turn motif is also ubiquitous in nature, with one in four residues in the PDB displaying a turn structure.³⁷ β -turns are a class of reverse turn and change the orientation of the peptide by 180 degrees.³⁸ Comprised of four peptide residues labelled i , $i+1$, $i+2$ and $i+3$ (**Figure 1.4**), β -turns are characterised by having a hydrogen bond between the i carbonyl oxygen and the $i+3$ amide proton residues, forming a 10-membered ring.

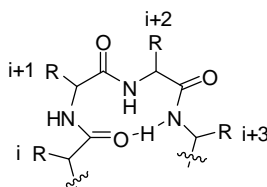


Figure 1.4. Structure of a tetra-peptide in a β -turn formation

Nine classes of β -turn have been identified, defined by the ϕ and ψ dihedral angles as shown in **Table 1.1**.³⁹ These turns generally occupy the surface of proteins, are

hydrophilic⁴⁰ and play an important role in recognition and binding of proteins.^{41, 42} β -Turn mimics have been developed to capitalise on their affinity to a wide variety of pharmacologically important receptors including bradykinin,⁴³ integrin,⁴⁴ dopamine,^{45, 46} somatostatin,⁴⁷ and opioid receptors.⁴⁸ This topic has been extensively reviewed.⁴⁹⁻⁵¹

The β -strand is the most simple peptide structural element with no internal hydrogen bonds. Isolated β -strands are not common in proteins, they are usually arranged, via inter-molecular hydrogen bonds, in a β -sheet. Originally considered to be a random structure, β -strands are now recognised as the crucial recognition element in proteolytic enzymes, major histocompatibility complex (MHC) proteins and transferases, as such, small molecules targeting this secondary structure are now widespread.⁵²⁻⁵⁴

1.4 Classes of peptidomimetic

Numerous synthetic strategies have emerged to restrict the ϕ , ψ , ω and χ angles in peptidomimetics to pre-organise the defined conformations discussed above. Broadly, these can be classified into three categories, side chain modification, backbone modification and the introduction of global restrictions.

1.4.1 Side chain modification

The side chain orientation of an α -amino acid is critical for molecular recognition and transduction processes.⁵⁵ There are three low energy staggered conformations that are possible (**Figure 1.5**).

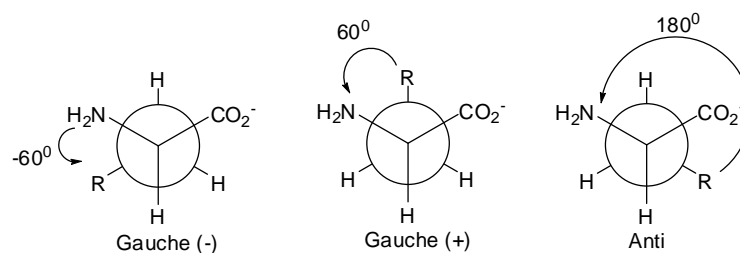


Figure 1.5. Newman projections of low energy staggered conformers in α -amino acids.

In the gauche (-) conformation, the side chain points towards the N-terminus, in the gauche (+) conformation the side chain is perpendicular to the peptide backbone and in the anti conformation the side chain points towards the C-terminus. Generally, all three conformations are accessible to a peptide due to the low energy barrier between them; however during interaction between a peptide and its receptor, each side chain moiety will adopt the specific conformation required for binding.⁵⁶ Fixing the side chain geometry by constraining the χ angles is a powerful tool in the synthesis of peptidomimetics. Generally, side chain modifications do not restrict the conformation of the peptide backbone²⁹.

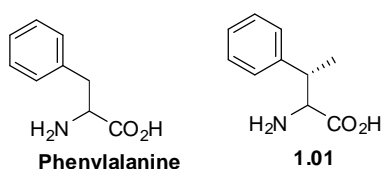


Figure 1.6. Natural phenylalanine and β -alkyl analogue **1.01**.

Side chain orientation can be constrained by alkylation of the β -carbon (**Figure 1.6**). The rationale behind this is to isolate the biologically active χ rotamer by steric hindrance of rotation about the χ_1 bond.⁵⁷ β -carbon alkylation has been used to modify a number of peptides including opioids,⁵⁸⁻⁶² oxytocin,⁶³ somatostatin,⁶⁴ and glucagen⁶⁵ to investigate topographical requirements and to better understand structure activity relationships. Replacement of natural amino acids with their

rigidified analogues can result in higher activity and bio-stability, for example when phenylalanine (**Figure 1.6**) is replaced with **1.01** in a peptide, activity at opioid receptors is successfully modified.⁵⁸

1.4.2 Strategies for restriction of ϕ , ψ and ω torsion angles

1.4.2.1 Backbone modification

Replacement of individual atoms			Extension of peptide chain	Replacement of amide bond
Replace NH	Replace CH	Replace CO	X	Replace CO-NH
N-alkyl	N (aza)	CS	CH₂	NH-CO
O	C-alkyl	CH ₂	O	CH(OH)CH ₂
S	BH	SO _n (n=1,2)	NH	CH=CH
		P=O(OH)		CH ₂ CH ₂
				P=O(OH)-CH ₂

Table 1.2. The most common forms of backbone modification of peptides to create peptidomimetics.

The most common forms of backbone modification are given in **Table 1.2**. These modifications generally reduce the mimic's affinity to proteolytic cleavage and, in some cases, restrict the flexibility of the backbone. Selected examples (highlighted in red) of mimics where the backbone flexibility is restricted by the modification, will be discussed.

Backbone modification may involve replacement of individual atoms, extension of the peptide or replacement of the amide bond. When considering replacement of individual atoms, the NH, the CH or the carbonyl/amide bond can be replaced to

improve cell permeation and bio-stability properties or to restrict the flexibility of the peptide. Replacement of the NH with an N-alkyl substituent, which generally restricts the ϕ torsion angle while eliminating any hydrogen bonding from the amide bond, can increase membrane permeability and proteolytic stability.^{1, 29} There are naturally occurring examples of peptides with N-alkylation, for example, Cyclomarin C, an anti-inflammatory cyclic heptapeptide,⁶⁶ and this is a common tool for creating synthetic peptidomimetic libraries to probe structure activity relationships. Due to the removal of hydrogen bonding ability from the nitrogen after N-methylation, successive alkylation of each backbone NH and subsequent measurement of biological activity for each derivative allows key hydrogen bonds for activity to be identified.⁶⁷

As first observed by Thorpe and Ingold and colleagues,⁶⁸ carbon-substitution is an effective method to restrict the conformation of a molecule to facilitate ring closure. Since early observations on the Thorpe-Ingold effect, alkylation of the α -carbon has been extensively studied as a strategy for peptidomimetic development due to the reduced rotation α -alkyl amino acids have around the ϕ and ψ torsion angles.⁶⁹ The most simple example of a tetra-substituted amino acid is naturally occurring α -aminoisobutyric acid (Aib) shown in **Figure 1.7**.⁶⁹

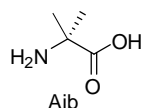


Figure 1.7. Structure of tetra-substituted Aib.

The tetra-substitution at $C\alpha$ imposes significant restrictions on the available conformational space of the amino acid and peptides incorporating Aib show a strong

helical tendency, for example, peptide **1.02** (**Figure 1.8**), is a deca-peptide with 80% of residues α -carbon-substituted. Peptide **1.02** adopts an α -helix and is an effective antibiotic.^{69, 70}

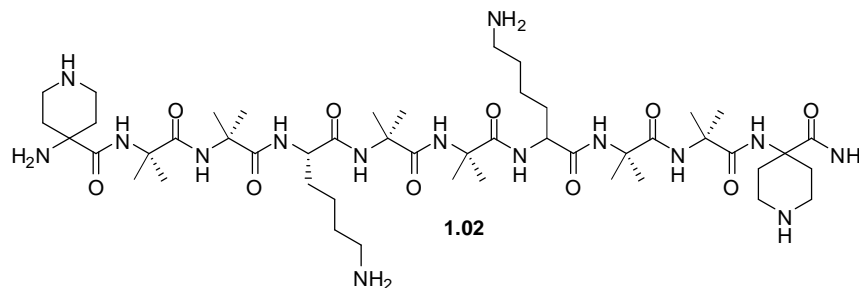


Figure 1.8. Structure of helical deca-peptide **1.02** stabilised by α -carbon substitution.

The replacement of an amide bond within a peptide with an isostere is a popular strategy in the design of peptidomimetics; however, often the novel compounds are not true mimics and may not be active at their desired biological targets.²⁹ Isosteres generally do not restrict global conformations, however they may improve the bioavailability of mimics.⁷¹ Replacement of the amide with, for example a thioamide, has been shown to increase plasma stability and cell permeability when incorporated into N-methyl-D-aspartate receptor inhibitors.⁷² A thioamide is a true isostere of the amide bond, where the number of atoms, the arrangement of atoms and the number of valence electrons are conserved with the parent amide. Thioamides confer some conformational restriction on the peptide due to the increased size of the sulfur atom compared to the oxygen in an amide. This enables the sulfur to better accommodate a negative charge which leads to a larger contribution from resonance structure III than in amides (**Figure 1.9**). This, in turn, restricts rotation of the ω torsion angle.⁷³

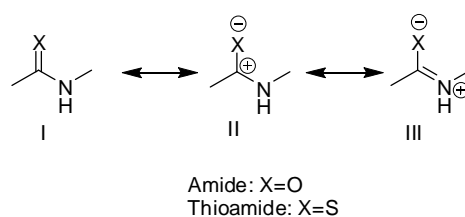


Figure 1.9. Resonance structures of amide or thioamide bonds.

Olefins have also been investigated as an amide bond isostere that restricts the peptide backbone conformation. Geometrically, the alkene is a good mimic of an amide bond, with both having a $C\alpha_i - C\alpha_{i+4}$ distance of approximately 3.8\AA .⁷⁴ Electronically, however, amides and alkenes are substantially different; olefins are not strong hydrogen bond donors or acceptors, where the amide is a strong hydrogen bond donor via the NH hydrogen and a strong hydrogen bond acceptor via the carbonyl oxygen.⁷³ The olefin isostere may have potential in the synthesis of β -turn mimics,^{75, 76} however it has been an ineffectual mimic of other structural conformations.⁷³

Peptidomimetics formed by extension of the peptide chain, for example, with a CH_2 group to give β -amino acids is discussed in detail in **Chapter 3** of this thesis.

1.4.2.2 Introduction of global restriction

The introduction of global restrictions on peptide conformation by cyclisation is a recognised universal method for the preparation of peptidomimetics.²⁹ The introduction of rigid bridges, of varying lengths between different parts of a peptide, can improve potency by fixing the backbone torsion angles and/or side chain orientation, locking the ligand into a preferred bioactive conformation.

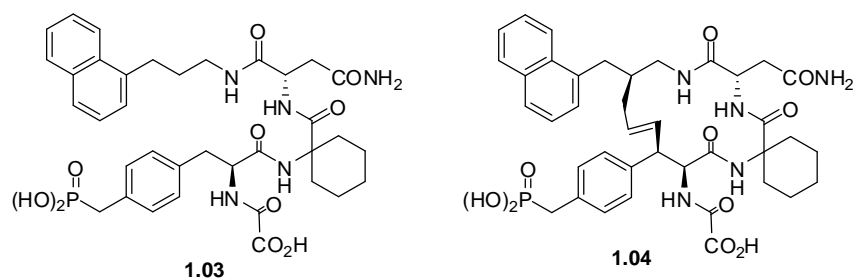


Figure 1.10. GRB2 binding peptidomimetic **1.03** and cyclic analogue **1.04**.⁷⁷

Peptidomimetic **1.03** was designed as a ligand for growth factor receptor-bound protein 2 (GRB2) (**Figure 1.10**). Ring closing metathesis was used to generate cyclic analogue **1.04**. The macrocycle stabilises the bent conformation required for binding to increase the affinity of the peptidomimetic by 140 fold compared to **1.03**.⁷⁷

There is evidence that the observed increase in activity conferred by cyclisation is due to off-set of the entropic loss that occurs when forming a protein-ligand complex.⁷⁷⁻⁷⁹

Cyclic peptidomimetics are generally designed to increase the mimics affinity for its associated receptor or enzyme active site compared to the native peptide, however, the exclusion of conformations that are capable of forming undesirable protein-peptide interactions also enhances the selectivity of the ligand for its target.^{29, 77}

Cyclic peptidomimetics have improved proteolytic stability, exhibiting enhanced resistance to exo- and endo-peptidases over their linear counterparts.¹

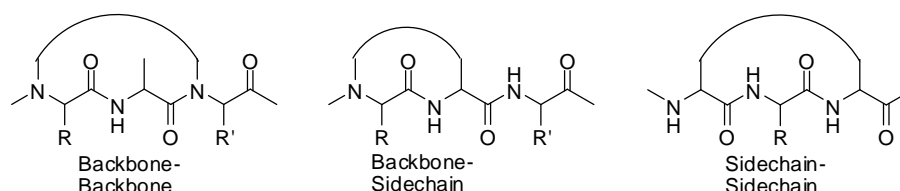


Figure 1.11. The three principle arrangements of peptide cyclisation.

There are three principle approaches to generating a cyclic peptidomimetic: through backbone-backbone (including head to tail), backbone-side chain or side chain-side chain cyclisations (**Figure 1.11**). By far the most common method of cyclisation has been the formation of a disulfide bridge or by lactamisation.⁸⁰ Numerous examples of natural cyclic peptides are known which contain either an amide linkage or a disulfide bridge – somatostatin, oxytocin, vasopressin ciclosporin and cyclotides to name a few.^{9, 10, 27, 81, 82} Given nature's propensity to constrain peptides by these methods, it is not surprising that a number of peptidomimetics, targeting a range of proteins, have been reported which contain lactam or disulfide bridges.^{49, 53, 83}

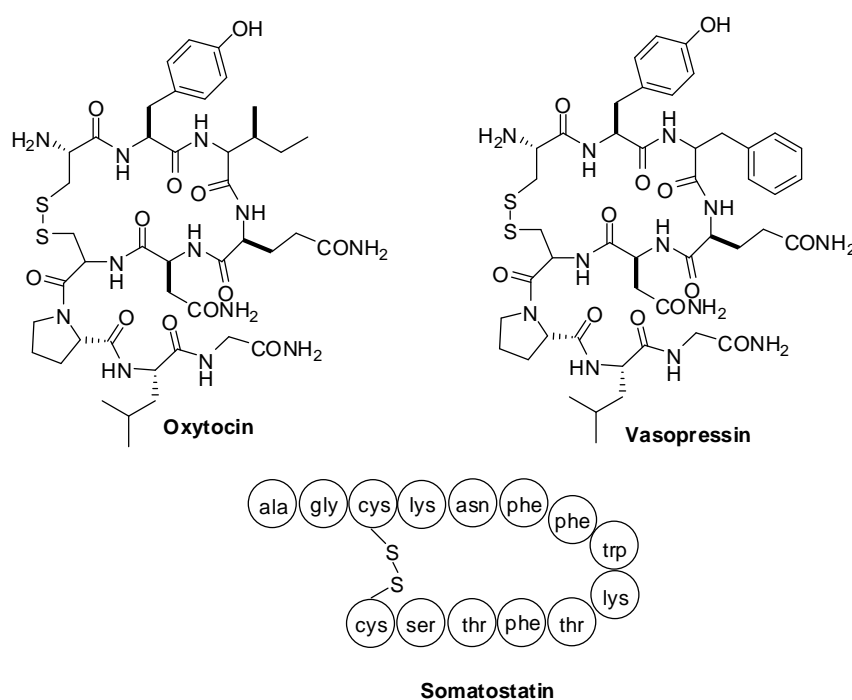


Figure 1.12. Hormones containing a disulfide bridge.

However, despite their ability to stabilise secondary structures, compounds containing lactam and disulfide bridges do not make ideal peptidomimetics. The lactam and disulfide bridges in natural systems and peptidomimetics are easily recognised as substrates *in vivo* and are prone to degradation. Hormones oxytocin, vasopressin and

somatostatin (**Figure 1.12**) are limited in their therapeutic use by short *in vivo* half lives (2-5 mins) and must be administered intravenously.⁵⁴ Octreotide (**Figure 1.13**), a marketed mimic of somatostatin, was developed retaining the disulfide bridge of the parent compound and suffers from a similarly short half life because of this.⁵⁴

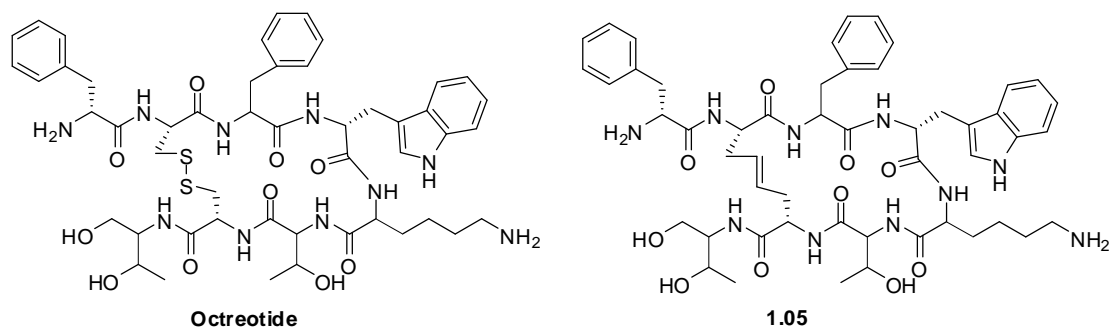


Figure 1.13. Octreotide and dicarba analogue **1.05**.

Ideally, peptidomimetics would use an alternative linker that is inert to *in vivo* reactions. A suitable analogue of a disulfide is the CH_2CH_2 (dicarba) moiety. The geometric properties (dihedral angle and inter-atomic distances) are approximately equal between the disulfide and the dicarba groups,⁷⁴ and dicarba analogues have more favourable half lives and/or selectivity *in vivo* while retaining activity against the desired receptor. For example **1.05** (**Figure 1.13**) is the alkene analogue of Octreotide and displays better biological stability than the parent, with excellent activity ($\text{IC}_{50} = 28 \text{ nM}$) against the biological target (in this case G-protein-coupled receptors).⁵⁴

1.5 A ring closing metathesis route to peptidomimetics

1.5.1 A brief history of metathesis.

Ring closing metathesis has emerged as an efficient method for the synthesis of carbon-carbon bonds in complex molecules including peptidomimetics. Ring closing metathesis describes the process by which alkylidene groups of alkenes exchange by the reversible mechanism proposed by Chauvin (**Figure 1.14**).^{84, 85}

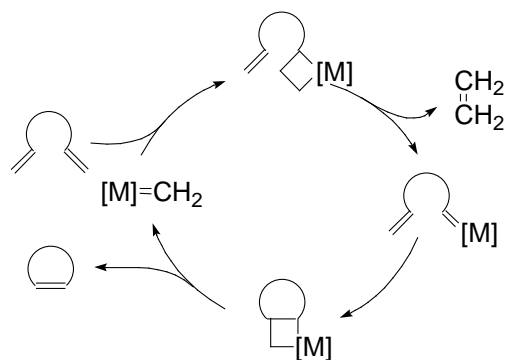


Figure 1.14. Ring closing metathesis mechanism.

Metathesis became a viable synthetic technique for organic chemists with the development of air stable, functional group tolerant ruthenium catalysts, specifically Grubbs' first generation catalyst.⁸⁶ The discovery of ruthenium based catalysts in the early 1990s⁸⁷ has enabled ring closing metathesis to become an important synthetic method in organic chemistry. Ruthenium catalysts are generally less active than earlier transition metal catalysts and are therefore more versatile for ring closing metathesis, reacting preferentially with olefins. Compare this to molybdenum, tungsten and titanium based catalysts which react with other functional groups in the molecule including esters, amides and ketones.⁸⁸ The development of highly active, stable, second generation catalysts capable of forming tri- and tetra- substituted olefins, has expanded the utility of the ring closing metathesis reaction.⁸⁹ Grubbs'

second generation catalyst is a ruthenium based system that has low sensitivity to moisture and air, which, combined with the favourable combination of high alkene activity and functional group compatibility, makes this the reagent of choice for olefin metathesis.⁸⁸

1.5.2 Peptidomimetics by ring closing metathesis

The first synthesis of a disulfide analogue by metathesis was reported by Grubbs in 1996 (**Figure 1.15**).⁹⁰ Here, cyclic tetra-peptide **1.07** was synthesised, and subsequent conformational studies revealed the dicarba analogue displayed the same hydrogen bonds, indicative of a β -turn, as the corresponding disulfide **1.06**.

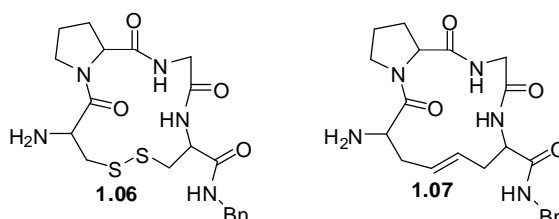


Figure 1.15. An early example of the use of ring closing metathesis to mimic a disulfide bond.

Ring closing metathesis has been used to prepare peptidomimetics pre-organised in all three of the key binding motifs discussed herein, specifically, there are α -helix mimics, β -turn mimics and β -strand mimics reported. This topic was reviewed extensively in 2011,⁵⁴ however some recently published examples that were not included in this review are shown in **Figure 1.16**.

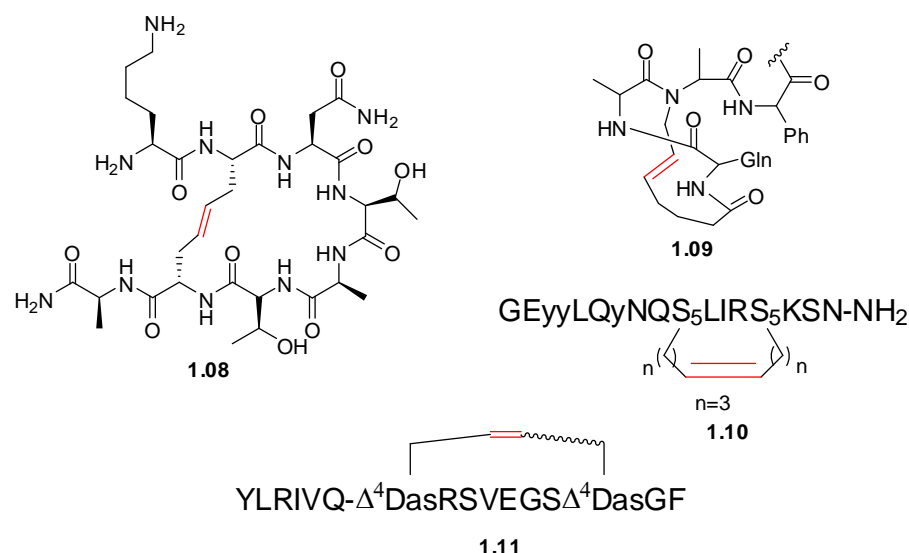


Figure 1.16. Recent peptidomimetics cyclised by ring closing metathesis. The bond highlighted red indicates the alkene formed in metathesis.

Amylin (1-8) is an octa-peptide that is effective as a promoter of the proliferation of osteoblasts (bone forming cells) which enhance bone volume and strength. While Amylin is a potential treatment of osteoporosis, it is not stable *in vivo*, due to a labile disulfide bridge, leading Kowalczyk and colleagues to investigate replacing the disulfide bridge with dicarba analogues for example **1.08** (Figure 1.16).⁹¹ The dicarba analogues displayed biological activity approximately equal to the parent peptide in *in vitro* assay and two of the most promising analogues have been progressed to *in vivo* testing. While no mention of the secondary structure of **1.08** is given, it should be noted that differences in biological activity were observed when cis and trans isomers were compared. This is presumably due to differing secondary structures imposed on the peptide by either of the two olefin moieties.

Cyclic peptide **1.09** (Figure 1.16) was synthesised by Henchey et al to investigate the helical forming properties conferred to an incorporating peptide and to investigate the binding affinity to MDM2.⁹² P53 is a tumour suppressor protein that signals cell

apoptosis in response to DNA damage or cellular stress. MDM2 binds to, and inhibits the action of, P53 at an α -helical interface. Inhibition of P53 by MDM2 is implicated in cancer proliferation, so peptides that can disrupt this interaction by binding to MDM2 may have potential as anticancer agents. Peptidomimetic **1.09** was designed to replace a hydrogen bond with a dicarba linkage to constrain the peptide in an α -helix conformation and displays highly selective binding to the target MDM2. The propensity of mimic **1.09** to adopt an α -helix is approximately double that of the parent peptide, and, interestingly, the binding affinity of **1.09** to MDM2 compared to the parent peptide is also approximately doubled ($K_D = 160$ nM compared to 340 nM).

Peptidomimetic **1.10** was proposed as a derivative of conantokins.⁹³ Conantokins are a class of anti-convulsant peptides, stabilised in a helical conformation by divalent cations. Replacement of the cation-mediated helix stabiliser with a covalent linkage as shown in **Figure 1.16** significantly improved the stability of the peptide while retaining the potency of the parent compound.

Finally, peptide **1.11** (**Figure 1.16**) is an analogue of a portion of human growth hormone, AOD9604, which was removed from clinical trials as an anti-obesity treatment when weight loss did not reach significance after oral application.⁹⁴ Structure **1.11**, where the disulfide bridge was replaced with a dicarba moiety, was proposed to improve the oral bioavailability of the peptide. Here, the replacement of the disulfide bridge with a mixture of cis and trans olefins lead to significant structural changes to the peptide. These structural changes manifested by **1.11** displaying the opposite effect to the parent *in vivo*. The truncated human growth

hormone promoted sustained weight loss in male New Zealand obese mice, while analogue **1.11** prompted sustained weight gain. The authors report future work to isolate each of the cis and trans isomers of the alkene and to independently analyse the structure and biological properties of the peptides. This surprising result stresses the importance that secondary structure plays in regulating protein-peptide interactions.

1.6 Research Described In This Thesis

The above examples were chosen to highlight the effectiveness of ring closing metathesis mediated cyclisations for controlling the structure and pharmacological properties of peptidomimetics. The increasing volume of research dedicated to peptidomimetics cyclised in this manner indicates the interest and potential of this field of research. The work in this thesis describes the design, synthesis and biological testing of conformationally constrained peptidomimetics. **Chapter 2** describes the synthesis of medium sized rings comprised of β -amino acids by ring closing metathesis and investigates their propensity to adopt a β -turn conformation. **Chapter 3** describes the use of ring closing metathesis to synthesis macrocycles, designed to adopt a β -strand conformation, as potential protease inhibitors. In **Chapter 4**, the *in vitro* activity of these macrocycles against calpain II, α -chymotrypsin and the 20S proteasome is reported. These results are discussed in the context of the full SAR study completed by the Abell group on these types of macrocycles and the most potent calpain II inhibitors are identified. **Chapter 5** describes the synthesis and *in vivo* testing of tritiated analogues of the most potent macrocyclic calpain II inhibitors in order to better understand the absorption and dispersion properties of our inhibitors.

1.7 References

1. Grauer, A.; König, B., *European Journal of Organic Chemistry* **2009**, 2009 (30), 5099-5111.
2. David, L. L.; Shearer, T. R., *Federation of European Biochemical Societies* **1993**, 324, 265-270.
3. David, L. L.; Shearer, T. R.; Shih, M., *Journal of Biological Chemistry* **1993**, 268, 1937-1940.
4. Nakamura, Y.; Fukiage, C.; Shih, M.; Ma, H.; David, L. L.; Azuma, M.; Shearer, T. R., *Investigative Ophthalmology & Visual Science* **2000**, 41, 1460-1466.
5. Mehellou, Y.; De Clercq, E., *Journal of Medicinal Chemistry* **2009**, 53 (2), 521-538.
6. Leung, D.; Abbenante, G.; Fairlie, D. P., *Journal of Medicinal Chemistry* **2000**, 43 (3), 305-341.
7. Petsalaki, E.; Russell, R. B., *Current Opinion in Biotechnology* **2008**, 19 (4), 344-350.
8. Rendell, M., *Drug Development Research* **2008**, 69 (3), 95-100.
9. Turner, R. A.; Pierce, J. G.; du Vigneaud, V., *Journal of Biological Chemistry* **1951**, 191 (1), 21-28.
10. du Vigneaud, V.; Ressler, C.; Trippett, S., *Journal of Biological Chemistry* **1953**, 205 (2), 949-957.
11. www.drugbank.ca (accessed 27 December 2012).
12. www.fda.gov/ (accessed 27 December 2012).
13. Vlieghe, P.; Lisowski, V.; Martinez, J.; Khrestchatsky, M., *Drug Discovery Today* **2010**, 15, 40-56.

14. Stevenson, C. L., *Current Pharmaceutical Biotechnology* **2009**, *10*, 122-137.
15. Pauletti, G. M.; Gangwar, S.; Siahhaan, T. J.; Jeffrey, A.; T. Borchardt, R., *Advanced Drug Delivery Reviews* **1997**, *27* (2â€³), 235-256.
16. Hirschmann, R., *Angewandte Chemie International Edition in English* **1991**, *30* (10), 1278-1301.
17. Nakayama, K.; Kawato, H. C.; Inagaki, H.; Ohta, T., *Organic Letters* **2001**, *3* (22), 3447-3450.
18. Smith, A. B.; Hirschmann, R.; Pasternak, A.; Akaishi, R.; Guzman, M. C.; Jones, D. R.; Keenan, T. P.; Sprengler, P. A., *Journal of Medicinal Chemistry* **1994**, *37* (2), 215-218.
19. Kumar Malik, D.; Baboota, S.; Ahuja, A.; Hasan, S.; Ali, J., *Current Drug Delivery* **2007**, *4* (2), 141-151.
20. Lee, V. H. L.; Yamamoto, A., *Advanced Drug Delivery Reviews* **1989**, *4* (2), 171-207.
21. Neurath, H., *Trends in Biochemical Sciences* **1989**, *14* (7), 268-271.
22. Beynon, R. J.; Bond, J. S., *American Journal of Physiology - Cell Physiology* **1986**, *251* (2), C141-C152.
23. Neurath, H.; Walsh, K. A., *Proceedings of the National Academy of Sciences* **1976**, *73* (11), 3825-3832.
24. Chin, J.; Foyez Mahmud, K. A.; Kim, S. E.; Park, K.; Byun, Y., *Drug Discovery Today: Technologies* **2012**, *9* (2), e105-e112.
25. Veber, D. F.; Freidinger, R. M., *Trends in Neurosciences* **1985**, *8* (0), 392-396.
26. Gante, J., *Angewandte Chemie International Edition in English* **1994**, *33* (17), 1699-1720.

-
27. Wiley, R. A.; Rich, D. H., *Medicinal Research Reviews* **1993**, *13* (3), 327-384.
 28. Loughlin, W. A.; Tyndall, J. D. A.; Glenn, M. P.; Fairlie, D. P., *Chemical Reviews* **2004**, *104* (12), 6085-6118.
 29. Hruby, V. J.; Balse, P. M., *Current Medicinal Chemistry* **2000**, *7* (9), 945-970.
 30. Stewart, D. E.; Sarkar, A.; Wampler, J. E., *Journal of Molecular Biology* **1990**, *214* (1), 253-260.
 31. Hutchinson, E. G.; Thornton, J. M., *Protein Science* **1994**, *3* (12), 2207-2216.
 32. Gillespie, P.; Cicariello, J.; Olson, G. L., *Peptide Science* **1997**, *43* (3), 191-217.
 33. Whitby, L. R.; Boger, D. L., *Accounts of Chemical Research* *45* (10), 1698-1709.
 34. Fairlie, D. P.; West, M. L.; Wong, A. K., *Current Medicinal Chemistry* **1998**, *5* (1), 29-62.
 35. Andrews, M. J. I.; Tabor, A. B., *Tetrahedron* **1999**, *55* (40), 11711-11743.
 36. Jochim, A. L.; Arora, P. S., *ACS Chemical Biology* **2010**, *5* (10), 919-923.
 37. www.pdb.org (accessed 30 December 2012).
 38. Arbor, S.; Kao, J.; Wu, Y.; Marshall, G. R., *Biopolymers* **2008**, *90* (3), 384-393.
 39. Hutchinson, E. G.; Thornton, J. M., *Protein Science* **1994**, *3* (12), 2207-2216.
 40. Kuntz, I. D., *Journal of the American Chemical Society* **1972**, *94* (11), 4009-4012.
 41. Wilmot, C. M.; Thornton, J. M., *Journal of Molecular Biology* **1988**, *203* (1), 221-232.
 42. Lewis, P. N.; Momany, F. A.; Scheraga, H. A., *Proceedings of the National Academy of Sciences* **1971**, *68* (9), 2293-2297.

-
43. Sejbal, J.; Cann, J. R.; Stewart, J. M.; Gera, L.; Kotovych, G., *Journal of Medicinal Chemistry* **1996**, *39* (6), 1281-1292.
 44. Belvisi, L.; Bernardi, A.; Colombo, M.; Manzoni, L.; Potenza, D.; Scolastico, C.; Giannini, G.; Marcellini, M.; Riccioni, T.; Castorina, M.; LoGiudice, P.; Pisano, C., *Bioorganic & Medicinal Chemistry* **2006**, *14* (1), 169-180.
 45. Vartak, A. P.; Johnson, R. L., *Org. Lett.* **2006**, *8* (5), 983-986.
 46. Vartak, A. P.; Skoblenick, K.; Thomas, N.; Mishra, R. K.; Johnson, R. L., *J. Med. Chem.* **2007**, *50* (26), 6725-6729.
 47. Veber, D. F.; Freidinger, R. M.; Perlow, D. S.; Paleveda, W. J.; Holly, F. W.; Strachan, R. G.; Nutt, R. F.; Arison, B. H.; Homnick, C.; Randall, W. C.; Glitzer, M. S.; Saperstein, R.; Hirschmann, R., *Nature* **1981**, *292* (5818), 55-58.
 48. Eguchi, M.; Shen, R. Y. W.; Shea, J. P.; Lee, M. S.; Kahn, M., *J. Med. Chem.* **2002**, *45* (7), 1395-1398.
 49. Tyndall, J. D. A.; Pfeiffer, B.; Abbenante, G.; Fairlie, D. P., *Chemical Reviews* **2005**, *105* (3), 793-826.
 50. Fairlie, D. P.; West, M. L.; Wong, A. K., *Current Medicinal Chemistry* **1998**, *5* (1), 29.
 51. Ruiz-Gomez, G.; Tyndall, J. D. A.; Pfeiffer, B.; Abbenante, G.; Fairlie, D. P., *Chemical Reviews* **2010**, *110* (4), PR1-PR41.
 52. Madala, P. K.; Tyndall, J. D. A.; Nall, T.; Fairlie, D. P., *Chemical Reviews* **2011**, *110* (6), PR1-PR31.
 53. Loughlin, W. A.; Tyndall, J. D. A.; Glenn, M. P.; Hill, T. A.; Fairlie, D. P., *Chemical Reviews* **2010**, *110* (6), PR32-PR69.

-
54. Pérez de Vega, M. J.; García-Aranda, M. I.; González-Muñiz, R., *Medicinal Research Reviews* **2010**, *31* (5), 677-715.
 55. Hruby, V. J., *Life Sciences* **1982**, *31* (3), 189-199.
 56. Jensen, K. J., *Peptide and Protein Design for Biopharmaceutical Applications*. Wiley: West Sussex, UK; Hoboken, NJ, 2009.
 57. Haskell-Luevano, C.; Toth, K.; Boteju, L.; Job, C.; Castrucci, A. M. d. L.; Hadley, M. E.; Hruby, V. J., *Journal of Medicinal Chemistry* **1997**, *40* (17), 2740-2749.
 58. Tourwe, D.; Mannekens, E.; Diem, T. N. T.; Verheyden, P.; Jaspers, H.; Toth, G.; Peter, A.; Kertesz, I.; Torok, G.; Chung, N. N.; Schiller, P. W., *Journal of Medicinal Chemistry* **1998**, *41* (26), 5167-5176.
 59. Mosberg, H. I.; Omnaas, J. R.; Lomize, A.; Heyl, D. L.; Nordan, I.; Mousigian, C.; Davis, P.; Porreca, F., *Journal of Medicinal Chemistry* **1994**, *37* (25), 4384-4391.
 60. Hruby, V. J.; Toth, G.; Gehrig, C. A.; Kao, L. F.; Knapp, R.; Lui, G. K.; Yamamura, H. I.; Kramer, T. H.; Davis, P.; Burks, T. F., *Journal of Medicinal Chemistry* **1991**, *34* (6), 1823-1830.
 61. Toth, G.; Russell, K. C.; Landis, G.; Kramer, T. H.; Fang, L.; Knapp, R.; Davis, P.; Burks, T. F.; Yamamura, H. I.; Hruby, V. J., *Journal of Medicinal Chemistry* **1992**, *35* (13), 2384-2391.
 62. Qian, X.; Koeber, K. E.; Shenderovich, M. D.; Lou, B.-S.; Misicka, A.; Zalewska, T.; Horvath, R.; Davis, P.; Bilsky, E. J., *Journal of Medicinal Chemistry* **1994**, *37* (12), 1746-1757.
 63. Lebl, M.; Toth, G.; Slaninova, J.; Hruby, V. J., *International Journal of Peptide and Protein Research* **1992**, *40* (2), 148-151.

-
64. Huang, Z.; He, Y. B.; Raynor, K.; Tallent, M.; Reisine, T.; Goodman, M., *Journal of the American Chemical Society* **1992**, *114* (24), 9390-9401.
 65. Azizeh, B. Y.; Shenderovich, M. D.; Trivedi, D.; Li, G.; Sturm, N. S.; Hruby, V. J., *Journal of Medicinal Chemistry* **1996**, *39* (13), 2449-2455.
 66. Wen, S.-J.; Yao, Z.-J., *Organic Letters* **2004**, *6* (16), 2721-2724.
 67. Rajeswaran, W. G.; Hocart, S. J.; Murphy, W. A.; Taylor, J. E.; Coy, D. H., *Journal of Medicinal Chemistry* **2001**, *44* (9), 1416-1421.
 68. Beesley, R. M.; Ingold, C. K.; Thorpe, J. F., *Journal of the Chemical Society, Transactions* **1915**, *107* (0), 1080-1106.
 69. Toniolo, C.; Crisma, M.; Formaggio, F.; Peggion, C., *Peptide Science* **2001**, *60* (6), 396-419.
 70. Vavrek, R. J.; Stewart, J. M., *Peptides* **1980**, *1* (3), 231-235.
 71. Vagner, J.; Qu, H.; Hruby, V. J., *Current Opinion in Chemical Biology* **2008**, *12* (3), 292-296.
 72. Bach, A.; Eildal, J. N. N.; Stuhr-Hansen, N.; Deeskamp, R.; Gottschalk, M.; Pedersen, S. W.; Kristensen, A. S.; Stromgaard, K., *Journal of Medicinal Chemistry* **2011**, *54* (5), 1333-1346.
 73. Choudhary, A.; Raines, R. T., *ChemBioChem* **2011**, *12* (12), 1801-1807.
 74. Liskamp, R. M. J.; Rijkers, D. T. S.; Kruijtzter, J. A. W.; Kemmink, J., *ChemBioChem* *12* (11), 1626-1653.
 75. Hoffmann, R. W.; Schopfer, U.; Müller, G.; Brandl, T., *Helvetica Chimica Acta* **2002**, *85* (12), 4424-4441.
 76. Spaltenstein, A.; Carpino, P. A.; Miyake, F.; Hopkins, P. B., *The Journal of Organic Chemistry* **1987**, *52* (17), 3759-3766.

-
77. Driggers, E. M.; Hale, S. P.; Lee, J.; Terrett, N. K., *Nature Reviews Drug Discovery* **2008**, *7* (7), 608-624.
78. Reid, R.; Kelso, K.; Scanlon, M.; Fairlie, D., *Journal of the American Chemical Society* **2002**, *124*, 5673-5683.
79. Tyndall, J. D. A.; Reid, R.; Tyssen, D. P.; Jardine, D. K.; Todd, B.; Passmore, M.; March, D. R.; Pattenden, L. K.; Bergman, D. A.; Alewood, D.; Hu, S.; Alewood, P. F.; Birch, C. J.; Martin, J. L.; Fairlie, D., *Journal of the American Chemical Society* **2000**, *43* (19), 3495-3504.
80. White, C. J.; Yudin, A. K., *Nature Chemistry* **3** (7), 509-524.
81. Peterson, D. H.; Reineke, L. M., *Journal of Biological Chemistry* **1949**, *181* (1), 95-108.
82. Tutschka, P. J.; Beschoner, W. E.; Allison, A. C.; Burns, W. H.; Santos, G. W., *Nature* **1979**, *280* (5718), 148-151.
83. Estieu-Gionnet, K.; Guichard, G., *Expert Opinion on Drug Discovery* **6** (9), 937-963.
84. Aitken, S. G.; Abell, A. D., *Australian Journal of Chemistry* **2005**, *58* (1), 3-13.
85. Jean-Louis Hérisson, P.; Chauvin, Y., *Die Makromolekulare Chemie* **1971**, *141* (1), 161-176.
86. Trnka, T. M.; Grubbs, R. H., *Accounts of Chemical Research* **2000**, *34* (1), 18-29.
87. Nguyen, S. T.; Johnson, L. K.; Grubbs, R. H.; Ziller, J. W., *Journal of the American Chemical Society* **1992**, *114* (10), 3974-3975.
88. Grubbs, R. H.; Trnka, T. M., *Accounts of Chemical Research* **2001**, *34* (1), 18-29.

-
89. Scholl, M.; Ding, S.; Lee, C. W.; Grubbs, R. H., *Organic Letters* **1999**, *1* (6), 953-956.
90. Miller, S. J.; Blackwell, H. E.; Grubbs, R. H., *Journal of the American Chemical Society* **1996**, *118* (40), 9606-9614.
91. Kowalczyk, R.; Brimble, M. A.; Callon, K. E.; Watson, M.; Cornish, J., *Bioorganic & Medicinal Chemistry* **2012**, *20* (20), 6011-6018.
92. Henchey, L. K.; Porter, J. R.; Ghosh, I.; Arora, P. S., *ChemBioChem* **2010**, *11* (15), 2104-2107.
93. van Lierop, B.; Whelan, A.; Andrikopoulos, S.; Mulder, R.; Jackson, W. R.; Robinson, A., *International Journal of Peptide Research and Therapeutics* **2010**, *16* (3), 133-144.
94. Platt, R. J.; Han, T. S.; Green, B. R.; Smith, M. D.; Skalicky, J.; Gruszczynski, P.; White, H. S.; Olivera, B.; Bulaj, G.; Gajewiak, J., *Journal of Biological Chemistry* **2012**, *287* (24), 20727-20736.

CHAPTER TWO

SYNTHESIS OF MEDIUM SIZED RINGS COMPRISED OF β -AMINO ACIDS BY RING CLOSING METATHESIS

2 Synthesis of medium sized rings comprised of β -amino acids by ring closing metathesis

2.1 Peptidomimetics from β -amino acids

As outlined in **Chapter 1**, cyclic structures provide an important class of peptidomimetics that can overcome many problems associated with linear peptides, including poor bio-availability, low solubility and low stability towards hydrolysis. A number of cyclic scaffolds are known to constrain small molecules into a β -turn motif as defined in **Chapter 1**. The most common classes of constrained β -turn mimics are the Freidinger lactams, spiro-bi- and -tri- cyclic lactams, ring fused lactams including benzodiazepines and azabicycloalkanones and macrocycles comprised of di-, tri- and tetra- peptides.^{1,2} However alternative scaffolds, with a wider range of turn geometries and biophysical properties are needed to better mimic natural diversity.² Cyclic peptides comprised of β -amino acids are an emerging class of peptidomimetics that have not been studied extensively, yet have potential as β -turn mimics, as discussed later in this introduction. Peptides comprised of β -amino acids are an attractive alternative to those derived from α -amino acids in drug design due to their enhanced chemical stability and hence improved resistance to degradation by enzymes in the body.³ Examples of β -peptides are known to form secondary structures, for example; turns, helices and sheets. These structures mimic those found in nature's proteins, however β -peptides offer high stability while providing a scaffold for interaction with α -amino acids.⁴

Incorporation of an S β 2-S β 3 dipeptide fragment (or its mirror image dipeptide, R β 2-R β 3) into a peptide has been shown to induce a β -turn arrangement (**Figure 2.1 a**).^{5,6}

Macrocycles comprised of β -amino acids cyclised by ring closing metathesis⁷ and lactamisation^{3,7} have been prepared as constrained β -turn mimics (**Figure 2.1, b and c**), however the synthesis of medium sized rings comprised of β -amino acids (or α -amino acids for that matter) has not been extensively studied, presumably due to the inherent difficulty in making such rings.

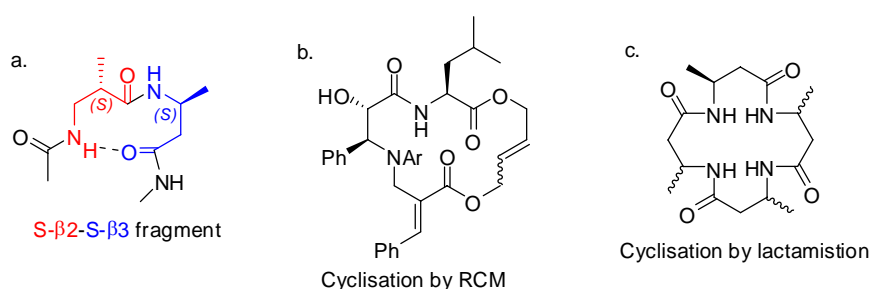


Figure 2.1. Examples of β -turn mimics comprised of β -amino acids

The major barriers to medium-sized ring formation are enthalpic, i.e.: ring strain (including angle strain, conformational strain and transannular strain) and entropic, i.e.: unwanted, competing side reactions such as dimer or polymer formation. The kinetics of ring closing reactions has been extensively studied.⁸⁻¹¹

The strain energies of the cyclo-alkanes from 3- to 23- membered rings are shown in **Figure 2.2**. The greatest strain energy exists for the smallest ring sizes (3- and 4-membered rings), with a second peak in strain energy corresponding to the 8- to 11-membered rings particularly the 10-membered ring.

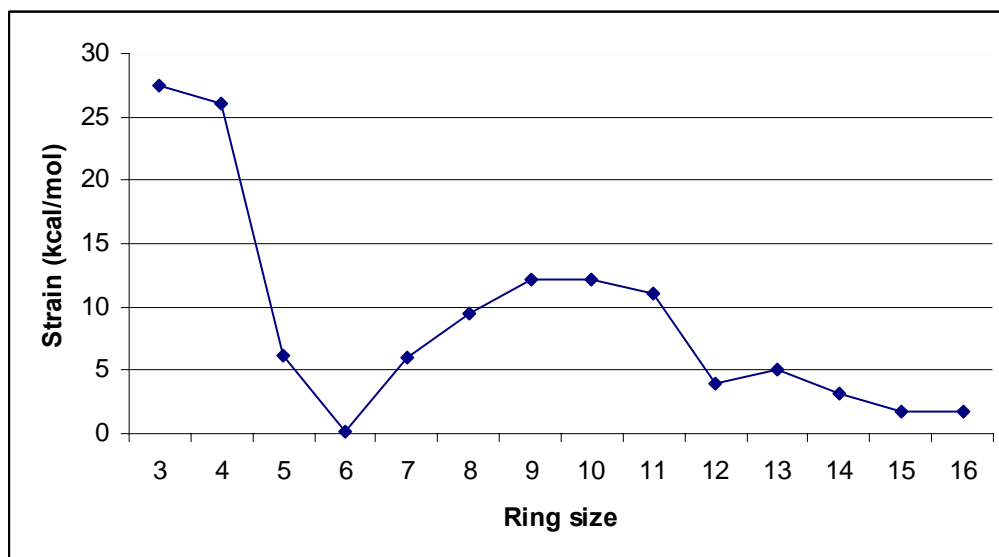


Figure 2.2. Strain energy of the cyclo-alkanes for ring sizes 3 – 16.⁸

This general trend in strain energy is apparent in the formation of cyclic lactones, where ring strain is high in the small (3-membered rings) and medium (8- to 10-membered) sized rings. Large macrocyclic lactones (>12-membered) are relatively strainless with the intra-molecular ring forming reaction having a ΔH approximately equal to the ΔH of the inter-molecular reaction.⁹ The cyclisation of medium sized rings is adversely affected by an increase in ring strain compared to larger macrocycles and also smaller (5- to 7- membered) rings.

With respect to entropic considerations, formation of small rings has the least negative entropy of activation.⁸ This is due to the close proximity of the two termini increasing the probability of ring formation and the relatively few degrees of freedom being restricted in the transition state. Medium and large sized ring formation is adversely affected by entropic factors, with ΔS sharply decreasing from 8-membered rings to 10-membered rings (**Figure 2.3**).^{10, 11} The effect of entropy begins to level off for ring sizes greater than 11, and the formation of large rings is less affected by entropy as the

macrocycles are less restricted in the transition state which is thought to compensate for the loss of degrees of freedom.

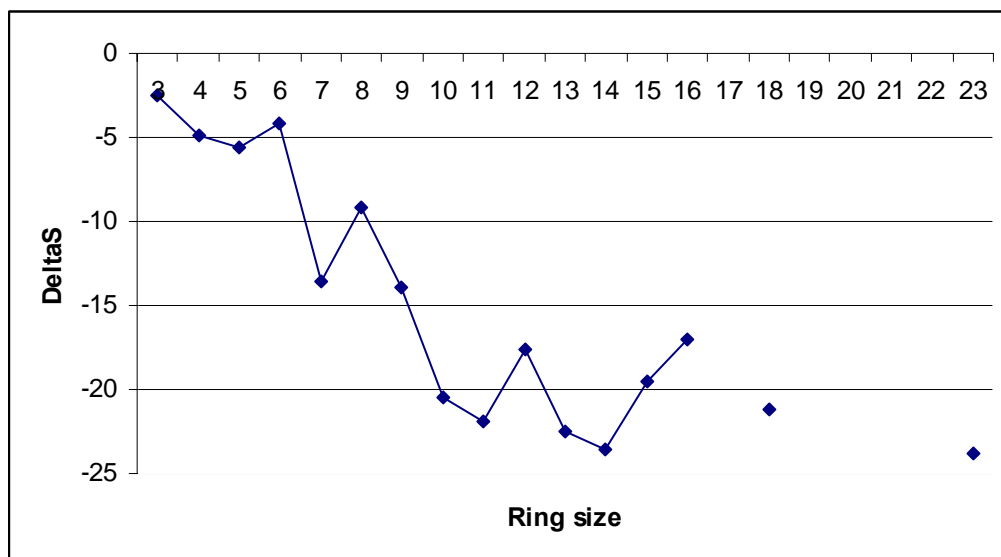


Figure 2.3. ΔS versus Ring size for lactone formation in 3-23 membered rings.^{10, 11}

Effective Molarity (EM) has been used extensively to quantitatively measure the ease of a ring closing reaction and takes both ΔH and ΔS into account (see **Equation 2.1**).⁸ The EM of a reaction gives the ratio of the intra-molecular (cyclisation) reaction versus the competing inter-molecular reaction. A low effective molarity indicates a more difficult intra-molecular reaction.

$$EM = \exp[-(\Delta H_{\text{intra}} - \Delta H_{\text{inter}})/RT] * \exp[\Delta S_{\text{intra}} - \Delta S_{\text{inter}}/R] \quad (2.1)$$

A plot of EM of lactone formation versus ring size as shown in **Figure 2.4** shows that medium sized rings have the least favourable (lowest) EM for cyclisation, with a minimum EM for the 8- and 9- membered rings.¹¹

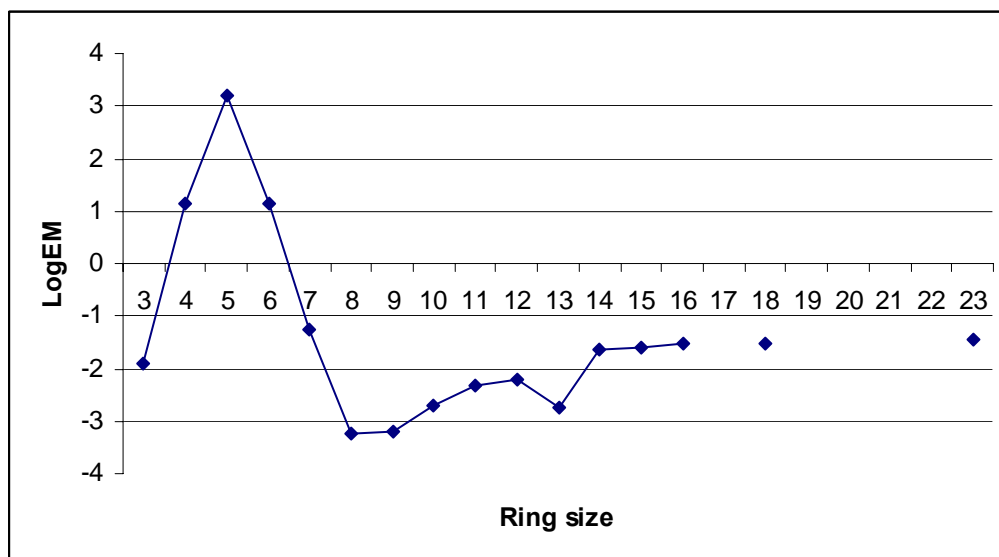


Figure 2.4. LogEM versus ring size for lactone formation.¹¹

The combination of unfavourable enthalpy and entropy associated with 8- to 11-membered ring formation means that these medium sized rings are the most difficult to synthesise. This presents a major challenge when trying to prepare compounds containing ring sizes in this region, particularly with regards to peptidomimetics as discussed in this chapter.

Metathesis has gained enormous popularity as a strategy for making small and large rings since the discovery of well defined molybdenum and ruthenium catalysts in the early 1990's.¹²⁻¹⁴ However, ring closing metathesis has only relatively recently been used to successfully prepare medium sized rings, for examples see **Figure 2.5**¹⁵⁻¹⁷ and **Figure 2.6**.¹⁸⁻²⁰

Metathesis mediated cyclisations of medium sized rings have been achieved by introducing a conformational constraint into the precursor diene, either by using a cyclic constraint such as **2.01**, **2.03** and **2.05** (**Figure 2.5**)¹⁵⁻¹⁷ or acyclic conformational constraint such as **2.09** shown in **Figure 2.6**.¹⁸⁻²⁰

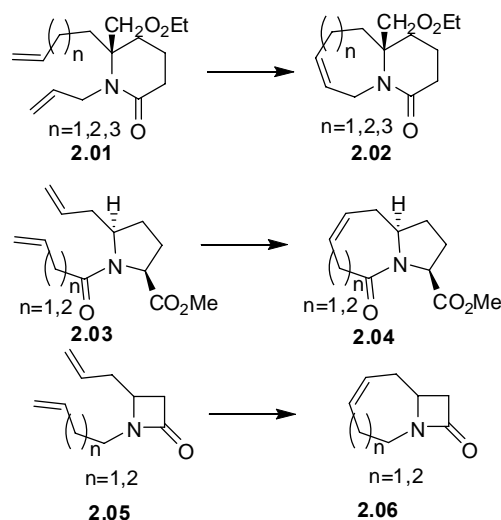


Figure 2.5. Examples of bi-cyclic lactams where ring closing metathesis is facilitated by cyclic constraint

As shown in **Figure 2.5**, the 7- to 9-membered bicyclic lactams **2.02**, **2.04** and **2.06** were prepared by cyclising dienes **2.01**, **2.03** and **2.05** respectively, where the component cycle constrains the geometry of the diene into that required for cyclisation.

An example of an acyclic constraint is to introduce an N-alkylate on an amide nitrogen with a 2,4-dimethoxy-benzyl (DMB) group. The DMB group stabilises the cis-amide conformation in the dipeptide shown in **Figure 2.6** to facilitate ring closing metathesis.¹⁸⁻²⁰ Diene **2.07** does not undergo ring closing metathesis on treatment with Grubbs' second generation catalyst, however diene **2.09**, where the DMB group favours a cis geometry about the central amide, is successfully cyclised to give **2.10**.

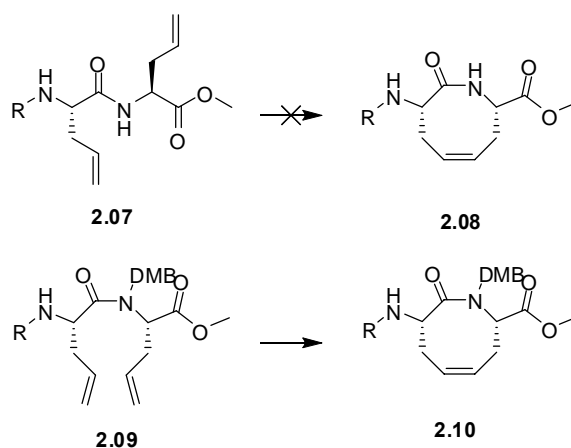


Figure 2.6. Top: ring closing metathesis is not possible with a trans-amide as the diene groups are too far apart for the intramolecular reaction. Bottom: the DMB group stabilises the cis geometry of the amide bond facilitating metathesis.

Much of the ring closing metathesis research reported on β -turn mimics has focused on making cyclic lactams from α -amino acids. For example see 8-membered ring **2.10** shown in **Figure 2.6**.^{2, 19-23} Work on the equivalent constraint of β -peptides has been much more limited. A literature review on small and medium sized cyclic peptides containing β -amino acids made by ring closing metathesis reveals five types of cyclisations have been reported as shown in **Figure 2.7**. These cyclisations give rise to the five scaffolds **2.11** – **2.15** depicted in **Figure 2.8**.

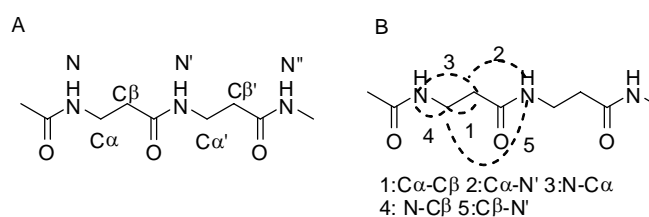


Figure 2.7. A: Atom labelling system used in this thesis. B: Cyclisations that have been reported in literature.

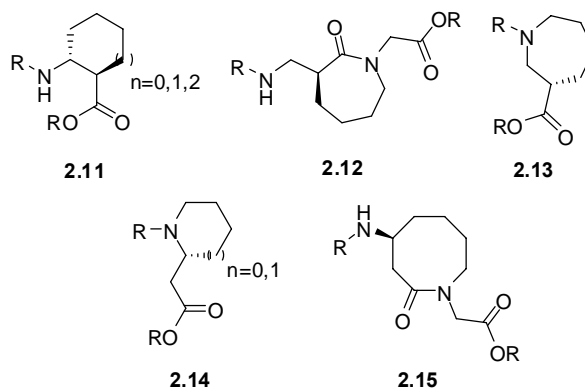


Figure 2.8. Existing β -peptide based scaffolds

Abell and co-workers²⁴ were the first to publish a ring closing metathesis-based synthesis of **2.17** (**Figure 2.9**) to give a cyclic β -peptide analogous to scaffold **2.11** in **Figure 2.8**. Formation of the six-membered ring, by connection of the C_{α} to C_{β} , was achieved by ring closing metathesis of diene **2.16** to give cycle **2.17**. This new metathesis based methodology allowed for substituents (either methyl or ethyl) at the C_{α} position and also functionalisation of the carbon-carbon double bond formed in the metathesis step.

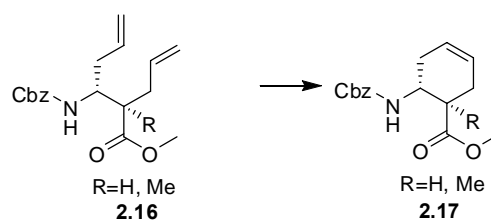


Figure 2.9. Cyclisation of C_{α} - C_{β} by RCM to give 6-membered ring **2.17**

Peptides derived from monomers containing a C_{α} to C_{β} cyclisation as in **2.17** (**Figure 2.9**) have been shown to adopt helices that resemble those comprised of α -amino acids.²⁴ The 6-membered monomer gives rise to a “12 helix” when incorporated into a peptide, while the 5-membered monomer gives rise to a “14 helix”.²⁵ The Abell group and others extended this work to the preparation of different ring sizes with the

synthesis of 5- to 7- membered rings,²⁶⁻²⁸ and the introduction of fluorine into the ring.²⁹

Subsequently, the Abell group³⁰ developed ring closing metathesis strategies to make scaffolds **2.12** and **2.13** (**Figure 2.8**). The connection of C α - to N' by ring closing metathesis is a convenient way to synthesis seven-membered lactams of the type **2.12**. Compounds containing this basic structure have been reported by Abell and co-workers as potential β -turn mimics.

Cyclisation from N to C α in a β -amino acid gives rise to compounds of type **2.13** (**Figure 2.8**).³⁰ Structures such as this have been shown by *in silico* modeling to adopt a β -turn geometry, with examples having been assayed against multiple biological targets such as GABA,³¹ calpain,³⁰ and aspartic protease.^{32, 33} Yamanaka and co-workers³⁴ used an enantio-selective allylation of **2.18** to give the diene **2.19** (**Figure 2.10**) which was then cyclised by ring closing metathesis to give the 7-membered cycle **2.20**.

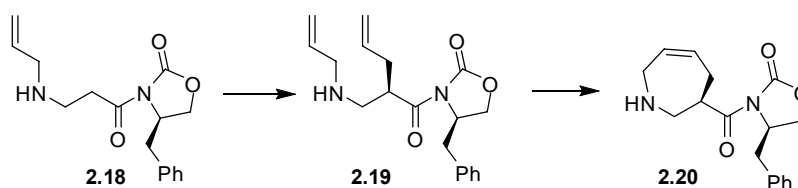


Figure 2.10. Cyclisation of N-C α by RCM to give cycle **2.20**.

The N to C β cyclisation of a β -amino acid gives homo-proline **2.14** (**Figure 2.8** where $n = 1$). Homo-proline is an important intermediate in the synthesis of biologically active

molecules, for example as a component of opioid receptor agonists and as GABA uptake inhibitors.^{35, 36} Davies and co-workers^{27, 37} reported the cyclisation of diene **2.21** by ring closing metathesis to give 6-membered ring **2.22** (Figure 2.11). This work was extended by Lesma and co-workers to include a 5-membered ring analogue and the introduction of a methyl or ketone group in the ring.³⁸

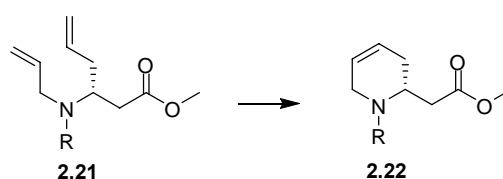


Figure 2.11. Cyclisation of N-C β by RCM to give 6-membered ring **2.22**.

Finally, cyclisation of **2.23** from C β to N' gives Homo-Freidinger lactam **2.24** (Figure 2.12). Freidinger lactams are examples of conformationally restrained peptidomimetics that are effective as inhibitors for a wide variety of proteases.³⁹ Hoffmann and co-workers have used ring closing metathesis to produce unsaturated Homo-Freidinger lactams, which are of interest due to the enhanced metabolic stability of β -amino acids over α -amino acids.⁴⁰

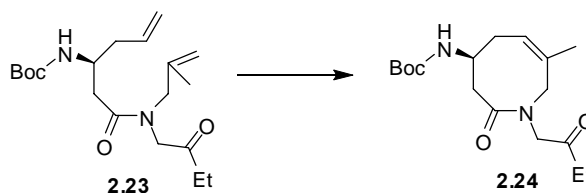


Figure 2.12. Cyclisation of C β -N' by RCM to give 8-membered ring **2.24**

The above review highlights that, while the backbone to backbone cyclisation of β -peptides have been reported, there has been very little work examining side chain to side chain cyclisations of β -peptides (with the exception of the C α -C β cyclisations

described above). Additionally, only one example of the preparation of a medium (8- to 12- membered) sized ring has been reported (see **2.15** in **Figure 2.8**). **Figure 2.13** shows cyclisations identified as being of importance to gain further knowledge into the synthesis of medium sized rings by ring closing metathesis and the potential of these compounds as β -turn mimics.

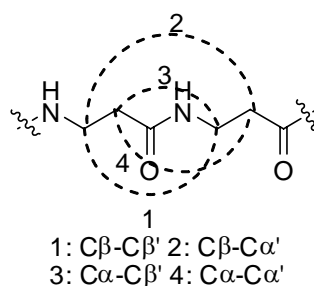


Figure 2.13: Cyclisations identified as important targets.

Work in this chapter aims to develop a methodology for the cyclisation of β -peptides depicted in **Figure 2.13** to give the six 8- 9- and 10- membered ring scaffolds **2.25** - **2.30** (**Figure 2.14**) by ring closing metathesis. The preparation of enantiomerically pure β 2 and β 3 amino acids containing an alkene group is described. These β -amino acids are coupled to give dipeptide dienes which can then be cyclised by ring closing metathesis followed by catalytic hydrogenation to give **2.25** - **2.30**.

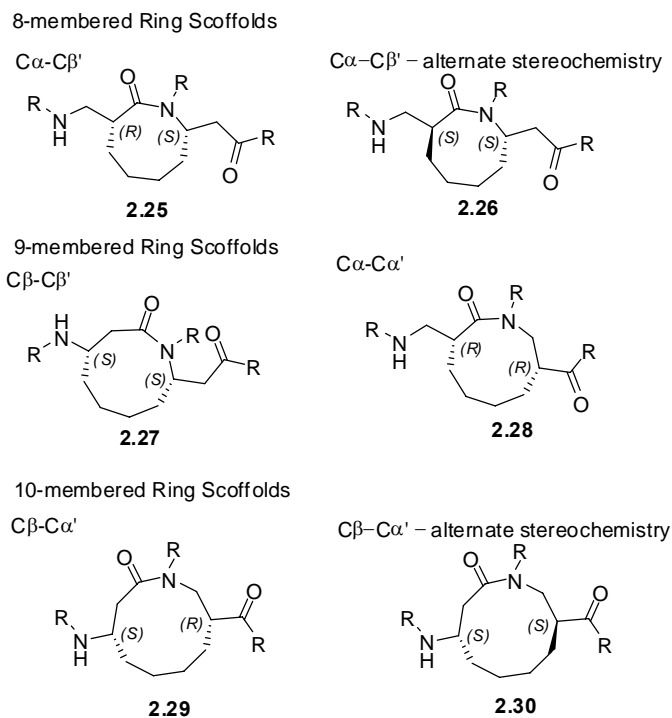


Figure 2.14. Six cyclic scaffolds selected as synthetic targets for this chapter

There is precedence that cyclic structures **2.26** and **2.30** may adopt a β -turn conformation based on these dipeptides having an $S\beta_2$ - $S\beta_3$ fragment as discussed above.^{5, 6} The remaining cyclic scaffolds (**2.25**, and **2.27** – **2.29**) were analysed by modelling (see later discussion) to assess their potential as β -turn mimics. The three cyclic scaffolds most likely to induce a β -turn in a peptide (identified by literature precedence or modeling results) were incorporated into a tri-peptide (**Figure 2.15**) which was assessed for its ability to adopt a β -turn conformation by ^1H NMR analysis. The conformation of tripeptides was assessed by ^1H NMR in CDCl_3 and $[\text{D}_6]\text{DMSO}$ to judge whether or not the required i carbonyl oxygen - $i+3$ amide proton hydrogen bond is present (shown in red, **Figure 2.15**).

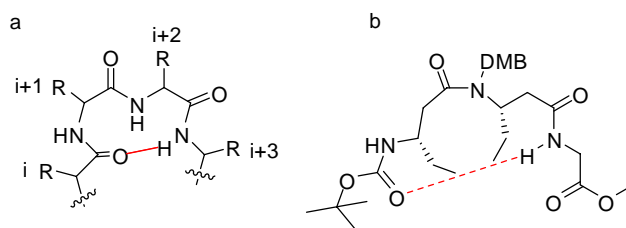


Figure 2.15. A. Structure of a tetrapeptide in a β -turn formation with the i C=O – $i+3$ NH hydrogen bond shown in red. B. Structure of tripeptide containing scaffold **2.27** with hydrogen bond shown in red.

2.2 Synthesis and analysis of cyclic scaffolds

2.2.1 Synthesis of building blocks 2.31 – 2.36

The synthesis of the six cycles, **2.25** – **2.30** identified in the introduction, required the preparation of six key precursor building blocks (see β -amino acids **2.31** – **2.36**, **Figure 2.16**).

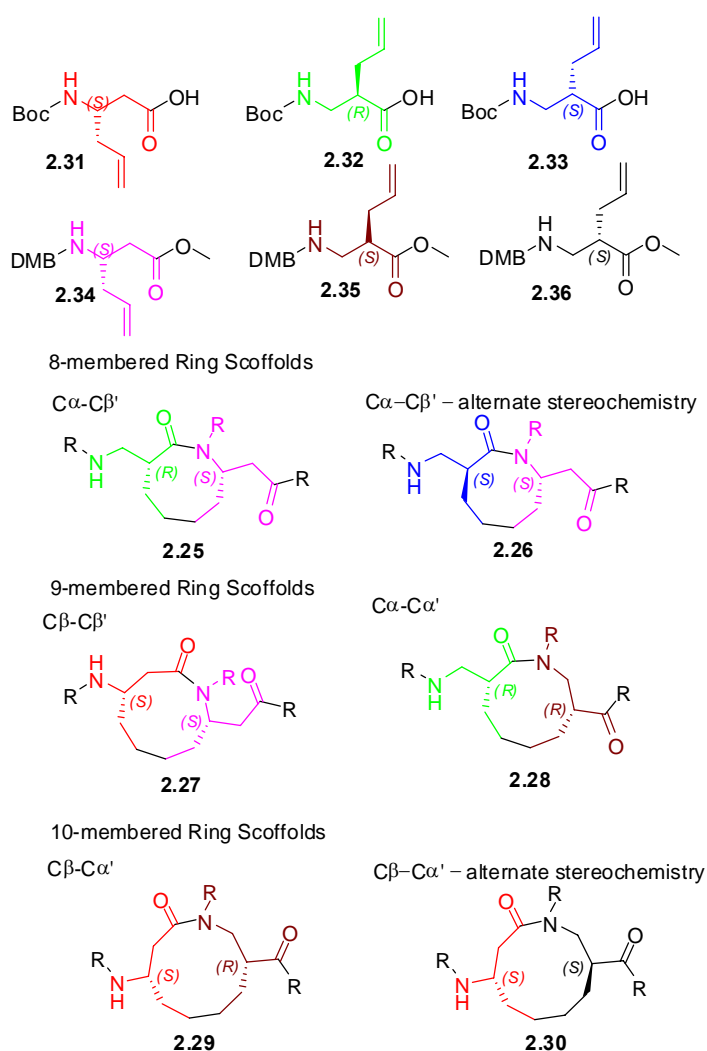
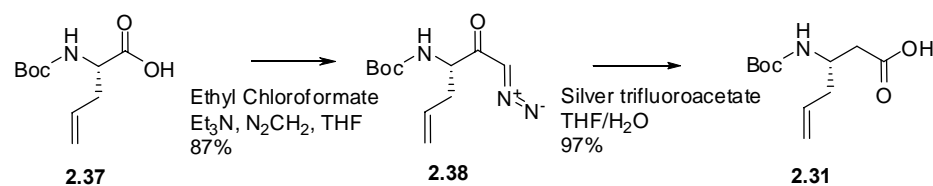


Figure 2.16. Building blocks **2.31** – **2.36** are required to make cycles **2.25** – **2.30**.

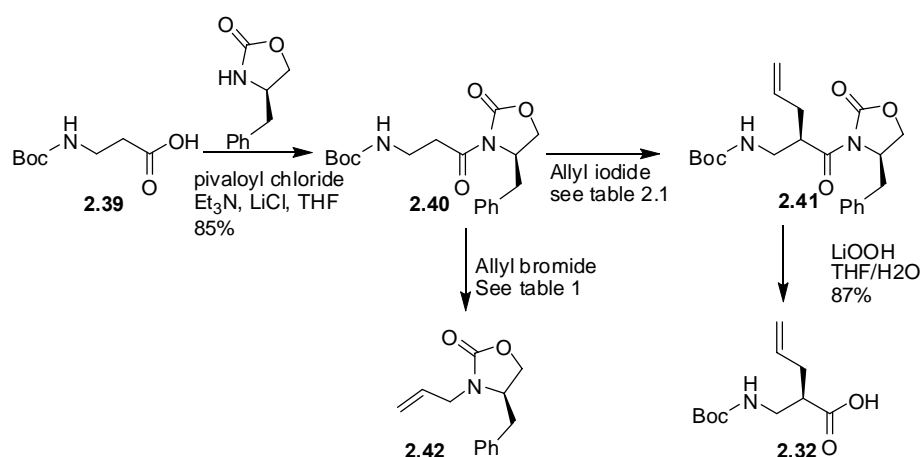
Arndt-Eistert homologation, followed by a Wolff rearrangement, was used to convert **2.37** to give key building block **2.31** as shown in **Scheme 2.1**. This proceeds by first

forming a mixed anhydride of the N-Boc amino acid **2.31** upon treatment with ethyl chloroformate. Treatment of the mixed anhydride with diazomethane gives the diazoketone **2.38** in 87%. Reaction of **2.38** with silver (I) trifluoroacetate in THF/water, in the absence of light, caused the diazoketone to undergo a Wolff rearrangement to give the required **2.31** in 97%.



Scheme 2.1. Synthesis of **2.31** by Arndt-Eistert homologation and Wolff rearrangement of **2.37**.

With **2.31** in hand, attention turned to the synthesis of the β 2 amino acid building blocks, enantiomers **2.32** and **2.33** (**Figure 2.16**). These were made using either the (*R*)-(-)-4-phenyl-2-oxazolidinone (for the *R* isomer **2.32**, see **Scheme 2.2**) or the (*S*)-(+)-4-phenyl-2-oxazolidinone (for the *S* isomer **2.33**, see **Scheme 2.3**) to direct the stereochemistry of the allylation reaction.



Scheme 2.2. Synthesis of β 2 amino acid **2.32**

(*R*)-(-)-4-Phenyl-2-oxazolidinone was coupled to **2.39** upon treatment with pivaloyl chloride, Et₃N and LiCl in THF at -30°C to give **2.40** in 85% yield.

An allyl halide was used as the electrophile, with the oxazolidinone auxiliary of **2.40** directing the stereochemistry of the reaction to give a high diastereoselectivity - the *R* isomer of the oxazolidinone gives the 'R' configuration at the C α position of **2.41** as shown in **Figure 2.17**. The level of diastereoselectivity was determined by ¹H NMR.

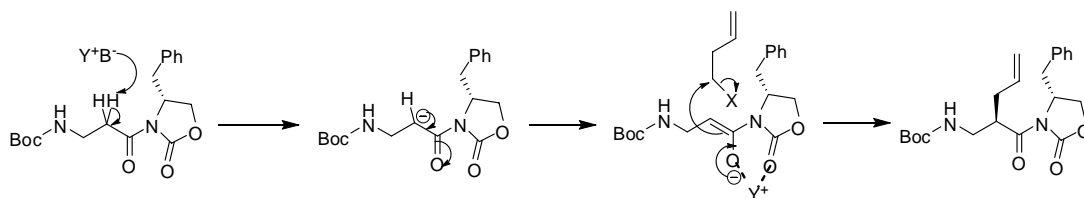


Figure 2.17. Mechanism of β_2 amino acid formation using the C-terminal oxazolidinone to direct stereochemistry.

The base and electrophile used were varied according to **Table 2.1** in order to optimize formation of **2.41**.

Entry	Base	Electrophile	Additives	Yield
1	LDA (3 eq)	Allyl-Br (4 eq)	LiCl (4 eq)	2.41 : 0%, 2.42 : 60%
2	LiHMDS (3eq)	Allyl-Br (1.5 eq)	LiCl (4 eq)	2.41 : 0%, 2.42 : 56%
3	LiHMDS (1.1 eq)	Allyl-Br (1.1 eq)	LiCl (2 eq)	2.41 : 0%, 2.42 : 30%
4	NaHMDS (1.5 eq)	Allyl-Br (1.5 eq)	-	2.41 : 0%, 2.42 : 47%
5	Et ₃ N (1.1)	Allyl-Br (1.05 eq)	TiCl ₄ (1.05 eq)	2.41 : 0%, 2.42 : 74%
6	NaHMDS (3)	Allyl-I (3 eq)	-	2.41 : 30%, 2.42 : 0%
7	NaHMDS (1.5)	Allyl-I (1.5 eq)	-	2.41 : 55%, 2.42 : 0%

Table 2.1 Reaction conditions for the addition of the allyl group to **2.40**.

Reaction of **2.40** with allyl bromide, in the presence of a base (either LDA, LiHMDS, NaHMDS or Et₃N/TiCl₄), gave the side product **2.42** as evidenced by ¹H NMR and mass spectrometry, presumably due to moisture in the allyl bromide (see **Scheme 2.2** and **Table 2.1** entries 1 – 5).

Reaction of **40** with freshly purchased allyl iodide, in the presence of NaHMDS in dry THF, gave **2.41** in a modest yield of 30% (see entry 6, **Table 2.1**). The optimum conditions for this reaction were found to be treatment of **2.40** with NaHMDS (1.5 eq) at -78°C, followed by addition of 1.5 eq allyl iodide, to give **2.41** in 55% yield. The product was assigned the (R,R)-isomer in >95% diastereomeric excess (d.e)¹ based on the absence of any doubling of resonances in the ¹H NMR spectrum (**Figure 2.18**). The oxazolidinone of **2.41** was hydrolysed on treatment with LiOOH in THF/H₂O to give **2.32** in 87% (**Scheme 2.2**). The acid **2.32** is presumed to form in >95% enantiomeric excess based on the diastereomeric excess of its precursor **2.41**.

¹ The >95% d.e is the upper limit of detection for the NMR machine

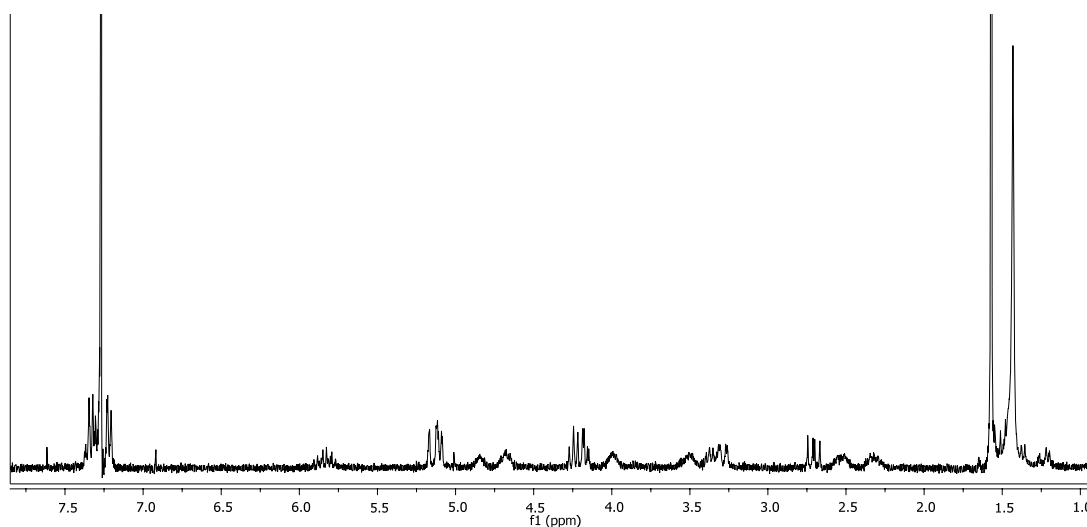
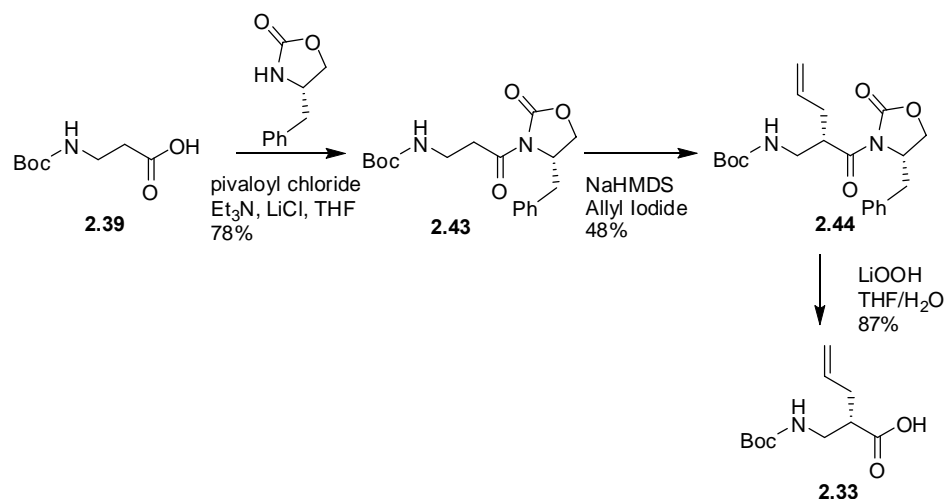


Figure 2.18. Proton NMR spectrum of **2.41**.

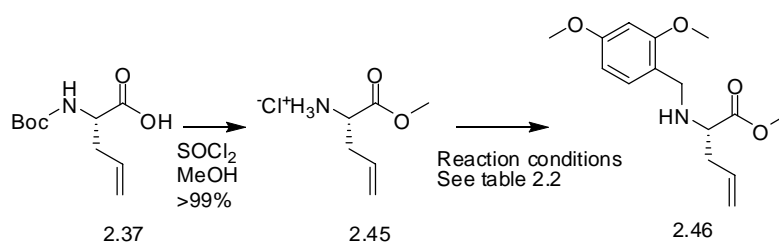
The optimum conditions thus developed to make **2.32** were applied to the synthesis of the enantiomer **2.33** (**Scheme 2.3**). In particular, acid **2.39** was coupled to the (*S*)-(+)-4-phenyl-2-oxazolidinone in the presence of pivaloyl chloride, Et₃N and LiCl in THF at -30°C. Purification of the resulting crude product, by flash chromatography on silica, gave **2.43** in 78% yield. Compound **2.43** was deprotonated with NaHMDS, at -78°C, and the resulting enolate reacted with allyl iodide to give **2.44** in 48% yield. Compound **2.44** is the enantiomer of **2.41**, and as such gave an identical ¹H NMR spectrum to that shown in **Figure 2.18**. There was no evidence of the formation of an epimer and as such **2.44** was judged >95% d.e. by proton NMR.



Scheme 2.3. Synthesis of **2.33**.

The oxazolidinone of **2.44** was cleaved on reaction with LiOOH in THF/H₂O to give **2.33** in 87% yield and >95% e.e. based on the d.e. of the precursor **2.44** (**Scheme 2.3**).

With the three key building blocks **2.31**, **2.32** and **2.33** in hand, attention turned to synthesizing the three methyl esters **2.34**, **2.35** and **2.36** (**Figure 2.16** and **Table 2.3**). The 2,4-dimethoxybenzyl (DMB) group was used as a conformational constraint to help promote ring closing metathesis.² As discussed in the introduction, the DMB group stabilises the geometry of the peptide bond of the resulting dipeptides in a cis conformation. Formation of the dipeptides is discussed in **Section 2.2.2**. The DMB group is introduced onto the nitrogen of an amino acid methyl ester by reductive amination with 2,4-dimethoxybenzaldehyde in the presence of Na(OAc)₃BH (**Scheme 2.4** and **Table 2.2**).



Scheme 2.4. Synthesis of N-DMB protected allyl-Gly-OMe (**2.46**).

Entry	Base	Aldehyde	Reducing agent	Solvent	2.46 yield
1	NaHCO ₃	2,4-DMB 1.1 eq	Na(OAc) ₃ BH 1.5 eq	DCM	22 %
2	NaHCO ₃	2,4-DMB 1.0 eq	Na(OAc) ₃ BH 1.5 eq	DCM	24 %
3	NaHCO ₃	2,4-DMB 0.9 eq	Na(OAc) ₃ BH 1.5 eq	DCM	35 %
4	NaOAc 4Å molecular sieves	2,4-DMB 0.9 eq	Na(OAc) ₃ BH 7.5 eq	MeOH	81 %

Table 2.2. Optimisation of reductive amination of **2.45** to give **46**.

Due to the limited availability of the key β -amino acids **2.31**, **2.32** and **2.33** (**Figure 2.16**), the reductive amination was first trialed on a model compound, i.e. commercially available Boc-allyl-glycine-OH (**2.37**) (**Scheme 2.4**). The Boc group was cleaved from **2.37** while simultaneously introducing the methyl ester at the C-terminus on treatment with SOCl₂/MeOH to give **2.45** in quantitative yield. The methyl ester **2.45** was reacted with excess NaHCO₃, followed by treatment with 1 equivalent of 2,4-dimethoxybenzaldehyde and 1.5 equivalents of Na(OAc)₃BH according to literature methodology,^{2, 19} to give **2.46** in 24% (**Scheme 2.4** and **Table 2.2**, entry 1). Increasing the amount of 2,4-dimethoxybenzaldehyde to 1.1 equivalents gave a slightly reduced yield of **2.46** (22% see **Table 2.2**, entry 2). However, a significant increase in yield (to 35%) was observed on reducing the equivalents of the 2,4-dimethoxybenzaldehyde to 0.9 with respect to **2.45** (**Table 2.2**, entry 3). The optimum conditions proved to be dissolving **2.45** and 0.9 equivalents of 2,4-dimethoxybenzaldehyde in super dry MeOH with the addition of NaOAc and 4Å molecular sieves. After 1 h the reducing agent Na(OAc)₃BH (7.5eq) was added to give **2.46** in 81%.⁴¹

Having developed an optimum procedure for the reductive amination of **2.45** with 2,4-dimethoxybenzaldehyde, these reaction conditions were applied to the synthesis of key building blocks **2.34**, **2.35** and **2.36** from precursors **2.31**, **2.32** and **2.33** (Table 2.3)

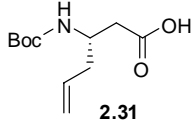
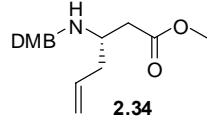
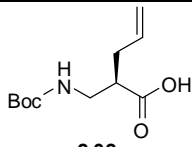
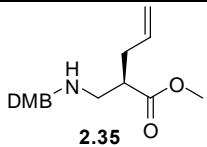
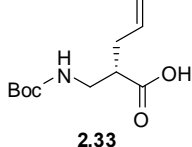
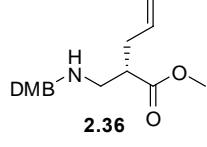
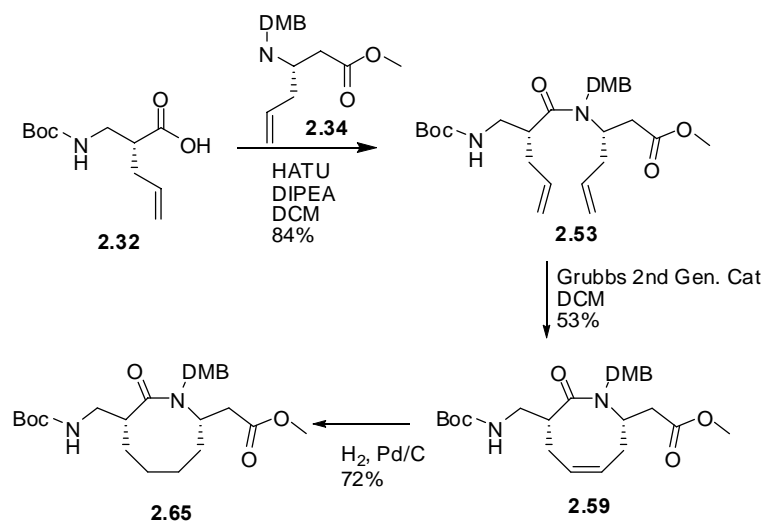
Acid	Reaction Conditions	Secondary amine
 <p>2.31</p>	1. SOCl ₂ , MeOH (2.47) 2. NaOAc, 4Å sieves 2,4-DMB Na(OAc) ₃ BH	 <p>2.34</p> <p>78%</p>
 <p>2.32</p>	1. SOCl ₂ , MeOH (2.48) 2. NaOAc, 4Å sieves 2,4-DMB Na(OAc) ₃ BH	 <p>2.35</p> <p>82%</p>
 <p>2.33</p>	1. SOCl ₂ , MeOH (2.49) 2. NaOAc, 4Å sieves 2,4-DMB Na(OAc) ₃ BH	 <p>2.36</p> <p>84%</p>

Table 2.3. Synthesis of **2.34**, **2.35**, **2.36** by reductive amination with 2,4-dimethoxybenzaldehyde

The β-amino acids **2.31** – **2.33** were treated with SOCl₂ in MeOH to give methyl esters **2.48** – **2.50** (each in quantitative yield). Each of these methyl esters was separately reacted with 2,4-dimethoxybenzaldehyde in the presence of NaOAc followed by addition of reducing agent Na(OAc)₃BH as defined for **2.45** to give **2.34**, **2.35** and **2.36** in 78%, 82% and 84% respectively.

2.2.2 Synthesis of cyclic scaffolds

Having synthesised the six precursor building blocks (**2.31** – **2.36**, **Figure 2.16**), the target cyclic peptidomimetics (**2.62** – **2.66**) were prepared by HATU mediated peptide coupling of the acids **2.31** – **2.33** to the methyl esters **2.34** – **2.36** to give dipeptide dienes **2.50** – **2.55** (see **Table 2.4**). These were then cyclised by ring closing metathesis, with the resulting alkene hydrogenated on treatment with H₂ and Pd/C to give the cyclised lactams **2.62** – **2.66**. **Scheme 2.5** depicts the synthesis and cyclisation of the dipeptide **2.53** to give cycle **2.59**, the alkene of which was hydrogenated on treatment with Pd/C to give **2.65**, as a representative synthesis.



Scheme 2.5. Synthesis and cyclisation of dipeptide **2.53** to give unsaturated cycle **2.59** followed by hydrogenation to give **2.65**.

N-Boc amino acid	DMB methyl ester	Diene	Unsaturated Cycle	Saturated Cycle
2.31	2.34	2.50 (84%)	2.56 (53%)	2.62 (72%)
2.31	2.35	2.51 (75%)	2.57 (59%)	2.63 (83%)
2.31	2.36	2.52 (72%)	2.58 (29%)	2.64 (79%)
2.32	2.34	2.53 (70%)	2.59 (49%)	2.65 (73%)
2.32	2.35	2.54 (74%)	2.60 (0%)	-
2.33	2.34	2.55 (65%)	2.61 (44%)	2.66 (82%)

Table 2.4. Peptide couplings and cyclisations of dienes **2.50** – **2.55** followed by hydrogenation to give 8-10 membered rings **2.62** – **2.66**.

The dipeptides **2.50** – **2.55** were similarly formed by HATU mediated peptide coupling of an acid (**2.31** – **2.33**) to a methyl ester (**2.34** – **2.36**) in DCM (see **Table 2.4**). This gave the desired dipeptides **2.50** - **2.55** in good yield (65%-87%) after purification by flash chromatography on silica gel.

In order to complete the synthesis of the cyclic scaffolds, the dienes **2.50** – **2.55** were cyclised by ring closing metathesis. Of the six cyclisations attempted, five were successful. The dienes **2.50** – **2.55** underwent ring closing metathesis to give 8- to 10-membered rings by treatment with Grubbs' second generation catalyst (5 mol %) in

refluxing DCM for one hour. The results of the cyclisations are summarised in **Table 2.4**. These conditions gave the unsaturated cyclic lactams **2.56** – **2.61** in 29% - 59% yield after purification by flash chromatography on silica. Cyclisation of diene **2.54** to give a 9-membered ring was repeatedly unsuccessful using both literature conditions and the modified conditions described above, with only small amounts of dimer (9%) and starting material (16%) being recovered. The literature method² for cyclisations of this type involves treatment of the diene with 20 mol% Grubbs second generation catalyst in refluxing DCM for 72 h. It was found that the cyclisations could be achieved equally well by reducing both the catalyst loading and the reaction time. This represents a significant 75% reduction in catalyst loading and a 98% reduction in reaction time.

The unsaturated cyclic lactams **2.56** – **2.61** were separately hydrogenated in the presence of Pd/C and H₂ to give the saturated cycles **2.62** – **2.66** in 72% - 83% yield (**Table 2.4** and **Scheme 2.5**).

2.2.3 Synthesis and NMR analysis of tripeptides containing cyclic scaffolds.

Having successfully synthesised five of the cyclic key targets **2.62** – **2.66** identified in the introduction (**Figure 2.14**), the next step was to explore the potential of these lactams to adopt a β -turn conformation.

Cycles **2.64** and **2.66** (**Figure 2.19**) have a S β 3-S β 2 fragment which is known^{5, 6} to induce β -turn as discussed in the introduction to this chapter. This makes **2.64** and **2.66** the optimum candidates to study and form a β -turn mimic, with the others providing useful references. However as 10-membered ring **2.64** was unable to be produced in

sufficient quantity (>50 mg required), this compound was excluded from the β -turn study at this time.

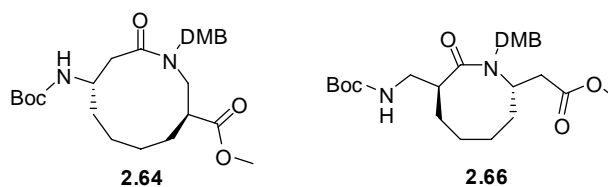


Figure 2.19. Cycles **2.64** and **2.66** with an a) S β 2-S β 3 or b) S β 3-S β 2 peptide arrangement

In order to evaluate the β -turn inducing potential of the three remaining cycles **2.62**, **2.63** and **2.65** (top, **Figure 2.20**), conformational searches were conducted by Dr Stephen McNabb⁴² on penta-peptides (bottom, **Figure 2.20**) containing each of the three cyclic scaffolds. The penta-peptides were used in the study to determine if the key hydrogen bond between the *i* and *i*+4 residues is formed.

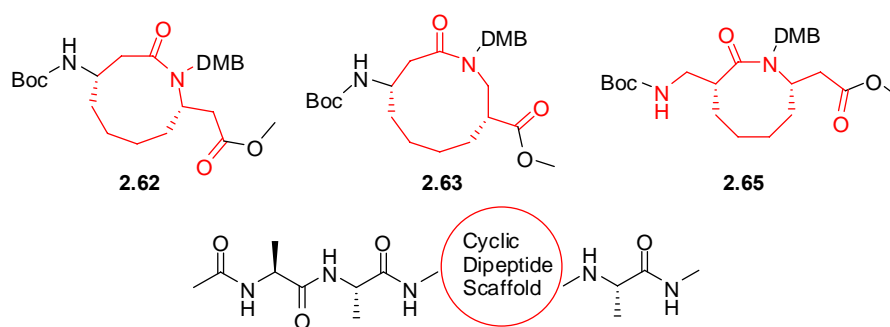


Figure 2.20. Top: cyclic scaffolds that were analysed in the conformational search. Bottom: Penta-peptide structure incorporating cyclic scaffold.

The ability of scaffolds **2.62**, **2.63** and **2.65** to induce a β -turn in the peptides was evaluated using MacroModel 9.1 to generate an ensemble of low energy conformers. The potential energy of the conformers was calculated by summing bond stretching, bending, torsional, and the non-bonded energies (e.g. van der Waals energy and hydrogen bonds). The searches were conducted with the MCMC method using a

GB/SA water model and the OPLS2005 force field, with 3000 steps for the conformational search and up to 5000 iterations for the minimisation of each generated structure. The minimisation was stopped with the default gradient convergence threshold of $d = 0.05 \text{ kJ}/(\text{mol}\cdot\text{\AA})$. The default Polak-Ribiere Conjugate Gradient method was used for all minimisations. The Boltzmann weighted percentage of conformers within the 12kcal per mole window of the global minimum that exhibited turn like structure was calculated.

The β -turn mimicry of each of the penta-peptides was evaluated using the following criteria as depicted in **Figure 2.21**:⁴³

1. A penta-peptide was judged as being turn-like if the inter-atomic distance of the $\alpha C_i - \alpha C_{i+3}$ carbons was less than 7\AA and;
2. The pseudo dihedral angle (P) defined by C1, C α 2, C α 3 and N4 of the penta-peptide model should lie between the specified limits defined in **Table 2.5**

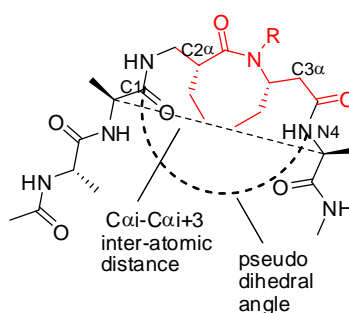


Figure 2.21. Scaffold **2.65** modelled as part of a penta-peptide showing the criteria for judging a β -turn – the $C_{\alpha i} - C_{\alpha i+3}$ inter atomic distance and the pseudo dihedral angle.⁴³

Type of β -turn	Pseudo dihedral angle
I	$10 < P < 80$

I'	-79<P<-10
	20<P<40
II	-69<P<-60
	-49<P<-40
	-29<P<40
II'	-59<P<-50
	-29<P<30

Table 2.5. Pseudo dihedral angle (P) defines the classes of β -turn.⁴³

The inter-atomic distances and pseudo-dihedral angle calculated from the lowest energy conformers identified from the conformational searches on the penta-peptides containing scaffolds **2.62**, **2.63** and **2.65** are given in **Table 2.6**.

Scaffold	Ave. $C_{ai}-C_{ai+3}$ Distance	Ave. pseudo-dihedral angle (P)
2.62	6.97	31.69
2.63	11.78	n/a
2.65	6.16	0.42

Table 2.6. Results of conformational search on scaffolds **2.62**, **2.63** and **2.65** predicting β -turn like properties

Two of the cycles (**2.62** and **2.65**) meet the criteria outlined above for inducing a turn like structure in a peptide. The lowest energy conformers of both **2.62** and **2.65** have $C_{ai} - C_{ai+3}$ inter-atomic distances of 6.97Å and 6.16Å respectively. However, the lowest energy conformer of **2.63** does not appear to induce a β -turn when incorporated into a peptide as evidenced by a $C_{ai} - C_{ai+3}$ inter-atomic distance of 11.78Å. The pseudo dihedral angles predicted by the conformational search suggest⁴³ that cycle **2.62**, with an angle of 31.60°, will induce a Type I' or Type II β -turn in a peptide. Cycle **2.65**, where a dihedral angle of 0.42°, is predicted⁴³ to induce either a Type II or Type

II' β -turn when incorporated into a peptide. **Figure 2.22** depicts the low energy conformers of cycles **2.62** and **2.65**.

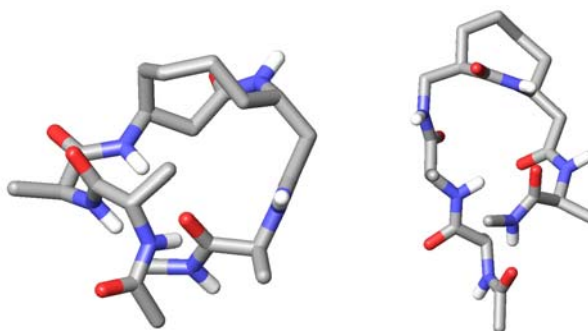
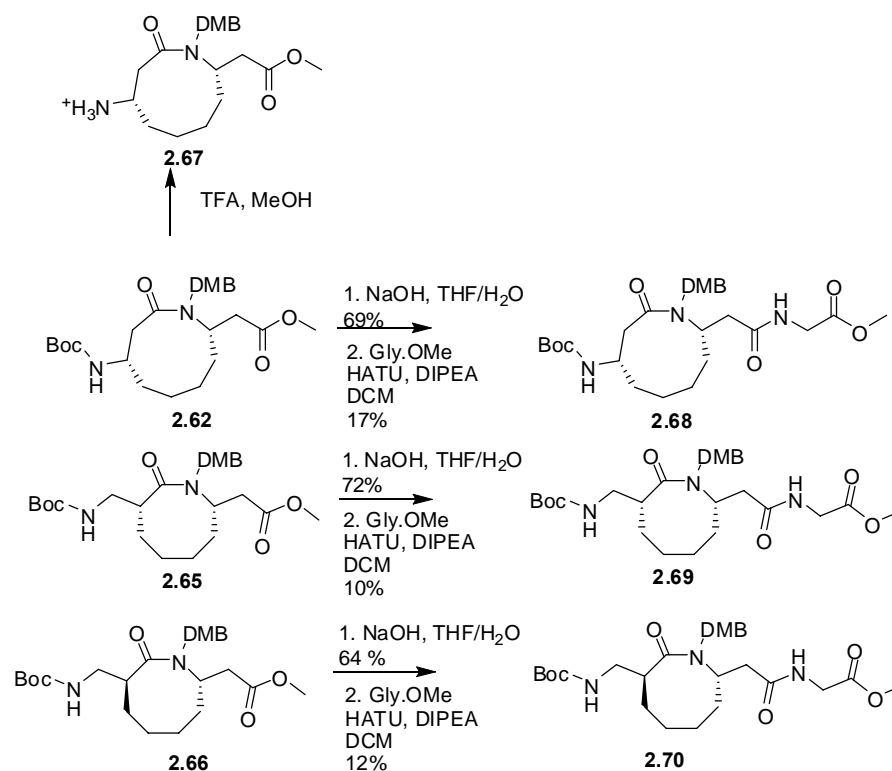


Figure 2.22. Best representative poses of: left hand side) **2.62** and right hand side) **2.65**.

Compounds **2.62**, **2.65** and **2.66** were chosen to be assessed further for their ability to form a β -turn on the basis of cycle **2.66** having the optimum arrangement of β -amino acids to form a β -turn (the S β 2-S β 3 arrangement) and the conformation of the low energy conformers of cycles **2.62** and **2.65**. The conformation of these three cycles was defined by ^1H NMR spectroscopy by determining the presence or otherwise of a hydrogen bond between the carbonyl oxygen of the C_i residue and the NH proton of the C_{i+3} residue. This hydrogen bond is indicative of a β -turn structure.⁴⁴ In order to determine if any of these scaffolds was able to induce a β -turn in a peptide, each of the cycles was incorporated into a tripeptide by coupling of Gly-OMe to the C-terminus of the dipeptide (see **Scheme 2.6**). Glycine was chosen since the lack of substituent at the C_α position simplifies analysis of the ^1H spectra. It was anticipated that if the cyclic scaffold induced a β -turn in these tripeptides, a hydrogen bond would be observed between the carbonyl oxygen of the N-terminal Boc group and the NH of the $i+3$ Gly residue.⁴⁴



Scheme 2.6. Synthesis of tripeptides **2.68**, **2.69** and **2.70** for NMR study.

Attempted removal of the DMB group from **2.62** on treatment with TFA was however unsuccessful, resulting in the Boc deprotected **2.67** with DMB intact. This is consistent with literature attempts to remove the DMB group in the presence of N-protecting Boc. We reasoned, by examining 3-D models of the tripeptides, that the DMB group is oriented perpendicular to the site of the hydrogen bond between the C_i and C_{i+3} residues (see **Figure 2.23**) and thus should not interfere with either the ability of the compounds to adopt a β -turn conformation or our ability to evidence this conformation in the ¹H NMR spectra of the cycles. Based on this observation it was decided to complete the synthesis with the DMB group intact.

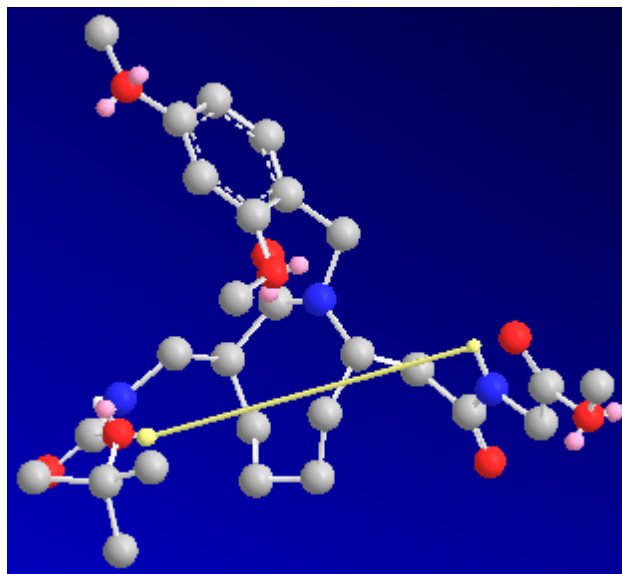


Figure 2.23. CS Chem3D representation of tri-peptide of tripeptide **2.70**. The DMB group is oriented at a 90° angle to the site of the intra-molecular hydrogen bond (shown in yellow).

After hydrolysis of each of the methyl ester of dipeptides **2.62**, **2.65** and **2.66** with NaOH, glycine-methyl ester was separately coupled to the C-terminus of the cycles in the presence of HATU to give the tripeptides **2.68**, **2.69** and **2.70** (Scheme 2.6), which were purified in 17% 10% and 12% yield respectively by reverse phase HPLC .

The presence or otherwise of an intra-molecular hydrogen bond in tripeptides **2.68** – **2.70** was then assessed by measuring the ^1H NMR spectra for **2.68** – **2.70** in CDCl_3 and $[\text{D}_6]\text{DMSO}$ to evaluate the effect switching from a non-hydrogen bonding solvent (CDCl_3) to a hydrogen bonding solvent ($[\text{D}_6]\text{DMSO}$) has on the chemical shift of the $\text{NH}(\text{Gly})$ proton. It is known that the chemical shift of a proton involved in an intra-molecular hydrogen bonds is much less influenced by type of solvent than a proton involved in an inter-molecular hydrogen bond to the solvent. Thus the presence of an intra-molecular hydrogen bond to a proton can be confirmed by a small up-field change in chemical shift of that proton when the ^1H NMR spectra in CDCl_3 and $[\text{D}_6]\text{DMSO}$ are compared.⁴⁴ A proton that is not involved in an intra-molecular hydrogen bond will

be observed to have a large downfield shift in a ^1H NMR spectra in $[\text{D}_6]\text{DMSO}$ compared to a ^1H NMR spectra in CDCl_3 (see **Figure 2.24** and **Table 2.7**).

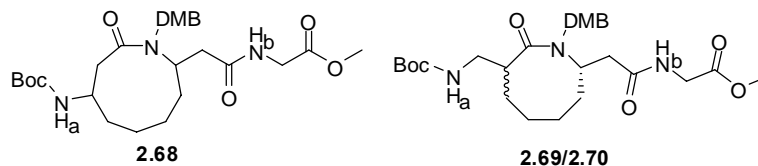


Figure 2.24. Proton labelling used in the NMR interpretation.

Compound	Proton	δ CDCl_3	δ $[\text{D}_6]\text{DMSO}$	$\Delta\delta$ CDCl_3 > $[\text{D}_6]\text{DMSO}$
2.68	Ha	5.649	7.796	2.147
	Hb	5.059	8.114	3.055
2.69	Ha	5.410	6.529	1.119
	Hb	5.338	8.225	2.887
2.70	Ha	5.189	8.274	3.085
	Hb	4.991	4.750	-0.241

Table 2.7. Solvent effect on NH protons Ha and H_b for tripeptides **2.68** – **2.70**.

^1H NMR spectra of the tripeptides **2.68** – **2.70** were run in CDCl_3 and $[\text{D}_6]\text{DMSO}$. Both the key protons Ha and H_b, as defined in **Figure 2.24** for compounds **2.68** and **2.69**, were downfield in the spectrum run in $[\text{D}_6]\text{DMSO}$ compared to the spectrum run in CDCl_3 (**Table 2.7**). This downfield shift indicates that these protons hydrogen bond to $[\text{D}_6]\text{DMSO}$ and as a consequence there is no intra-molecular hydrogen bond to these protons.⁴⁴ These results suggest compounds **2.68** and **2.69** do not have the $i - i+3$ hydrogen bond indicative of a β -turn.

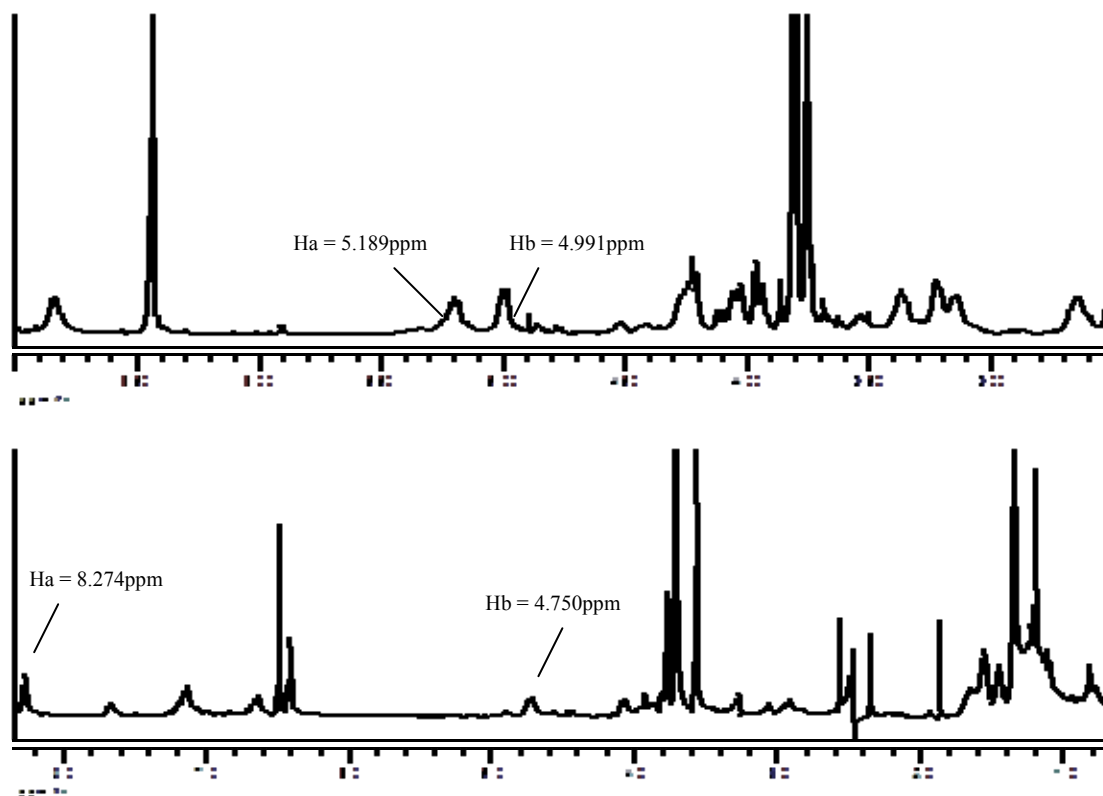


Figure 2.25. Proton NMR spectra of **2.70** in CDCl_3 (top) and $[\text{D}_6]\text{DMSO}$ (bottom).

In contrast, in the ^1H NMR spectra of **2.70** in CDCl_3 and $[\text{D}_6]\text{DMSO}$ (see **Figure 2.25**), Ha is observed to have a downfield shift (3.085 ppm) in $[\text{D}_6]\text{DMSO}$ while Hb is only weakly affected (-0.241 ppm) by the change from non-hydrogen bonding CDCl_3 to strongly hydrogen bonding $[\text{D}_6]\text{DMSO}$. This is consistent with proton Hb being involved in an intra-molecular hydrogen bond which shields the proton from solvent effects.

Given the observance of a potential intra-molecular H-bond to Hb in **2.70**, the ability of **2.70** to form a β -turn was further investigated by measuring the effect of a change in temperature on the observed hydrogen bond. Temperature coefficients between 0 and -4 ppb/K indicate the proton is solvent-shielded by an intra-molecular bond, while temperature coefficients less than -4 ppb/K indicate an unstructured peptide.⁴⁵ ^1H NMR spectra of **2.70** were recorded in $[\text{D}_6]\text{DMSO}$ over the temperature range 295K to 343K

in increments of 5K . The temperature coefficient for Ha and Hb (**Figure 2.24**) of **2.70** was then calculated by measuring the change in temperature / change in ppm. Ha of **2.70** had a temperature coefficient of -5.1 ppb/K which indicates, as expected, that it is not involved in an intra-molecular hydrogen bond. However, the Gly-NH resonance (Hb of **2.70**) had a reduced temperature coefficient of -0.65 ppb/K which further provides strong evidence that this proton is deshielded from the solvent by an intra-molecular hydrogen bond, presumably to the carbonyl oxygen of the N-terminal Boc. These two NMR experiments provide evidence that tripeptide **2.70** has a hydrogen bond from the *i* carbonyl oxygen to the *i*+3 NH and is in a β -turn conformation.

2.3 Conclusions

The work presented in this chapter describes the synthesis of five new cyclic dipeptide scaffolds comprised of β -amino acids, compounds **2.62** – **2.66**. Ring closing metathesis of a diene, using DMB to stabilise the cis-geometry about the central peptide bond, was found to be an effective strategy to overcome the inherent difficulties in synthesizing medium sized rings of this type. This work establishes a methodology for the synthesis of traditionally challenging targets (medium sized rings) by ring closing metathesis where the catalyst loading is reduced by 75% and the reaction time is reduced by 98% compared with literature procedures. This optimisation of the ring closing metathesis step significantly lowers the cost to produce compounds of this type and makes this synthetic approach more suitable should large scale synthesis of the compounds described herein be required.

Of the five cyclic dipeptides prepared by ring closing metathesis, two (**2.62** and **2.65**) were chosen as potential β -turn mimics based on results from a conformational search.¹¹ Cycle **2.66** has a S β 2S β 3 arrangement of amino acids which is known to induce a β -turn.^{5, 6} Of these, cycle **2.66**, when incorporated into peptide **2.70**, provides strong ¹H NMR evidence from solvent effect and temperature effect experiments that there is an intra-molecular hydrogen bond in the peptide between the nitrogen proton of the glycine and the carbonyl oxygen of the Boc group. This indicates **2.66** induces a β -turn conformation in peptide **2.70**.

As predicted by observation of a 3-D model (**Figure 2.23**), the DMB group on the central amide does not disrupt the ability of peptide **2.70** to form a β -turn. This observation is important as DMB is a large bulky group that provides potential to introduce a wide range of other substituents at this position of the peptide without disrupting the formation of a β -turn. Furthermore, the alkene resulting from ring closing metathesis can be functionalised, for example by dihydroxylation or epoxidation. Aspects of such functionalisation are discussed in **Chapter 3**. With this added potential, scaffold **2.66** provides a basic β -turn scaffold with conceivable opportunity to be optimized for binding to a specific receptor. While it is known that an S β 2-S β 3 fragment will induce a β -turn, scaffold **2.66** is pre-organised in this conformation. Preorganisation of a molecule into the required geometry for binding to a biological target limits the flexibility of the molecule and thus reduces the unfavorable loss of entropy when binding to a target enzyme or receptor.⁴⁶ Cycle **2.66** is predicted to have better drug-like properties conferred by the ring, for example, additional stability to degradation and higher bioavailability than an acyclic peptide.⁴⁷⁻⁴⁹ Based on these results, there is potential that scaffold **2.64** could also have a β -turn conformation (this

¹¹ Dr Stephen Mc Nabb performed all conformational searches described herein.

peptide has an S β 3-S β 2 arrangement). As discussed in the introduction to this chapter, there is a need for a wider range of turn geometries to mimic natural diversity. Larger scale synthesis and conformational analysis of peptide **2.64** would be an interesting comparison to **2.66** and this has been highlighted as important future work.

2.4 References

1. Che, Y.; Marshall, G. R., *Expert Opinion on Therapeutic Targets* **2008**, *12* (1), 101-114.
2. Kaul, R.; Surprenant, S.; Lubell, W., *Journal of Organic Chemistry* **2005**, *70* (10), 3838-3844.
3. Seebach, D.; Matthews, J. L., *Chemical Communications* **1997**, 2015-2022.
4. Humuro, Y.; Schneider, J. P.; DeGrado, W. F., *Journal of the American Chemical Society* **1999**, *121* (51), 12200-12201.
5. Daura, X.; Gademann, K.; Schafer, H.; Jaun, B.; Seebach, D.; van Gunsteren, W. F., *Journal of the American Chemical Society* **2001**, *123* (10), 2393-2404.
6. Lelais, G.; Seebach, D.; Jaun, B.; Mathad, R. I.; Flögel, O.; Rossi, F.; Campo, M.; Wortmann, A., *Helvetica Chimica Acta* **2006**, *89* (3), 361-403.
7. Rajesh, S.; Banerji, B.; Iqbal, J., *Journal of Organic Chemistry* **2002**, *67* (22), 7852-7857.
8. Galli, C.; Mandolini, L., *European Journal of Organic Chemistry* **2000**, *2000* (18), 3117-3125.
9. Illuminati, G.; Mandolini, L., *Accounts of Chemical Research* **1981**, *14* (4), 95-102.
10. Mandolini, L., *Journal of the American Chemical Society* **1978**, *100* (2), 550-554.

11. Galli, C.; Illuminati, G.; Mandolini, L.; Tamborra, P., *Journal of the American Chemical Society* **1977**, *99* (8), 2591-2597.
12. Schrock, R. R., *Accounts of Chemical Research* **1990**, *23* (5), 158-165.
13. Dias, E. L.; Nguyen, S. T.; Grubbs, R. H., *Journal of the American Chemical Society* **1997**, *119* (17), 3887-3897.
14. Novak, B. M.; Grubbs, R. H., *Journal of the American Chemical Society* **1988**, *110* (3), 960-961.
15. Diedrichs, N.; Westermann, B., *Synlett* **1999**, 1127-1129.
16. Grossmith, C. E.; Senia, F.; Peterson, S. L., *Synlett* **1999**, 1660-1662.
17. Tarling, C.; Holmes, A.; Markwell, R.; Pearson, N., *Journal of the Chemical Society, Perkin Transactions I* **1999**, (12), 1695-1702.
18. Derrer, S.; Davies, J. E.; Holmes, A. B., *Journal of the Chemical Society, Perkin Transactions I* **2000**, (17), 2943-2956.
19. Creighton, C.; Leo, G.; Du, T.; Reitz, A., *Bioorganic and Medicinal Chemistry* **2004**, *12*, 4375-4385.
20. Creighton, C. J.; Reitz, A. B., *Organic Letters* **2001**, *3* (6), 893-895.
21. Grubbs, R. H.; Miller, S. J., *Journal of the American Chemical Society* **1995**, *117* (21), 5855-5856.
22. Reichwein, J. F.; Liskamp, R. M. J., *European Journal of Organic Chemistry* **2000**, 2335-2344.
23. Abell, A. D.; Brown, K.; Coxon, J. M.; Jones, M. A.; Miyamoto, S.; Neffe, A. T.; Nikkel, J. M.; Stuart, B. G., *Peptides* **2005**, *26*, 251-258.
24. Abell, A. D.; Gardiner, J., *Organic Letters* **2002**, *4* (21), 3663-3666.
25. Barchi, J. J.; Huan, X.; Appella, D.; Christianson, L.; Durell, S.; Gellman, S., *Journal of the American Chemical Society* **2000**, *122*, 2711-2718.

-
26. Perlmutter, P.; Rose, M.; Vounatsos, F., *European Journal of Organic Chemistry* **2003**, 756-760.
 27. Chippindale, A. M.; Davies, S. G.; Iwamoto, K.; Parkin, R. M.; Smethurst, C. A. P.; Smith, A. D.; Rodriguez-Solla, H., *Tetrahedron* **2003**, *59*, 3263-3265.
 28. Gardiner, J.; Andersson, K.; Downard, A.; Abell, A. D., *Journal of Organic Chemistry* **2004**, *69*, 3375-3382.
 29. Fustero, S.; Bartolome, A.; Sanz-Cervera, J. F.; Sanchez-Rosello, M.; Soler, J. G.; deArellano, C.; Fuentes, A. S., *Organic Letters* **2003**, *5* (14), 2523-2526.
 30. Gardiner, J.; Aitken, S. G.; McNabb, S. B.; Zaman, S.; Abell, A. D., *Journal of Organometallic Chemistry* **2006**, *691* (24-25), 5487-5496.
 31. Ramachandran, P. V.; Burghardt, T. E.; Bland-Berry, L., *Journal of Organic Chemistry* **2005**, *70* (20), 7911-7918.
 32. Brass, S.; Chan, N.-S.; Gerlach, C.; Luksch, T.; Bottcher, J.; Diederich, W., *Journal of Organometallic Chemistry* **2006**, *691*, 5406-5422.
 33. Brass, S.; Gerber, H.-D.; Dorr, S.; Diederich, W., *Tetrahedron* **2006**, *62*, 1777-1786.
 34. Yamanaka, T.; Ohkubo, M.; Kato, M.; Kawamura, Y.; Nishi, A., *Synlett* **2005**, (4), 631-634.
 35. Cardillo, G.; Gentilucci, L.; Qasem, A. R.; Sgarzi, F.; Spampinato, S., *Journal of Medicinal Chemistry* **2002**, *45*, 2571-2578.
 36. Fulep, G. H.; Hoesl, C. E.; Hofner, G.; Wanner, K. T., *European Journal of Medicinal Chemistry* **2006**, *41*, 809-824.
 37. Davies, S. G.; Iwamoto, K.; Smethurst, C. A. P.; Smith, A. D.; Rodriguez-Solla, H., *Synlett* **2002**, (7), 1146-1148.

-
38. Lesma, G.; Danieli, B.; Sacchetti, A.; Silvani, A., *Journal of Organic Chemistry* **2006**, *71*, 3317-3320.
 39. Wolfe, M. S.; Dutta, D.; Aube, J., *Journal of Organic Chemistry* **1997**, *62*, 654-663.
 40. Hoffmann, T.; Gmeiner, P., *Synlett* **2002**, (6), 1014.
 41. Walker, S., Reductive amination. Unpublished work. Postdoctoral Fellow. Monash University: Melbourne, 2008.
 42. McNabb, S. B., Unpublished work. Post Doctoral Fellow. University of Canterbury. 2009.
 43. Ball, J. B.; Hughes, R. A.; Alewood, P. F.; Andrews, P. R., *Tetrahedron* **1993**, *49* (17), 3467-3478.
 44. Van Rompaey, K.; Ballet, S.; Tömböly, C.; De Wachter, R.; Vanommeslaeghe, K.; Biesemans, M.; Willem, R.; Tourwé, D., *European Journal of Organic Chemistry* **2006**, (13), 2899-2911.
 45. Halab, L.; Lubell, W. D., *The Journal of Organic Chemistry* **1999**, *64* (9), 3312-3321.
 46. Cowell, S. M.; Lee, Y. S.; Cain, J. P.; Hruby, V. J., *Current Medicinal Chemistry* **2004**, *11* (21), 2785-2798.
 47. Marsault, E.; Peterson, M. L., *Journal of Medicinal Chemistry* **2011**, *54*, 1961-2004.
 48. Rezai, T.; Yu, B.; Millhauser, G. L.; Jacobson, M. P.; Lokey, R. S., *Journal of the American Chemical Society* **2006**, *128* (8), 2510-2511.
 49. Driggers, E. M.; Hale, S. P.; Lee, J.; Terrett, N. K., *Nature Reviews Drug Discovery* **2008**, *7* (7), 608-624.

CHAPTER THREE

SYNTHESIS OF MACROCYCLIC PROTEASE INHIBITORS

3 Synthesis of macrocyclic protease inhibitors

3.1 Calpain and its inhibition

Calpains are a family of 15 calcium dependent cysteine proteases, each encoded by a different gene, that are found ubiquitously in all tissues.¹ Two major isoforms of calpain have been identified and extensively studied, calpain I (or μ -calpain) and calpain II or (m-calpain), which require micro-molar and milli-molar concentrations of calcium, respectively, for *in-vitro* activation.² Each protease consists of two subunits, a large ~80kDa subunit that is isoform specific with approximately 62% sequence homology between the two isoforms, and a conserved small 20kDa subunit (Figure 3.1).³

NOTE:

This figure/table/image has been removed to comply with copyright regulations. It is included in the print copy of the thesis held by the University of Adelaide Library.

Figure 3.1. Crystal structure of calpain II with domains DI-DVI and active site residues labeled. Protein data bank code 1KFU³

The large subunit of calpain is comprised of four domains, DI-DIV, while the small subunit is comprised of two domains, DV and DVI.⁴ DI is made up of residues 20-210 and consists of a single helix flanked by a cluster of α -helices and two anti parallel β -sheets.⁵ DII is similar to other cysteine proteases in that it consists of two three-stranded anti-parallel β -sheets. DII can be divided into two sub domains, DIIa and DIIb.⁶ The catalytic triad is located at the interface between DIIa (Cys105) and DIIb (His262 and Asn286).^{7,8}

DIII is an 8-stranded anti parallel β -sandwich and is similar to the C2 domain in protein Kinase C. DIII has the potential to bind Ca^{2+} at ten acidic side chains. Binding of Ca^{2+} is thought to be involved in structural changes leading to the activation of calpain.⁹ DIV lacks secondary structure with the exception of a short anti-parallel β -sheet (residues 516-518). DIV and DVI each contain five EF-hands, four of which are involved in Ca^{2+} binding while the fifth EF-hand of each domain interact with each other to form a heterodimer.^{4, 5, 10} Domain V is a very flexible glycine rich domain and it is believed to interact with phospholipids.⁵

The crystal structure of Ca^{2+} free calpain II shows the catalytic triad residues are not correctly aligned for catalysis.⁶ In other cysteine proteases the inter-atomic distance of the CysS and HisN is $\sim 3.7\text{\AA}$.¹¹ At this distance the HisN forms a hydrogen bond to the proton on the sulfur of cysteine enhancing the nucleophilicity of the thiol for hydrolysis. The proposed mechanism for proteolytic cleavage by cysteine proteases is shown in **Figure 3.2**.¹²

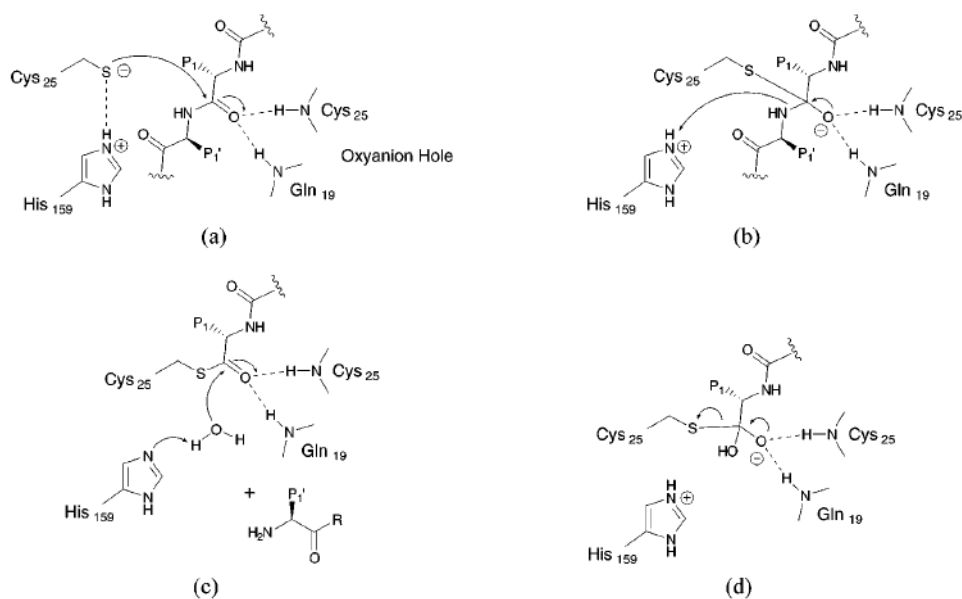


Figure 3.2. Proposed mechanism for proteolytic activity of cysteine proteases¹²

The key tetrahedral intermediate (see step b, **Figure 3.2**) is stabilised by hydrogen bonding to Gln19 and Cys25. This then leads to acylation of the enzyme with release of the C-terminal substrate fragment. Hydrolysis of the acylated enzyme to form a second tetrahedral intermediate (see step c), followed by collapse of this intermediate and release of the N-terminal substrate fragment in step d, completes the cycle to regenerate the free enzyme.

The crystal structure of the protease core of calpain I (domains I and II) has been reported.^{6, 8} This portion of the protease retains the minimal functional and structural requirements of a cysteine protease in the presence of Ca^{2+} . Two Ca^{2+} ions are bound, one in each domain, and binding of the calcium is shown to change the relative orientation of the two domains, bringing the active site Cys115 S 3.7 Å away from the His262 N (**Figure 3.3**) enabling the enzyme to be active.

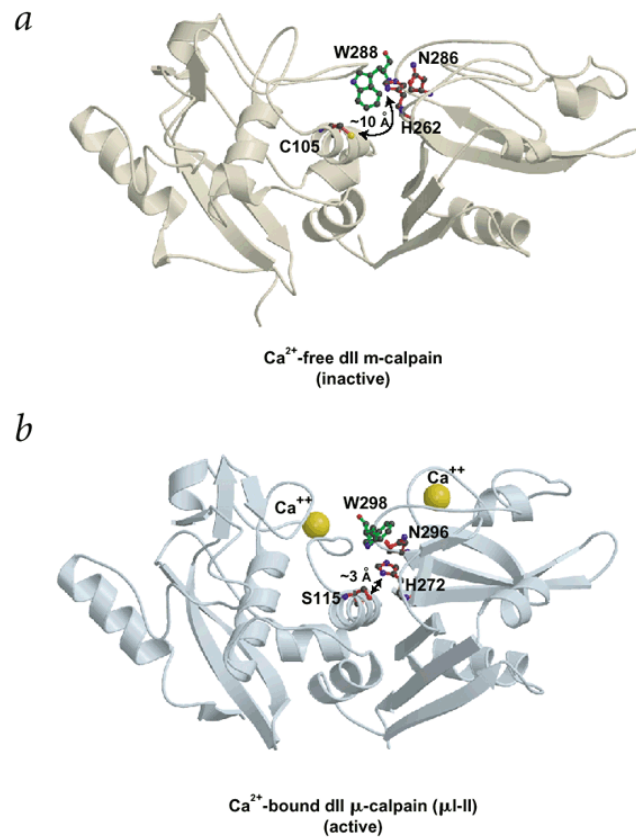


Figure 3.3. The proteolytic core of calpain I with⁶ and without⁸ Ca²⁺.

3.1.1 The role of calpain in pathological conditions

Disruption of calpain activity has been implicated in a number of pathological conditions including stroke, brain trauma, Alzheimer's disease, spinal cord injury and cardiac ischemia.^{13, 14} The role of calpain in these conditions is summarised in **Table 3.1**.

Disease	Role of calpain	Reference
Stroke	Degradation of cytoskeleton proteins leads to neural cell death and tissue damage	13 14 15
Brain trauma	Similar mechanism to stroke	13
Alzheimer's disease	Amyloid pre-cursor generated by calpain fragmentation of amyloid precursor protein	13, 14, 16 15
Spinal cord injury	Degradation of myelin proteins by calpain	13 14
Cardiac ischemia	Break down of myofibril proteins leads to cell death and tissue damage	13 17, 18

Table 3.1. Potential role of calpain in a number of diseases.

Calpain over activation has also been implicated in the formation of cataracts,¹⁹⁻²¹ a condition where opacification has occurred in all or part of the lens. This distorts and even prevents visible light reaching the retina.²² Cataract is the leading cause of visual impairment worldwide.^{23, 24} The only current treatment for cataract is surgery, which, while successful, may involve long delays with the patient experiencing further vision loss.²⁵ Furthermore there are associated risks and side effects associated with surgery. A pharmaceutical that could slow cataract progression, postponing deterioration of sight, while patients wait for surgery would greatly improve quality of life and present significant savings in health care dollars. There is an urgent need for a less expensive non-surgical treatment.¹⁹

The main structural components of the lens are soluble α - β - and γ -crystallins. Under normal conditions these crystallins exist in a highly ordered state which is essential for lens transparency. The over-activation of calpain occurs when an insult to the lens caused by UV light, ageing, oxidants and diabetes leads to an influx of calcium.^{19, 22}

In these cases, calpain catalysed hydrolysis of the crystallins leads to precipitation of insoluble protein fragments. The transparent nature of the lens is compromised causing light scattering and cataract formation.²⁶ Preliminary work has shown that calpain inhibitors prevent opacification in *in vitro* lens culture tests on rabbit²⁷ and ovine²⁸ lenses and slow cataract formation in *in vivo* trials (see **Chapter 5**). Thus the inhibition of calpain is a logical approach to cataract prevention.

3.1.2 Calpain inhibitors

Due to its role in a wide range of pathological conditions, calpain has emerged as an attractive drug target. A number of calpain inhibitors are known in the literature.^{3, 29, 30} These are generally peptide based, conformationally flexible molecules, with a reactive C-terminus. One of the most potent inhibitors, with an IC_{50} of 49 nM, is **SJA6017** (**Figure 3.4**), patented in 1999 by Senju Pharmaceuticals.^{31, 32}

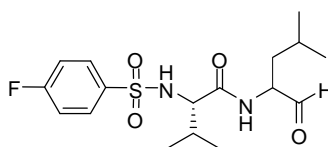


Figure 3.4. SJA6017

SJA6017 has been reported to reduce cataract formation in a lens culture assay and has a good toxicity profile, however, due to its peptidic nature it has poor membrane permeability, binding readily to plasma proteins to be quickly metabolised.²⁹

To overcome these shortcomings, it is desirable to synthesise inhibitors that have a higher bioavailability and improved drug profile. The introduction of a ring or bridge is commonly used to constrain a peptidomimetic into a biologically active

conformation. This effectively preorganises conformation for binding to the enzyme while increasing stability to protease hydrolysis by decreasing peptide characteristics (see **Chapter 1**).

The binding of an inhibitor to the active site of a protease, including calpain, can be described by nomenclature defined by Schechter and Berger as depicted in **Figure 3.5**.³³ Sub-sites that bind residues on the N-terminal side of the scissile bond of the substrate (non-primed sites) are numbered as $S_1 - S_n$. Sub-sites that bind from the C-terminus (primed sites) are numbered as $S_{1'} - S_{n'}$ from the scissile bond. The corresponding substrate residues are numbered $P_1 - P_n$ and $P_{1'} - P_{n'}$, respectively (**Figure 3.5**). The zigzag arrangement of the binding pockets of the protease favours an extended β -strand conformation for substrates (and inhibitors) binding to the protease active site.

NOTE:
This figure/table/image has been removed
to comply with copyright regulations.
It is included in the print copy of the thesis
held by the University of Adelaide Library.

Figure 3.5: Schechter and Berger nomenclature of substrates bound in an extended β -strand geometry in the active site of a protease.³⁴

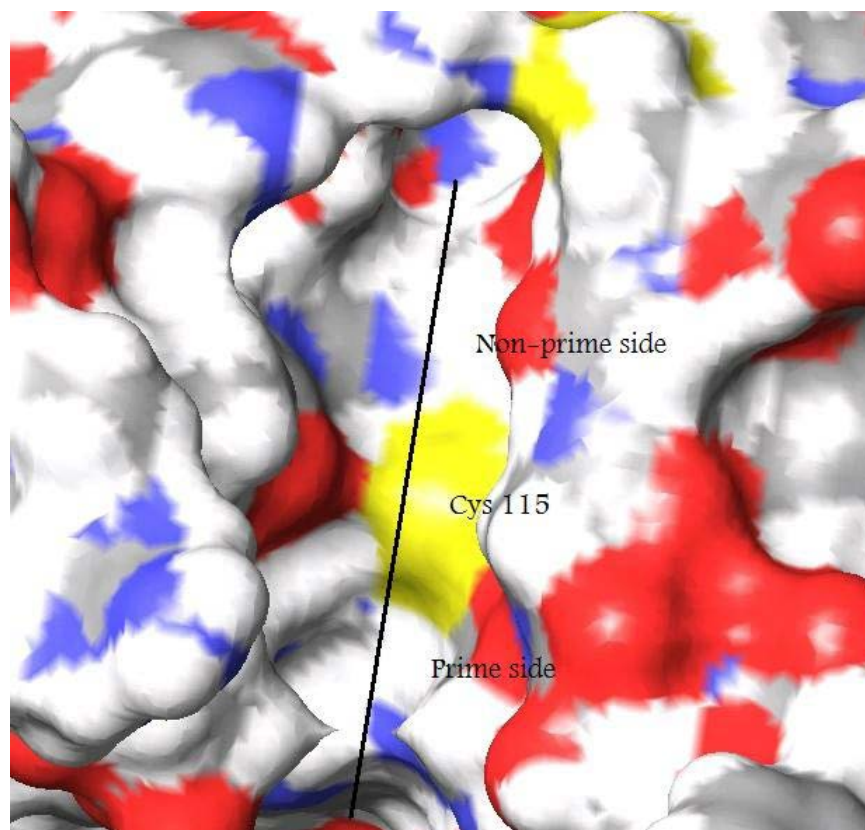


Figure 3.6. Surface diagram of 1KXR showing the active site cleft of calpain (black line).

The active site of calpain consists of a rigid, narrow groove with steep surfaces. The groove is narrowest around the S_1 site ($<7\text{\AA}$ across) and widest at the S_3 site ($>15\text{\AA}$ across) (**Figure 3.6**).³⁵ Classic calpain inhibitors (such as **SJA6017**, see **Figure 3.4**) consist of an “address region” for active site recognition and binding which contains amino acids chosen to fit into the S_1 - S_n pockets. A wide variety of residues are tolerated at P_1 ,³⁶ L-Leucine or L-valine are preferred at P_2 ³² and a bulky aromatic group is favored at P_3 . The C-terminus consists of a reactive “warhead” – an electrophilic group replacing the scissile amide bond that forms a reversible covalent interaction with the active site cysteine. The warhead is typically an aldehyde, but may also be an α -keto carbonyl group, an α -keto phosphorus group, or other electrophile.³⁶

Computational docking studies³⁷ have shown that known inhibitors bind to calpain with their backbone in a β -strand^I conformation, with the side chains of the amino acid residues of the inhibitor interacting with the S_1 - S_3 pockets of the protease. This allows the formation of three key hydrogen bonds to Gly208 and Gly271 residues of the enzyme, labeled A, B and C in Figure 3.7. This is consistent with other studies on proteases including a 2005 review which surveyed >1500 protease-ligand crystal structure in the PDB and found that proteases almost universally bind their substrates in an extended β -strand conformation (also see **Chapter 1**).³⁸

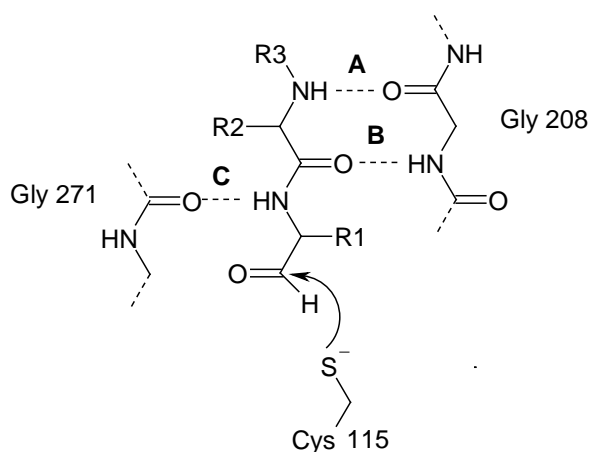


Figure 3.7. Key hydrogen bonds for β -strand formation.

Further emphasising the importance of the β -strand conformation, an analogue of **SJA6017** was prepared by the Abell group.³⁹ Modification and linkage of the leucine and valine residues of the parent compound to form an 8-membered ring gave rise to lactam **3.01** (**Figure 3.8**). This strategy restricted the conformation of **3.01** by reducing the flexibility around the amide bond and fixed the geometry of the inhibitor backbone in a non- β -strand conformation. The lack of activity of **3.01** against calpain,

^I The backbone of substrates and inhibitors are able to adopt a conformation that complements the geometry dictated by active site binding. Throughout this thesis this conformation is referred to as a β -strand.

despite it possessing a potent aldehyde warhead, suggests the β -strand conformation is crucial component for calpain binding and inhibition.

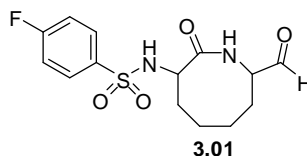


Figure 3.8. Cyclic analogue of SJA6017

Macrocycles (>12 membered rings) have been reported that constrain a peptide into a β -strand geometry.⁴⁰ Cyclic peptidomimetics linking the P₁ and P₃ residues adopt a β -strand conformation and have been developed, for example, into inhibitors of the aspartic protease HIV-1 (**Figure 3.9**).⁴¹

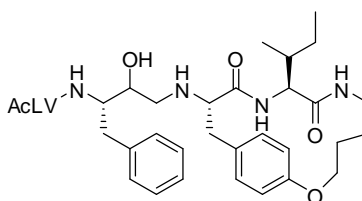


Figure 3.9. HIV-1 Protease inhibitor

The introduction of a macrocyclic bridge, as well as fixing the geometry of the compound, should also overcome many of the problems associated with known linear inhibitors such as poor cell permeability, plasma binding and proteolysis. Macrocyclisation has been shown to increase passive membrane permeability particularly if the conformational constraint induces internal hydrogen bonds.⁴² This reduces the affinity of the macrocycle to the solvent allowing higher bioavailability. By reducing the accessibility of the peptide bonds in the molecule to proteolytic cleavage, macrocyclisation further improves the drug profile of an inhibitor by

improving metabolic stability while retaining potency against and specificity towards the target protease.^{43, 44}

An objective of the Abell group is to design macrocycles constrained in a β -strand conformation in order to develop potent calpain inhibitors. To achieve this goal we developed a general template for inhibitor design consisting of a tripeptide in which the P_1 and P_3 residues are linked by an appropriate macrocycle (**Figure 3.10**).

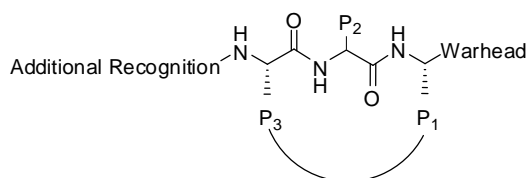


Figure 3.10. General structure of macrocycle inhibitors

The tyrosine-X-glycine (where X is an α -amino acid) series of macrocycles were chosen as an attractive class of inhibitors for synthesis. Tyrosine at the P_3 position satisfies the preference of the calpain for a bulky aromatic group in the S_3 pocket. Additionally, tyrosine, by nature of its aromaticity, reduces flexibility in the macrocyclic bridge, enhancing the effect of the constraint in inducing the β -strand conformation.⁴⁵

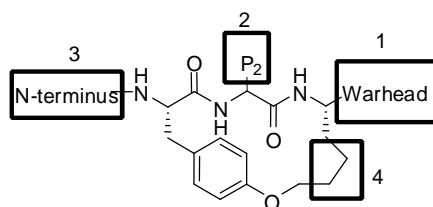


Figure 3.11. Four key areas of the macrocycle inhibitor

The tripeptide macrocycle contains four domains (**Figure 3.11**). It was found a C-terminal aldehyde with leucine at the P₂, tyrosine at P₃ and Cbz at the N-terminus gave the most potent inhibitor, **CAT0811**, which has an IC₅₀ of 30 nM against calpain II (**Figure 3.12** and discussion in **Chapter 4**).²⁸

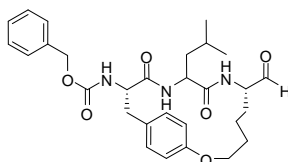


Figure 3.12. CAT0811

CAT0811 was chosen as the lead molecule for the macrocycle modification described herein. **CAT0811** is highly potent against calpain II and is relatively easily synthesised in reasonable quantities from commercially available starting materials making it a good lead compound. This chapter describes the synthesis of four analogues of **CAT0811** shown in **Figure 3.13**.

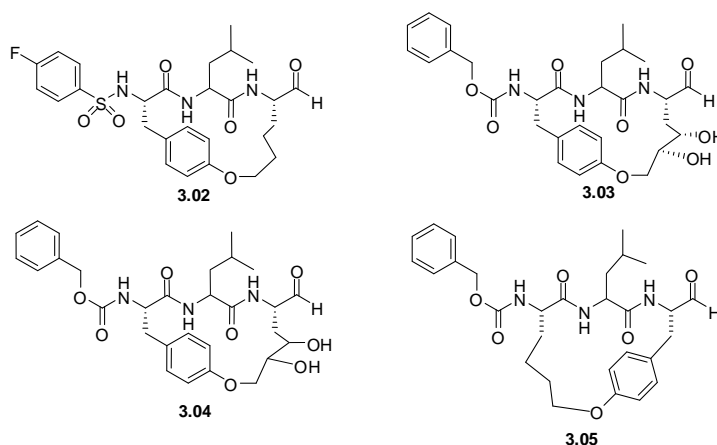


Figure 3.13. Macrocyclic analogues of CAT0811 prepared in this Chapter

As described in **Section 3.2**, macrocycle **3.02** was made to investigate the suitability of the 4-fluoro-benzyl-sulfonyl (FBS) group as an N-terminal group and to compare three synthetic routes to the macrocycle.

Macrocycles **3.03** and **3.04** were made to explore possible hydrophilic interactions with the active site and the diol oxygens as detailed in **Section 3.3**.

Macrocycle **3.05** (**Section 3.4**) was designed to investigate the relative importance of P₁ and P₃ towards the activity of calpain II, α -chymotrypsin and the 20S core of the 26S proteasome given that calpain favours aromatic substituents at P₃ while α -chymotrypsin favours aromatic at P₁.

3.2 Synthesis of the N-terminal FBS macrocycle 3.02

The N-terminal capping group of calpain inhibitors, such as the Cbz group of **CAT0811** (**Figure 3.12**), extends into the S₄ binding pocket of calpain. These groups thus provide additional recognition for binding, enhancing inhibitor selectivity while also increasing the stability of the ligand to metabolism by proteolysis.⁴⁶ Modelling studies on calpain II show the S₄ pocket is a hydrogen-bonding rich region of the enzyme that prefers an aromatic group at the P₄ position.⁴⁷ Hydrogen bonding between the S₄ pocket of the enzyme and P₄ substituents increases the affinity of the inhibitor for the enzyme and hence selectivity for calpain over other proteases such as cathepsin B and papain, neither of which have this H-bond rich region at S₄.

Despite the significance of **CAT0811**,²⁸ its synthesis (described in detail in **Chapter 5**) is low yielding (1% overall) with large catalyst loading (30 mol%) of Grubbs' second generation catalyst in the key ring closing metathesis cyclisation step. Difficulty in the cyclisation step is a phenomenon often observed in macrocycle synthesis. Macrocyclisations can be plagued by low yields and require high dilution conditions to offset entropic loss.⁴⁴

Given these problems with the synthesis of **CAT0811**, a comparative study on three metathesis-based approaches to macrocycle synthesis was investigated, two involving ring closing metathesis (RCM) and the third cross metathesis (CM) as outlined in **Figure 3.14**. The methodology is demonstrated by specifically targeting a new analogue of **CAT811** that contains an N-terminal 4-fluorobenzylylsulfonyl (FBS) group (see structure **3.02** in **Figure 3.14**).

The sulfonyl oxygens of the FBS group could potentially form hydrogen bonds to the S₄ pocket of calpain. Further, it is known to be a suitable N-terminal capping group for calpain providing potent acyclic inhibitors such as **SJA6017** (**Figure 3.4**).^{26, 31, 32} Unlike the Cbz N-terminus of **CAT0811**, FBS is stable to hydrogenation making it is more versatile for use in synthesis as it can be introduced at any step of the synthesis, including before the metathesis/hydrogenation. The proposed macrocycle **3.02** should give a potent calpain inhibitor.

Target macrocycle aldehyde **3.02** is readily prepared from key intermediate **3.06** (**Figure 3.14**). Key intermediate **3.06** has been prepared by Dr Seth Jones⁴⁸ by cross metathesis of terminal alkene **3.07** with alkene **3.08** followed by catalytic hydrogenation to give pseudo-peptide **3.09**. Macro-lactamisation gives key intermediate **3.06** (**Figure 3.14, Route A**). This synthesis gave macrocycle **3.06** in 5% yield over 6 steps.

In an attempt to improve the over all yield of macrocycles of this type we investigated two ring closing metathesis routes to macrocycle **3.06** (**Figure 3.14 - Routes B and C**). The first, **Route B**, is directly analogous to the synthesis of **CAT0811**²⁸ with ring closing metathesis of diene **3.10** followed by incorporation of the FBS group at the N-terminus of the macrocycle to give **3.06** (see **Scheme 3.1** for detail). The second, **Route C**, involves introduction of the FBS group to give dipeptide **3.11** which is coupled to alkene **3.12** to give diene **3.13**. Ring closing metathesis of diene **3.13** followed by catalytic hydrogenation gave **3.06** (see **Scheme 3.2** for detail).

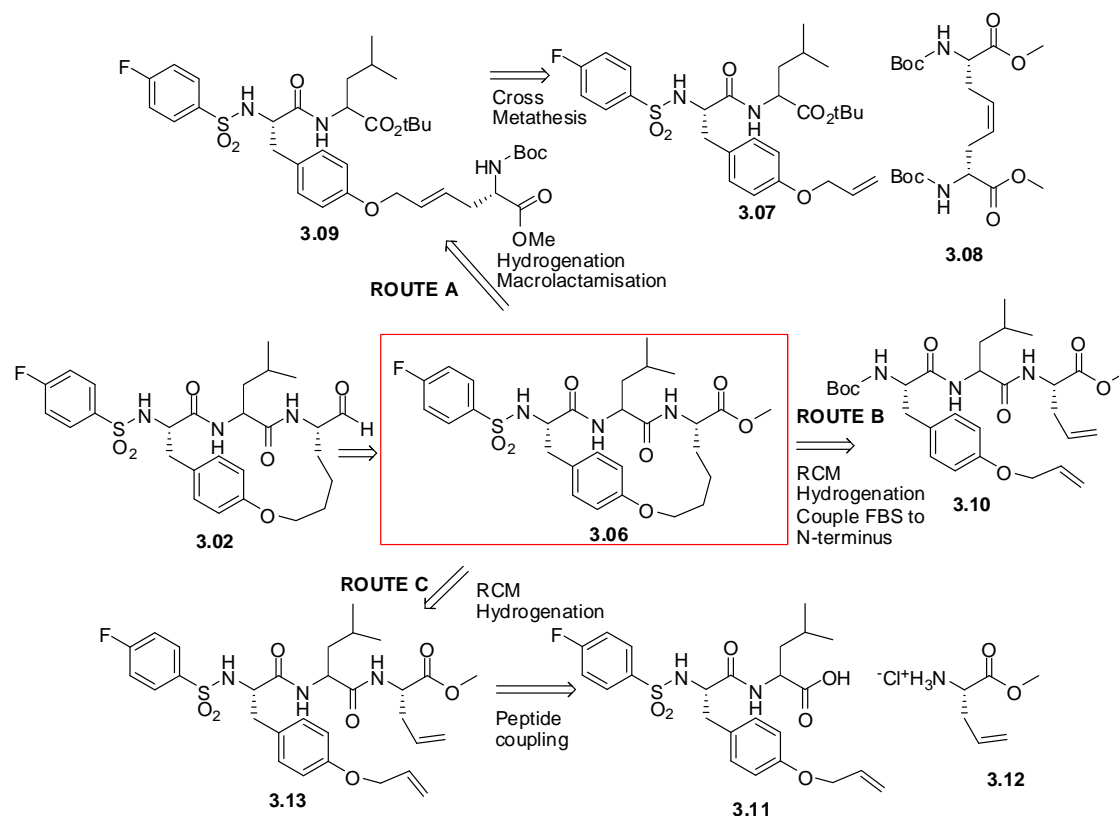


Figure 3.14. N-terminal FBS inhibitor **3.02** and key intermediate methyl ester **3.06**.

The first step in **Route B**, as shown in **Scheme 3.1**, involved coupling alkene **3.14** to Leu-OMe.HCl using HATU to give dipeptide **3.15** in 92% yield after purification by flash chromatography on silica gel. Hydrolysis of the methyl-ester of **3.15**, on treatment with NaOH, gave **3.16** and this was coupled to allyl-Gly-OMe.HCl in the presence of HATU to give the diene **3.10** in 74% yield over two steps. Microwave mediated ring closing metathesis, using three portions of Grubbs' Second Generation catalyst in TCE (3 x 10 mol%) gave **3.17** in 22% yield after purification by flash chromatography on silica gel. Alkene **3.17** was isolated after metathesis and subsequent purification was assigned the E isomer on the basis of ^1H NMR (**Figure 3.15**). The coupling constants of the alkene protons H_a and H_b of **3.17** (5.40 ppm and 5.55 ppm) were measured to be $J = 15.7$ Hz. This is consistent with the assigned E geometry (11 – 18 Hz).⁴⁹ The corresponding Z alkene would be expected to give

coupling constants of between 6 – 14 Hz. The lack of any doubling of resonances in both the ^1H and ^{13}C spectra confirmed only one isomer was present.

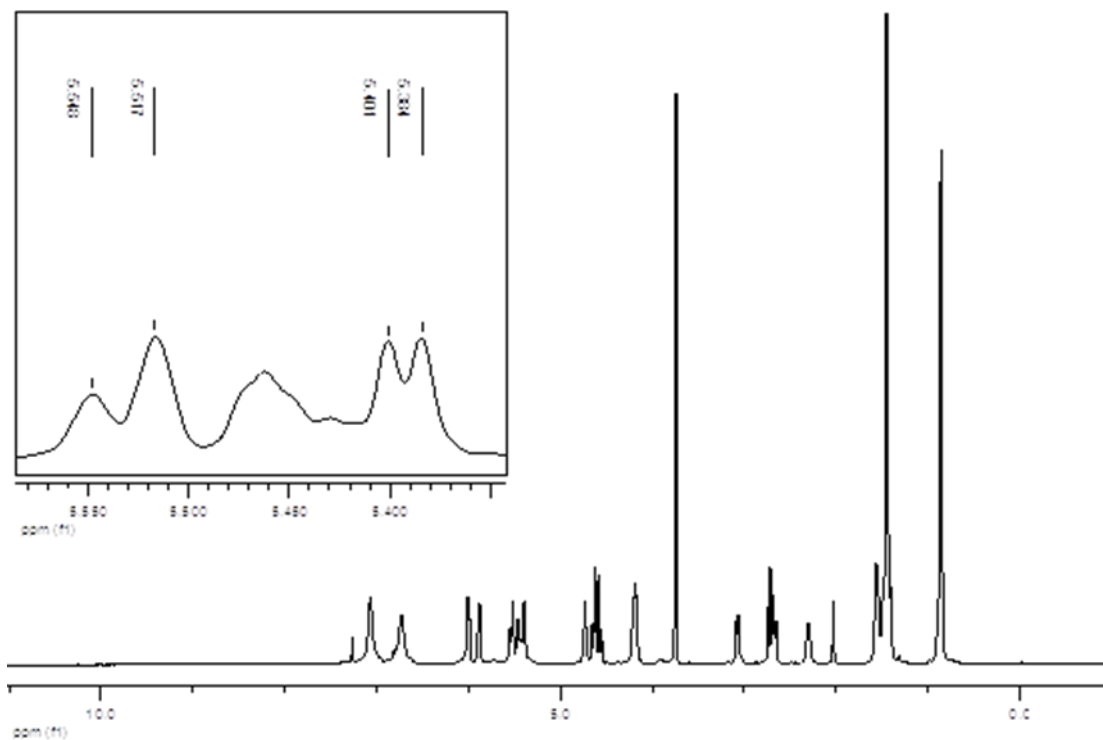
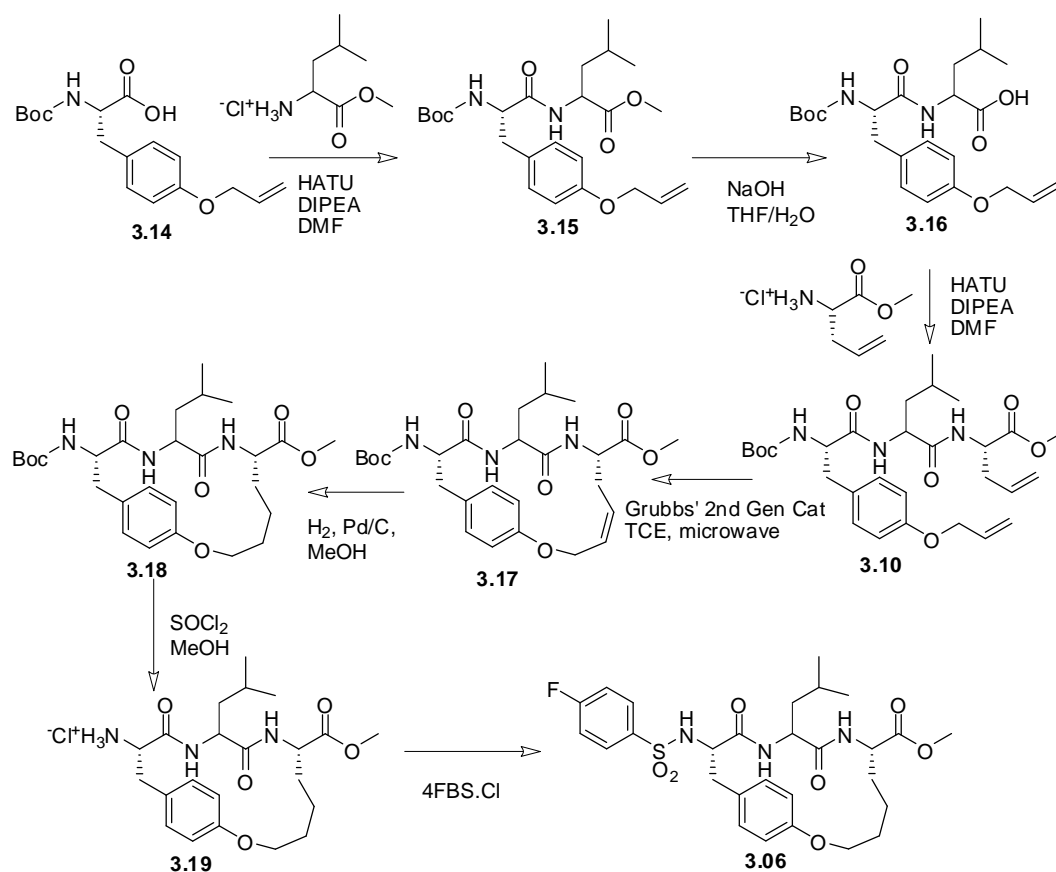


Figure 3.15. ^1H NMR of alkene **3.17** showing only the trans isomer of the alkene is formed.

Subsequent hydrogenation of the alkene of **3.17** with Pd/C and H_2 gave the saturated macrocycle **3.18** in 87% yield. Deprotection of the N-terminal Boc of **3.18** upon treatment with thionyl chloride in methanol gave amine **3.19** in quantitative yield. Coupling of the FBS chloride to the N-terminus of **3.19** gave the required **3.6** in a low 7% yield after purification by flash chromatography on silica gel.⁵⁰

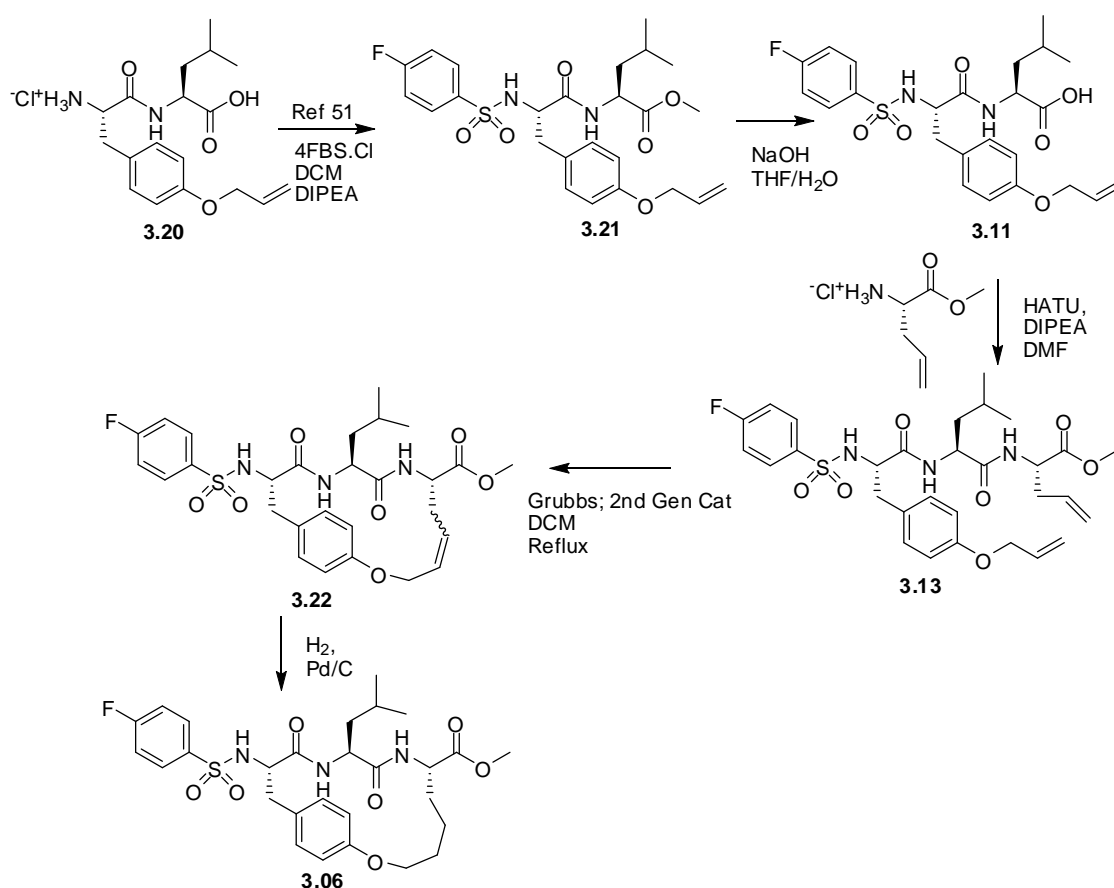


Scheme 3.1. Synthesis of macrocycle **3.06**.

Two significant inefficiencies were identified in this synthesis of **3.06**. The low yielding (7%) coupling of the FBS group onto macrocycle **3.19** significantly reduced the overall yield of the synthesis to 1%. This low yield is likely associated with the low solubility of macrocycle **3.19** during reaction and purification. Secondly, the ring closing metathesis step required 30 mol % of Grubbs' second generation catalyst and microwave irradiation. This renders **Route A** costly and unsuitable for large scale synthesis.

The second route (**B**) was then investigated,⁵¹ where the N-terminal capping group is introduced to dipeptide **3.11** (see **Figure 3.14** and **Scheme 3.2**). The dipeptide **3.20** is less polar and more soluble in organic solvents than the macrocycle. We hypothesised

that the yield of the coupling of the FBS group would be enhanced by the improved solubility of the dipeptide. The ring closing metathesis step has also been optimised for this synthesis to proceed thermally with 90% reduction in catalyst loading. This synthesis is shown in detail in **Scheme 3.2**.



Scheme 3.2. Alternate synthesis of **3.06** where FBS is introduced at the dipeptide.

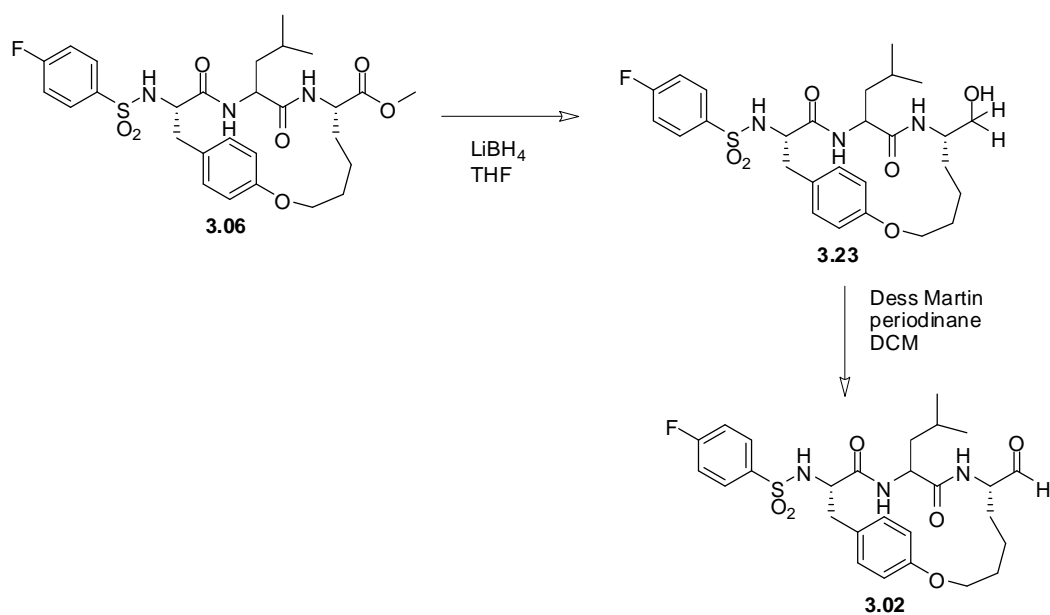
Hydrolysis of the methyl ester of **3.21**⁴⁸ on treatment with **NaOH** gave acid **3.11** which was coupled with allyl-Gly-OMe.HCl using **HATU** to give the diene **3.13** in 84% across two steps. The diene underwent ring closing metathesis under thermal conditions with one portion of Grubbs' second generation catalyst (3 mol %) in refluxing **DCM**, to give the macrocyclic alkene **3.22** in 68% after recrystallisation. Alkene **3.22** was determined to be a 9:1 mixture of **E/Z** isomers as judged by the

relative integral ratios of the methyl ester peaks in the ^1H NMR. The double bond of the E/Z mixture of alkenes was hydrogenated with Pd/C and H_2 to give the macrocycle **3.06** in 89%.

This route is an improvement on that shown in **Scheme 3.1** as the yield for the coupling reaction of FBS onto dipeptide **3.20** is increased to 87%⁴⁸ compared to a 7% yield when coupling to macrocycle **3.19**. This reaction likely proceeds more efficiently due to the increased solubility and ease of purification of the dipeptide compared with the highly insoluble and polar macrocycle. Secondly, we reduced the amount of catalyst used in the ring closing metathesis from 30 mol% to 3 mol% and did the reaction under thermal rather than microwave conditions. These conditions, as well as recrystallisation of macrocycle **3.22**, rather than purification by flash chromatography, gave an increase in yield of the metathesis step from 22% to 68%. The overall yield of **3.06** is increased from 1 % to 47 %. Thus the synthesis shown in **Scheme 3.2** is a much more efficient route to the target precursor **3.06**.

A comparison of the three synthetic routes reveals that attaching the FBS moiety before the ring closing metathesis of the subsequent diene (**Route C** and **Scheme 3.2**) is the most efficient method of preparing **3.06** (proceeding in 47% from **20**). The preparation of **3.06** by cross metathesis of terminal alkene **3.07** and alkene **3.08**, and subsequent macrolactamisation of the resulting pseudo-peptide gave **3.06** in an overall yield of 5%.⁴⁸ The preparation of **3.06** by coupling the FBS moiety to the previously reported macrocycle **3.19**²⁸ proceeded in 1% yield from **3.14** – this was the least efficient of the three routes investigated.

The synthesis of calpain inhibitor aldehyde **3.02** was achieved by transformation of the methyl ester of **3.06** to the aldehyde warhead in two steps (**Scheme 3.3**). Methyl ester **3.06** was treated with LiBH_4 in THF to give the alcohol **3.23** in 87% yield. The alcohol **3.23** was oxidised using Dess-Martin periodinane to give the aldehyde **3.02** in 79% yield.



Scheme 3.3. Synthesis of aldehyde **3.02** from methyl ester **3.06**.

The activity of aldehyde **3.02** was assessed against calpain II as discussed in **Chapter 4**.

3.3 Design, synthesis and testing of diol-containing macrocycles 3.03 and 3.04

This section describes work on the introduction of a hydrophilic group (specifically a diol substituent) to the macrocyclic ring of **CAT0811**. Examination of a site map of calpain residues generated in Glide³⁷ shows the active site cleft is largely hydrophobic deep in the S₁-S₄ region where the amino acid side chains (P₁ – P₄) of the inhibitor are bound (copper regions, **Figure 3.16**). The surface of the active site cleft is largely hydrophilic (light blue regions, **Figure 3.16**).

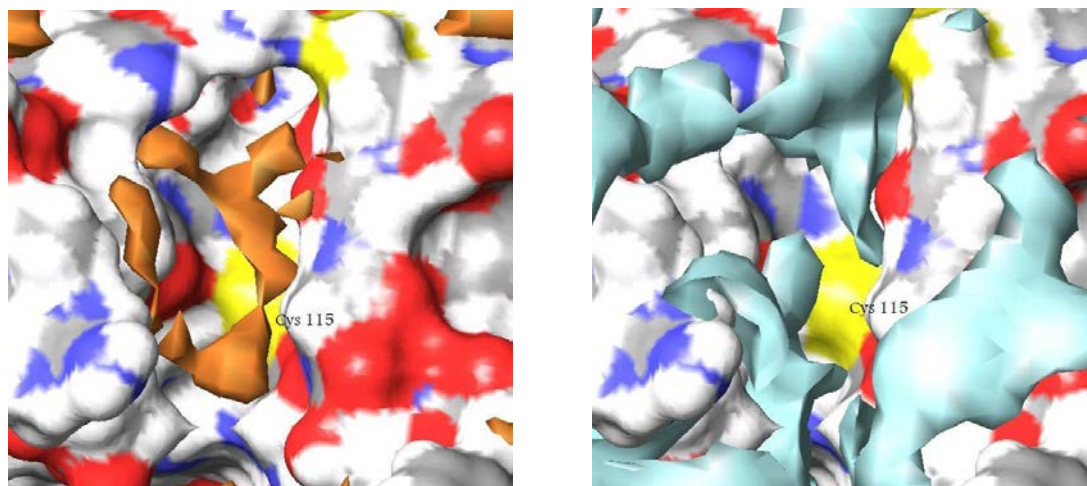


Figure 3.16. Active site of calpain with hydrophobic regions shown in copper (LHS) and hydrophilic regions of the active site shown in pale blue (RHS)

Docking studies³⁷ show that the peptide backbone of **Cat0811** binds in the active site of calpain with the macrocyclic ring orientated towards the opening of the active site cleft. The ring is situated in the hydrophilic region of the enzyme facing out towards the aqueous environment of the enzyme (**Figure 3.17**).

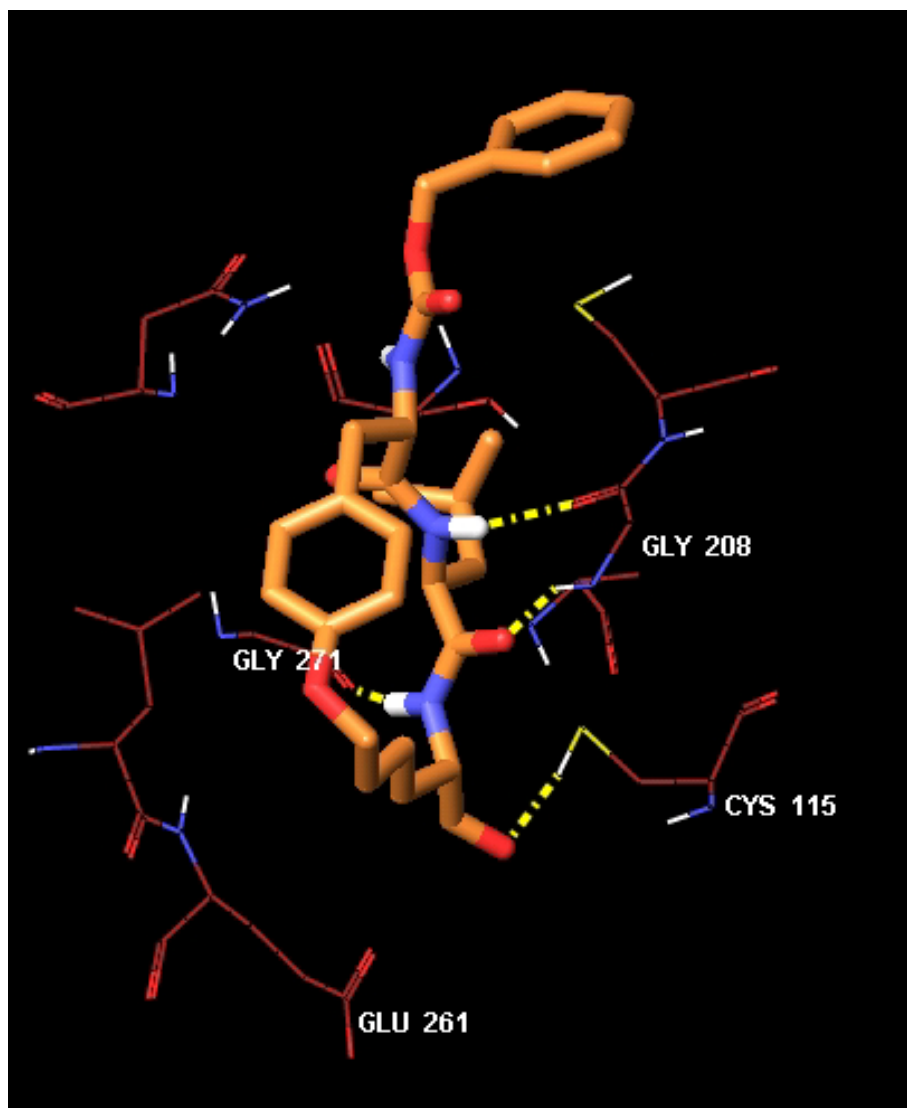


Figure 3.17. CAT0811 bound to ovine calpain II – the ring of the macrocycle is in the aqueous environment of the enzyme and separated from any residues from the protease.

It is hypothesised that introduction of a hydrophilic group in the macrocyclic ring of **CAT0811** would enhance the affinity of the macrocycle to the hydrophilic opening of the active site of the enzyme to potentially allow hydrogen bonding with residues in this region. Additional hydrogen bonds between the inhibitor and the enzyme might then lead to a more potent and selective inhibitor of calpain.

With this in mind, the two diastereomeric diols, compounds **3.03** and **3.04**, were prepared from **3.10** as depicted in **Figure 3.18**. Ring closing metathesis of diene **3.10**,

followed by coupling of Cbz to the N-terminus, would give the macrocycle **3.24**, the alkene of which can then be functionalised by Sharpless' dihydroxylation with potassium osmate to give the corresponding cis-diols **3.25** and **3.26** (Figure 3.18).

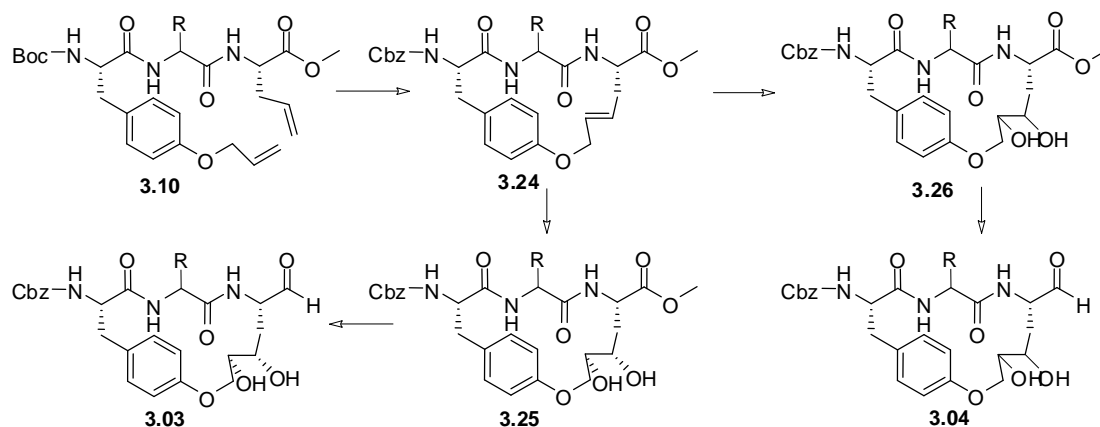


Figure 3.18. Proposed synthesis of diol macrocycles **3.03** and **3.04**

3.3.1 Computational modelling of diols **3.03** and **3.04**

The potential of the diols **3.03** and **3.04** to bind to calpain was studied *in silico* in collaboration with Dr. Stephen McNabb using Schrodinger suite of software 2005. Three key parameters were used to evaluate the potential of macrocycles **3.03** and **3.04** as calpain inhibitors: (i) whether or not the macrocycle forms a β -strand conformation (ii) the Glide Emodel score to assess binding strength between the macrocycle and calpain and (iii) the distance of the electrophilic aldehyde warhead from the Cys105 residue. These parameters are discussed below.

Conformational Search:

The ability of the diols to form a β -strand was evaluated by conducting conformational searches on structures **3.03** and **3.04** using MacroModel 9.1 to

generate an ensemble of low energy conformers. The energy of the conformers is a potential energy, calculated by summing bond stretching, bending, torsional, and the non-bonded energies (e.g. van der Waals energy and hydrogen bonds). The searches were conducted with the MCMM method using a GB/SA water model and the OPLS2005 force field, with 3000 steps for the conformational search and up to 5000 iterations for the minimisation of each generated structure. The minimisation was stopped with the default gradient convergence threshold of $d = 0.05 \text{ kJ}/(\text{mol} \cdot \text{\AA})$. The default Polak-Ribiere Conjugate Gradient method was used for all minimisations. The Boltzmann weighted percentage of conformers within the 12kcal per mole window of the global minimum that exhibited in a β -strand was calculated. For **3.03** it was found that 59.2% of the ensemble were in a β -strand conformation, whereas for **3.04** only 0.6% were in a β -strand. Thus it would appear that **3.03** has a much higher propensity to form the required β -strand motif for binding to the enzyme and therefore is predicted to be a more effective inhibitor of calpain.

Docking Studies:

The lowest energy conformer for each diol generated in the conformational search detailed above was docked into a rigid Glide model of calpain in order to assess the binding affinities of compounds **3.03** and **3.04**. When this synthesis was undertaken, the only crystal structure of calpain available was that of rat mini calpain (pdb code 1KXR). Thus rat mini calpain was used as the model to assess the potential of the compounds to inhibit calpain.

Rat mini calpain model

The crystal structure of rat mini calpain I (pdb code 1KXR) was prepared, using the protein preparation facility in GLIDE 4.0, by:

- deleting water molecules
- correcting the incorrect amino acids from the pdb file.
- mutation of Ser₁₁₅->Cys₁₁₅ to mimic the active site of calpain
- deprotonation of the Cys₁₁₅, and protonation of His₂₇₂ to mimic physiological conditions.
- The structure was minimized using the OPLS2005 force field with a GB/SA water model over 500 iterations. All residues within a 5 Å distance to the calcium ions, the calcium ions and the key residues Gly₂₀₈, Gly₂₇₁ and Cys₁₁₅ of the structure were kept frozen during this minimisation. The RMSD (root mean squared standard deviation) of the minimized structure to the crystal structure was 0.96 Å for the heavy atoms (C, N, O, and S).
- The centre of the docking grid was defined as the centroid of the residues Cys₁₁₅, Gly₂₀₈, and Gly₂₇₁ and was generated with GLIDE 4.0 using default settings. The centre of any docked ligand had to be within a 12 Å box.

Docking of ligands 3.03 and 3.04 to the calpain model:

The docking of flexible ligands **3.03** and **3.04** to the rigid rat model with GLIDE was performed with the following parameters:

- OPLS2005 force field
- extra precision mode
- 10000 poses per ligand for the initial docking
- scoring window for keeping 100 initial poses

-
- keep best 1000 poses per ligand for energy minimization
 - energy minimization with a distance dependent dielectric constant of 2 and a maximum of 5000 conjugate gradient steps.

For both aldehydes **3.03** and **3.04** the Glide Emodel score was calculated, the distance of the inhibitor aldehyde to the cysteine 105 sulfur was measured and the hydrogen bonding between the inhibitor and the enzyme was predicted.

*Evaluation of compounds **3.03** and **3.04** as calpain inhibitors:*

The Glide Emodel score is a combination of the energy grid score, the prediction of the relative binding energy of each ligand to the enzyme as predicted by the GlideScore⁵² and the internal strain energy of the ligand. The glide score is a reflection of the relative binding energy of each ligand to the enzyme, with a lower value being more favourable. A large number of parameters are used to calculate this score, however the number and strength of hydrogen bonds that the molecule forms with calpain provides a major contribution. A glide score of -9.5 was found for **3.03** which is comparable to the glide score for **CAT0811** of -8.60. This is consistent with the earlier prediction that **3.03** has low energy conformers in a β -strand conformation.

The warhead distance (WHD) is the distance from the aldehyde warhead of the inhibitor to the Cys105 residue of the enzyme. This distance must be less than 5 Å if the aldehyde is to undergo nucleophilic attack and form a covalent interaction with the enzyme active site.³⁷ For compound **3.03** 11 out of 22 poses were within the required warhead distance. For compound **3.04** 10 out of 28 poses generated were within the required warhead distance.

The computational studies were also used to predict hydrogen bonding to the enzyme. The three key hydrogen bonds ABC between the inhibitor and the Gly208 and Gly271 residues of the enzyme described previously (**Figure 3.7**) are required for binding in a β -strand conformation, with any additional hydrogen bonds potentially increasing binding efficiency. Diol **3.03** was predicted to form the ABC hydrogen bonds as well as an additional hydrogen bond between the alcohol and the Glu261 residue of the enzyme (**Figure 3.19**). Diol **3.04** was predicted to form only two of the three key hydrogen bonds (B and C) with two additional hydrogen bonds between each OH and Glu261 and Ser206 (**Figure 3.20**).

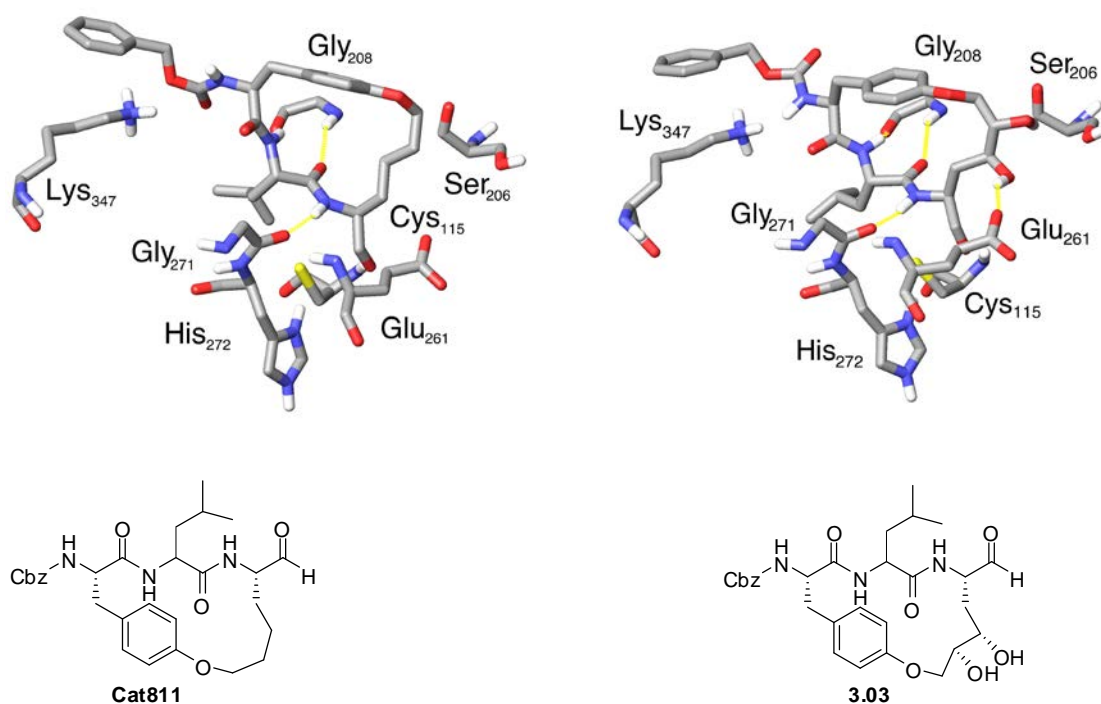


Figure 3.19. LHS: best pose of **CAT0811** and RHS: best pose of diol **3.03** showing H-bonding to the active site of the rat min calpain I construct. H-bonds to Gly208 and Gly271 indicate crucial β -strand formation. Extra H-bonding in **3.03** from OH groups to Glu261 may indicate increased binding to active site.

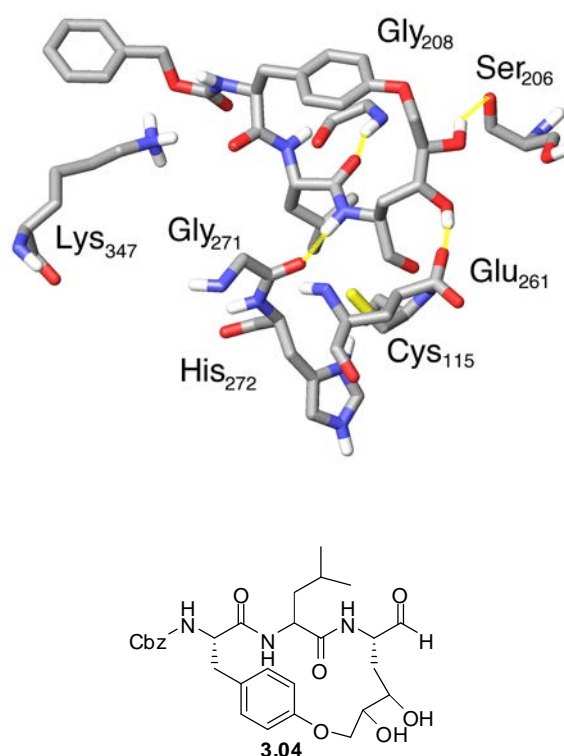


Figure 3.20. Best pose of **3.04** showing H-bonding to the active site of the rat mini calpain I construct. Two H-bonds are made to the Gly208 and Gly271 along with additional hydrogen bonds to the Ser206 and Glu261 residues.

Summary of *in silico* studies

A summary of the computational studies of compounds **3.03** and **3.04** using the rat mini calpain I model are summarised and compared to results for **CAT0811** in **Table 3.2**.

Compound	% β -strand	No. poses generated	No. poses with WHD < 5 Å	best representative pose		
				H-bonds	WHD	Emodel
3.03	59.2%	22	11	A,B,C,Glu ₂₆₁	4.42	-67.15
3.04	0.62%	28	10	B,C,Glu ₂₆₁ ,Ser ₂₀₆	4.15	-62.05
CAT0811		9	7	B,C	3.74	-65.50

Table 3.2. Modeling results of compounds **3.03** and **3.04** compared with **CAT0811** in the rat mini calpain I model. WHD stands for warhead distance - the distance from the aldehyde warhead to the Cys115 residue. Hydrogen bonds ABC are from the carbonyl of Gly208, the NH of Gly208 and the carbonyl of Gly 271. Additional hydrogen bonds can be formed between the OH groups of the diol and Glu261 and Ser 206.

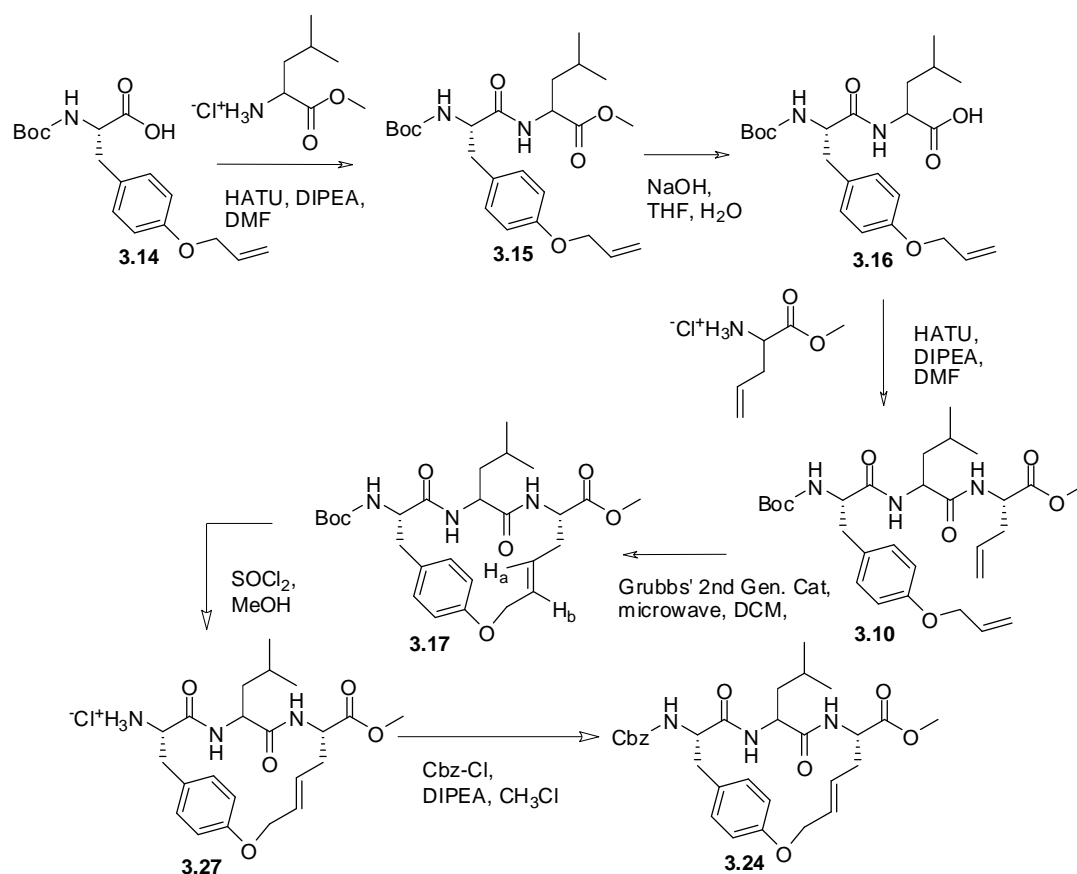
The three key hydrogens bonds (ABC) and the additional hydrogen bond to Glu261 predicted for diol **3.03** compare favourably to the two hydrogen bonds predicted for **CAT0811**. The Emodel score of **3.03** is also favourable and lower than that of **CAT0811**, -67.15 versus -65.50. This, in combination with its increased propensity to adopt a β -strand geometry, suggested diol **3.03** to be a likely inhibitor of calpain.

Diol **3.04** is also predicted to form four hydrogen bonds to calpain – the B and C bonds as well as hydrogen bonds from each hydroxyl group to the Ser206 and Glu261 residues as illustrated in **Figure 3.20**. However **3.04** has significantly reduced ability (0.6% of the ensemble of poses generated) to form the β -strand conformation necessary for binding to calpain and thus was not predicted to be a good inhibitor.

The modelling results suggest that the diol groups form hydrogen bonds to electrophilic residues in the hydrophilic area of enzyme as hypothesised by examination of the site map of calpain (**Figure 3.16**). Based on these results the synthesis was undertaken.

3.3.2 Synthesis of diol-based inhibitors

Alkene **3.24** is the key intermediate to the diols **3.03** and **3.04**; its synthesis is outlined in **Scheme 3.4**.

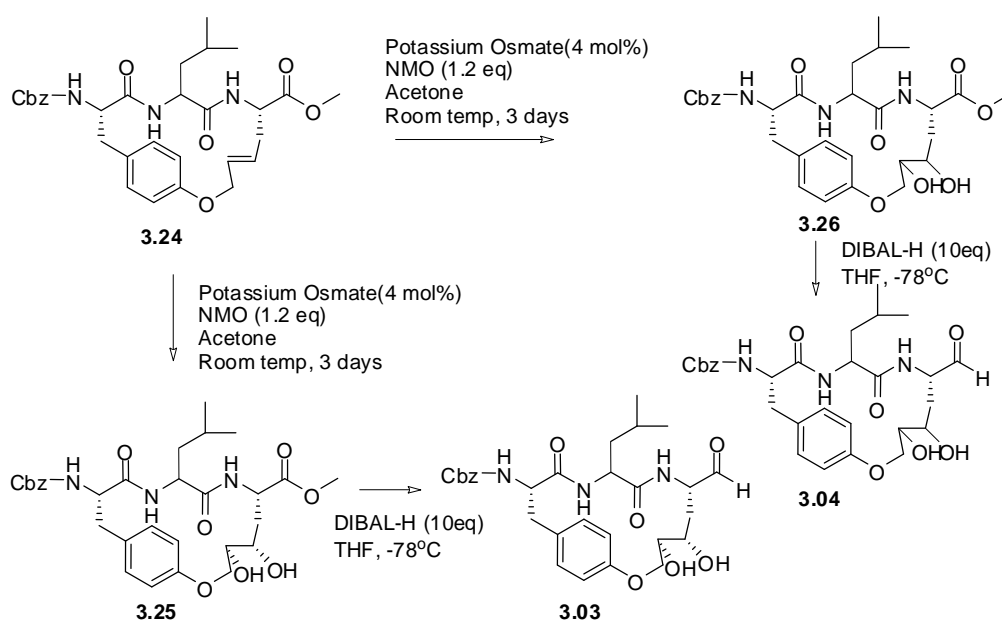


Scheme 3.4. Synthesis of macrocycle core **3.24**.

The acid **3.14** was coupled to Leu–OMe, in the presence of HATU to give dipeptide **3.15** in 93% yield. The methyl ester of **3.15** was hydrolysed on treatment with NaOH and the dipeptide acid **3.16** was then coupled to allyl–Gly–OMe.HCl on treatment with HATU to give diene **3.10** in 85% over two steps. Ring closing metathesis of diene **3.10** on treatment with Grubbs' second generation catalyst (3 mol %), under microwave conditions gave **3.17** in 62% after purification by recrystallisation from ethyl acetate. Alkene **3.17** was isolated after the metathesis and subsequent purification was assigned the E isomer on the basis of ^1H NMR (**Figure 3.15**). The coupling constants of the alkene protons H_a and H_b of **3.17** (5.40 ppm and 5.55 ppm) were measured to be $J = 15.7$ Hz. This is consistent with the assigned E geometry (11

– 18 Hz).⁴⁹ The lack of any doubling of resonances in both the ¹H and ¹³C spectra confirmed only one isomer was present.

Removal of the Boc protecting group of **3.17**, on treatment with thionyl chloride in methanol, gave **3.27** in >99% yield. The resulting amine **3.27** was treated with benzyl chloroformate to give **3.24** in 80% yield after recrystallisation.



Scheme 3.5. Synthesis of dihydroxylated inhibitors **3.03** and **3.04** from alkene precursor **3.24**.

Alkene **3.24** was treated with potassium osmate in the presence of N-methyl morpholine N-oxide over 72 h to give diastereoisomers **3.25** and **3.26** (**Scheme 3.5**). Purification of the mixture of diastereoisomers **3.25** and **3.26** by flash chromatography on silica gel gave a pure sample of **3.25** (>95% pure) and a mixture of **3.26** and **3.25** in an 85:15 ratio. The ¹H NMR of **3.25** did not reveal any of corresponding isomer **3.26**. The configuration of the purified diol was assigned on the basis of the coupling constants of the protons adjacent to the OH groups (protons H₁ – H₆ in **Figure 3.21**).

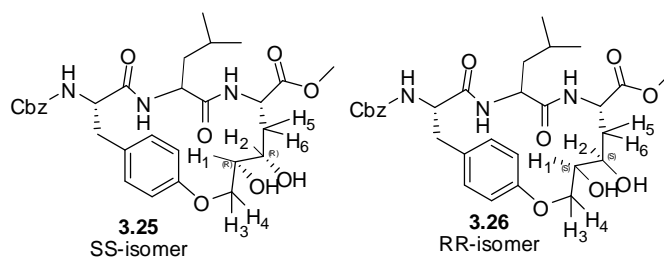


Figure 3.21. Diastereoisomers **3.25** and **3.26** with stereochemistry shown and key protons labeled H_1 - H_6

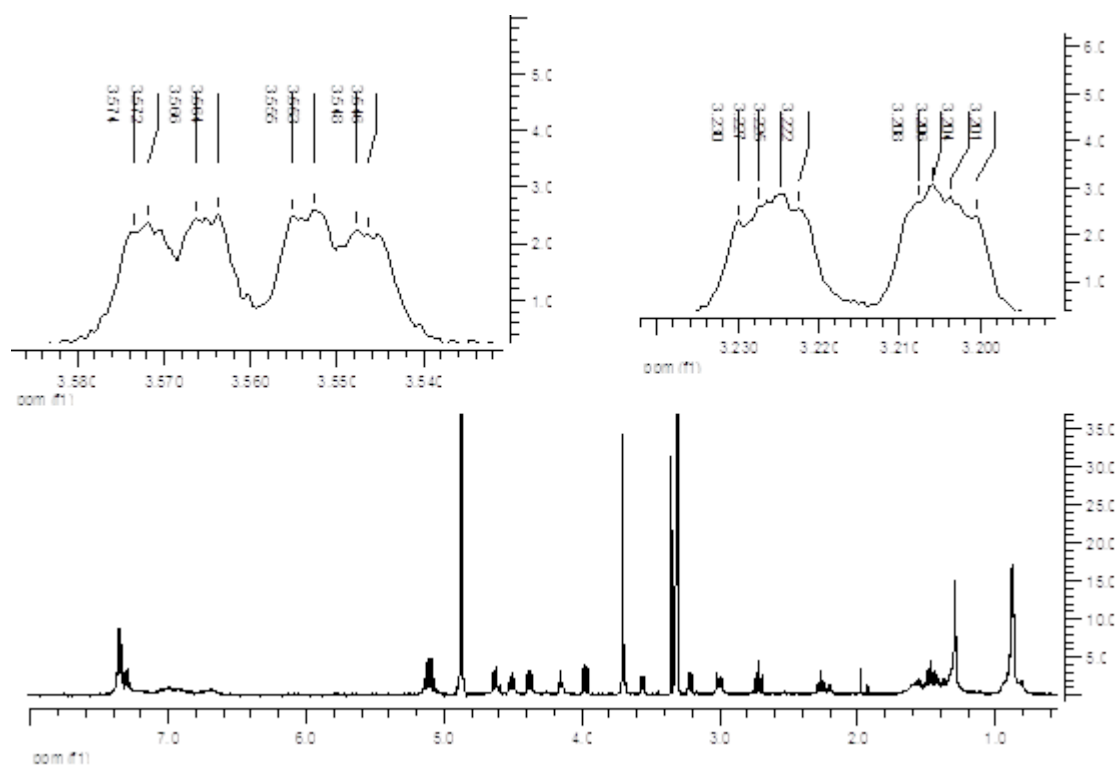
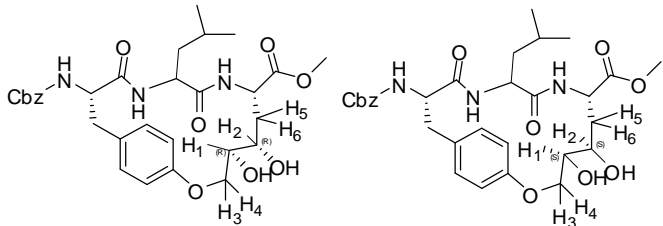


Figure 3.22. ^1H NMR spectrum of **3.25**. The ddd at 3.56 ppm corresponds to H_1 and the ddd at 3.22 ppm corresponds to H_2 . The coupling constants are calculated as $J=1.0, 4.0, 9.5$ Hz (for H_1) and $J=1.0, 2.5$ and 11.0 Hz for H_2 .

The coupling constants of H_1 (3.56 ppm, ddd, $J = 1.0, 4.0$ and 9.5 Hz) and H_2 (3.22 ppm, ddd, $J = 1.0, 2.5$ and 11.0 Hz) were measured from the ^1H NMR spectrum shown in **Figure 3.22**.

These coupling constants were compared to those predicted *in silico* for diols **3.25** and **3.26** by Dr Mc Nabb using molecular modelling. Models of the SS-isomer and

the RR-isomer were minimized and a conformational search was done on all conformers within 12 kJ/mol of the minimum. The dihedral angles (H_1-H_2 , H_1-H_3 , H_1-H_4 , H_2-H_5 and H_2-H_6 , **Figure 3.21**) of these conformers were calculated and used to generate the predicted coupling constants. These generated coupling constants were given a weighting according to the Boltzmann distribution and a Boltzmann weighted coupling constant for each coupling of H_1 and H_2 in the two isomers (SS- or RR-) was predicted. The measured coupling constants of H_1 and H_2 were compared to the predicted coupling constants to assign which isomer had been isolated (**Table 3.3**).



Coupling	J measured (Hz)	J predicted (Hz) SS isomer	J predicted (Hz) RR isomer
H_1-H_2	1.0	0.7-1.6	7.5
H_1-H_3	4.0	3.4	5.5
H_1-H_4	9.5	9.5	2.2
H_2-H_5	2.5	2.4	10.28
H_2-H_6	11.0	11.0	1.75

Table 3.3. Coupling constants predicted by conformational search and coupling constants measured by ^1H MNR for diastereoisomers **3.25** and **3.26**.

The measured coupling constants for H_1 and H_2 of **3.25** match very closely to the predicted coupling constants for the SS-isomer, indicating **3.25** is the SS-isomer.

Finally, the methyl ester **3.25** and the mixture of **3.26** and **3.25** (85:15) were separately reduced with 10 equivalents DIBAL at -78°C to give aldehyde **3.03** in 9% yield and an mixture of **3.04** and **3.03** (85:15) in 7% yield (**Scheme 3.5**). The low yields for the reduction reflect the small scale of reaction and reported difficulties with this kind of reduction.⁵³ Nevertheless sufficient samples of **3.03** and the **3.04:3.03** mixture were obtained for assay against calpain II (see **Chapter 4**).

3.4 Design and synthesis of novel macrocycle 3.05

A recent aim of the Abell group is to investigate the selectivity of our macrocycles in binding to more than one class of proteasome. Here, we begin to investigate the effect the P₁ and P₃ residues have on the selectivity of these macrocycles towards calpain II, α -chymotrypsin, and the chymotrypsin-like catalytic site of the 20S core.

3.4.1 Designing a macrocycle to investigate selectivity towards calpain II, α -chymotrypsin and 20S proteasome

In order to investigate the relative importance the P₁ and P₃ residues have in determining the selectivity of our macrocycles, a novel macrocyclic core was developed (**Figure 3.23**). Macrocycle **3.05** has the tyrosine residue at the P₁ position, rather than at the P₃ position in **CAT0811**.

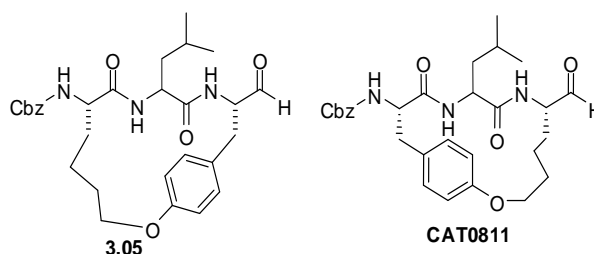


Figure 3.23. Proposed novel macrocycle 3.05

By synthesising macrocycle **3.05** and comparing the assay results against calpain II, α -chymotrypsin and the 20S core of the 26S proteasome with those of **CAT0811**, we aim to investigate the effect the P₃ and P₁ residues have on the selectivity of these macrocycles against the three target enzymes.

α -chymotrypsin was chosen for this study as it is a benchmark serine protease. The enzymes catalytic mechanism is well documented.^{54, 55}

The 20S core of the 26S proteasome was chosen due to its therapeutic importance. The 20S proteolytic core is a component of the 26S proteasome, which itself is part of the ubiquitin pathway.⁵⁶ The ubiquitin pathway is the major proteolytic system in eukaryote cells that plays an important role in cell turnover, apoptosis, transcription and cell signalling, as well as being a key process in the proliferation of tumour cells and inflammation due to proteolysis of the I κ B protein.⁵⁷ This makes the proteasome an attractive target for inhibition as potential anti-cancer and anti-inflammatory treatments. There are six β -units containing the catalytic sites of the proteasome which have the same proteolytic mechanism⁵⁶ but differ based on their substrate specificity and are named according to this preference rather than the active site residue.⁵⁸ The β_1 and β_1' sites cleave peptide bonds at the C-terminus of acidic residues and thus called capase-like. The β_2 and β_2' sites cleave after basic residues and are trypsin-like. The β_5 and β_5' sites are chymotrypsin-like.⁵⁶⁻⁵⁹ The chymotrypsin-like site will be the target of this work.

	P ₁	P ₂	P ₃
Calpain II	Wide variety tolerated	Leu Val	aromatic
α -chymotrypsin	Aromatic Tyr, Trp, Phe	Leu Val	α -amino acid
20S core	Aromatic or Leucine	Ill- defined	Wide variety tolerated

Table 3.4. Specificities of calpain II, α -chymotrypsin and the 20S core

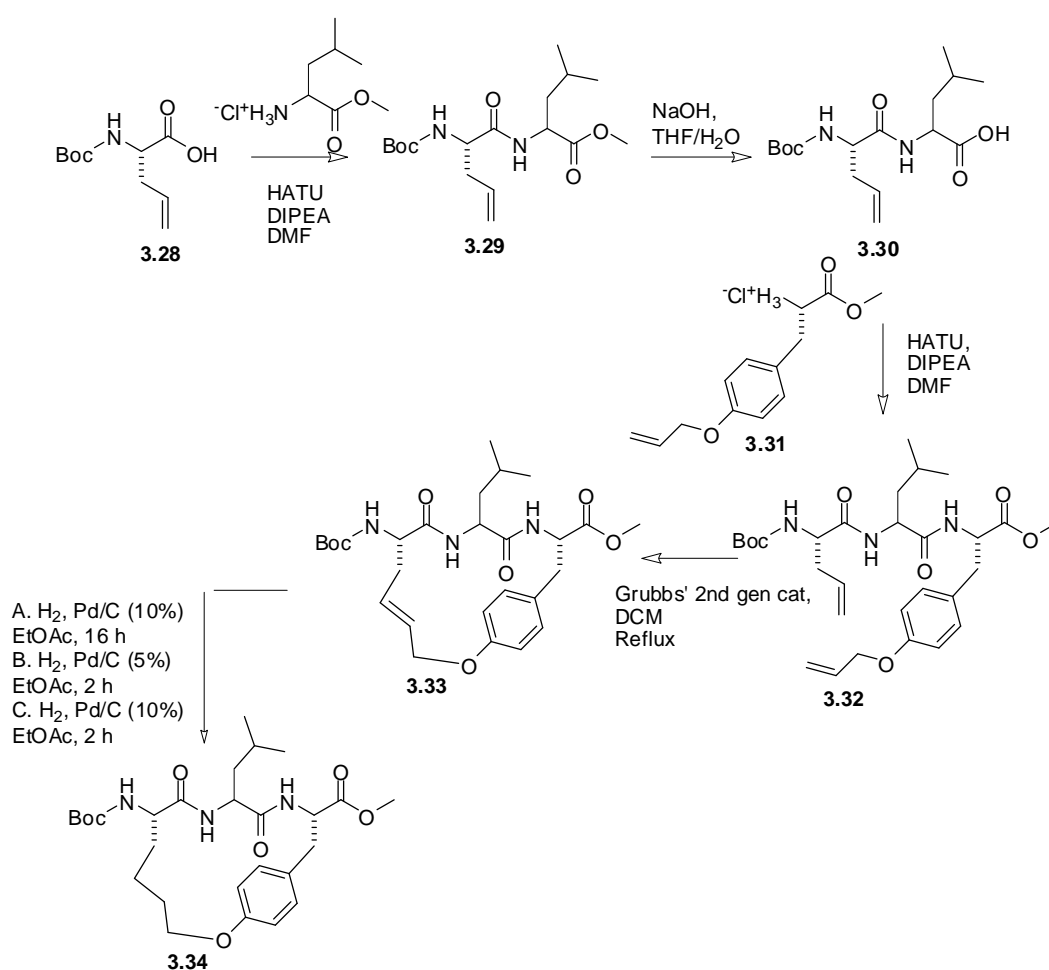
Examination of the substrate specificity of the calpain II, α -chymotrypsin and the 20S core (**Table 3.4**) reveals that the P₁ and P₃ residues should play an important role in determining selectivity. α -Chymotrypsin requires an aromatic group at the P₁ position to bind in the S₁ sub-site. Tyrosine is preferred here, followed by tryptophan and phenylalanine.⁶⁰ Calpain tolerates a wide variety of residues at P₁.³⁶ Both calpain and α -chymotrypsin favour leucine or valine at the P₂ position, however leucine is preferred for both enzymes.^{32, 61} Chymotrypsin is not specific as to what binds in the S₃ sub-site although unnatural (D-configured) amino acids are not tolerated.⁶⁰ The S₃ site of calpain is large and bulky aromatic groups are favoured at P₃.³⁶

Structure activity relationship studies on the specificity of 20S proteasome indicate there is evidence that the proposed macrocycle **3.05** could inhibit the chymotrypsin-like catalytic site of the proteasome.⁶²⁻⁶⁵ While leucine is the most common P₁ substituent of 20S proteasome inhibitors, there are a number of compounds published that have an aromatic group at P₁.⁶² The S₂ pocket of the chymotrypsin like sub-site of the 20S core is ill defined and is thought to be not critical for binding.^{59, 66} Bulky substituents are favoured at the P₂ site and leucine has precedence as an effective P₂ substituent.⁶⁷ The specificity of the proteasome at P₃ is more varied and a wider variety of residues are tolerated.⁶³

Macrocycle **3.05**, with tyrosine at P₁, should be a suitable comparator to **CAT0811** to determine the importance of the P₁ and P₃ residues on macrocyclic selectivity towards calpain II, α -chymotrypsin and the chymotrypsin-like sub-site of the 20S proteasome.

3.4.2 Synthesis of macrocycle 3.05

The synthesis of **3.05** is shown in **Scheme 3.6** and **Scheme 3.7**. **Scheme 3.6** describes the synthesis of compound **3.34**, the key precursor to **3.05**, by ring closing metathesis of a suitable diene. **Scheme 3.7** describes the transformation of **3.34** into the target **3.05** by functionalisation of the N-terminus with a Cbz group and conversion of the methyl ester to the C-terminal aldehyde.

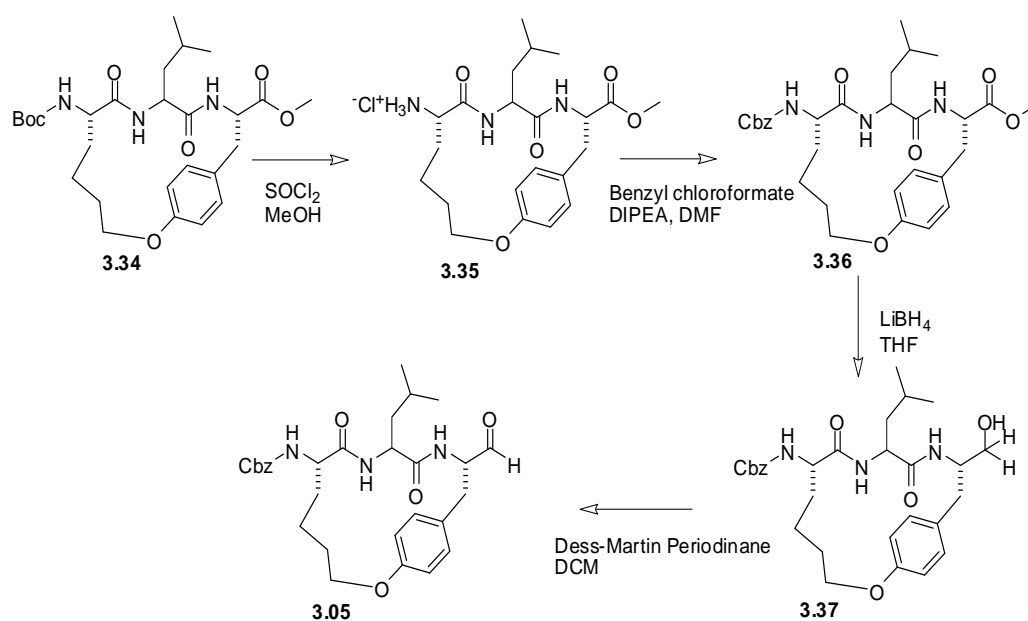


Scheme 3.6. Synthesis of the macrocyclic core **3.34**

Coupling of acid **3.28** to Leu-OMe.HCl in the presence of HATU and DIPEA gave dipeptide **3.29** in 89% yield. The methyl ester of **3.29** was hydrolysed on treatment with NaOH in THF/H₂O to give **3.30**. Coupling of the resulting acid **3.30** to methyl

ester **3.31** with HATU and DIPEA gave diene **3.32** in 73% yield over two steps. Ring closing metathesis of diene **3.32** on treatment with Grubbs' second generation catalyst (3 mol%) in refluxing DCM for 1 h gave **3.33** in 64%. Hydrogenation of alkene **3.33** with H₂ in the presence of 10% Pd/C (20% w/w) in methanol for 16 h (conditions **A**) gave **3.34** however two unidentified products were observed in the ¹H NMR. Milder hydrogenation conditions (**B**), where alkene **3.33** was treated with H₂ in the presence of 5% Pd/C (20% w/w catalyst/alkene) in ethyl acetate for 2 h, gave a mixture of starting material **3.33** and hydrogenated product **3.34** in a 2:1 ratio as judged by the relative integral ratios of the methyl ester peaks at 3.80 and 3.74 ppm in the ¹H NMR. The optimum conditions for the hydrogenation of alkene **3.33** involved treatment with H₂ in the presence of freshly purchased 10% Pd/C (50% w/w catalyst/alkene) in ethyl acetate for 2 h which gave **3.34** in 80% yield.

With the macrocyclic core **3.34** in hand; the synthesis of the aldehyde **3.05** was completed as shown in **Scheme 3.7**.



Scheme 3.7. Synthesis of aldehyde **3.05**

The Boc group of macrocycle **3.34** was cleaved on treatment with SOCl_2 in MeOH to give **3.35** in quantitative yield. Benzyl chloroformate was coupled to the resulting amine **3.35** to give **3.36** in 65% yield. Reduction of the methyl ester of **3.36** by LiBH_4 in THF gave alcohol **3.37** in 86%. Oxidation of the alcohol **3.37** by Dess-Martin periodinane in DCM gave aldehyde **3.05** in 62%.

The assay of aldehyde **3.05** against calpain II, α -chymotrypsin and the chymotrypsin-like site of the 20S core is described in **Chapter 4**.

3.5 Conclusions

Four macrocyclic calpain inhibitors based on modifications of **CAT0811** were synthesised. Firstly macrocyclic aldehyde **3.02** with an N-terminal FBS group was made by two ring closing metathesis routes. The first synthesis was analogous to the synthesis of **CAT0811** and involved coupling FBS onto macrocyclic core **3.19**. This gave **3.02** in 1% yield over all. This low yield is most likely due to the insolubility of the macrocycle during synthesis and purification. The second, novel, synthesis of **3.02** involved coupling the FBS moiety onto the more soluble dipeptide **3.20**. This, combined with an optimised ring closing metathesis step, gave the desired aldehyde in 33% over all. Should large quantities of these inhibitors be required to be made by ring closing metathesis for testing, compound **3.02** is an attractive alternative to **CAT0811**.

Secondly, diastereoisomers **3.03** and **3.04** (as a mixture of **3.04** and **3.03** in an 85:15 ratio) were prepared by Sharpless dihydroxylation of the alkene resulting from ring closing metathesis to give a diol group at the P₁ position of the macrocyclic ring. The aim of this modification is to increase the binding affinity of the inhibitor to calpain II and to increase specificity by targeting hydrophilic regions of calpain specific to the enzyme. The effectiveness of these modifications in the inhibition of calpain II is discussed in **Chapter 4**.

Thirdly, macrocycle **3.05** was prepared by a ring closing metathesis based synthesis. Aldehyde **3.05** has an aromatic substituent at P₁, in contrast with **CAT0811** which has an aromatic substituent at P₃. We intend to investigate the relative importance of having an aromatic substituent at P₁ or P₃ on the inhibition and selectivity of **3.05** and

CAT0811 against calpain II, α -chymotrypsin and the 20S core of the 26S proteasome. The effectiveness of this strategy is discussed in **Chapter 4**.

References

1. Dear, T. N.; Boehm, T., *Gene* **2001**, *274*, 245-252.
2. Mellgren, R. L., *Federation of American Societies for Experimental Biology* **1987**, *1*, 110-115.
3. Goli, D. E.; Thompson, V. F.; Li, H.; Wei, W.; Cong, J., *Physiological Reviews* **2003**, *83*, 731-801.
4. Ohno, S.; Emori, Y.; Imajoh, S.; Kawasaki, H.; Kisaragi, M.; Suzuki, K., *Nature* **1984**, *312*, 566-570.
5. Sorimachi, H.; Suzuki, K., *Journal of Biochemistry* **2001**, *129*, 653-664.
6. Moldoveanu, T.; Hosfield, C. M.; Lim, D.; Elce, J. S.; Jia, Z.; Davies, P. L., *Cell* **2002**, *108*, 649-660.
7. Hosfield, C. M.; Elce, J. S.; Davies, P. L.; Jia, Z., *European Molecular Biology Organization Journal* **1999**, *18*, 6880-6889.
8. Strobl, S.; Fernandez-Catalan, C.; Braun, M.; Huber, R.; Masumoto, H.; Nakagawa, K.; Irie, A.; Sorimachi, H.; Bourenkow, G.; Bartunik, H.; Suzuki, K., *Proceedings of the National Academy of Sciences USA* **2000**, *97*, 588-592.
9. Tompa, P.; Emori, Y.; Sorimachi, H.; Suzuki, K.; Friedrich, P., *Biochemical and Biophysical Research Communications* **2001**, *280*, 1333-1339.
10. Dutt, P.; Spriggs, C. N.; Davies, P. L.; Jia, Z.; Elce, J. S., *Biochemical Journal* **2002**, *367*, 263-269.
11. Kamphuis, I. G.; Kalk, K. H.; Swarte, M. B. A.; Drenth, J., *Journal of Molecular Biology* **1984**, *179*, 233-256.

12. Leung, D.; Abbenante, G.; Fairlie, D. P., *Journal of Medicinal Chemistry* **2000**, *43*, 305-341.
13. Wang, K. K. W.; Po-Wai, Y., *Trends in Pharmacological Sciences* **1994**, *15* (11), 412-419.
14. Biswas, S.; Harris, F.; Singh, J.; Phoenix, D., *Molecular and Cellular Biochemistry* **2004**, *261* (1), 151-159.
15. Vanderklish, P. W.; Bahr, B. A., *International Journal of Experimental Pathology* **2000**, *81* (5), 323-339.
16. Tsuji, T.; Shimohama, S.; Kimura, J.; Shimizu, K., *Neuroscience Letters* **1998**, *248* (2), 109-112.
17. Papp, Z. n.; van der Velden, J.; Stienen, G. J. M., *Cardiovascular Research* **2000**, *45* (4), 981-993.
18. Sandmann, S.; Yu, M.; Unger, T., *British Journal of Pharmacology* **2001**, *132* (3), 767-777.
19. David, L. L.; Shearer, T. R., *Federation of European Biochemical Societies* **1993**, *324*, 265-270.
20. David, L. L.; Shearer, T. R.; Shih, M., *Journal of Biological Chemistry* **1993**, *268*, 1937-1940.
21. Nakamura, Y.; Fukiage, C.; Shih, M.; Ma, H.; David, L. L.; Azuma, M.; Shearer, T. R., *Investigative Ophthalmology & Visual Science* **2000**, *41*, 1460-1466.
22. Biswas, S.; Harris, F.; Dennison, S.; Singh, J.; Phoenix, D. A., *Trends in Molecular Medicine* **2004**, *10*, 78-84.
23. www.cvr.org.au (accessed 9 August 2011).

-
24. Congdon, N.; O'Colmain, B.; Klaver, C. C.; Klein, R.; Munoz, B.; Friedman, D. S.; Kempen, J.; Taylor, H. R.; Mitchell, P., *Archives of Ophthalmology* **2004**, *122* (4), 477-85.
 25. Hodge, W.; Horsley, T.; Albiani, D.; Baryla, J.; Belliveau, M.; Buhrmann, R.; O'Connor, M.; Blair, J.; Lowcock, E., *Canadian Medical Association Journal* **2007**, *176* (9), 1285-1290.
 26. Azuma, M.; Fukiage, C.; David, L. L.; Shearer, T. R., *Experimental Eye Research* **1997**, *64*, 529-538.
 27. Fukiage, C.; Azuma, M.; Nakamura, Y.; Tamada, Y.; Nakamura, M.; Shearer, T. R., *Biochimica et Biophysica Acta (BBA) - Molecular Basis of Disease* **1997**, *1361* (3), 304-312.
 28. Abell, A. D.; Jones, M. A.; Coxon, J. M.; Morton, J. D.; Aitken, S. G.; McNabb, S. B.; Lee, H. Y.-Y.; Mehrtens, J. M.; Alexander, N. A.; Stuart, B. G.; Neffe, A. T.; Bickerstaffe, R., *Angewandte Chemie International Edition* **2009**, *48*, 1455-1458.
 29. Neffe, A. T.; Abell, A. D., *Current Opinion in Drug Discovery and Development* **2005**, *8*, 684-700.
 30. Pietsch, M.; Chua, K. C. H.; Abell, A. D., *Current Topics in Medicinal Chemistry* **Accepted**.
 31. Azuma, M.; Yoshida, Y.; Sakamoto, Y.; Inoue, J. Pharmaceutical composition containing an arylsulfonyl dipeptide aldehyde for prophylaxis and therapy of diseases associated with ocular fundus tissue cytopathy. **1999**.
 32. Inoue, J.; Nakamura, M.; Cui, Y.-S.; Sakai, Y.; Sakai, O.; Hill, J. R.; Wang, K. K. W.; Yuen, P.-W., *Journal of Medicinal Chemistry* **2003**, *46*, 868-871.

-
33. Schechter, I.; Berger, A., *Biochemical and Biophysical Research Communications* **1967**, 27 (2), 157-162.
 34. Turk, B., *Nat Rev Drug Discov* **2006**, 5 (9), 785-799.
 35. Moldoveanu, T.; Campbell, R. L.; Cuerrier, D.; Davies, P. L., *Journal of Molecular Biology* **2004**, 343, 1313-1326.
 36. Donkor, I. O., A survey of Calpain Inhibitors. In *Current Medicinal Chemistry*, Bentham Science Publishers Ltd.: 2000; Vol. 7, p 1171.
 37. Stuart, B. Molecular Modelling for Enzyme-Inhibition: A Search for a New Treatment for Cataract and New Antimicrobials and Herbicides Christchurch, **2010**.
 38. Tyndall, J. D. A.; Nall, T.; Fairlie, D. P., *Chemical Reviews* **2005**, 105, 973-999.
 39. Abell, A. D.; Brown, K. M.; Coxon, J. M.; Jones, M. A.; Miyamoto, S.; Neffe, A. T.; Nikkel, J. M.; Stuart, B. G., *Peptides* **2005**, 26, 251-258.
 40. Loughlin, W. A.; Tyndall, J. D. A.; Glenn, M. P.; Fairlie, D. P., *Chemical Reviews* **2004**, 104 (12), 6085-6118.
 41. Abbenante, G.; March, D. R.; Bergman, D. A.; Hunt, P. A.; Garnham, B.; Dancer, R. J.; Martin, J. L.; Fairlie, D. P., *Journal of the American Chemistry Society* **1995**, 117, 10220 - 10226.
 42. Rezai, T.; Yu, B.; Millhauser, G. L.; Jacobson, M. P.; Lokey, R. S., *Journal of the American Chemical Society* **2006**, 128 (8), 2510-2511.
 43. Driggers, E. M.; Hale, S. P.; Lee, J.; Terrett, N. K., *Nature Reviews Drug Discovery* **2008**, 7 (7), 608-624.
 44. Marsault, E.; Peterson, M. L., *Journal of Medicinal Chemistry* **2011**, 54, 1961-2004.

-
45. Fairlie, D. P.; Abbenante, G.; March, D. R., *Current Medicinal Chemistry* **1995**, 2 (2), 654-686.
 46. Donkor, I. O., *Current Medicinal Chemistry* **2000**, 7, 1171-1188.
 47. Jiao, W. *Clan CA Cystein Proteases: Selectivity and Structure Comparison*. University of Canterbury, Christchurch, **2007**.
 48. Jones, S. A. *Beta-Strand Mimicry as the Basis for a Universal Approach to Protease Inhibitor*. University of Adelaide, Adelaide, **2011**.
 49. Pavia, D. L.; Lampman, G. M.; Kriz, G. S.; Vyvyan, J. M., *Introduction to Spectroscopy*. 2009.
 50. Duncan, J., Honours thesis. 2006.
 51. Aitken, S. G. *Design, synthesis and testing of β -strand mimics as protease inhibitors* University of Canterbury, Christchurch, **2006**.
 52. The glide score is a reflection of the relative binding energy of each ligand to the enzyme. A large number of parameters are used to calculate this score, however the number and strength of hydrogen bonds that the molecule forms with calpain provides a major contribution. For 6 the glide score is -9.5 which is comparable to the glide score for CAT0811 of -8.60. The lower the glide score the better the estimated binding energy.
 53. Dondoni, A.; Perrone, D., *Organic Syntheses* **2000**, 77, 64.
 54. Leung, D.; Abbenante, G.; Fairlie, D. P., *Journal of Medicinal Chemistry* **2000**, 43 (3), 305-341.
 55. Walker, B.; Lynas, J. F., *Cellular and Molecular Life Sciences* **2001**, 58 (4), 596-624.
 56. Kisselev, A. F.; Goldberg, A. L., *Chemistry & Biology* **2001**, 8 (8), 739-758.

-
57. Meiners, S.; Ludwig, A.; Stangl, V.; Stangl, K., *Medicinal Research Reviews* **2008**, 28 (2), 309-327.
 58. Groll, M.; Ditzel, L.; Lowe, J.; Stock, D.; Bochtler, M.; Bartunik, H. D.; Huber, R., *Nature* **1997**, 386 (6624), 463-471.
 59. Borissenko, L.; Groll, M., *Chemical Reviews* **2007**, 107 (3), 687-717.
 60. Schellenberger, V.; Braune, K.; Hofmann, H.-J.; Jakubke, H.-D., *European Journal of Biochemistry* **1991**, 199 (3), 623-636.
 61. Bauer, C.-A., *European Journal of Biochemistry* **1980**, 105 (3), 565-570.
 62. Huber, E. M.; Groll, M., *Angewandte Chemie International Edition* 51 (35), 8708-8720.
 63. Harris, J. L.; Alper, P. B.; Li, J.; Rechsteiner, M.; Backes, B. J., *Chemistry & Biology* **2001**, 8 (12), 1131-1141.
 64. de Bettignies, G.; Coux, O., *Biochimie* 92 (11), 1530-1545.
 65. Zhu, Y.-Q.; Pei, J.-F.; Liu, Z.-M.; Lai, L.-H.; Cui, J.-R.; Li, R.-T., *Bioorganic & Medicinal Chemistry* **2006**, 14 (5), 1483-1496.
 66. Braun, H. A.; Umbreen, S.; Groll, M.; Kuckelkorn, U.; Mlynarczuk, I.; Wigand, M. E.; Drung, I.; Kloetzel, P.-M.; Schmidt, B., *Journal of Biological Chemistry* **2005**, 280 (31), 28394-28401.
 67. Rock, K. L.; Gramm, C.; Rothstein, L.; Clark, K.; Stein, R.; Dick, L.; Hwang, D.; Goldberg, A. L., *Cell* **1994**, 78 (5), 761-771.

CHAPTER FOUR

IN VITRO TESTING OF MACROCYCLES SYNTHESISED IN CHAPTER 3

4 *In vitro* testing of macrocycles synthesised in Chapter 3.

4.1 Introduction

In Chapter 3 the design rationale and synthesis of compounds **3.02**, **3.03**, **3.04** and **3.05** (Figure 4.1) was described. In Sections 4.2 and 4.3 we report the assay results against calpain II for compounds **3.02**, **3.03** and **3.04**. These results are discussed in the context of the full SAR study completed by the Abell group on these types of macrocycles to identify the criteria for the most potent macrocyclic calpain inhibitor.

In Section 4.4 the assay results for compound **3.05** against calpain II, α -chymotrypsin and the 20S proteasome are reported. The effect the P₁ P₂ and P₃ residues have on the selectivity of the macrocycles against these three targets is discussed.

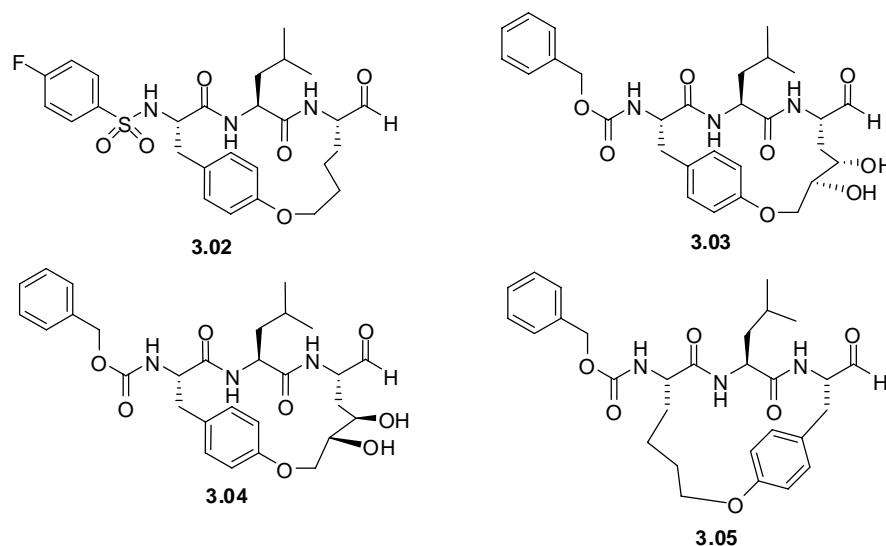


Figure 4.1 Macrocycles designed and synthesised in Chapter 3.

4.2 Assay of compounds **3.02**, **3.03** and **3.04** against ovine calpain II

The inhibitory activity of **3.02**, **3.03** and an inseparable mixture, containing **3.04** and **3.03** in a ratio of 85:15, was determined by measuring inhibition constants (IC_{50}) in a competitive binding assay against ovine calpain II.¹ The assays were performed using calpain II, which was purified from sheep lung by ion-exchange chromatography.² The calpain was diluted to give a linear response over the course of the assay. Casein labelled with fluorophore 4,4-difluoro-5,7-dimethyl-4-bora-3a,4a-diaza-s-indacene-3-propionic acid (BODIPY) was used as the substrate. BODIPY does not fluoresce in the absence of proteolysis of the casein by calpain. This is due to auto-quenching of adjacent fluorophores, however in the presence of activated calpain, the casein is proteolysed and fluorescence from the BODIPY is observed. Inhibition of calpain results in less proteolysis of casein and a corresponding reduction of BODIPY fluorescence. This change in fluorescence enables the IC_{50} to be calculated. The assay results of compounds **3.02**, **3.03** and the mixture of **3.04** and **3.03** are reported in **Table 4.1**.

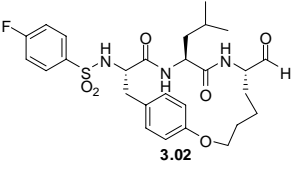
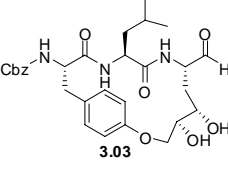
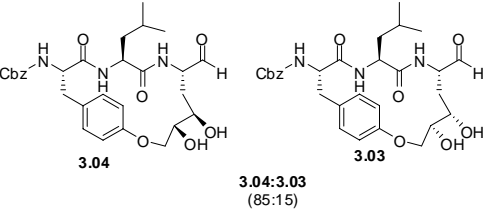
Compound	IC ₅₀ Calpain II (μM)
 <p style="text-align: center;">3.02</p>	0.045
 <p style="text-align: center;">3.03</p>	3.7
 <p style="text-align: center;">3.04 3.03 3.04:3.03 (85:15)</p>	>50

Table 4.1. IC₅₀ values of **3.02**, **3.03** and the mixture of **3.04** and **3.03** against ovine calpain II. IC₅₀ values given in μM concentrations.

Compound **3.02** was found to be a potent inhibitor of calpain II with an IC₅₀ of 0.045 μM that is comparable to that of **CAT0811** (IC₅₀ = 0.03 μM).³ An FBS group was incorporated at the N-terminus of **3.02** to allow for hydrogen bonding to the S₄ pocket of the enzyme (through the sulfonyl oxygens). The FBS moiety also enabled new synthetic approaches to the base macrocycle to be investigated that were otherwise not possible with Cbz group (see **Chapter 3** for more detail). This assay result confirms our hypothesis that the FBS moiety is a potent N-terminal group for macrocyclic inhibitors of calpain II. This is in line with results from acyclic inhibitors, where **SJA6017**, a di-peptidic aldehyde with an N-terminal FBS group, has an IC₅₀ of 0.049 μM against calpain II.⁴ Macrocycle **3.02**, with a comparable IC₅₀ and more efficient synthesis, is an attractive alternative to **CAT0811** should large

quantities of the inhibitor be required, for example in *in vivo* testing. The optimised yield of **3.02**, as reported in **Chapter 3**, is 33% which compares to a reported yield of 1% for **CAT0811**.³

Compound **3.03** was found to have an IC_{50} of 3.7 μ M against calpain while the mixture containing **3.04** and **3.03** (in an 85:15 ratio) had an IC_{50} of >50 μ M against calpain. These results reveal **3.03** as a modest inhibitor of ovine calpain II and **3.04** as essentially inactive. We concluded that incorporation of a diol substituent at P₁ was not compatible with binding to calpain. Given that diol **3.03** was significantly less active than the modelling suggested (as described in **Chapter 3**), we thus decided to further investigate the modelling of these compounds using an improved ovine model that had recently become available. This model was not available when the synthesis of these compounds was undertaken, however it is now thought to be the best available to rationalise the assay results.⁵ Compound **3.03** was thus docked in the ovine calpain II model prepared by Dr Stephen McNabb in the same manner as the mini-rat calpain model (**Chapter 3**). The modelling results are summarised in **Table 4.2**.

Compound	No. poses generated	No. poses with WHD < 4.5	best representative pose			
			H-bonds	WHD	Emodel	Gscore
3.03	19	9	B,C	3.41	-69.07	-6.09
CAT0811	11	4	A,B,C	3.95	-63.04	-5.67

Table 4.2. Modelling results of compound **3.03** compared with **CAT0811** in the ovine calpain II model. WHD stands for warhead distance - the distance from the aldehyde warhead to the Cys115 residue. Hydrogen bonds ABC describe hydrogen bonds to the carbonyl of Gly208, the NH of Gly208 and the carbonyl of Gly 271 respectively.

The ovine modelling results reported in **Table 4.2** suggest that the diol aldehyde **3.03** forms only two of the three key hydrogen bonds to calpain (the B and C bonds shown in **Figure 4.2a**). In comparison, **CAT0811** forms three hydrogen bonds to calpain under the same docking conditions (**Figure 4.2b**). The fact that there are low energy conformers of **3.03** that do not adopt a β -strand configuration (40% of low energy conformers did not adopt a β -strand conformation – see **Chapter 3**), and its inability to form the A hydrogen bond to Gly208, (**Figure 4.2**) provides a possible explanation for the reduced activity of **3.03** against ovine calpain II compared to **CAT0811**.

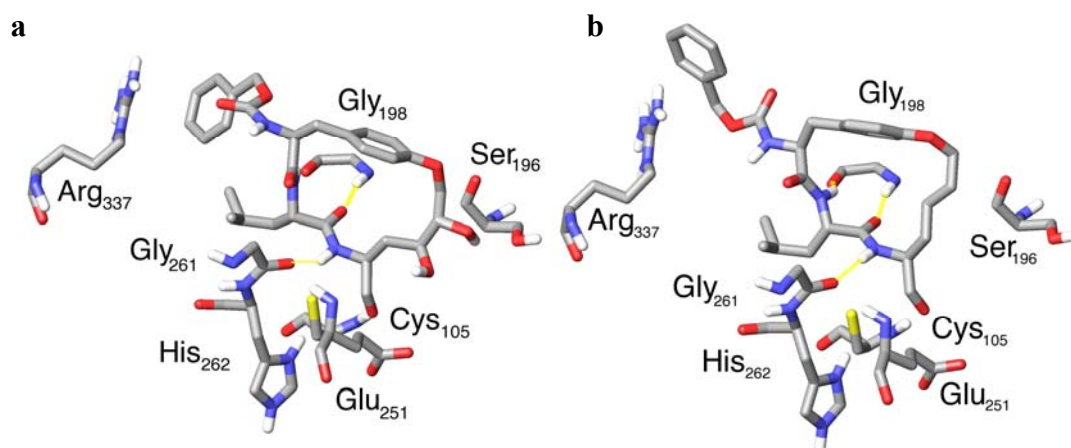


Figure 4.2. Best pose of **3.03** (a) and **CAT0811** (b) showing H-bonding to the active site of the ovine calpain II construct. The diol **3.03** has a cis conformation at the Cbz amide bond and has only two hydrogen bonds compared to the three hydrogen bonds shown for **CAT0811**.

The differences observed between the ovine calpain II modelling results and the rat calpain I modelling results described in **Chapter 3** presumably arose from the differences in the enzymes' homology. There is only 51% sequence homology between rat calpain I and ovine calpain II.⁵ This is largely due to differences between the calpain I and II isoforms. As all our IC₅₀ values are measured by assay against ovine calpain II, the ovine model would reasonably be expected to give a more

accurate prediction of the potency of potential inhibitors in our assay than the rat model. Additionally, the human calpain sequences have a higher sequence homology with ovine calpain than rat calpain (94% compared to 89%).⁵ This makes the ovine model more useful for predicting the potential for these inhibitors to be used as human therapeutics. Based on these results we would suggest that all future modelling in this area be done using an ovine calpain model.

4.3 Analysis of calpain II inhibition data

The compounds reported in **Section 4.1** of this chapter were developed as part of a series of tri-peptidic macrocyclic calpain II inhibitors. A total of 31 macrocycles have been synthesised in the Abell group that focus on each of the four domains identified in **Figure 4.3**,⁶⁻⁸ the N-terminus (domain 1), the P₂ position (domain 2), the C-terminus (domain 3), and the macrocycle (domain 4).

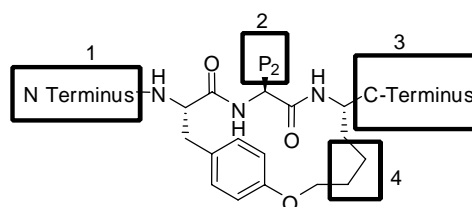


Figure 4.3. Four key areas of the macrocycle

A summary of the IC₅₀ values for the macrocycles, including the new derivatives reported in this thesis, is shown in **Table 4.3**, **Table 4.4** and **Table 4.5**, with a discussion of this series described below.

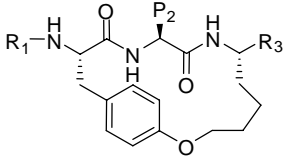
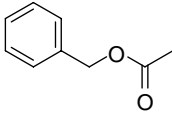
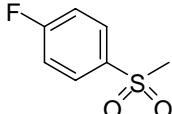
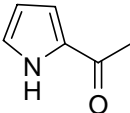
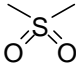
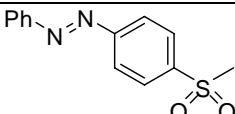
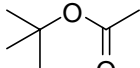
 General macrocyclic structure				
R ₁	Compound	P ₂	R ₃	IC ₅₀
	CAT0811	Leu	CHO	0.03
	4.01	Val	CHO	0.24
	4.02	Ileu	CHO	5.0
	4.03	Leu	CHN ₂ CONH ₂	0.16
	4.04	Leu	CH ₂ OH	0.7
	4.05	Val	CH ₂ OH	1.6
	4.06	Ileu	CH ₂ OH	7.1
	4.07	Leu	C(OH)CN	8.9
	4.08	Leu	CH ₂ N ₃	>50
	3.02	Leu	CHO	0.045
	4.09	Val	CHO	0.28
	4.10	Ileu	CHO	2.6
	4.11	Leu	CH ₂ OH	0.9
	4.12	Val	CH ₂ OH	1.1
	4.13	Ileu	CH ₂ OH	>50
	4.14	Val	CO ₂ CH ₃	>50
	4.15	Val	CHO	0.7
	4.16	Val	CH ₂ CHO	>50
	4.17	Val	CHO	0.95
	4.18	Val	CH ₂ CHO	>50
	4.19	Leu	CHO	1.5
	4.20	Leu	CH ₂ OH	2.5
	4.21	Val	CH ₂ OH	>50

Table 4.3. IC₅₀ values for macrocyclic calpain inhibitors showing the effect on calpain II potency of changing the electrophilic C-terminus (R₁), the P₂ amino acid and the N-terminal group (R₃). IC₅₀ values shown are reported in μM concentrations.

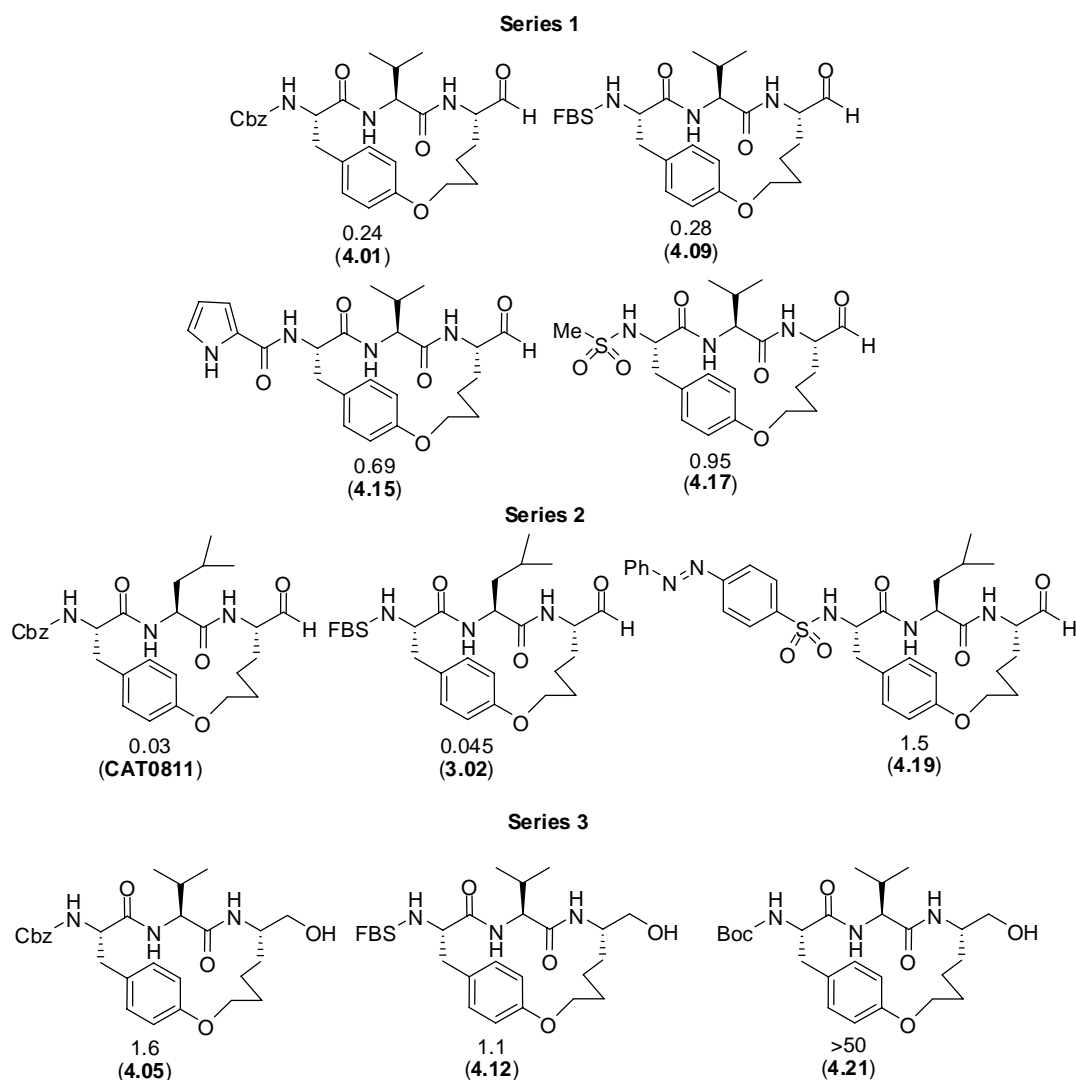
Modification at R_1 (N-terminus):

Figure 4.4. Effect of varying the N-terminus. IC_{50} values are listed below each macrocycle and are reported in μM concentrations. Compound codes are listed in parentheses.

The N-terminal group of the macrocycles is thought to extend into the S_4 binding pocket of calpain II where an aromatic group, with hetero atoms able to hydrogen bond to the enzyme, is preferred.⁹ We have compared the effect of six N-terminal groups – Cbz, FBS, MeSO₂, pyrrole, 4-(phenyldiazo) benzene sulfonyl and Boc substituents – across three series of compounds (**Figure 4.4**). The first series has valine at P_2 and a C-terminal aldehyde, see **4.01** (N-terminal Cbz), **4.09**, (FBS) **4.15** (pyrrole) and **4.17** (MeSO₂). The second series has leucine at P_2 and a C-terminal

aldehyde, see **CAT0811** (N-terminal Cbz), **3.02** (FBS) and **4.19** (4-(phenyldiazo) benzene sulfonyl). The third series has valine at P₂ and a C-terminal alcohol, see **4.05** (N-terminal Cbz), **4.12** (FBS) and **4.21** (Boc).

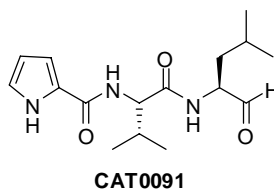


Figure 4.5. CAT0091 with an N-terminal pyrrole.

An N-terminal Cbz group has been shown in our labs to be favoured for inhibition, for example **CAT0811** has an IC₅₀ of 0.03 μM.³ Similarity, FBS results in compounds that are potent inhibitors of calpain, for example **3.02** (IC₅₀ = 0.045 μM). An N-terminal pyrrole conferred excellent activity in acyclic calpain inhibitors such as **CAT0091** (**Figure 4.5**) which has an IC₅₀ of 0.14 μM against calpain II.⁵ By comparison, the macrocyclic pyrrole analogue **4.15** was less potent than the Cbz analogue **4.01** or FBS analogue **4.09** with an IC₅₀ of 0.69 μM. Macrocyclic **4.17** (IC₅₀ = 0.95 μM), with an N-terminal MeSO₂ group, is significantly less potent than the FBS analogue **4.09** (IC₅₀ = 0.28 μM). MeSO₂, a truncated analogue of FBS, was chosen to investigate the relative importance of an aromatic substituent in the S₄ binding pocket, thus an aromatic group at S₄ would appear important for optimum enzyme binding in line with previous literature.⁹ Macrocyclic **4.19** (IC₅₀ = 1.5 μM), with an N-terminal 4-(phenyldiazo) benzene sulfonyl moiety, was 50 fold less active against calpain II than Cbz analogue **CAT0811**. The 4-(phenyldiazo) benzene sulfonyl group is a larger substituent than Cbz and the lower activity of **4.19** compared to **CAT0811** is possibly due to Cbz being a better fit in the S₄ binding pocket. Docking studies of **4.19** and **CAT0811** in the ovine calpain II model support

this hypothesis with **CAT0811** having a lower Glide score than **4.19** (-9.32 and -6.22 respectively). These Glide scores suggest **CAT0811** has a higher binding affinity to the enzyme than **4.19**. The macrocycle **4.21**, with an N-terminal Boc group, was essentially inactive against calpain ($IC_{50} > 50 \mu M$), while Cbz analogue **4.05** and FBS analogue **4.12** had IC_{50} values of 1.6 and 1.1 μM respectively. The reduced activity imparted by an N-terminal Boc group is not surprising given the already mentioned preference for an aromatic group at this position. Interestingly an N-Boc group is hydrophobic but this does not appear to be sufficient for binding.

Given the excellent inhibition conferred by Cbz and FBS (see compounds **CAT0811**, and **3.02**, **Figure 4.4**) compared to the other N-terminal groups discussed above, we suggests either FBS or Cbz to be the optimum R_1 substituents for future work.

Modification at P_2 :

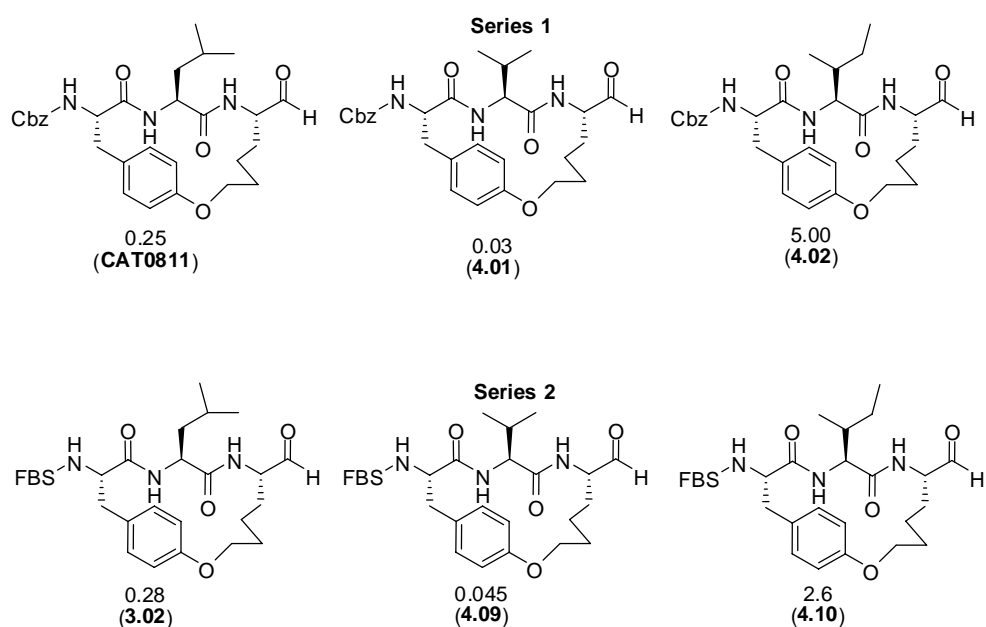


Figure 4.6. Effect of changing the P_2 amino acid. IC_{50} values are listed below each macrocycle and are reported in μM concentrations. Compound codes are listed in parentheses.

The relative effect of incorporating leucine, valine or iso-leucine at the P₂ position of calpain II inhibitors has been studied through two series of compounds typified by **CAT0811**, **4.01** and **4.02** (series one, **Figure 4.6**) and **3.02**, **4.09** and **4.10** (series two, **Figure 4.6**) The first series has Cbz at the N-terminus and the second FBS. Both series contain an optimum C-terminal aldehyde for activity. Macrocycles with a leucine residue at P₂ are 6 – 8 times more active than corresponding macrocycles with a valine residue at this position, for example compare **CAT0811** (IC₅₀ = 0.03 μM) with **4.01** (IC₅₀ = 0.25 μM) or compare **3.02** (IC₅₀ = 0.045 μM) with **4.09** (IC₅₀ = 0.28 μM). Docking of macrocycles **CAT0811** and **4.01** into the ovine calpain II model suggests leucine to be a better fit into the deep hydrophobic S₂ pocket of calpain.¹⁰ This is consistent with other studies on calpain inhibitors that similarly identify a preference for leucine at P₂.¹¹ Incorporation of iso-leucine at P₂ of the macrocycles results in a significant loss of activity against calpain II compared to leucine analogues. Macrocycle **4.02** (IC₅₀ = 5.0 μM) is 166 times less active than **CAT0811** and **4.10** (IC₅₀ = 2.6 μM) is 58 times less active than **3.02**.

Modification at R₃ (C-terminus).

A range of C-terminal groups within the macrocyclic inhibitors were investigated, particularly an aldehyde, alcohol, azide, semicarbazone, cyanohydrin, methyl ester or homologated aldehyde. Each of the C-terminal groups was expected to interact with the active site cysteine of calpain II.

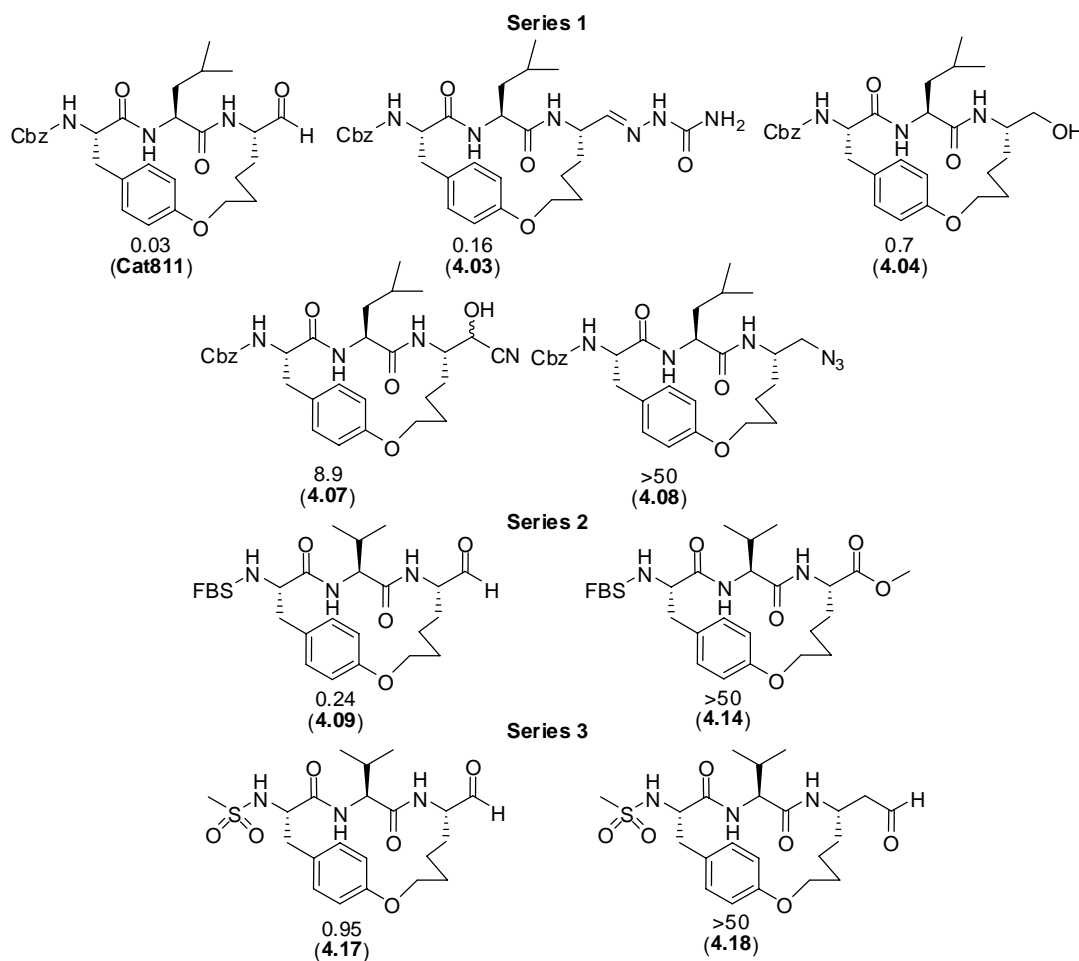


Figure 4.7. Macrocycles with C-terminal group varied. IC_{50} values are listed below each macrocycle and are reported in μM concentrations. Compound codes are listed in parentheses.

We have compared the effect of the seven C-terminal groups across three series of compounds as shown in **Figure 4.7**. The first series has Cbz at the N-terminus and leucine at P_2 , see aldehyde **CAT0811**, semicarbazone **4.03**, alcohol **4.04**, cyanohydrin **4.07** and azido **4.08**. The second series has FBS at the N-terminus and valine at P_2 , see aldehyde **4.09** and methyl ester **4.14**. The third series has MeSO_2 at the N-terminus and valine at P_2 , see aldehyde **4.17** and homologated aldehyde **4.18**. As expected¹² an aldehyde proved the most effective C-terminal group; **CAT0811**, **4.09** and **4.17** all display potent inhibition of calpain (IC_{50} values = 0.03, 0.24 and 0.95 μM respectively). The aldehyde group is known to allow covalent (reversible) inhibition of calpain.¹² However, this group does allow for indiscriminate interaction with other

nucleophiles, particularly *in vivo*. For example aldehydes are also known to be potent inhibitors of numerous cysteine and serine proteases, not exclusively calpain.¹²⁻¹⁴ Aldehydes are not optimal for incorporation into a drug due to low bioavailability and selectivity and hence undesired side effects.¹⁴ Macrocycle **4.03**, with a C-terminal semicarbazone, is the most potent non-aldehyde-based inhibitor with an $IC_{50} = 0.16 \mu\text{M}$ against calpain II. The semicarbazone might also be expected to form a reversible interaction with the enzyme via a tetrahedral adduct resulting from attack of the active site cysteine on the protected carbonyl carbon.¹² Such a group is considered non-drug-like due to its promiscuous reactivity and poor stability.¹⁵ In order to avoid the potential problems associated with the aldehyde and semicarbazone C-terminal groups outlined above, a series of macrocycles with C-terminal groups designed to form non-covalent interactions within the calpain II active site were developed. These macrocycles contained a C-terminal alcohol (**4.04**), cyanohydrin (**4.07**) or azido (**4.08**) substituent.

The alcohol moiety forms a non-covalent interaction with the active site of calpain through hydrogen bonding and as such is considered non-reactive.¹⁴ C-terminal macrocyclic alcohols with a Cbz or FBS substituent at R_1 and also a leucine or valine residue at P_2 (identified as the optimum substituents above) are good inhibitors of calpain II (compounds **4.04**, **4.05**, **4.11** and **4.12**, **Table 4.3**). Alcohol **4.04** (**Figure 4.7**) is a particularly potent non-aldehyde-containing inhibitor of calpain ($IC_{50} = 0.7 \mu\text{M}$). This is a significant result and to the best of our knowledge **4.04** is the most potent non-covalent binding calpain inhibitor known.⁷ The macrocycle containing a C-terminal cyanohydrin (**4.07**) showed moderate activity against calpain ($IC_{50} = 8.9 \mu\text{M}$). While this group has not been reported in cysteine protease inhibitors it might

be expected to equilibrate back to the aldehyde under the assay conditions.⁶ A C-terminal azido group has been reported in acyclic capase inhibitors that have IC₅₀ values in the low nM range.¹⁶ Interestingly **4.08** was inactive against calpain II. Docking of **4.08** into the ovine calpain II model suggests the orientation of the N₃ group is such that it is unable to form a non-covalent interaction with the oxianion hole of the active site of the enzyme.⁶ Within series two macrocycle **4.14**, with a C-terminal methyl-ester, was inactive against calpain (IC₅₀ > 50 μM). By comparison the aldehyde analogue **4.09** is a potent calpain inhibitor with an IC₅₀ = 0.28 μM. In series three, a homologated C-terminal aldehyde was incorporated at the P₁ position to give macrocycle **4.18**. All attempts to incorporate a β-amino acid into the macrocyclic calpain II inhibitors have lead to inactive compounds, for example, β-peptide derivatives **4.18** and **4.21** (**Table 4.3**) are inactive against calpain while the α-peptidic aldehyde analogues **4.15** and **4.17** had IC₅₀ values of 0.7 and 0.95 μM respectively. This is consistent with other literature based work^{17, 18} that has shown that β-peptides are not recognised as protease substrates. However, the Abell group has recently reported α-chymotrypsin inhibitors comprised of a fluorinated β₂ or β₃ phenyl alanine derivatives which have Ki values in the μM range.¹⁹ This suggests there may be potential for this inhibition strategy in the future.

Modification of Ring Size:

Macrocycles ranging in size from 14- to 22- membered rings are known to adopt a β-strand conformation.²⁰ Members of the Abell group have synthesised, by ring closing metathesis, 15- to 19- membered ring macrocycles with a C-terminal aldehyde. The activity of these macrocycles against calpain II is reported in **Table 4.4**.

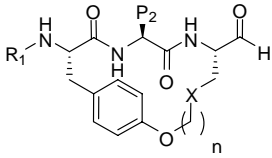
						
Compound	R ₁	P ₂	n	Ring size	X	IC ₅₀ μM
4.22	Cbz	Leu	1	16	CH ₂	0.85
CAT0811	Cbz	Leu	2	17	CH ₂	0.03
4.23	Cbz	Leu	3	18	CH ₂	0.18
4.24	Cbz	Leu	4	19	S	1.01
4.25	FBS	Val	0	15	CH ₂	3.71
4.26	FBS	Val	1	16	CH ₂	3.7
4.09	FBS	Val	2	17	CH ₂	0.28
4.27	FBS	Val	4	19	S	2.4

Table 4.4. Effect of modifying the macrocyclic ring by varying the ring size. IC₅₀ values are reported as μM concentrations.

The limited SAR study on the eight compounds shown in **Table 4.4** demonstrates that a 17-membered macrocycle (as in **CAT0811** and **4.09**) is optimal for inhibition of calpain II. The 17-membered **CAT0811**, with an IC₅₀ of 0.03 μM, is more potent than 16-membered macrocycle **4.22**, 18-membered macrocycle **4.23** and 19-membered macrocycle **4.24** (IC₅₀ values = 0.85, 0.18 and 1.01 μM respectively). Similarly, the 17-membered macrocycle **4.09** with an IC₅₀ of 0.28 μM is more potent than 15-membered macrocycle **4.25**, 16-membered macrocycle **4.26** and 19-membered macrocycle **4.27** (IC₅₀ values = 3.71, 3.7 and 2.4 μM respectively). Conformational searches on the macrocycles reported in **Table 4.4** suggests that 17-membered macrocycles have the greatest propensity of the 15- to 19- membered rings to adopt a β-strand conformation.^{10, 20, 21} This may explain the increased activity of macrocycles of this size against calpain II.

Modification of Domain 4

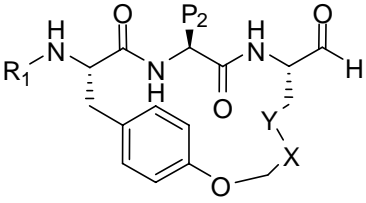
						
Compound	R ₁	P ₂	X	Y	Ring modification	IC ₅₀ μM
4.09	FBS	Val	CH ₂	CH ₂	None	0.28
4.28	FBS	Val	CH	CH	Alkene	2.68
CAT0811	Cbz	Leu	CH ₂	CH ₂	None	0.03
3.03	Cbz	Leu	CHOH	CHOH	SS-diol	3.7
3.04:3.03 (85:15)	Cbz	Leu	CHOH	CHOH	RR-diol:SS-diol (85:15)	>50

Table 4.5. Modification of Domain 4. IC₅₀ values are reported in μM concentrations.

The introduction of a diol into the macrocyclic ring at P₁ was shown earlier in this chapter to reduce the activity of the inhibitor against calpain II, with the SS-diol **3.03** reporting a 125-fold reduction in activity compared to **CAT0811** (IC₅₀ = 3.7 μM compared to IC₅₀ = 0.03 μM, **Table 4.5**). The RR-diol **3.04** (tested as an 85:15 mixture with **3.03**) was inactive against calpain II (IC₅₀ >50 μM). The alkene **4.28** was 10-fold less active (IC₅₀ = 2.68 μM) compared to the saturated analogue **4.09** (IC₅₀ = 0.28 μM) (see **Table 4.5**). A conformational search conducted on structure **4.28** suggests the alkene has a lower propensity to adopt a β-strand motif than **4.09** (32.6% of low energy conformers were in a β-strand conformation compared to 81.2% for **4.09**).⁷ These *in silico* results may rationalise the reduced activity of **4.28** compared to **4.09**.

4.4 Biological testing of 3.05

CAT0811 remains the most potent macrocyclic calpain inhibitor synthesised to date by the Abell group (**Figure 4.8**). In order to gain an understanding of the selectivity of **CAT0811**, the macrocycle was assayed against calpain II, α -chymotrypsin and the 20S core of the 26S proteasome. It has been reported that calpain II has a preference for an aromatic residue binding in the S_3 pocket,²² while α -chymotrypsin favours an aromatic substituent binding in the S_1 pocket.²³ As discussed in **Chapter 3**, macrocyclic aldehyde **3.05** was designed as a comparator to **CAT0811** where the aromatic tyrosine residue is at the P_1 site rather than at P_3 (**Figure 4.8**). Macrocycle **3.05** was similarly assayed against calpain II, α -chymotrypsin and the 20S core of the 26S proteasome. These results were compared to those obtained for **CAT0811** to investigate what contribution the P_1 and P_3 groups make to the selectivity of these macrocycles. As part of a wider SAR study to determine the most potent macrocyclic inhibitors of the 20S proteasome, macrocycle **4.02** (**Figure 4.8**) was synthesised.⁸ Compound **4.02** is an analogue of **CAT0811** with iso-leucine at the P_2 position instead of leucine.

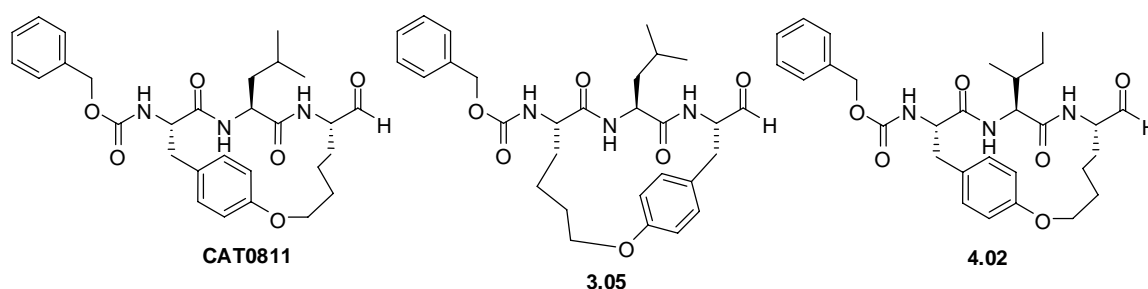


Figure 4.8. **CAT0811**, **3.05** and **4.02**.

The inhibitory activity of **3.05**, **CAT0811** and **4.02** against the calpain II, α -chymotrypsin and the three sub-sites of the 20S proteasome was determined as detailed in **Table 4.6**.^{I,II,III}

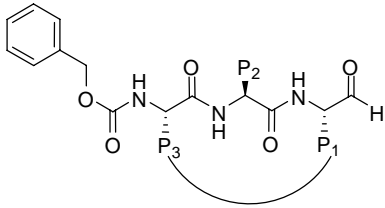
								
Compound	P ₁	P ₂	P ₃	Activity μM				
				Calpain	α -Chymo	20S proteasome		
						Chymo-	Trypsin	Capase
CAT0811	(CH ₂) ₄	Leu	Tyr	0.03	>10,000	1.51	>100	>100
3.05	Tyr	Leu	(CH ₂) ₄	0.15	-	1.46	>100	>100
4.02	(CH ₂) ₄	Ileu	Tyr	5.0	686	0.025	>100	>100

Table 4.6. IC₅₀ values of against calpain II, and the 20S proteasome. Ki values of **CAT0811**, **3.05** and **4.02** against α -chymotrypsin. All activity values are given as μM concentrations.

Comparison of Calpain II Inhibition

Aldehyde **3.05** (IC₅₀ = 0.15 μM) showed a modest 5-fold reduction in activity against calpain II compared to **CAT0811**, with an IC₅₀ of 0.03 μM . This is an interesting result since **3.05** does not have an aromatic residue at P₃. This suggests that there is not an absolute requirement for an aromatic residue at the P₃ site for binding to calpain II in these types of macrocycles. This observation is contrary to reported SAR studies on acyclic calpain inhibitors²² where an aromatic substituent at P₃ was required for potent inhibition of the enzyme. Subsequently, **3.05** was docked into the

^I Activity against calpain II was determined as described earlier in this chapter by Dr Ondrej Zvarec.

^{II} Activity against α -chymotrypsin was analysed spectrophotometrically and the measure of dissociation of the enzyme inhibitor complex – Ki, was calculated. Assay details are reported in Appendix 2.

^{III} Activity against the 20S proteasome was determined by a fluorescence based assay conducted by Dr Paul Nielsen and Limei (May) Sieu of the School of Medicine, University of Adelaide.

ovine calpain II model (prepared as previously discussed) to rationalise this assay result.

Modelling Results

Compound	H-bonds	WHDdistance	Glide score	Glide lipo
3.05	ABC + Lys347	3.9	-9.2	-3.87

Table 4.7. Results from InducedFit docking of **3.05**. Data shown is from the best enzyme-ligand pose. Column 2: the number of hydrogen bonds formed between the ligand and the enzyme model. Column 3: Warhead distance - the distance between the enzymes active site sulfur and the ligands electrophilic carbon. Column 4: the Glide score, a binding energy estimate.

Based on the docking studies, aldehyde **3.05** displays the three essential hydrogen bonds between the macrocycle backbone and the Gly208 and Gly271 residues of the enzyme. An additional hydrogen bond from the carbonyl oxygen of the Cbz group to Lys347 NH_3^+ group is apparent (**Figure 4.9**). The distance between the aldehyde carbon of the ligand and the nucleophilic sulfur of the enzymes active site Cys115 (war head distance) is within 5\AA , close enough for nucleophilic attack by the cysteine sulfur. The backbone of the macrocycle of **3.05** is positioned within the active site in the favoured β -strand conformation. The leucine side chain is positioned deep in the hydrophobic region of the active site. The Glide score of **3.05** is low (-9.2) which indicates strong binding energies for the enzyme ligand complex.

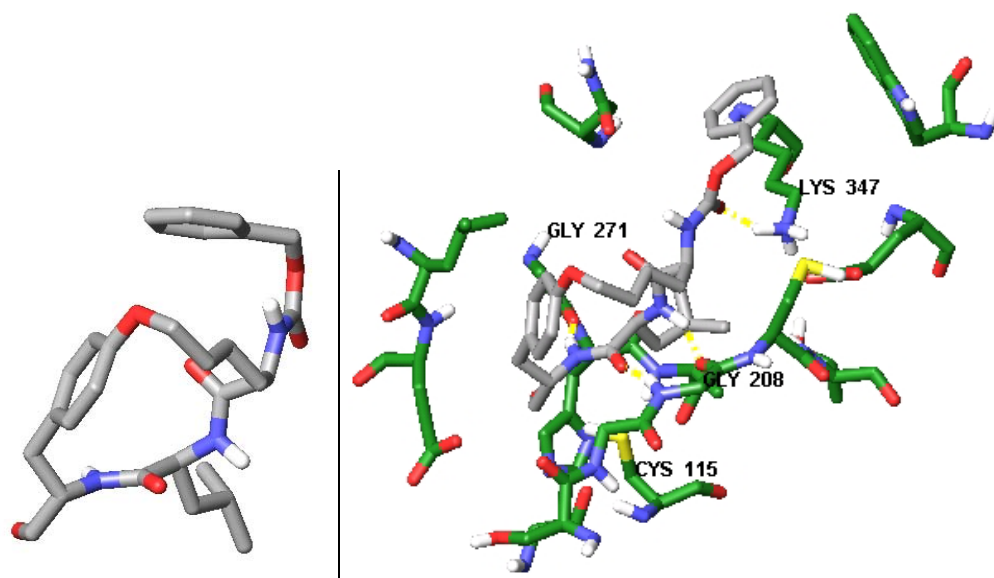


Figure 4.9. Left - lowest energy conformer of compound **3.05**. Right – best pose of lowest energy conformer of compound **3.05** docked into 1kxr. Dotted yellow lines show hydrogen bonds between ligand and enzyme.

This modelling suggests that despite **3.05** not having an aromatic group at P₃, it should bind to calpain II. We believe the additional hydrogen bond between the calpain Lys347 residue and **3.05**, not apparent for active site bound **CAT0811**, may mitigate the effect of the aromatic residue being at P₁ rather than the preferred P₃ site.

As previously discussed, the effect of incorporating isoleucine at P₂ (as in **4.02**) rather than leucine (as in **CAT0811**) has a dramatic effect on the inhibitory activity of the macrocycle against calpain. Macrocycle **4.02**, with an IC₅₀ of 5.0 μM, is less potent than **CAT0811** by a factor of 166 (**Table 4.6**).

Comparison of α-Chymotrypsin Inhibition.

Macrocycle **3.05** has an IC₅₀ of 686 μM against α-chymotrypsin, this favourably compares to **CAT0811** which shows no inhibitory activity against the enzyme.³ α-Chymotrypsin is known to prefer at aromatic residue at P₁, which is present in **3.05**

and absent in **CAT0811**. This structural difference between the two macrocycles presumably explains the difference in activity.

Comparison of 20S Proteasome Inhibition

Macrocycle **3.05** has moderate activity against the proteasome with an IC_{50} of 1.46 μ M, which compares favourably to **CAT0811** ($IC_{50} = 1.51 \mu$ M). These results are consistent with literature reports that have found inhibitors of calpain will similarly inhibit the 20S proteasome.²⁴ The comparable activity of **CAT0811** and **3.05** against the proteasome suggests there is no preference for an aromatic residue at P_1 or P_3 for the chymotrypsin-like sub-site of the 20S proteasome.

A dramatic effect on proteasome inhibition was observed when the P_2 position of the macrocycles was modified. Macrocycle **4.02**, with a P_2 isoleucine is 60 times more active than **CAT0811** with a P_2 leucine (IC_{50} values = 0.025 and 1.5 μ M respectively). These results are consistent with other recent findings in our group that have shown that iso-leucine likely provides a better fit for the S_2 pocket of the chymotrypsin-like sub-site of the 20S proteasome than leucine.²⁵ The S_2 pocket of the chymotrypsin-like sub-site of 20S proteasome is ill-defined and has a preference for bulky substituents, however, crystallographic data about the S_2 pocket is not available at this time so we cannot fully rationalise why iso-leucine is a substantially better P_2 substituent than leucine in these macrocycles.^{24, 26}

The activities of **3.05**, **CAT0811** and **4.02** against the proteasome were significantly lower than that of benchmark proteasome inhibitor **MG132** which has high potency against the chymotrypsin-like, trypsin-like and capase-like sub-sites of the

proteasome ($IC_{50} = 0.0012, 1.998$ and $0.545 \mu\text{M}$ respectively). However, unlike **MG132**, all three macrocycles displayed selective activity against the chymotrypsin-like sub-site and were inactive against both the trypsin-like and capase-like sub-sites up to the highest concentrations tested ($100 \mu\text{M}$)

Additionally, all three macrocycles selectively induced cyto-toxicity in cancer cell lines WE-68 and HCT116, while displaying no cyto-toxicity towards non-cancerous human embryonic fibroblasts.^{IV} In contrast, **MG132** is toxic towards non-cancerous cell lines at relatively low concentrations (**Table 4.8**).

Compound	WE-68	HCT116	Human Embryonic Fibroblasts
MG132	$0.68 \mu\text{M}$	$0.76 \mu\text{M}$	$1.7 \mu\text{M}$
3.05	$29 \mu\text{M}$	$53 \mu\text{M}$	$>80 \mu\text{M}$
CAT0811	$>80 \mu\text{M}$	$57 \mu\text{M}$	$>80 \mu\text{M}$
4.02	$11 \mu\text{M}$	$19 \mu\text{M}$	$>80 \mu\text{M}$

Table 4.8. Cell based assay results for **MG132**, **3.05**, **CAT0811** and **4.02**

The ability of the **3.05**, **CAT0811** and **4.02** to induce cell death in cancer cells was determined by cell viability assays with tumour cell lines WE-68 and HTC116. WE-68, a sarcoma cell line and HTC116, a carcinoma cell line, were incubated with either **CAT0811**, **3.05**, **4.02** or **MG132**. The percentage of cells that had undergone apoptosis or necrosis was assessed and this percentage was used to calculate an IC_{50} value of cell death for each inhibitor. Compound **3.05** induced cell death in both the WE-68 and HCT116 cancer cell lines with IC_{50} values for cell death of $29 \mu\text{M}$ and $53 \mu\text{M}$ respectively. **CAT0811** similarly induced cell death in the HCT116 cell line (IC_{50}

^{IV} Cytotoxicity data obtained from Dr Paul Nielsen of the School of Medicine, University of Adelaide.

= 57 μM) however it did not cause cyto-toxicity in WE-68 cells up to concentrations of 80 μM . Macrocycle **4.04** was approximately twice as active as **3.05**, with IC_{50} values for cell death in WE-68 and HCT116 cells of 11 μM and 19 μM respectively. In accordance with the inhibition data presented above, **MG132** was a more potent cyto-toxic agent of WE-68 and HCT116 cell lines (IC_{50} = 0.31 μM and 0.76 μM).

Human embryonic fibroblast cells were used as a control to see if **MG132**, **3.05**, **CAT0811** and **4.02** were toxic to normal cells. Interestingly, **MG132** did induce cell death in the normal human cells at relatively low concentrations (IC_{50} = 1.7 μM) while **3.05** and **CAT0811** and **4.02** were not cyto-toxic to these cells up to concentrations of 80 μM . This indicates that macrocycles of this type could be promising lead compounds as inhibitors of the 20S proteasome.

4.5 Conclusions.

After detailed examination of the macrocyclic compounds designed by the Abell group,^V we confirmed that a C-terminal aldehyde, an aromatic residue at P₄ and leucine or valine at P₂ are required for potent calpain II inhibition. **CAT0811**, with an IC₅₀ of 0.03 μM is the most potent inhibitor of the protease. Macrocycle **3.02**, with an N-terminal FBS group, also results in potent inhibition of calpain II (IC₅₀ = 0.045 μM). As detailed in **Chapter 3**, the synthesis of **3.02** is higher yielding than that of **CAT0811** (33% compared to 1%). As such macrocycle **3.02** is a good alternative to **CAT0811** for studies requiring large scale synthesis. While **CAT0811** is an excellent calpain inhibitor *in vitro*, its C-terminal aldehyde may not be optimum for many drug applications. The C-terminal alcohol **4.04** is a potent calpain inhibitor (IC₅₀ = 0.7 μM) that lacks a potent electrophile. The *in vivo* anti-cataract potential of both **CAT0811** and **4.04** is detailed in **Chapter 5**, along with investigation of the adsorption, distribution and excretion properties of tritiated analogues of **CAT0811** and **4.04**.

Introduction of the diol moiety to the macrocycle at the P₁ position, as in macrocycle **3.03**, reduced the ability of the macrocycle to inhibit calpain II by a factor of 120 compared to **CAT0811**. We hypothesise this is due to the fact only two key hydrogen bonds are predicted (by *in silico* docking studies) to form to the protease. This compares to three hydrogen bonds predicted to form between **CAT0811** and calpain II. Diol **3.04** (tested as an 85:15 mixture with **3.03**) was found to be essentially inactive against calpain II. We hypothesise this is due to **3.04** having a low propensity

^V Synthesised by myself as described in Chapter 3 and by Dr. Seth Jones, Dr. Janna Mehrtens, Dr. Steve Aitken and Dr. Ashok Pehere where stated. Assayed by Dr. Matthew Jones, Dr. Markus Pietsch and Dr Ondrej Zvarec where otherwise stated.

to adopt a β -strand conformation. As predicted by a conformational search,^{VI} only 1% of low energy conformers of **3.04** adopt this requisite geometry for binding to calpain II.

Macrocycle **3.05** ($IC_{50} = 0.157 \mu\text{M}$), with an aromatic residue at P_1 , displayed modest reduction in potency against calpain II compared to **CAT0811** ($IC_{50} = 0.03 \mu\text{M}$), which has an aromatic residue at P_3 . However, the fact that **3.05** is a potent inhibitor of calpain II suggests that having an aromatic group at P_1 is not essential for these macrocycles to inhibit the protease.

Both **3.05** and **CAT0811** are moderate inhibitors of the chymotrypsin-like sub-site of the 20S proteasome.^{VII} By comparing the inhibitor data from **CAT0811**, **3.05** and **4.02** we can gain some idea as to the selectivity of the proteasome. We observed little affect on inhibitory action when modifying the P_1 and P_3 residues with the macrocycle, with a modest decrease in the inhibition of the chymotrypsin-like sub-site of the 20S proteasome when comparing **3.05** ($IC_{50} = 1.46 \mu\text{M}$) to **CAT0811** ($IC_{50} = 1.51 \mu\text{M}$). However, changing the P_2 residue from leucine (as in **CAT0811**) to isoleucine (as in **4.02**) has a dramatic affect on the selectivity of the macrocycles to both calpain II and the chymotrypsin sub-site of the 20S proteasome. Macrocycle **4.02** is 167 times less potent than **CAT0811** against calpain II, and 60 times more potent against the chymotrypsin-like sub-site of the 20S proteasome. Further exploration of the binding requirements of the S_2 pocket of the 20S proteasome to identify the optimum residue for the P_2 position of these macrocycles is the next step to in our attempts selectively inhibit the 20S proteasome.

^{VI} Conformational search carried out by Dr Stephen Mc Nabb or Dr Blair Stuart where indicated.

^{VII} Dr. Paul Nielsen carried out all assay and cytotoxicity studies regarding the 20S proteasome.

References

1. Thompson, V. F.; Saldana, S.; Cong, J.; Goll, D. E., *Analytical Biochemistry* **2000**, *279* (2), 170-178.
2. Muir, M. Unpublished work. Lincoln University.
3. Abell, A. D.; Jones, M. A.; Coxon, J. M.; Morton, J. D.; Aitken, S. G.; McNabb, S. B.; Lee, H. Y.-Y.; Mehrtens, J. M.; Alexander, N. A.; Stuart, B. G.; Neffe, A. T.; Bickerstaffe, R., *Angewandte Chemie International Edition* **2009**, *48*, 1455-1458.
4. Azuma, M.; Yoshida, Y.; Sakamoto, Y.; Inoue, J. Pharmaceutical composition containing an arylsulfonyl dipeptide aldehyde for prophylaxis and therapy of diseases associated with ocular fundus tissue cytopathy. **1999**.
5. Jones, M. A.; Morton, J. D.; Coxon, J. M.; McNabb, S. B.; Lee, H. Y. Y.; Aitken, S. G.; Mehrtens, J. M.; Robertson, L. J. G.; Neffe, A. T.; Miyamoto, S.; Bickerstaffe, R.; Gately, K.; Wood, J. M.; Abell, A. D., *Bioorganic & Medicinal Chemistry* **2008**, *16* (14), 6911-6923.
6. Mehrtens, J. M. The Design, Synthesis and Biological Assay of Cysteine Protease Specific Inhibitors. University of Canterbury, Christchurch, **2007**.
7. Aitken, S. G. Design, synthesis and testing of β -strand mimics as protease inhibitors University of Canterbury, Christchurch, **2006**.
8. Jones, S. A. Beta-Strand Mimicry as the Basis for a Universal Approach to Protease Inhibitor. University of Adelaide, Adelaide, **2011**.
9. Jiao, W. Clan CA Cystein Proteases: Selectivity and Structure Comparison. University of Canterbury, Christchurch, **2007**.

-
10. Stuart, B. *Molecular Modelling for Enzyme-Inhibition: A Search for a New Treatment for Cataract and New Antimicrobials and Herbicides* University of Canterbury, Christchurch, **2010**.
 11. Iqbal, M.; Messina, P. A.; Freed, B.; Das, M.; Chatterjee, S.; Tripathy, R.; Ming, T.; Josef, K. A.; Dembofsky, B.; Dunn, D.; Griffith, E.; Siman, R.; Senadhi, S. E.; Biazzo, W.; Bozyczko-Coyne, D.; Meyer, S. L.; Ator, M. A.; Bihovsky, R., *Bioorganic & Medicinal Chemistry Letters* **1997**, *7* (5), 539-544.
 12. Otto, H.-H.; Schirmeister, T., *Chemical Reviews* **1997**, *97* (1), 133-172.
 13. Walker, B.; Lynas, J. F., *Cellular and Molecular Life Sciences* **2001**, *58* (4), 596-624.
 14. Rishton, G. M., *Drug Discovery Today* **2003**, *8* (2), 86-96.
 15. Rishton, G. M., *Drug Discovery Today* **1997**, *2* (9), 382-384.
 16. Le, G. T.; Abbenante, G.; Madala, P. K.; Hoang, H. N.; Fairlie, D. P., *Journal of the American Chemical Society* **2006**, *128* (38), 12396-12397.
 17. Seebach, D.; Gardiner, J., *Accounts of Chemical Research* **2008**, *41* (10), 1366-1375.
 18. Seebach, D.; Beck, A. K.; Bierbaum, D. J., *Chemistry & Biodiversity* **2004**, *1* (8), 1111-1239.
 19. Peddie, V.; Pietsch, M.; Bromfield, K. M.; Pike, R. N.; Duggan, P. J.; Abell, A. D., *Synthesis* **2010**, *11*, 1845-1859.
 20. Loughlin, W. A.; Tyndall, J. D. A.; Glenn, M. P.; Fairlie, D. P., *Chemical Reviews* **2004**, *104* (12), 6085-6118.

-
21. Fairlie, D. P.; Tyndall, J. D. A.; Reid, R. C.; Wong, A. K.; Abbenante, G.; Scanlon, M. J.; March, D. R.; Bergman, D. A.; Chai, C. L. L.; Burkett, B. A., *Journal of Medicinal Chemistry* **2000**, *43* (7), 1271-1281.
 22. Inoue, J.; Nakamura, M.; Cui, Y.-S.; Sakai, Y.; Sakai, O.; Hill, J. R.; Wang, K. K. W.; Yuen, P.-W., *Journal of Medicinal Chemistry* **2003**, *46*, 868-871.
 23. Schellenberger, V.; Braune, K.; Hofmann, H.-J.; Jakubke, H.-D., *European Journal of Biochemistry* **1991**, *199* (3), 623-636.
 24. Borissenko, L.; Groll, M., *Chemical Reviews* **2007**, *107* (3), 687-717.
 25. Pehere, A. New Peptide-Based Templates Constrained into a Beta-Strand by Huisgen Cycloaddition. University of Adelaide, Adelaide, **2012**.
 26. Braun, H. A.; Umbreen, S.; Groll, M.; Kuckelkorn, U.; Mlynarczuk, I.; Wigand, M. E.; Drung, I.; Kloetzel, P.-M.; Schmidt, B., *Journal of Biological Chemistry* **2005**, *280* (31), 28394-28401.

CHAPTER FIVE

IN VIVO TESTING OF TRITIATED MACROCYCLES

5 *In vivo* testing of tritiated macrocycles

5.1 Introduction

CAT0811 (Figure 5.1), has been established in Chapter 4 as a potent inhibitor of calpain II in with an IC_{50} value of 0.03 μ M, while its precursor alcohol, **4.04**, has an IC_{50} value of 0.7 μ M (Figure 5.1).¹

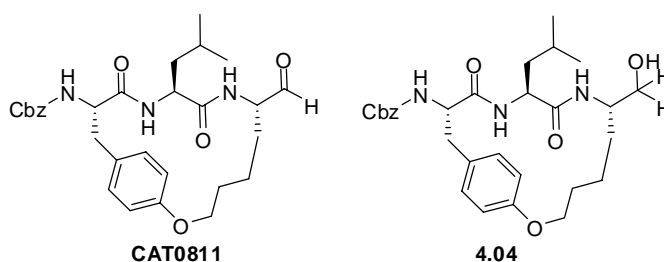


Figure 5.1. Structures of **CAT0811** and **4.04**

The anti-cataract potential of **CAT0811** has also been investigated in *in vitro* ovine lens culture studies,¹ where the compound was shown to slow the development of calcium induced cortical cataracts (Figure 5.2). Lenses treated with calcium alone (Figure 5.2b) showed substantial opacity as associated with cataract formation.¹ However lenses treated with both calcium and **CAT0811** (Figure 5.2c) remained essentially transparent after incubation, thus **CAT0811** significantly reduced lens opacity ($p < 0.005$ in a paired t-test).

¹ To calculate the opacity all lenses were photographed over a grid, and the opacity was graded by using the software Image-Pro 4.1.

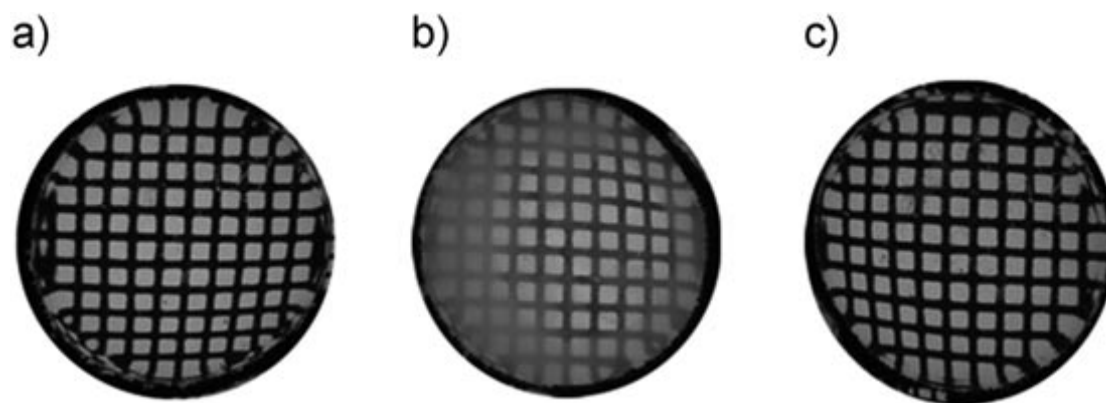


Figure 5.2 Effect of **CAT0811** on opacity in lenses treated with: a. Control (no treatment), b. Calcium only and c. Calcium and **CAT0811**.

The *in vitro* calpain assays (discussed in **Chapter 4**) and lens culture studies demonstrated that **CAT0811** has potential as an anti-cataract therapeutic. However the efficacy of **CAT0811** *in vivo* had not been investigated.

Collaborators at Lincoln University have developed a sheep flock predisposed to cataract formation, which can be used as a model for cataractogenesis.² This model is advantageous for three reasons: the formation of the ovine cataracts follows reproducible stages, the cataracts are congenital rather than induced, and the cataracts show rapid progression. Therefore, these sheep provide an ideal model to study inhibitor effectiveness *in vivo*. The flock of sheep for the study were sired by a cataractous Romney ram, and gestated by a normal-eyed unrelated Coopworth ewe.³ The level of the cataract formation in these animals is scored using a one to seven scoring system as depicted in **Figure 5.3**. Stages one and two show suture lines, stages three to five show cortical nuclear involvement, and stages six and seven have complete cataract.

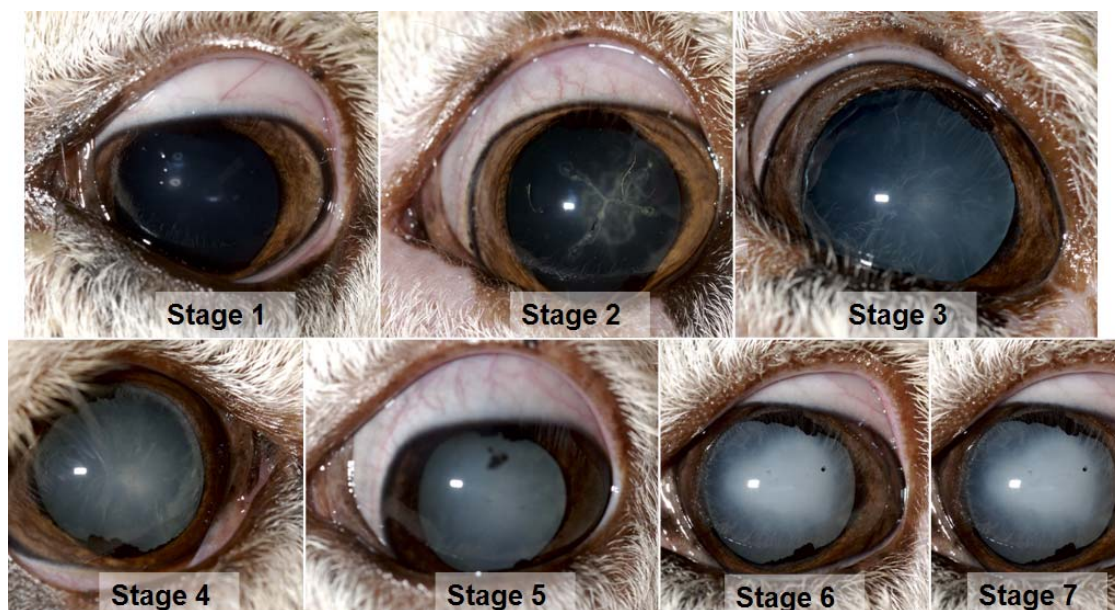


Figure 5.3. (1) Anterior suture lines (2) Anterior & posterior suture lines (3) 0-33% cortical nuclear involvement (4) 33-66% cortical nuclear involvement (5) Greater than 66% cortical nuclear involvement (6) Total immature cataract (7) Total mature cataract³

5.1.1 Summary of *in vivo* trials of CAT0811

A trial using the cataractous flock was conducted at Lincoln University beginning on 16th November 2005 and running until 26th February 2006. The objective was to establish whether there is a difference in cataract development between the left and right eye when **CAT0811** is topically applied to the left eye only.

A sample of 24 3-month old lambs was chosen from the cataractous flock with all lambs in the sample having a cataract score of between 1 and 2. The mean score for the sample was 1.50 in the left eye and 1.54 in the right eye. The left eye of each lamb was treated with 25 mg ointment (formulated as 1% (w/w) **CAT0811**, cetyl stearyl alcohol (25%), lanolin (35%) paraffin oil (39%)) twice daily for the duration of the trial (102 days). The progression of cataracts in both eyes was determined by a veterinary ophthalmologist using a slit-lamp microscope as described by Robertson *et al.*³

The results from the 2005 trial showed no significant difference in cataract progression between the treated and untreated eye within the sample. However, when the rate of progression of cataracts in this trial was evaluated and compared to the rate of cataract progression in an untreated quasi control group, it was found that eyes in treated sheep displayed slower rates of cataract progression than those of control sheep.

This observation led to the development of a new protocol for conducting the *in vivo* trials.⁴ In December 2006, 63 lambs with cataract scores between 1 and 2 were selected and split into three groups by an independent statistician.ⁱⁱ 21 sheep were treated twice daily in the left eye with 17 - 23 mg of **CAT0811** ointment (formulated as above) and 21 sheep were treated twice daily in the left eye with 17 - 23 mg of **4.04** ointment formulated as 1% (w/w) **4.04**, cetyl stearyl alcohol (25%), lanolin (35%) paraffin oil (39%). The remaining placebo group of 21 sheep were treated in the left eye twice daily with 17 – 23 mg of placebo ointment containing neither **4.04** nor **CAT0811** (Cetyl stearyl alcohol (26%), lanolin (35%) paraffin oil (39%).

Cataract progression was measured and recorded for both eyes of all sheep. Again the progression of cataracts, in both eyes, was determined by a veterinary ophthalmologist using a slit-lamp microscope. The pre-determined key point for analysis of efficacy was 3 months after ointment administration. At this time the mean lens opacity of the control group had increased from 1.82 to 4.66 (an increase in score of 2.84). Over the same period the mean cataract score of the lambs treated with

ⁱⁱ Three sheep were removed from analysis as there was no change in their lens opacity over the course of the trial.

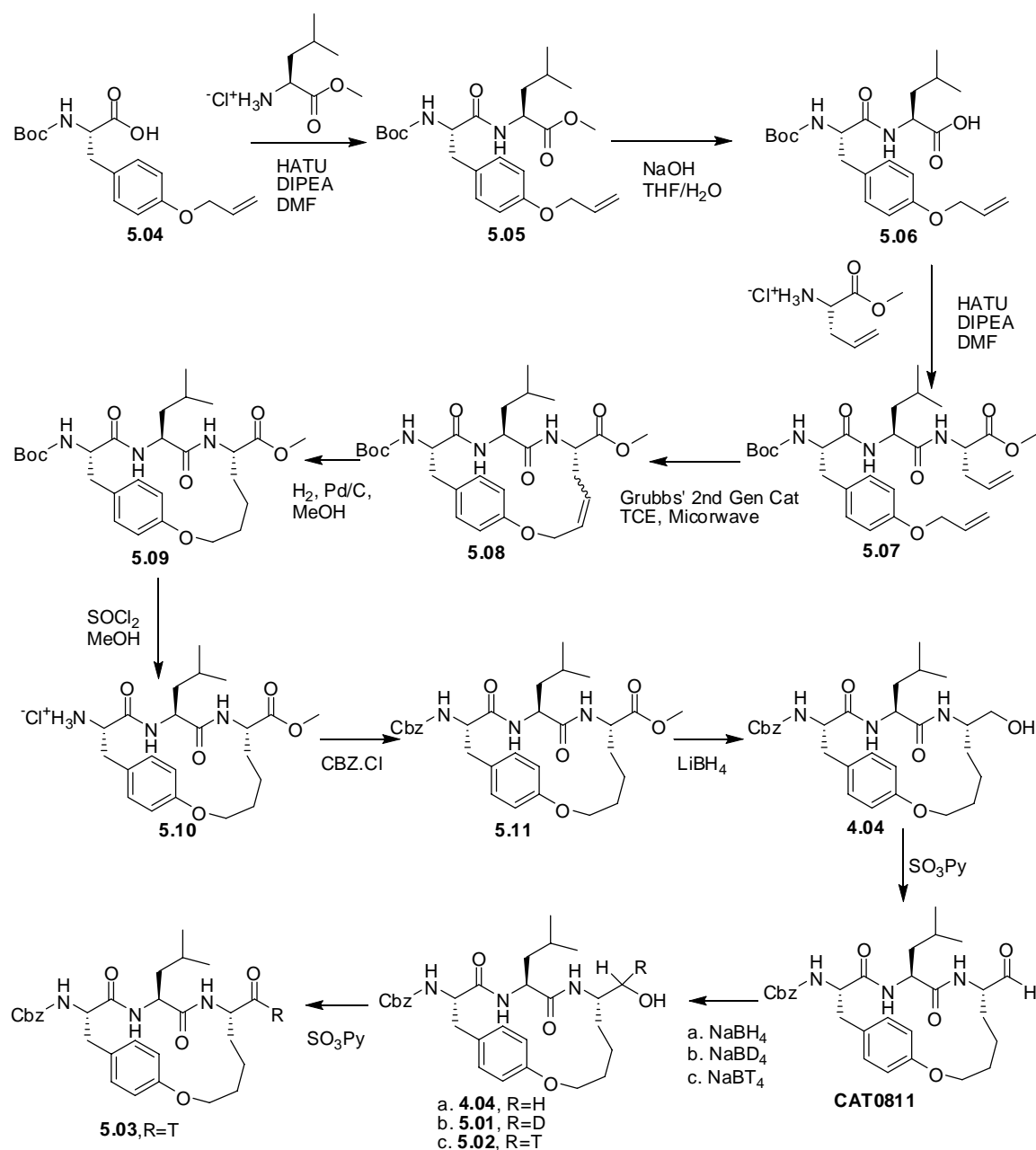
CAT0811 increased by 2.08 and the mean cataract score for lambs treated with **4.04** increased by 2.26. Treatment with **CAT0811** resulted in a 27 % slowing of cataract progression ($p < 0.05$). The opacity of lenses in lambs treated with **4.04** showed a 16 % reduction in cataract progression, however, this was not significantly different to the control group ($p = 0.12$). Again, there was no difference in cataract progression between the treated and untreated eyes. It was concluded that crossover of the drug from the treated eye to the untreated eye was occurring and thus that treatment of one eye is effective in slowing cataract in both eyes.⁴ This cross over phenomena has been reported, but is not well understood.³

The experiments described in this chapter were devised to further explore this crossover phenomenon and as an initial attempt to elucidate more information on the bioavailability, absorption and dispersion properties of **CAT0811** and **4.04**. Tritium labelled analogues of **CAT0811** and **4.04** were synthesised, each of which was administered to the left eye of one sheep from the cataract flock. Liquid scintillation counting was used to measure the uptake of tritium in the treated and untreated lenses of the sheep in order to observe whether drug crossover had occurred. The levels of tritium in the organs, tissues, and urine of the sheep were measured in order to get a preliminary picture of the absorption, distribution and excretion patterns of the inhibitors.

5.2 Results and discussion

5.2.1 Synthesis and formulation of radio-labelled analogues

As depicted in **Scheme 5.1**, it was envisaged that tritiated **CAT0811** (**5.03**) and tritiated **4.04** (**5.02**) could be accessed by reduction of the aldehyde functionality of **CAT0811** using NaBT_4 to give the tritiated alcohol **5.02**, followed by re-oxidation to give the desired tritiated analogue **5.03**.



Scheme 5.1 Synthesis of tritiated macrocycles **5.02** and **5.03**.

CAT0811 was prepared as previously reported (**Scheme 5.1**).¹ Alkene **5.04** was coupled to Leu-OMe.HCl in the presence of HATU to give dipeptide **5.05** in 89% yield after purification by flash chromatography on silica gel. Hydrolysis of the methyl-ester of **5.05** on treatment with NaOH gave **5.06** and this was coupled to allyl-Gly-OMe.HCl in the presence of HATU to give the diene **5.07** in 78% yield over two steps. Ring closing metathesis, using three portions of Grubbs' second generation catalyst in TCE (3 x 10 mol%) gave **5.08** in 20% yield after purification by flash chromatography on silica gel. Subsequent hydrogenation of **5.08** with Pd/C and H₂ gave the macrocycle **5.09** in 85% yield. Deprotection of the N-terminal Boc group upon treatment of **5.09** with thionyl chloride in methanol gave amine **5.10** in near quantitative yield. Coupling of benzyl chloroformate to the N-terminus of **5.10** gave the required **5.11** in 49% yield after purification by flash chromatography on silica gel. The methyl ester of **5.11** was reduced on treatment with LiBH₄ to give alcohol **4.04** in 83% yield. Parikh-Doering oxidation⁵ of the alcohol of **4.04** gave the aldehyde **CAT0811** in 80% yield.

With **CAT0811** in hand, we envisioned reduction of the aldehyde of **CAT0811** with LiBT₄ to give **5.02** followed by oxidation of the resultant aldehyde to give **5.03** (**Scheme 5.1**, conditions c). Due to the need to minimise radioactive contamination and by-product formation, it was not possible to purify the labelled products by flash chromatography, nor could the purity of the products be determined using NMR or mass spectrometry due to their radioactive nature.ⁱⁱⁱ An efficient, reliable and reproducible synthesis of the tritiated analogues was required. Owing to the expense

ⁱⁱⁱ We did not have access to NMR or Mass spec facilities equipped to handle radioactive species.

of tritium, reaction conditions were optimised using NaBH₄ (**Scheme 5.1**, conditions a) which is considerably cheaper.

A mole of NaBH₄ may donate up to four moles of hydride ions; therefore initially **CAT0811** was treated with 0.25 mol equivalents of NaBH₄. The reduction of **CAT0811** was monitored by proton NMR, with the integral ratio of the aldehyde proton resonance at 10 ppm and the alcohol CH₂ multiplet at 3.30-3.33 ppm used to calculate the % conversion to **4.04**. Complete disappearance of the aldehyde peak was deemed a >95% conversion to the alcohol. The reaction was monitored for 14 days (**Table 5.1**), and the reaction was judged complete after 72 h.

Reaction Conditions	Time	% reduction
A NaBH ₄	24 hr	85%
B NaBH ₄	48 hr	93%
C NaBH ₄	72 hr	>95%
D NaBH ₄	14 days	>95%
E NaBD ₄	72 hr	>95%

Table 5.1. Reaction conditions of reduction to aldehyde. 16mg of **CAT0811** was reduced with 0.25 eq NaBH₄ (Rows A-D) or 0.25 eq NaBD₄ (E) in a 1:1 mixture of water:THF. The % reduction was calculated by measuring integral ratios between the starting material and product resonances within ¹H NMR spectra.

The optimised reaction conditions were repeated using NaBD₄ in order to assess any kinetic isotope effect, and to see how this effect could potentially influence the reaction time with NaBT₄ (**Scheme 5.1**, conditions b and **Table 1**, E). **CAT0811** was treated with 0.25 mol equivalents of NaBD₄ in a 1:1 mixture of H₂O:THF to give **5.01** in >95 % yield. The reaction was monitored by proton NMR as above and judged

complete by the absence of aldehyde resonance at 10 ppm after 72 h. No discernible kinetic isotope effect was observed, as the rate limiting step does not involve the breaking of the B-H (or B-D) bond, which is consistent with reported kinetic studies on the reduction of aldehydes by NaBH₄.⁶

The reduction of **CAT0811** by NaBT₄ was carried out in the radioactive suite at Lincoln University, and TLC analysis was used to monitor the reaction. After 72 h conversion of **CAT0811** to the alcohol **5.02** was judged to be complete by TLC. The reaction was quenched with 1 M aqueous HCl and the product extracted with ethyl acetate to give 15 mg of **5.02**. A 2 mg sample of **5.02** was retained for use in the animal trial, the remainder of the sample (13 mg) was oxidised to give the tritiated aldehyde **5.03**, presumed to be in >95% yield based on results from trial E (**Table 5.1** and **Scheme 5.1**).

It has been observed in our labs that in order to achieve complete oxidation from **4.04** to **CAT0811** the oxidation is ideally performed on a greater than 200 mg scale. Thus, in order to ensure effective and pure synthesis of the tritiated aldehyde **5.03**, the 13 mg sample of **5.02** was blended with 187 mg of non-tritiated **4.04** (**Scheme 5.1**). The blended mixture was oxidised with SO₃.Py complex in DMSO. After two hours, TLC analysis showed complete oxidation to the aldehyde **5.03**. The aldehyde was extracted into EtOAc to give **5.03** in 80% yield. Previous studies have reported oxidations requiring the breaking of a C-H bond are typically 5 – 10 times faster than those requiring the breaking of a C-D bond.^{7, 8} Using the Swain equation⁹ we estimated the kinetic isotope effect for oxidation our tritiated alcohol to be between 7 – 14, hence

we anticipated that the tritium would be preferentially retained in the aldehyde after oxidation.

The samples of **5.02** and **5.03** were formulated according to the specifications developed for the sheep trials: inhibitor (1% w/w), cetyl/stearyl alcohol (30% w/w), lanolin (35% w/w) and paraffin (34% w/w) to give the formulations **5.02f** and **5.03f**. The specific radioactivity of the formulations was determined by dilution of a known mass of ointment (in triplicate) in 1 mL of scintillation fluid (Optiphase Supermix) followed by scintillation counting using a Wallac 1409 liquid scintillation counter. For details of the theory and procedure for liquid scintillation counting including calibration curve see **Appendix 1**. The specific activity of **5.02f** was 61 $\mu\text{Ci}/\text{mg}$ and the specific activity of **5.03f** was 0.50 $\mu\text{Ci}/\text{mg}$.

5.2.2 *In Vivo* study methods

These experiments were carried out in collaboration with Lincoln University in accordance with their Animal Ethics Protocols ACE#154 as reviewed by the New Zealand Animal Ethics Committee and the ARVO Statement for the Use of Animals in Ophthalmic and Vision Research. Dr Hannah Lee of Lincoln University was responsible for the care of the animals and for the collection of all biological samples at the conclusion of the experiments. Liquid scintillation counting of all samples was done under the guidance of Dr Matthew Jones.

Animals: Three sheep born in August 2006 (aged 14 months) were selected from cataract trial flock. The sheep were brought into the experiment room several days prior to application of ointment and were fed and cared for by Dr Hannah Lee. Sheep

were placed into an elevated cage with a plastic cover below for waste collection, with food and water supplies attached to sides. 18 gauge catheters were inserted into the jugular of the sheep and flushed with heparin to avoid blood clots. Prior to dosing, a blank blood sample was taken from each of the three sheep. Three experiments were conducted: in each case the ointment (either **5.02f** or **5.03f**) was administered to the sclera under the lower eyelid in the left eye of each sheep.

Experiment 1 (48 h): 13 μL of ointment **5.02f** was administered to the left eye of one sheep weighing 34.0kg. Blood samples were collected by Dr Hannah Lee via the cannula at $t = 5, 7, 9, 12, 15, 30, 60, 90, 120, 180, 300, 420, 600, 2160$ and 2880 min and stored in Eppendorf tubes containing heparin. Whole blood samples were centrifuged for 5 minutes to isolate plasma as soon as possible to prevent possible contamination from lysed red cells. Plasma samples (1 mL) were then mixed with 10 mL scintillation fluid (Optiphase Supermix) in 20 mL scintillation vials (Econoglass) and scintillation counted for tritium content as described in **Appendix 1**.

Urine was collected and analysed for tritium content at $t = 35$ and $t = 2880$ min. Aliquots (1 mL) of the urine collected at these time periods were analysed for tritium-content by mixing with 10 mL Optiphase Supermix and scintillation counted as described in **Appendix 1**. Total urinary output was calculated from the tritium in each aliquot and the measured volume of urine collected over the experiment duration.

For the biodistribution studies, the sheep was euthanized 48 h after dosing. The major organs and tissue of interest (aqueous humour, lens, cornea, globe, vitreous humour, eye lid, heart, liver, kidney, pituitary gland, muscle, brain, eye orbit and cheek) were removed, weighed and a sample homogenised in 5 – 10 mL MilliQ water. Each of the

organ and tissue samples was then scintillation counted to determine the tritium-content.

Experiment 2 (216 hours): 25 μL of **5.02f** was administered to a left eye of one sheep weighing 33.5 kg. Blood samples were collected by Dr Hannah Lee via the cannula at $t = 3, 5, 7, 9, 12, 15, 30, 45, 60, 75, 90, 120, 150, 180, 312, 435, 570, 720, 1230, 1578, 1896, 2160, 2880, 3240, 4362, 5640, 5796, 6480, 7200, 7890, 8640, 9000, 9936, 11376$ and 12900 min. Plasma aliquots were prepared as described above. Urine samples were collected between 48 – 120 h, at 96 h, and at 216 h. Urine aliquots were counted as described above. For the biodistribution studies, the sheep was euthanized 216 h after dosing. The major organs and tissue of interest (aqueous humour, lens, cornea, globe, vitreous humour, eye lid, heart, lung, liver, kidney, pituitary gland, muscle, brain, rumin, eye orbit and cheek) were removed, weighed, prepared and counted as described above.

Experiment 3 (216 hours): A third sheep weighing 34.5 kg had 25 μL **5.03f** administered to its left eye. Blood samples were collected by Dr Hannah Lee via the cannula at $t = 3, 5, 7, 9, 12, 15, 20, 30, 45, 60, 75, 90, 120, 150, 180, 312, 435, 570, 720, 1230, 1578, 1896, 2160, 2880, 3240, 4362, 5640, 5796, 6480, 7200, 9000, 9936, 11376,$ and 12840 min. Plasma aliquots were prepared as described above. Urine samples were collected at 5 h, 20 h, 54 h and at 216 h. Urine aliquots were counted as described above. For the biodistribution studies, the sheep was euthanized 216 h after dosing. The major organs and tissue of interest (aqueous humour, lens, cornea, globe, vitreous humour, eye lid, heart, lung, liver, kidney, pituitary gland, muscle, brain,

rumin, eye orbit, and cheek) were removed, weighed, prepared and counted as described above.

5.2.3 Liquid scintillation counting results

Plasma:

Figure 5.4 shows the plasma concentration – time profile for Experiments 1 and 2 with tritium content reported as picogram equivalents of **5.02** per mL. The disintegrations per minute (DPM) of radiolabel in plasma samples were converted to picogram equivalent concentrations using the specific activity of **5.02f**, however these, and subsequent results, should be viewed with the caveat that this approach assumes that the tritium content is still associated with the intact inhibitor (**5.02** or **5.03**).

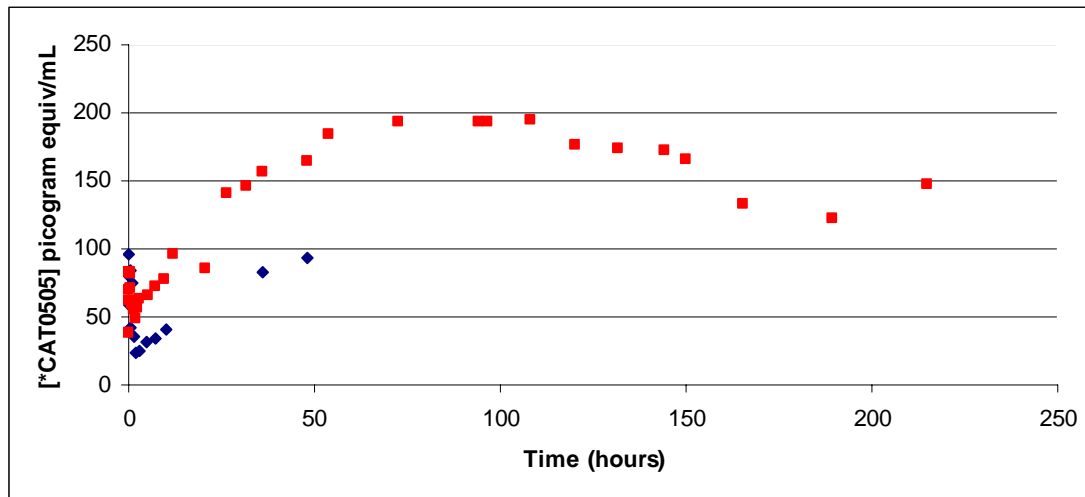


Figure 5.4. Plasma concentration – time profiles for **5.02**. Experiment 1, 48 h, blue series. Experiment 2, 216 h, red series.

A rapid increase followed by an initial drop in plasma concentration of **5.02** was evident in the first 1 h post dose in Experiment 1 (**Figure 5.4**, blue series). From approximately 2 h post dose the concentration of tritium in the plasma increased for

the remainder of the experiment. Experiment 2 (**Figure 5.4**, red series) showed a qualitatively similar plasma concentration profile. An initial peak followed by rapid clearance of tritium from the plasma was observed in the first 1.5 h post dose. From approximately 2 h post dose the concentration of tritium in the plasma increased to reach a maximum of 195 pg/mL at 108 h, (4.5 days) post dose. Between 108 h and 190 h the plasma tritium concentration decreased, presumably as tritium is cleared from the body. The final measurement of the experiment at 215 h (9 days) post dose may indicate the plasma tritium concentration is again increasing. This is an unusual plasma profile however this observation is not unheard of – in a study¹⁰ reporting a similar plasma concentration profile, the second peak in plasma concentration is due to enzymatic degradation of the radio-labelled peptide followed by release of a radio labelled amino acid into the plasma after metabolism. Further studies are necessary to determine if this was the cause of the unusual plasma concentration profile of **5.02**.

Figure 5.5 shows the plasma concentration – time profile for Experiment 3 with tritium content reported as picogram equivalents of **5.03** per mL. The DPM of radiolabel in plasma samples were converted to picogram equivalent concentrations using the specific activity of **5.03f**.

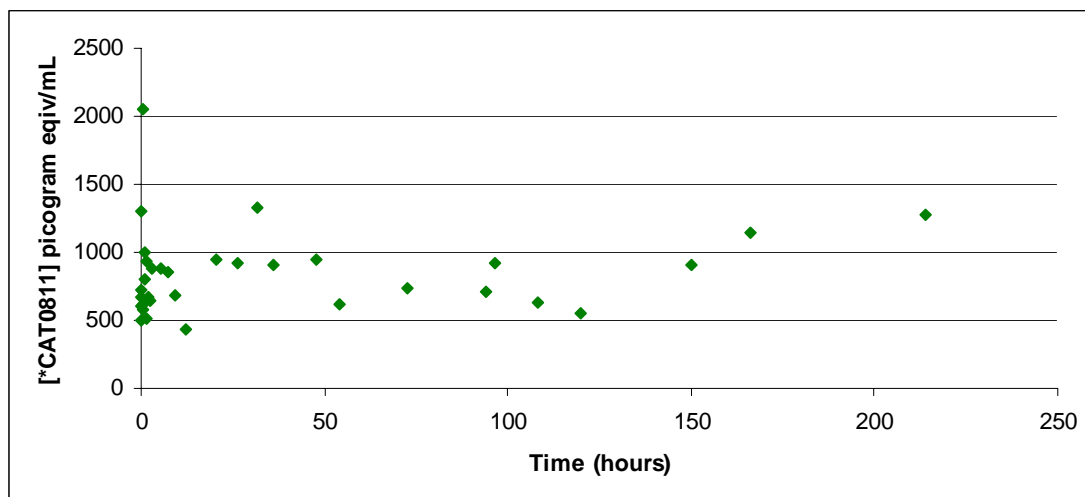


Figure 5.5. Plasma concentration – time profiles for **5.03**. Experiment 3, 216 hours, green series.

Because the aldehyde ointment **5.03f** used in Experiment 3 had much lower tritium levels (0.6% of the activity), detection of the tritium in the biological samples was more difficult and no obvious peaks in plasma tritium levels was observed, however generally, plasma concentration increased rapidly after application to reach a peak 20 minutes post dose. This was followed by a sharp decrease in plasma concentration until 2 h post dose. The plasma concentration then remained between 500-1500 picogram/mL for the remainder of the experiment. Comparing the plasma concentration profile of Experiments 2 and 3, we observed 10-fold higher plasma levels of **5.03** than **5.02**.

Lens Data

The key measurements of this study involved the determination of levels of **5.02** and **5.03** in the lenses of the treated and untreated eyes. If tritiated species were found in both eyes this would support our hypothesis from the 2006 sheep trial that crossover of the drug was occurring. The amount of tritium measured in each sample is reported

as a % of tritium applied per g of tissue. Data for **5.02**, is given in **Figure 5.6**, data for **5.03** is given in **Figure 5.7**.

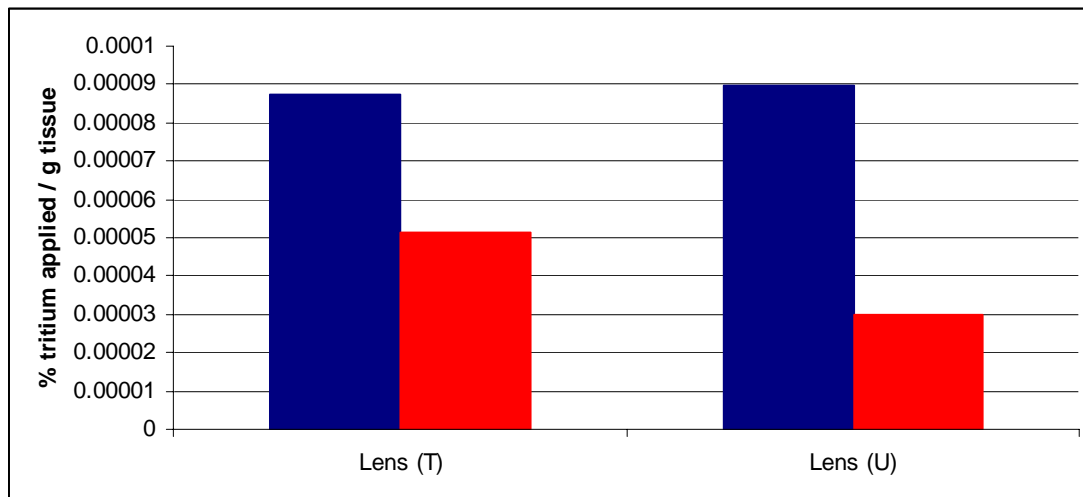


Figure 5.6. Distribution of administered **5.02** in the treated (T) and untreated lenses (U) for Experiment 1 (blue series) and Experiment 2 (red series).

Two days after dosage with **5.02f** (Experiment 1), approximately 8.7×10^{-5} % of applied **5.02** was measured in the treated lens and 9.0×10^{-5} % was measured in the untreated lens. That an approximately equal amount of **5.02** was found in both lenses strongly supports our hypothesis that crossover of the inhibitor is occurring. Nine days after dosage with **5.02f** (Experiment 2), the % of applied **5.02** measured in the treated lens is 40 % lower (5.15×10^{-5} %) and the levels of **5.02** in the untreated eye are 67 % lower (2.98×10^{-5} %). We hypothesise that the different levels of **5.02** found in the lenses nine days post dose are due to tissue surrounding the treated lens, (for example the cornea, **Figure 5.8**) which were found to have higher tritium levels than those adjacent to the untreated lens, therefore this tissue may have acted as a reservoir for **5.02**.

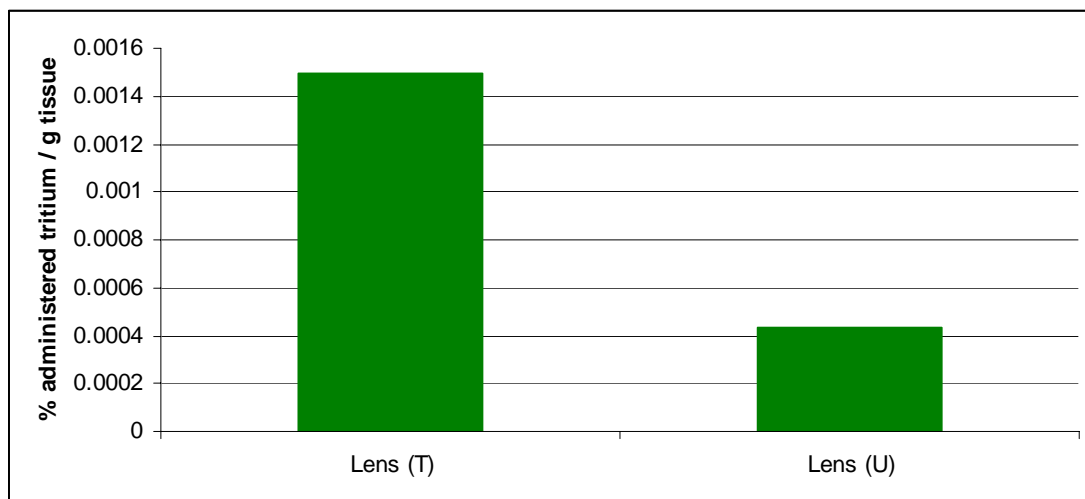


Figure 5.7. Distribution of administered **5.03** in the treated and untreated lenses for Experiment 3.

The amount of **5.03** (as a % of administered dose) measured in the treated and untreated lenses 9 days post dose is shown in **Figure 5.7** (Experiment 3). The treated lens had 0.0015% of administered **5.03** while the untreated lens had 71% lower levels of inhibitor with 0.00043% of administered dose recovered. This is consistent with the pattern of results for Experiment 2, however in Experiment 3 we observed much higher amounts (thirty times more) of **5.03** compared to **5.02**. This suggests that **5.03** has a higher affinity to the lens than **5.02**, possibly due to the increased reactivity of the aldehyde compared to the alcohol. The % of administered **5.03** that was recovered in the treated and untreated lenses was converted to nanogram equivalents of **5.03** to give a theoretical mass of inhibitor in the lens. The lenses of both the treated and untreated eyes were found to contain 3.7 and 1.1 nanograms respectively of tritiated inhibitor after topical application of **5.03f**.

Bio distribution:

At the conclusion of the three experiments, samples of selected tissue and organs of the three sheep were collected to determine the pattern of distribution of **5.02** and

5.03. Figure 5.8 shows the distribution of **5.02** in major organs and tissue sample for Experiments 1 and Experiment 2. The results are presented as the percentage of tritium applied per g of tissue. Where applicable, samples from the treated eye or surrounding tissue is denoted T, samples from the untreated eye or surrounding tissue is denoted U.

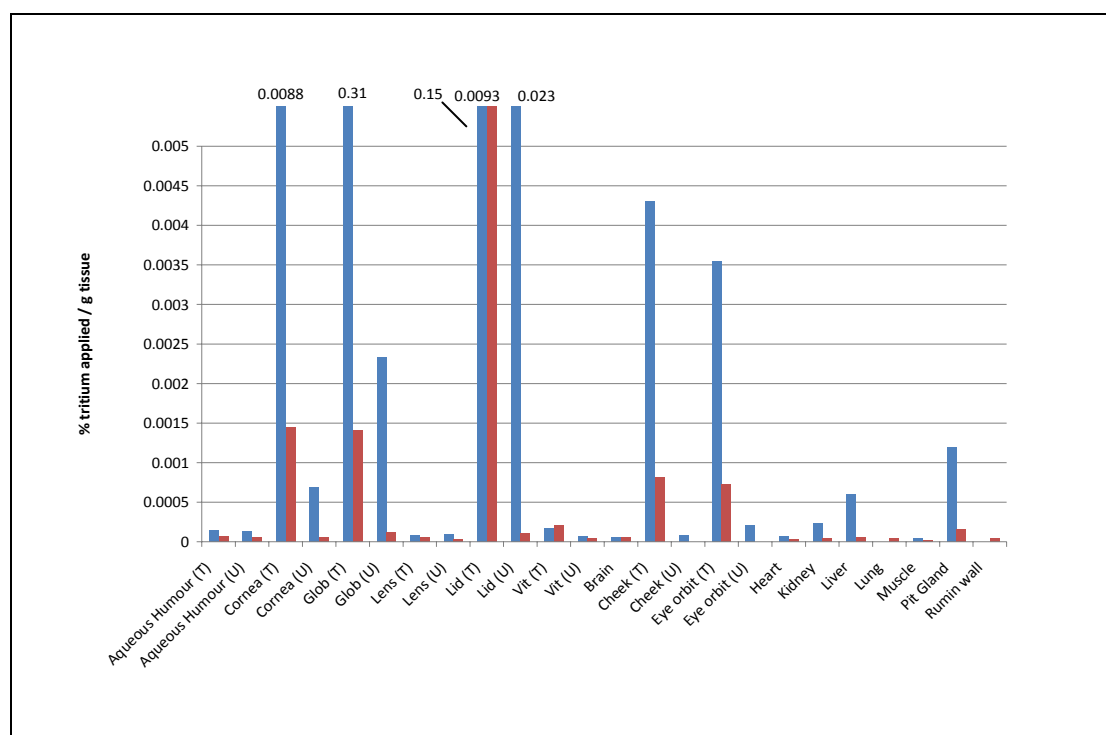


Figure 5.8. Tissue distribution profiles for **5.02**. Experiment 1, 48 hours, blue series. Experiment 2, 216 hours, red series. The results are presented as the percentage of tritium applied per g of tissue. Where applicable, samples from the treated eye or surrounding tissue is denoted T, samples from the untreated eye or surrounding tissue is denoted U

Tritium, presumed to be alcohol **5.02**, was detected in all organ and tissue samples recovered, with tritium levels in Experiment 1 (collected 48 h post dose) consistently higher than samples from Experiment 2 (collected 216 h post dose). In Experiment 1, samples with the highest proportion of **5.02** per g were those associated with the application site of the formula (the sclera). The comparatively high levels of **5.02** recorded in the cheek muscles on the treated side of the animal are most likely due to

leakage of the formula from the eye and subsequent absorption of **5.02** through the skin. Similarly we note the eyelid (T), cornea (T), globe (T) and eye orbit muscles (T) have a comparatively high tritium count due to their proximity to the application site of the formula. Interestingly, the untreated globe, eye lid and, to a lesser extent, cornea, also had comparatively elevated tritium levels. We hypothesis this is also due to being in close proximity to the application site. The liver and kidney showed moderately elevated tritium levels 48 hours post dose, however as these are the organs involved in metabolism and excretion of drugs this is not surprising. The levels of tritium in the pituitary gland were also moderately elevated (0.0012% of administered dose). The pituitary gland is located at the base of the brain near the nasal cavity, meaning this result is possibly due to being in close proximity to either the application site of the ointment or to an excretion route of the formula through the nasal cavity into the stomach. In Experiment 2 tritium levels were lower in all tissue samples than those measured in Experiment 1 as **5.02** is presumably cleared from the body over time.

Figure 5.9 shows the distribution of **5.03** in major organs and tissue sample for Experiment 3. The results are presented as the percentage of tritium applied per g of tissue. Where applicable, samples from the treated eye or surrounding tissue is denoted T, samples from the untreated eye or surrounding tissue is denoted U.

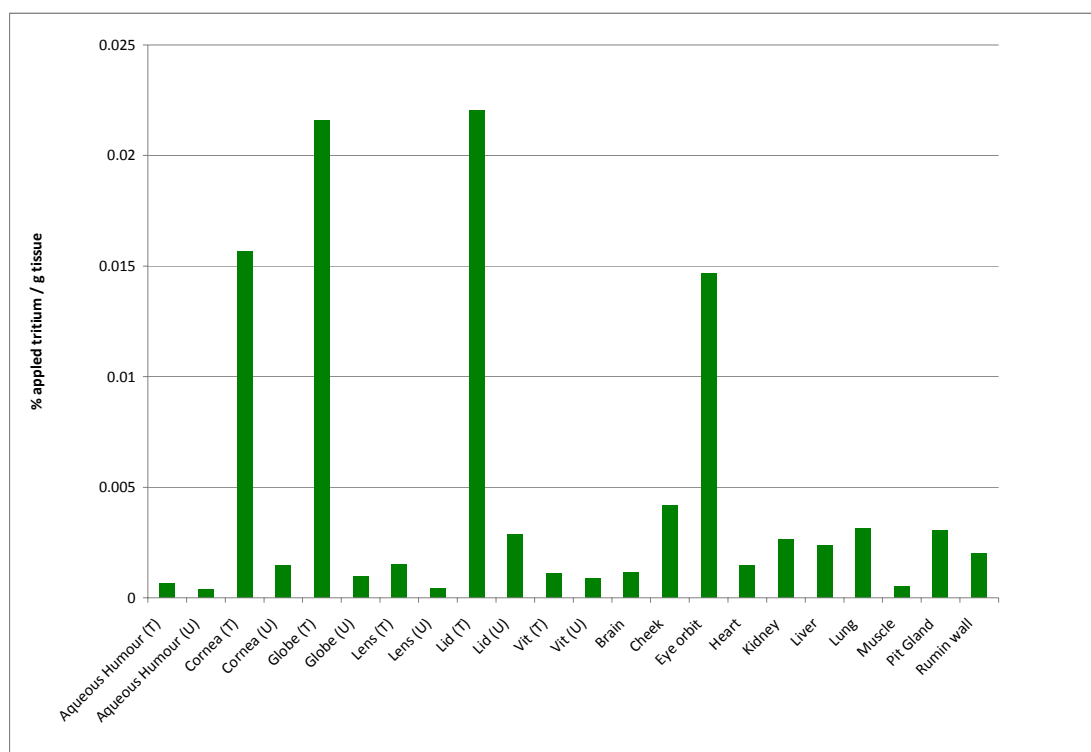


Figure 5.9. Tissue distribution profile for **5.03**. Experiment 3, 216 hours, green series. The results are presented as the percentage of tritium applied per g of tissue. Where applicable, samples from the treated eye or surrounding tissue is denoted T, samples from the untreated eye or surrounding tissue is denoted U.

The distribution of **5.03** (or a breakdown product thereof) measured in Experiment 3 (nine days post dose) is consistent with the pattern of distribution observed for the **5.02** experiment (Experiment 2). The tissue surrounding the application site of the formula (globe (T), eye lid (T), cornea (T) and eye orbit muscles (T)) had the highest levels of tritium recovered. Distribution across the other tissue and organ samples was approximately even.

Excretion:

Significant renal excretion was not observed for either **5.02** in Experiments 1 and 2 or **5.03** in Experiment 3. For Experiments 1 and 2, 0.3% of the administered **5.02** was measured in the urine. For Experiment 3, 1.5% of administered **5.03** was measured in

the urine. Most (95%) of the tritium excreted was in urine samples taken in the first 48 h after application.

Generally, a very low percentage of the administered **5.02** (or a breakdown product thereof) was recovered in the tissue and organ samples. For Experiment 1 0.94% of the administered **5.02** was recovered in the tissue and organ samples. For Experiment 2 0.32% of the administered **5.02** was recovered. In Experiment 3, 10.9 % of administered **5.03** was recovered in the organ and tissue samples. This is 30 times higher than the total % recovered of **5.02** in Experiment 2, suggesting **5.03** is retained more readily *in vivo*.

The low % of tritium observed in the tissue, plasma and urine samples is consistent with known topically applied ocular pharmaceuticals.¹¹⁻¹³ There are three major barriers to absorption, leakage from the eye, systemic absorption via the tear duct to the nasal cavity and low corneal permeability.¹⁴ Typically corneal permeability is less than 1% of the total applied dosage.¹⁵ We hypothesise that a large proportion of the applied formulations of **5.02** and **5.03** is being lost from the eye at or very close to the time of application via ointment leakage. This is evidenced by the high levels of tritium recorded in the cheek muscles under the treated eye. The second major route for topically applied ocular ointments is loss through the tear ducts into the nasal cavity, the gut and finally excretion in the faeces. Determination of the amount of applied **5.02** and **5.03** excreted in the faeces was unable to be determined due to high colour quenching of the faecal samples.

5.3 Conclusions

The lens data from Experiment 2 shows that equal amounts of **5.02** were found in both treated and untreated lenses 48 h after application of **5.02f**. This supports the findings of previous *in vivo* trials that showed topical application of **5.02f** to one eye slowed cataract formation in both eyes by an equal amount.

All biological samples in this study (collected by Dr Hannah Lee) showed elevated levels of tritium compared to blank samples. This tells us that tritium in some form at least is circulating in the biological system 9 days post dose; however we have not attempted to determine whether this tritium is still attached to **5.02** and **5.03**, a metabolite of the inhibitors or another species. We do have some limited evidence from our unusual plasma concentration profiles that this tritium may be due to metabolism of our inhibitors, however further experiments would need to be conducted to establish that this was the case. It would also be useful to confirm that a major excretion route of the inhibitors is through the gut to the faeces in order to help account for the large percentage of applied tritium that was not recovered in these experiments. This could be achieved by developing a procedure to bleach the highly coloured faeces samples so that they may be liquid scintillation counted.

As previously reported,⁴ **CAT0811** significantly slows cataract formation in *in vivo* animal studies. The next phase in developing **CAT0811**, or a related macrocycle, as a pharmaceutical suitable for human consumption is to expand the pilot study described here into a rigorous ADME-tox investigation to establish any side effects that may result from topical application of **CAT0811**. This is especially pertinent due to

the C-terminal aldehyde of **CAT0811**, identified in **Chapter 4** as being a potentially unsuitable pharmaceutical moiety.

The work described in this thesis has demonstrated the effectiveness of ring closing metathesis as a technique to prepare challenging synthetic targets, namely 8- to 10-membered rings and macrocycles, in the synthesis of peptidomimetics designed to adopt either a β -turn or β -strand conformation. In **Chapter 2** compound **2.66** was found to have an intra-molecular hydrogen bond indicative of a β -turn and compound **2.64** is indicated to adopt this conformation also. This work lays the preliminary foundations on the road to developing these scaffolds into pharmaceutically relevant compounds. Future work on this project involves the synthesis of analogues of these initial scaffolds and the development of recognition elements to bind potently and specifically to a desired receptor. In comparison, the macrocycles described in **Chapter 3** are components of a more established investigation into the binding of cyclic tripeptides to protease active sites. Macrocycles **3.02**, **3.03**, **3.04**, **3.05**, **5.02** and **5.03** show the progression from the initial design of potential calpain II inhibitors in collaboration with molecular docking studies described in **Chapter 3** to the *in vitro* assay results reported in **Chapter 4** finally arriving at the pilot *in vivo* trials described in **Chapter 5**. The next phase for this project will be the running of more comprehensive *in vivo* studies as described above, and the exploration of individuals in this class of macrocycles as inhibitors of a wider range of proteases, for example the preliminary work on α -chymotrypsin and 20S proteasome inhibition reported in **Chapter 4**.

5.4 References for Chapter 5

1. Abell, A. D.; Jones, M. A.; Coxon, J. M.; Morton, J. D.; Aitken, S. G.; McNabb, S. B.; Lee, H. Y.-Y.; Mehrtens, J. M.; Alexander, N. A.; Stuart, B. G.; Neffe, A. T.; Bickerstaffe, R., *Angewandte Chemie International Edition* **2009**, *48*, 1455-1458.
2. Brooks, H. V.; Jolly, R. D.; Paterson, C. A., *Current Eye Research* **1993/1993**, *2* (9), 625-632.
3. Robertson, L. J. G.; Morton, J. D.; Yamaguchi, M.; Bickerstaffe, R.; Shearer, T. R.; Azuma, M., *Investigative Ophthalmology & Visual Science* **2005**, *46* (12), 4634-4640.
4. Morton, J. D.; Lee, H. Y. Y.; McDermott, J. D.; Robertson, L. J. G.; Bickerstaffe, R.; Jones, M. A.; Coxon, J. M.; Abell, A. D., *Investigative Ophthalmology & Visual Science* **2013**, *54*, 389-395.
5. Parikh, J. R.; Doering, W. v. E., *Journal of the American Chemical Society* **1967**, *89* (21), 5505-5507.
6. Yamataka, H.; Hanafusa, T., *Journal of the American Chemistry Society* **1986**, *108* (21), 6643.
7. Liu, K. E.; Johnson, C. C.; Newcomb, M.; Lippard, S. J., *Journal of the American Chemical Society* **1993**, *115* (3), 939-947.
8. Westheimer, F. H., *Chemical Reviews* **1961**, *61* (3), 265-273.
9. Swain, C. G.; Stivers, E. C.; Reuwer, J. F.; Schaad, L. J., *Journal of the American Chemical Society* **1958**, *80* (21), 5885-5893.
10. Boyd, B. J.; Kaminskas, L. M.; Karellas, P.; Krippner, G.; Lessene, R.; Porter, C. J. H., *Molecular Pharmaceutics* **2006**, *3* (5), 614-627.

-
11. Jarvinen, K.; Jarvinen, T.; Urtti, A., *Advanced Drug Delivery Reviews* **1995**, *16* (1), 3-19.
 12. Sigurdsson, H. H.; Konráðsdóttir, F.; Loftsson, T.; Stefánsson, E., *Acta Ophthalmologica Scandinavica* **2007**, *85* (6), 598-602.
 13. Ali, Y.; Lehmussaari, K., *Advanced Drug Delivery Reviews* **2006**, *58* (11), 1258-1268.
 14. Souto, E. B.; Doktorovova, S.; Gonzalez-Mira, E.; Egea, M. A.; Garcia, M. L., *Current Eye Research* **2010**, *35* (7), 537-552.
 15. Kaur, I. P.; Garg, A.; Singla, A. K.; Aggarwal, D., *International Journal of Pharmaceutics* **2004**, *269* (1), 1-14.

CHAPTER SIX

EXPERIMENTAL

6 Experimental

6.1 General methods and experimental procedures

Nuclear Magnetic Resonance

Proton NMR spectra were acquired on a Varian Inova 500 spectrometer (operating at 500 MHz), a Varian Gemini 2000 spectrometer (operating at 300 MHz) or a Varian Inova 600 spectrometer (operating at 600 MHz). Carbon NMR spectra were acquired on a Varian Unity XL 300 MHz Fourier Transform spectrometer operating at 75 MHz with a delay (D1) of 1 s or on a Varian Inova 600 spectrometer (operating at 125 MHz) with a delay (D1) of 1 s. All spectra were obtained at 23 °C and chemical shifts are reported in parts per million (ppm) and are referenced relative to residual solvent (e.g. CHCl₃ at δ H 7.26 ppm for CDCl₃, DMSO at δ H 2.50 ppm for [D₆]DMSO, and CH₃OH at δ H 3.31 ppm for CD₃OD). Spin multiplicities are represented by the following signals: s (singlet), bs (broad singlet), d (doublet), dd (doublet of doublets), t (triplet), ddd (doublet of doublet of doublets), dt (doublet of triplets), q (quartet), sex (sextet) and m (multiplet).

Mass Spectrometry

ESI high resolution mass spectra (HRMS) were recorded at the University of Canterbury, New Zealand on a Micromass LCT spectrometer using a probe voltage of 3200 V, an operating temperature of 150 °C and a source temperature of 80 °C. Direct ionization used 10 μ L of a 10 μ g mL⁻¹ solution, using a carrier solvent of 50% acetonitrile/water at a flow rate of 20 μ L min⁻¹. Ionization was assisted by the addition of 0.5% formic acid. Electrospray ionisation (ESI) mass spectra were determined using a Finnigan LCQ Ion Trap mass spectrometer at the University of

Adelaide. Electrospray conditions were as follows: needle potential, 4500 V; tube lens, 60 V; heated capillary, 200 °C, 30 V; sheath gas flow, 30 psi.

High Performance Liquid Chromatography

The chromatography system consisted of a Hewlett Packard HPLC equipped with an HP Series 1100 degasser, HP Series 1100 quaternary pump, HP Series 1100 diode-array detector, and Agilent Technologies 1200 Series fraction collector. The column used for analytical HPLC was a reverse phase Phenomenex Jupiter Proteo 90 Å (4 µm C₁₂, 250 x 4.60 mm), and for semipreparative purification a reverse phase Supelco Discovery BIO Wide Pore (5 µm C₅, 250 x 10.0 mm). For analytical HPLC, the mobile phase was pumped at 1 mL/min as a binary system over 35 min, starting at 10% TFA/MeCN/Milli-Q water (1:99:900 v/v/v), 90% TFA/Milli-Q water (1:1000 v/v), and ending with 100% TFA/MeCN/Milli-Q water (1:99:900 v/v/v). For semipreparative HPLC, the mobile phase was pumped at 3 mL/min as a binary system over 35 min, starting at 10% TFA/MeCN/Milli-Q water (1:99:900 v/v/v), 90% TFA/Milli-Q water (1:1000 v/v), and ending with 100% TFA/MeCN/Milli-Q water (1:99:900 v/v/v), with 0.5 mL fractions collected.

Specific Rotation

Specific rotation values were determined using an Atago Automatic Polarimeter AP-100, and a 100 mm observation tube (1 mL capacity).

Reagents, Solvents and Laboratory Methodology

All chemicals commercially obtained were utilised as received. Oven dried glassware was used in all reactions which were performed under an inert atmosphere (dry nitrogen or argon).

Thin-layer chromatography (TLC) was done using Merck aluminium sheets coated with silica gel 60 F254 or plastic backed Merck Kieselgel KG60F254 silica plates. Products were visualised with a Vilber Lourmat VL-60C (6W – 254 nm tube) UV lamp and/or vanillin dip (6 g vanillin, 95 mL ethanol, and 2 mL concentrated sulfuric acid), a potassium permanganate stain (10 g K_2CO_3 , 1.5 g of $KMnO_4$, 150 mL water, then 1.5 mL of 10% aq. NaOH solution), or a phosphomolybdate dip (10 g phosphomolybdic acid and 100 mL ethanol). Flash column chromatography was performed using Merck or Scharlau silica gel 60 (230 – 400 mesh).

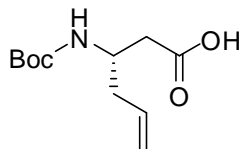
THF was distilled from sodium benzophenone ketyl under an inert atmosphere immediately prior to use. Dichloromethane and TCE were distilled from calcium hydride under an inert atmosphere. Petroleum ether refers to the fraction collected between 50 - 70 °C.

Concentration *in vacuo* refers to removal of solvent by rotary evaporation followed by application of a high vacuum for a minimum of thirty minutes.

Microwave irradiation refers to heating in a domestic microwave at 1200 W, with a QuickFit reflux condenser attached, under an inert atmosphere. Boiling points under microwave reflux were 110 – 115 °C for TCE, and 40 – 45 °C for dichloromethane.

6.2 Experimental for Chapter 2

Preparation of (*S*)-3-(tert-butoxycarbonylamino)hex-5-enoic acid (**2.31**)



To a solution of **2.37** (2.11 g, 9.8 mmol) in dry THF (5 mL) under inert atmosphere at -20 °C was added N-methyl-morpholine (1.13 mL, 10.2 mmol) and iso-butylchloroformate (1.34 mL, 10.2 mmol) to form a white suspension. The reaction mixture was stirred at -20 °C for 30 minutes then warmed to 0 °C in an ice bath and ethereal diazomethane (~12.7 mmol) was added dropwise over ten minutes. This solution was stirred at 0 °C for 2 h and then at room temperature for a further 16 h. Glacial acetic acid was added to quench the reaction followed by aqueous NaOH (1M) to adjust the solution to pH 8. The mixture was partitioned between ethyl acetate (20 mL) and water (20 mL). The aqueous phase was separated and extracted again with ethyl acetate (20 mL). The combined organic extracts were washed sequentially with saturated aqueous NH₄Cl (20 mL) and brine (20 mL), before being dried over MgSO₄. Organic solvents were removed *in vacuo* to yield the diazoketone **2.38** (2.04 g, 87%) as a yellow oil that was used without purification.

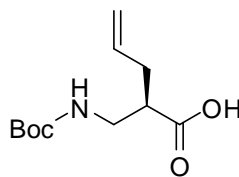
To a solution of **1.38** (1.68 g, 7.0 mmol) in THF (75 mL) and water (25 mL), in the absence of light, was added silver trifluoroacetate (153 mg, 0.7 mmol) and the reaction mixture was sonicated for 3 h. Solvents were removed *in vacuo*. Purification of the residue by flash chromatography on silica gel (eluting with 9/1

dichloromethane/methanol with 0.5 mL glacial acetic acid) gave **2.31** (1.59 g, 99%) as a white foam.

^1H NMR (600 MHz, CDCl_3) δ 5.81 – 5.70 (1H, m, $\text{NHCHCH}_2\text{CHCH}_2$), 5.18 – 5.09 (2H, m, $\text{NHCHCH}_2\text{CHCH}_2$), 4.91 (1H, bs, NHCHCH_2CO), 4.14 – 3.83 (1H, m, NHCHCH_2CO), 2.60 – 2.51 (2H, m, NHCHCH_2CO), 2.36 – 2.28 (2H, m, $\text{NHCHCH}_2\text{CHCH}_2$), 1.43 (9H, s, $(\text{CH}_3)_3$).

HRMS (ES^+) calc. for $\text{C}_{11}\text{H}_{19}\text{NO}_4$ ($\text{M}+\text{H}^+$) 230.1392, found 230.1398

Preparation of (*R*)-2-((tert-butoxycarbonylamino)methyl)pent-4-enoic acid (**2.32**)



To a solution of **2.41** (670 mg, 1.7 mmol) in THF (8 mL) at 0 °C was added H_2O_2 (30% w/w, 1 mL, 8.5 mmol) in water (10 mL). The mixture was stirred at 0 °C for 2 h then stirred at room temperature for 16 h. The solvents were removed *in vacuo* and saturated aqueous NaHCO_3 (10 mL) was added. The aqueous phase was washed with ethyl acetate (2 x 10 mL) then aqueous HCl (1 M, 40 mL) was added to acidify the solution to pH 1. The aqueous phase was extracted with ethyl acetate (2 x 20 mL) and the combined organic extracts were dried over MgSO_4 . Removal of the solvents *in vacuo* gave **2.32** (370 mg, 95 %) as a white foam.

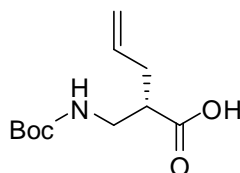
^1H NMR (600 MHz, CDCl_3) δ 5.81 – 5.77 (1H, m, $\text{NHCH}_2\text{CHCH}_2\text{CHCH}_2$), 5.13 – 5.08 (2H, m, $\text{NHCH}_2\text{CHCH}_2\text{CHCH}_2$), 4.96 (1H, bs, NHCH_2CHCO), 3.43 – 3.37 (2H, m, NHCH_2CHCO), 3.27 – 3.24 (1H, m, NHCH_2CHCO), 2.74 – 2.67 (1H, m, $\text{NHCH}_2\text{CHCH}_2\text{CHCH}_2$), 2.43 – 2.39 (1H, m, $\text{NHCH}_2\text{CHCH}_2\text{CHCH}_2$), 1.44 (9H, s, $(\text{CH}_3)_3$).

^{13}C NMR (75 MHz, CDCl_3) δ 177.6, 155.9, 134.2, 117.8, 79.7, 45.5, 41.1, 33.8, 28.3

HRMS (ES^+) calc. for $\text{C}_{11}\text{H}_{19}\text{NO}_4$ ($\text{M}+\text{H}^+$) 230.1392, found 230.1396

$[\alpha]_{\text{D}} = -12.5$ (c 0.1, MeOH)

(S)-2-((tert-butoxycarbonylamino)methyl)pent-4-enoic acid (2.33)



A solution of **2.44** (740 mg, 1.9 mmol) in THF (10 mL) was cooled to 0 °C and H_2O_2 (1.5 mL, 30% w/w) in water (13 mL) was added dropwise. The mixture was stirred at 0 °C for 2 h then allowed to warm to room temperature while stirring for 16 h. The solvents were removed *in vacuo* and saturated aqueous NaHCO_3 (10 mL) was added. The aqueous phase was washed with ethyl acetate (2 x 10 mL) then aqueous HCl (1 M, 40 mL) was added to acidify the solution to pH 1. The aqueous phase was extracted with ethyl acetate (2 x 20 mL) and the combined organic extracts were dried

over MgSO₄. Removal of the solvent *in vacuo* gave **2.33** (380 mg, 87 %) as a white foam.

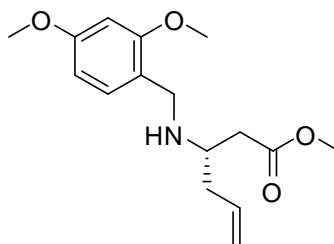
¹H NMR (600 MHz, CDCl₃) δ 5.81 – 5.77 (1H, m, NHCH₂CHCH₂CH₂CH₂), 5.13 – 5.08 (2H, m, NHCH₂CHCH₂CH₂CH₂), 4.96 (1H, bs, NHCH₂CHCO), 3.43 – 3.37 (2H, m, NHCH₂CHCO), 3.27 – 3.24 (1H, m, NHCH₂CHCO), 2.74 – 2.67 (1H, m, NHCH₂CHCH₂CHCH₂), 2.43 – 2.39 (1H, m, NHCH₂CHCH₂CHCH₂), 1.44 (9H, s, (CH₃)₃).

¹³C NMR (75 MHz, CDCl₃) δ 177.6, 155.9, 134.2, 117.8, 79.7, 45.5, 41.1, 33.8, 28.3

HRMS (ES⁺) calc. for C₁₁H₁₉NO₄ (M+H⁺) 230.1392, found 230.1387

[α]_D = 371.5 (c 0.1, MeOH)

Preparation of (*S*)-methyl 3-(2,4-dimethoxybenzylamino)hex-5-enoate (**2.34**)



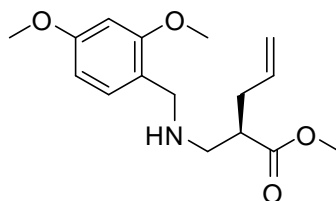
To a solution of **2.31** (815 mg, 3.3 mmol) in MeOH (6 mL) at 0 °C was added SOCl₂ (1.2 mL, 16.5 mmol). The reaction was stirred at room temperature for 16 h. Removal of the solvent *in vacuo* gave **2.47** (600 mg, >99 %) as a yellow oil.

To a solution of **2.47** (600 mg, 3.3 mmol), in anhydrous methanol (14 mL) was added 2,4-dimethoxybenzaldehyde (500 mg, 3.0 mmol), sodium acetate (550 mg, 6.7 mmol) and 4Å mol sieves (3.3 g). The mixture was stirred at room temperature for 1 h, then Na(OAc)₃BH (4.95 g, 23.4 mmol) was added. The reaction was stirred at room temperature for 16 h. The reaction mixture was filtered through celite and the solvents were removed *in vacuo*. The residue was dissolved in DCM (20 mL) and the organic phase was washed with saturated aqueous NaHCO₃ (10 mL), dried over MgSO₄ and the solvents removed *in vacuo*. Purification of the residue by flash chromatography on silica gel (eluting with 3/1 ethyl acetate/petroleum ether) gave **2.34** (760 mg, 78 %) as a yellow oil.

¹H NMR (600 MHz, CDCl₃) δ 7.13 (1H, d, *J* = 7.8 Hz, ArH), 6.47 – 6.41 (2H, m, 2 x ArH), 5.77 – 5.68 (1H, m, NHCHCH₂CHCH₂), 5.11 – 5.06 (2H, m, NHCHCH₂CHCH₂), 3.86 – 3.70 (3H, m, CH₂Ar, NHCHCH₂CO), 3.81 (3H, s, ArOCH₃), 3.80 (3H, s, ArOCH₃), 3.68 (3H, s, COOCH₃), 3.08 – 3.00 (1H, m, NHCHCH₂CO), 2.60 – 2.52 (1H, m, NHCHCH₂CO), 2.48 – 2.41 (1H, m, NHCHCH₂CO), 2.31 – 2.27 (2H, m, NHCHCH₂CHCH₂).

HRMS (ES⁺) calc. for C₁₆H₂₃NO₄ (M+H⁺) 294.1705, found 294.1706

Preparation of (*R*)-methyl 2-((2,4-dimethoxybenzylamino)methyl)pent-4-enoate (2.35)



To a solution of **2.32** (750 mg, 3.1 mmol) in MeOH (6 mL) at 0 °C was added SOCl₂ (1.1 mL, 15.5 mmol). The reaction was stirred at room temperature for 16 h. Removal of the solvent *in vacuo* gave **2.48** (550 mg, >99 %) as a yellow oil.

To a solution of **2.48** (550 mg, 3.1 mmol) in anhydrous methanol (14 mL) was added 2,4-dimethoxybenzaldehyde (320 mg, 2.8 mmol), sodium acetate (510 mg, 6.2 mmol) and 4Å mol sieves (3.1 g). The mixture was stirred at room temperature for 1 h, then Na(OAc)₃BH (4.57 g, 21.7 mmol) was added. The reaction was stirred at room temperature for 16 h. The reaction mixture was filtered through celite and the solvents were removed *in vacuo*. The residue was dissolved in DCM (20 mL) and the organic phase was washed with saturated aqueous NaHCO₃ (10 mL), dried over MgSO₄ and the solvent removed *in vacuo*. Purification of the residue by flash chromatography on silica gel (eluting with 3/1 ethyl acetate/petroleum ether) gave **2.35** (740 mg, 82 %) as a yellow oil.

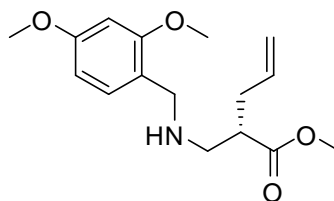
¹H NMR (600 MHz, CDCl₃) δ 7.12 (1H, d, *J* = 7.8 Hz, ArH), 6.46 – 6.41 (2H, m, 2 x ArH), 5.79 – 5.68 (1H, m, NHCH₂CHCH₂CHCH₂), 5.02 – 4.99 (2H, m, NHCH₂CHCH₂CHCH₂), 3.83 – 3.77 (2H, m, CH₂Ar), 3.81 (3H, s, ArOCH₃), 3.80 (3H, s, ArOCH₃), 3.68 (3H, s, COOCH₃), 2.80 – 2.83 (1H, m, NHCH₂CHCO), 2.79

(1H, bs, NHCH₂CHCO), 2.75 – 2.69 (1H, m, NHCH₂CHCO), 2.56 – 2.52 (1H, m, NHCH₂CHCO), 2.40 – 2.36 (1H, m, NHCH₂CHCH₂CHCH₂), 2.31 – 2.23 (1H, m, NHCH₂CHCH₂CHCH₂).

¹³C NMR (75 MHz, CDCl₃) δ 175.14, 161.5, 158.6 134.9, 130.8, 117.1, 105.7, 103.9, 98.1, 55.4, 51.7, 47.4, 41.1, 34.2

HRMS (ES⁺) calc. for C₁₆H₂₃NO₄ (M+H⁺) 294.1705, found 294.1702

Preparation of (S)-methyl 2-((2,4-dimethoxybenzylamino)methyl)pent-4-enoate (2.36)



To a solution of **2.33** (720 mg, 3.0 mmol) in MeOH (6 mL) at 0 °C was added SOCl₂ (1.1 mL, 15.5 mmol). The reaction was stirred at room temperature for 16 h. Removal of the solvent *in vacuo* gave **2.49** (530 mg, >99 %) as a yellow oil.

To a solution of **2.49** (530 mg, 3.0 mmol) in anhydrous methanol (12 mL) was added 2,4-dimethoxybenzaldehyde (310 mg, 2.8 mmol), sodium acetate (490 mg, 6.0 mmol) and 4Å mol sieves (3.0 g). The mixture was stirred at room temperature for 1 h, then Na(OAc)₃BH (4.39 g, 20.7 mmol) was added. The reaction was stirred at room temperature for 16 h. The reaction mixture was filtered through celite and the solvents were removed *in vacuo*. The residue was dissolved in DCM (20 mL) and the organic

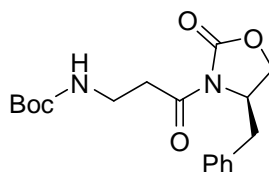
phase was washed with saturated aqueous NaHCO_3 (10 mL), dried over MgSO_4 and the solvent removed *in vacuo*. Purification of the residue by flash chromatography on silica gel (eluting with 3/1 ethyl acetate/petroleum ether) gave **2.36** (730 mg, 84 %) as a yellow oil.

^1H NMR (600 MHz, CDCl_3) δ 7.12 (1H, d, $J = 7.8$ Hz, ArH), 6.46 – 6.41 (2H, m, 2 x ArH), 5.79 – 5.68 (1H, m, $\text{NHCH}_2\text{CHCH}_2\text{CHCH}_2$), 5.02 – 4.99 (2H, m, $\text{NHCH}_2\text{CHCH}_2\text{CHCH}_2$), 3.83 – 3.77 (2H, m, CH_2Ar), 3.81 (3H, s, ArOCH_3), 3.80 (3H, s, ArOCH_3), 3.68 (3H, s, COOCH_3), 2.80 – 2.83 (1H, m, NHCH_2CHCO), 2.79 (1H, bs, NHCH_2CHCO), 2.75 – 2.69 (1H, m, NHCH_2CHCO), 2.56 – 2.52 (1H, m, NHCH_2CHCO), 2.40 – 2.36 (1H, m, $\text{NHCH}_2\text{CHCH}_2\text{CHCH}_2$), 2.31 – 2.23 (1H, m, $\text{NHCH}_2\text{CHCH}_2\text{CHCH}_2$).

^{13}C NMR (75 MHz, CDCl_3) δ 175.14, 161.5, 158.6, 134.9, 130.8, 117.1, 105.7, 103.9, 98.1, 55.4, 51.7, 47.4, 41.1, 34.2

HRMS (ES^+) calc. for $\text{C}_{16}\text{H}_{23}\text{NO}_4$ ($\text{M}+\text{H}^+$) 294.1705, found 294.1709

Preparation of (*R*)-tert-butyl 3-(4-benzyl-2-oxooxazolidin-3-yl)-3-oxopropylcarbamate (2.40)



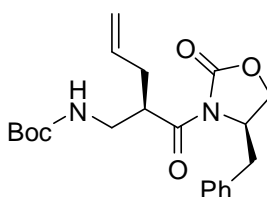
To a solution of **2.39** (0.5 g, 2.6 mmol) in anhydrous THF (25 mL) was added Et₃N (0.91 mL, 6.6 mmol) and the mixture was cooled to -30 °C. Pivaloyl chloride (0.33 mL, 2.6 mmol) was added dropwise and the resulting white suspension was stirred at -30 °C for 1.5 h. Anhydrous LiCl (123 mg, 2.9 mmol) and *R*-(*R*)-(-)-4-phenyl-2-oxazolidinone (0.45 g, 2.5 mmol) were added and the reaction was stirred at room temperature for 16 h. The solvents were removed *in vacuo* and the residue was diluted with ethyl acetate (25 mL). The organic layer was washed with saturated aqueous NH₄Cl (2 x 20 mL) aqueous HCl (1 M, 2 x 20 mL), aqueous NaOH (1 M, 20 mL) and brine (20 mL) before being dried over MgSO₄. The solvents were removed *in vacuo*. Purification of the residue by flash chromatography on silica gel (eluting with 1/2 ethyl acetate/petroleum ether) gave **2.40** (0.78 g, 85%) as a yellow oil.

¹H NMR (600 MHz, CDCl₃) δ 7.34 (2H, t, *J* = 6.8 Hz, ArH), 7.28 (1H, t, *J* = 6.8 Hz, ArH), 7.21 (2H, d, *J* = 6.8 Hz, ArH), 5.00 (1H, bs, NHCH₂CH₂CO), 4.69 – 4.66 (1H, m, OCH₂CHCH₂Ar), 4.24 – 4.17 (2H, m, NHCH₂CH₂CO), 3.50 (2H, bs, OCH₂CHCH₂Ar), 3.29 (1H, dd, *J* = 3.8, 13.8 Hz, OCH₂CHCH₂Ar), 3.17 – 3.10 (2H, m, NHCH₂CH₂CO), 2.79 (1H, dd, *J* = 10.2, 13.8 Hz, OCH₂CHCH₂Ar), 1.44 (9H, s, (CH₃)₃).

^{13}C NMR (75 MHz, CDCl_3) δ 172.1, 155.8, 153.4, 135.2, 129.9, 129.5, 128.5, 127.9, 126.6, 77.9, 66.4, 54.6, 37.5, 35.7, 34.2, 28.8.

HRMS (ES^+) calc. for $\text{C}_{18}\text{H}_{24}\text{N}_2\text{O}_5$ ($\text{M}+\text{H}^+$) 349.1763, found 349.1774

Preparation of Tert-butyl (*R*)-2-((*R*)-4-benzyl-2-oxooxazolidine-3-carbonyl)pent-4-enylcarbamate (2.41**)**



Method A

To a solution of **2.40** (750 mg, 2.2 mmol) in anhydrous THF (20 mL) under inert atmosphere at $-78\text{ }^\circ\text{C}$ was added NaHMDS (3.3 mL, 1M in THF) dropwise. The mixture was stirred at $-78\text{ }^\circ\text{C}$ for 30 minutes. Allyl iodide (0.3 mL, 3.3 mmol) was added and the reaction was stirred at $-78\text{ }^\circ\text{C}$ for 3 h. The reaction was quenched with saturated aqueous NH_4Cl (5 mL) and the solvents were removed *in vacuo*. The residue was dissolved in ethyl acetate (10 mL) and the organic phase was washed with water (10 mL) and brine (10 mL) before being dried over MgSO_4 . The solvents were removed *in vacuo*. Purification of the residue by flash chromatography on silica gel (eluting with 1/3 ethyl acetate/petroleum ether) gave **2.41** (460 mg, 55%) as a yellow oil.

^1H NMR (600 MHz, CDCl_3) δ 7.33 (2H, t, $J = 6.8$ Hz, ArH), 7.29 (1H, t, $J = 6.8$ Hz, ArH), 7.21 (2H, d, $J = 6.8$ Hz, ArH), 5.86 – 5.79 (1H, m, $\text{NHCH}_2\text{CHCH}_2\text{CHCH}_2$), 5.15 – 5.09 (2H, m, $\text{NHCH}_2\text{CHCH}_2\text{CHCH}_2$), 4.83 (1H, bs, NHCH_2CHCO), 4.69 –

4.65 (1H, m, OCH₂CHCH₂Ar), 4.23 (1H, t, $J = 8.2$ Hz, NHCH₂CHCO), 4.16 (1H, dd, $J = 3.4, 8.2$ Hz, NHCH₂CO), 4.00 – 3.96 (1H, m, OCH₂CHCH₂Ar), 3.51 – 3.47 (1H, m, OCH₂CHCH₂Ar), 3.36 – 3.34 (1H, m, NHCH₂CHCO), 3.30 – 3.27 (1H, m, OCH₂CHCH₂Ar), 2.69 (1H, dd, $J = 10.2, 14.4$ Hz, OCH₂CHCH₂Ar), 2.53 – 2.50 (1H, m, NHCH₂CHCH₂CHCH₂), 2.35 – 2.30 (1H, m, NHCH₂CHCH₂CHCH₂), 1.42 (9H, s, (CH₃)₃)

¹³C NMR (75 MHz, CDCl₃) δ 174.4, 155.8, 153.2, 135.3, 134.5, 129.4, 128.9, 127.4, 117.8, 79.4, 66.2, 55.5, 43.5, 41.0, 38.2, 34.0, 28.3.

HRMS (ES⁺) calc. for C₂₁H₂₈N₂O₅ (M+H⁺) 389.2076, found 389.2082

Method B

To a solution of **2.40** (50 mg, 0.1 mmol) in anhydrous THF (5 mL) under inert atmosphere at -78 °C was added NaHMDS (0.3 mL, 1M in THF) dropwise. The mixture was stirred at -78 °C for 30 minutes. Allyl iodide (0.028 mL, 0.3 mmol) was added and the reaction was stirred at -78 °C for 3 h. The reaction was quenched with saturated aqueous NH₄Cl (5 mL) and the solvents were removed *in vacuo*. The residue was dissolved in ethyl acetate (10 mL) and the organic phase was washed with water (10 mL) and brine (10 mL) before being dried over MgSO₄. The solvents were removed *in vacuo*. Purification of the residue by flash chromatography on silica gel (eluting with 1/3 ethyl acetate/petroleum ether) gave **2.41** (16 mg, 30%) as a yellow oil.

Method C

To a suspension of anhydrous LiCl (13 mg, 0.3 mmol) in anhydrous THF (5 mL) at -78 °C under inert atmosphere was added LDA (0.3 mL, 2M in THF). The solution was stirred at -78 °C for 10 minutes. **2.40** (27 mg, 0.08 mmol) was added and the mixture was stirred at -78 °C for 1 h. Allyl bromide (0.02 mL, 0.3 mmol) was added dropwise and the mixture was stirred at -78 °C for a further 2 h. The reaction was allowed to warm to room temperature and was then quenched with saturated aqueous NH₄Cl (5 mL). The solvents were removed *in vacuo* and the residue was diluted with ethyl acetate (10 mL). The organic phase was washed with saturated aqueous NaHCO₃ (10 mL), saturated aqueous NH₄Cl (10 mL) and brine (10 mL) before being dried over MgSO₄. The solvents were removed *in vacuo* and the residue was purified by flash chromatography on silica gel (eluting with 1/3 ethyl acetate/petroleum ether) to give side product **2.42** (10 mg, 60%) as a yellow oil.

Method D

To a solution of **2.40** (200 mg, 0.6 mmol) in anhydrous THF (25 mL) at -78 °C under inert atmosphere was added LiCl (68 mg, 2.4 mmol) and LiHMDS (1.8 mL, 1M in THF). The mixture was stirred at -78 °C for 15 minutes. Allyl bromide (0.07 mL, 0.9 mmol) was added and the reaction was stirred for a further 2 h at -78 °C before being allowed to warm to room temperature. The reaction was quenched with saturated aqueous NH₄Cl (25 mL) and the solvents were removed *in vacuo*. The residue was dissolved in ethyl acetate (20 mL) and the organic phase was washed with saturated aqueous NaHCO₃ (10 mL), saturated aqueous NH₄Cl (10 mL) and brine (10 mL) before being dried over MgSO₄. The solvents were removed *in vacuo* and the residue

was purified by flash chromatography on silica gel (eluting with 1/3 ethyl acetate/petroleum ether) to give side product **2.42** (73 mg, 56%) as a yellow oil.

Method E

To a solution of **2.40** (50 mg, 0.1 mmol) in anhydrous THF (5 mL) at -78 °C under inert atmosphere was added LiCl (12 mg, 0.2 mmol) and LiHMDS (0.1 mL, 1M in THF). The mixture was stirred at -78°C for 15 minutes then allyl bromide (0.09 mL, 0.1 mmol) was added. The reaction was stirred for a further 2 h at -78°C before being allowed to warm to room temperature. The reaction was quenched with saturated aqueous NH₄Cl (5 mL) and the solvents were removed *in vacuo*. The residue was dissolved in ethyl acetate (5 mL) and the organic phase was washed with saturated aqueous NaHCO₃ (5 mL), saturated aqueous NH₄Cl (5 mL) and brine (5 mL) before being dried over MgSO₄. The solvents were removed *in vacuo* and the residue was purified by flash chromatography on silica gel (eluting with 1/3 ethyl acetate/petroleum ether) to give side product **2.42** (9 mg, 30%) as a yellow oil.

Method F

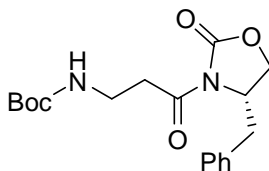
To a solution of **2.40** (50 mg, 0.1 mmol) in anhydrous THF (5 mL) under inert atmosphere at -78 °C was added NaHMDS (0.1 mL, 1M in THF) dropwise. The mixture was stirred at -78 °C for 30 minutes. Allyl bromide (0.013 mL, 0.15 mmol) was added and the reaction was stirred at -78 °C for 3 h. The reaction was quenched with saturated aqueous NH₄Cl (5 mL) and the solvents were removed *in vacuo*. The residue was dissolved in ethyl acetate (5 mL) and the organic phase was washed with water (5 mL) and brine (5 mL) before being dried over MgSO₄. The solvents were removed *in vacuo*. Purification of the residue by flash chromatography on silica gel

(eluting with 1/3 ethyl acetate/petroleum ether) gave side product **2.42** (10 mg, 47%) as a yellow oil.

Method G

To a solution of **2.40** (50 mg, 0.1 mmol) in anhydrous DCM (0.8 mL) under inert atmosphere at -30 °C was added TiCl₄ (0.017 mL, 0.1 mmol) followed by Et₃N (0.022 mL, 0.1 mmol). The mixture was stirred at -30 °C for 30 minutes. Allyl bromide (0.013 mL, 0.1 mmol) was added and the reaction was stirred at -15 °C for 4 h. The reaction was quenched with saturated aqueous NH₄Cl (5 mL). The reaction was diluted with DCM (5 mL) and the organic phase was washed with aqueous HCl (1 M, 2 x 5 mL), aqueous NaOH (1M, 5 mL) and brine (5 mL) before being dried over MgSO₄. The solvents were removed *in vacuo*. Purification of the residue by flash chromatography on silica gel (eluting with 1/3 ethyl acetate/petroleum ether) gave side product **2.42** (16 mg, 74%) as a yellow oil.

Preparation of (S)-tert-butyl 3-(4-benzyl-2-oxooxazolidin-3-yl)-3-oxopropylcarbamate (2.43)



To a solution of **2.39** (0.5 g, 2.6 mmol) in anhydrous THF (25 mL) was added Et₃N (0.91 mL, 6.6 mmol) and the mixture was cooled to -30 °C. Pivaloyl chloride (0.33 mL, 2.6 mmol) was added dropwise and the resulting white suspension was stirred at

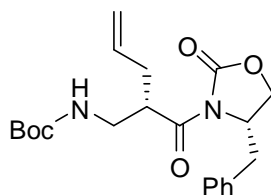
-30 °C for 1.5 h. Anhydrous LiCl (123 mg, 2.9 mmol) and (*S*)-(+)-4-phenyl-2-oxazolidinone (0.45 g, 2.5 mmol) were added and the reaction stirred at room temperature for 16 h. The solvents were removed *in vacuo* and the residue was diluted with ethyl acetate (25 mL). The organic layer was washed with saturated aqueous NH₄Cl (2 x 20 mL) aqueous HCl (1 M, 2 x 20 mL), aqueous NaOH (1 M, 20 mL) and brine (20 mL) before being dried over MgSO₄. The solvents were removed *in vacuo*. Purification of the residue by flash chromatography on silica gel (eluting with 1/2 ethyl acetate/petroleum ether) gave **2.43** (0.71 g, 78%) as a yellow oil.

¹H NMR (600 MHz, CDCl₃) δ 7.34 (2H, t, *J* = 6.8 Hz, ArH), 7.28 (1H, t, *J* = 6.8 Hz, ArH), 7.21 (2H, d, *J* = 6.8 Hz, ArH), 5.00 (1H, bs, NHCH₂CH₂CO), 4.69 – 4.66 (1H, m, OCH₂CHCH₂Ar), 4.24 – 4.17 (2H, m, NHCH₂CH₂CO), 3.50 (2H, bs, OCH₂CHCH₂Ar), 3.29 (1H, dd, *J* = 3.8, 13.8 Hz, OCH₂CHCH₂Ar), 3.17 – 3.10 (2H, m, NHCH₂CH₂CO), 2.79 (1H, dd, *J* = 10.2, 13.8 Hz, OCH₂CHCH₂Ar), 1.44 (9H, s, (CH₃)₃).

¹³C NMR (75 MHz, CDCl₃) δ 172.1, 155.8, 153.4, 135.2, 129.9, 129.5, 128.5, 127.9, 126.6, 77.9, 66.4, 54.6, 37.5, 35.7, 34.2, 28.8.

HRMS (ES⁺) calc. for C₁₈H₂₄N₂O₅ (M+H⁺) 349.1763, found 349.1761

Preparation of tert-butyl (S)-2-((S)-4-benzyl-2-oxooxazolidine-3-carbonyl)pent-4-enylcarbamate (2.44)



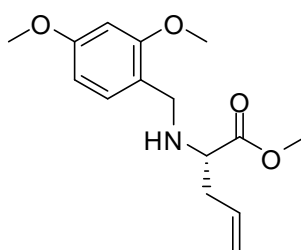
To a solution of **2.43** (850 mg, 2.4 mmol) in anhydrous THF (20 mL) under inert atmosphere at $-78\text{ }^{\circ}\text{C}$ was added NaHMDS (3.7 mL, 1M in THF) and the mixture was stirred at $-78\text{ }^{\circ}\text{C}$ for 30 minutes. Allyl iodide (0.34 mL, 3.7 mmol) was added and the reaction was stirred at $-78\text{ }^{\circ}\text{C}$ for 3 h. The reaction was quenched with saturated aqueous NH_4Cl (10 mL) and the solvents were removed *in vacuo*. The residue was dissolved in ethyl acetate (15 mL) and the organic phase was washed with water (10 mL) and brine (10 mL) before being dried over MgSO_4 . The solvents were removed *in vacuo*. Purification of the residue by flash chromatography on silica gel (eluting with 1/3 ethyl acetate/petroleum ether) gave **2.44** (455 mg, 48%) as a yellow oil.

^1H NMR (600 MHz, CDCl_3) δ 7.33 (2H, t, $J = 6.8$ Hz, ArH), 7.29 (1H, t, $J = 6.8$ Hz, ArH), 7.21 (2H, d, $J = 6.8$ Hz, ArH), 5.86 – 5.79 (1H, m, $\text{NHCH}_2\text{CHCH}_2\text{CHCH}_2$), 5.15 – 5.09 (2H, m, $\text{NHCH}_2\text{CHCH}_2\text{CHCH}_2$), 4.83 (1H, bs, NHCH_2CHCO), 4.69 – 4.65 (1H, m, $\text{OCH}_2\text{CHCH}_2\text{Ar}$), 4.23 (1H, t, $J = 8.2$ Hz, NHCH_2CHCO), 4.16 (1H, dd, $J = 3.4, 8.2$ Hz), 4.00 – 3.96 (1H, m, $\text{OCH}_2\text{CHCH}_2\text{Ar}$), 3.51 – 3.47 (1H, m, $\text{OCH}_2\text{CHCH}_2\text{Ar}$), 3.36 – 3.34 (1H, m, NHCH_2CHCO), 3.30 – 3.27 (1H, m, $\text{OCH}_2\text{CHCH}_2\text{Ar}$), 2.69 (1H, dd, $J = 10.2, 14.4$ Hz, $\text{OCH}_2\text{CHCH}_2\text{Ar}$), 2.53 – 2.50 (1H, m, $\text{NHCH}_2\text{CHCH}_2\text{CHCH}_2$), 2.35 – 2.30 (1H, m, $\text{NHCH}_2\text{CHCH}_2\text{CHCH}_2$), 1.1.42 (9H, s, $(\text{CH}_3)_3$)

^{13}C NMR (75 MHz, CDCl_3) δ 174.4, 155.8, 153.2, 135.3, 134.5, 129.4, 128.9, 127.4, 117.8, 79.4, 66.2, 55.5, 43.5, 41.0, 38.2, 34.0, 28.3.

HRMS (ES^+) calc. for $\text{C}_{21}\text{H}_{28}\text{N}_2\text{O}_5$ ($\text{M}+\text{H}^+$) 389.2076, found 389.2079

Preparation of (*S*)-methyl 2-(2,4-dimethoxybenzylamino)pent-4-enoate (**2.46**)



To a solution of **2.37** (400 mg, 1.9 mmol) in MeOH (5 mL) at 0 °C was added SOCl_2 (0.7 mL, 9.3 mmol) dropwise. The reaction was stirred at room temperature for 16 h. Removal of the solvent *in vacuo* gave **2.45** (308 mg, >99 %) as a yellow oil.

Method A

To a solution of **2.45** (140 mg, 0.9 mmol) in anhydrous methanol (3.5 mL) was added 2,4-dimethoxybenzaldehyde (138 mg, 0.9 mmol), sodium acetate (136 mg, 1.8 mmol) and 4Å molecular sieves (900 mg). The mixture was stirred at room temperature for 1 h, then $\text{Na}(\text{OAc})_3\text{BH}$ (1.31 g, 6.3 mmol) was added. The reaction was stirred at room temperature for 16 h. The reaction mixture was filtered through celite and the solvents removed *in vacuo*. The residue was dissolved in DCM (5 mL) and the organic phase was washed with saturated aqueous NaHCO_3 (5 mL), dried over MgSO_4 and the solvents removed *in vacuo*. Purification of the residue by flash chromatography on

silica gel (eluting with 3/1 ethyl acetate/petroleum ether) gave **2.46** (140 mg, 81 %) as a yellow oil.

^1H NMR (600 MHz, CDCl_3) δ 7.08 (1H, d, $J = 7.8$ Hz, ArH), 6.49 – 6.35 (2H, m, 2 x ArH), 5.71 – 5.62 (1H, m, $\text{NHCHCH}_2\text{CHCH}_2$), 5.07 – 4.99 (2H, m, $\text{NHCHCH}_2\text{CHCH}_2$), 4.52 (1H, bs, NHCHCO), 3.73 (3H, s, ArOCH_3), 3.72 (3H, s, ArOCH_3), 3.70 – 3.60 (2H, m, CH_2Ar), 3.60 (3H, s, COOCH_3), 3.30 – 3.25 (1H, m, NHCHCHO), 2.37 (t, $J = 8.2$ Hz, NHCHCHO), 2.39 – 2.30 (2H, m, $\text{NHCHCH}_2\text{CHCH}_2$)

Method B

Methyl ester **2.45** (50 mg, 0.3 mmol) was stirred in saturated aqueous NaHCO_3 (20 mL) for 30 minutes. The aqueous phase was extracted with DCM (3 x 15 mL) and the combined organic layers were dried over MgSO_4 . To this solution was added 2,4-dimethoxy-benzaldehyde (55 mg, 0.3 mmol) and $\text{Na(OAc)}_3\text{BH}$ (96 mg, 0.5 mmol). The reaction was stirred at room temperature for 16 h. Saturated aqueous NaHCO_3 (15 mL) was added to quench the reaction and the aqueous phase was washed with DCM (2 x 15 mL). The combined organic layers were dried over MgSO_4 and solvents were removed *in vacuo*. Purification by flash chromatography on silica gel (eluting with 3/1 ethyl acetate/petroleum ether) gave **2.46** (14 mg, 22 %) as a yellow oil.

Method C

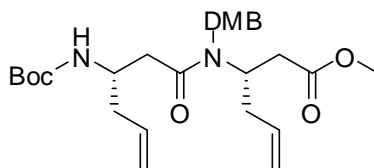
Methyl ester **2.45** (50 mg, 0.3 mmol) was stirred in saturated aqueous NaHCO_3 (20 mL) for 30 minutes. The aqueous phase was extracted with DCM (3 x 15 mL) and the combined organic layers were dried over MgSO_4 . To this solution was added 2,4-

dimethoxy-benzaldehyde (50 mg, 0.3 mmol) and Na(OAc)₃BH (96 mg, 0.5 mmol). The reaction was stirred at room temperature for 16 h. Saturated aqueous NaHCO₃ (15 mL) was added to quench the reaction and the aqueous phase was washed with DCM (2 x 15 mL). The combined organic layers were dried over MgSO₄ and the solvent was removed *in vacuo*. Purification by flash chromatography on silica gel (eluting with 3/1 ethyl acetate/petroleum ether) gave **2.46** (16 mg, 24 %) as a yellow oil.

Method D

Methyl ester **2.45** (50 mg, 0.3 mmol) was stirred in saturated aqueous NaHCO₃ (20 mL) for 30 minutes. The aqueous phase was extracted with DCM (3 x 15 mL) and the combined organic layers were dried over MgSO₄. To this solution was added 2,4-dimethoxy-benzaldehyde (45 mg, 0.3 mmol) and Na(OAc)₃BH (96 mg, 0.5 mmol). The reaction was stirred at room temperature for 16 h. Saturated aqueous NaHCO₃ (15 mL) was added to quench the reaction and the aqueous phase was washed with DCM (2 x 15 mL). The combined organic layers were dried over MgSO₄ and the solvent was removed *in vacuo*. Purification by flash chromatography on silica gel (eluting with 3/1 ethyl acetate/petroleum ether) gave **2.46** (23 mg, 22 %) as a yellow oil.

Preparation of methyl (3S)-3-[[[(3S)-3-(tert-butoxycarbonylamino)hex-5-enoyl]-[(2,4-dimethoxyphenyl)methyl]amino]hex-5-enoate (2.50)



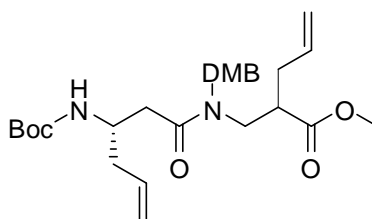
To a solution of **2.31** (66 mg, 0.3 mmol), **2.34** (70 mg, 0.2 mmol) and HATU (136 mg, 0.5 mmol) in anhydrous DCM (1 mL) was added DIPEA (0.2 mL, 1.2 mmol) dropwise. The reaction was stirred at room temperature for 16 h. The solvents were removed *in vacuo* and the reaction was diluted with ethyl acetate (5 mL) and washed with aqueous HCl (1 M, 2 x 5 mL), saturated aqueous NaHCO₃ (5 mL) and brine (5 mL). The organic phase was separated and dried over MgSO₄. The solvent was removed *in vacuo* and the residue purified by flash chromatography on silica gel (eluting with 1/3 ethyl acetate/petroleum ether) to give **2.50** (100 mg, 84 %) as a yellow oil.

¹H NMR (600 MHz, CDCl₃) δ 7.02 (1H, d, *J* = 8.2 Hz, ArH), 6.45 - 6.39 (3H, m, 3 x ArH), 5.78 - 5.71 (1H, m, CHCH₂), 5.63 - 5.55 (1H, m, CHCH₂), 5.16 - 4.97 (4H, m, 2 x CHCH₂), 4.44 (1H, bs, NH), 4.34 (2H, d, *J* = 1.8 Hz, CH₂Ar), 4.05 - 4.00 (1H, m, N(DMB)CHCH₂CO), 3.93 - 3.89 (1H, m, NHCHCH₂CO), 3.83 (3H, s, ArOCH₃), 3.77 (3H, s, ArOCH₃), 3.61 (3H, s, COOCH₃), 2.84 - 2.81 (1H, m, NHCHCH₂CO), 2.68 (1H, dd, *J* = 8.4, 15.6 Hz, N(DMB)CHCH₂CHCH₂), 2.59 - 2.55 (2H, m, N(DMB)CHCH₂CHCH₂, NHCHCH₂CO), 2.51 (1H, dd, *J* = 9.0, 15.7 Hz, N(DMB)CHCCH₂CHCH₂), 2.45 - 2.40 (1H, m, NHCHCH₂CHCH₂), 2.39 - 2.33 (2H, m, N(DMB)CHCCH₂CHCH₂, NHCHCH₂CHCH₂), 1.42 (9H, s, (CH₃)₃).

^{13}C NMR (75 MHz, CDCl_3) δ 172.2, 160.6, 159.8, 157.9, 155.5, 135.2, 134.9, 133.6, 128.9, 118.8, 117.5, 117.3, 103.8, 98.6, 55.4, 55.2, 53.5, 51.7, 47.8, 45.9, 38.7, 37.7, 37.1, 36.9, 29.7, 28.4

HRMS (ES^+) calc. for $\text{C}_{22}\text{H}_{32}\text{N}_2\text{O}_5$ ($\text{M}+\text{H}^+$) 505.2889, found 505.2909

Preparation of methyl (2*R*)-2-[[[(3*S*)-3-(tert-butoxycarbonylamino)hex-5-enoyl]-[(2,4-dimethoxyphenyl)methyl]amino]methyl]pent-4-enoate (2.51)



To a solution of **2.31** (160 mg, 0.7 mmol), **2.35** (175 mg, 0.6 mmol) and HATU (340 mg, 0.9 mmol) in anhydrous DCM (2 mL) was added DIPEA (0.4 mL, 2.4 mmol) dropwise. The reaction was stirred at room temperature for 16 h. The solvents were removed *in vacuo* and the reaction was diluted with ethyl acetate (5 mL) and washed with aqueous HCl (1 M, 2 x 5 mL), aqueous NaHCO_3 (5 mL) and brine (5 mL). The organic phase was separated and dried over MgSO_4 . The solvent was removed *in vacuo* and the residue purified by flash chromatography on silica gel (eluting with 1/3 ethyl acetate/petroleum ether) to give **2.51** (225 mg, 75 %) as a yellow oil.

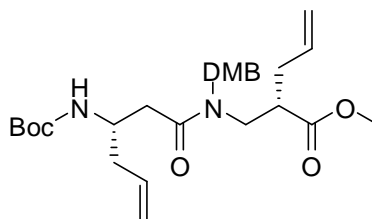
^1H NMR (600 MHz, CDCl_3) δ 6.89 (1H, d, $J = 7.8$, ArH), 6.44 – 6.42 (3H, m, 3 x ArH), 5.81 – 5.63 (m, 2H, 2 x CHCH₂), 5.57 (1H, bs, NH), 5.09 – 5.01 (4H, m, 2 x CHCH₂), 4.50 (1H, d, $J = 16.8$ Hz, CH₂Ar), 4.30 (1H, d, $J = 16.8$ Hz, CH₂Ar), 3.93 – 3.88 (1H, m, NHCHCH₂CO), 3.80 (3H, s, ArOCH₃), 3.79 (3H, s, ArOCH₃), 3.67

(3H, s, COOCH₃), 3.53 (1H, dd, $J = 5.4, 13.8$ Hz, N(DMB)CH₂CHCO), 3.38 (1H, dd, $J = 9.6, 13.7$ Hz, N(DMB)CH₂CHCO), 2.96 – 2.91 (1H, m, N(DMB)CH₂CHCO), 2.71 – 2.68 (1H, m, N(DMB)CH₂CHCH₂CHCH₂), 2.47 (1H, dd, $J = 4.2, 15.6$ Hz, N(DMB)CH₂CHCH₂CHCH₂), 2.43 – 2.41 (1H, m, NHCHCH₂CO), 2.38 – 2.32 (2H, m, NHCHCH₂CO, NHCHCH₂CHCH₂), 2.23 – 2.19 (1H, m, NHCHCH₂CHCH₂), 1.42 (9H, s, (CH₃)₃).

¹³C NMR (75 MHz, CDCl₃) δ 174.8, 172.2, 160.6, 160.3, 158.4, 158.2, 155.5, 135.2, 134.6, 133.9, 128.3, 117.7, 117.5, 117.2, 103.9, 98.7, 55.4, 51.9, 47.8, 44.3, 43.7, 41.8, 35.8, 35.6, 34.5, 28.4

HRMS (ES⁺) calc. for C₂₂H₃₂N₂O₅ (M+H⁺) 505.2889, found 505.2895

Preparation of methyl (2*S*)-2-[[[(3*S*)-3-(tert-butoxycarbonylamino)hex-5-enoyl]-[(2,4-dimethoxyphenyl)methyl]amino]methyl]pent-4-enoate (2.52)



To a solution of **2.31** (164 mg, 0.7 mmol), **2.36** (175 mg, 0.6 mmol) and HATU (340 mg, 0.9 mmol) in anhydrous DCM (2 mL) was added DIPEA (0.4 mL, 2.4 mmol) dropwise. The reaction was stirred at room temperature for 16 h. The solvents were removed *in vacuo* and the reaction was diluted with ethyl acetate (5 mL) and washed with aqueous HCl (1 M, 2 x 5 mL), saturated aqueous NaHCO₃ (5 mL) and brine (5 mL). The organic phase was separated and dried over MgSO₄. The solvent was

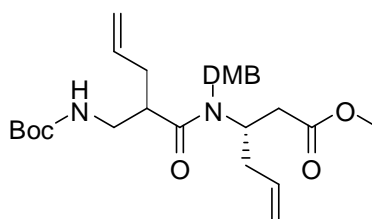
removed *in vacuo* and the residue purified by flash chromatography on silica gel (eluting with 1/3 ethyl acetate/petroleum ether) to give **2.52** (215 mg, 72 %) as a yellow oil.

^1H NMR (600 MHz, CDCl_3) δ 6.88 (1H, d, $J = 7.8$ Hz, ArH), 6.45 – 6.43 (2H, m, 2 x ArH), 5.81 – 5.67 (2H, m, 2 x CHCH₂), 5.57 (1H, bs, NH), 5.09 – 5.01 (4H, m, 2 x CHCH₂), 4.43 (1H, d, $J = 16.8$ Hz, CH₂Ar), 4.35 (1H, d, $J = 16.8$ Hz, CH₂Ar), 3.94 – 3.89 (1H, m, NHCHCH₂CO), 3.80 (3H, s, ArOCH₃), 3.79 (3H, s, ArOCH₃), 3.67 (3H, s, COOCH₃), 3.51 (1H, dd, $J = 3.6, 12.6$ Hz, N(DMB)CH₂CHCO), 3.43 (1H, dd, $J = 3.9$ Hz, 12.7 Hz, N(DMB)CH₂CHCO), 2.95 – 2.89 (1H, m, N(DMB)CH₂CHCO), 2.63 – 2.53 (2H, m, NHCHCH₂CO), 2.46 – 2.38 (1H, m, N(DMB)CH₂CHCH₂CHCH₂), 2.36 – 2.31 (2H, m, N(DMB)CH₂CHCH₂CHCH₂, NHCHCH₂CHCH₂), 2.23 – 2.19 (1H, m, NHCHCH₂CHCH₂), 1.42 (9H, s, (CH₃)₃).

^{13}C NMR (75 MHz, CDCl_3) δ 174.8, 160.6, 158.5, 155.5, 135.1, 134.6, 130.6, 128.1, 117.6, 116.8, 103.9, 98.7, 55.4, 55.2, 51.8, 48.1, 47.7, 44.2, 43.8, 41.7, 35.8, 28.4

HRMS (ES^+) calc. for $\text{C}_{22}\text{H}_{32}\text{N}_2\text{O}_5$ ($\text{M}+\text{H}^+$) 505.2889, found 505.2895

Preparation of methyl (3S)-3-[[[(2R)-2-[(tert-butoxycarbonylamino)methyl]pent-4-enoyl]-[(2,4-dimethoxyphenyl)methyl]amino]hex-5-enoate (2.53)



To a solution of **2.32** (94 mg, 0.4 mmol), **2.34** (100 mg, 0.3 mmol) and HATU (194 mg, 0.5 mmol) in anhydrous DCM (1 mL) was added DIPEA (0.3 mL, 1.6 mmol) dropwise. The reaction was stirred at room temperature for 16 h. The solvents were removed *in vacuo* and the reaction was diluted with ethyl acetate (5 mL) and washed with aqueous HCl (1 M, 2 x 5 mL), saturated aqueous NaHCO₃ (5 mL) and brine (5 mL). The organic phase was separated and dried over MgSO₄. The solvent was removed *in vacuo* and the residue purified by flash chromatography on silica gel (eluting with 1/3 ethyl acetate/petroleum ether) to give **2.53** (120 mg, 70 %) as a yellow oil.

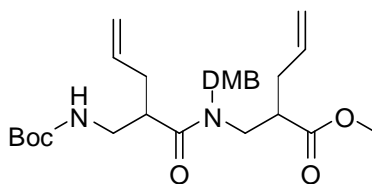
¹H NMR (600 MHz, CDCl₃) δ 7.02 (1H, d, *J* = 7.8 Hz, ArH), 6.49 – 6.42 (2H, m, 2 x ArH), 5.76-5.68 (1H, m, CH₂CHCH₂) 5.64 – 5.58 (1H, m, CH₂CHCH₂), 5.20 – 5.17 (1H, m, NH), 5.09 – 4.98 (4H, m, 2 x CH₂CHCH₂), 4.45 (1H, d, *J* = 16.6, CH₂Ar), 4.37 – 4.34 (1H, m, N(DMB)CHCH₂CO), 4.31 (1H, d, *J* = 16.5, CH₂Ar), 3.80 (3H, s, ArOCH₃), 3.79 (3H, s, ArOCH₃), 3.62 (3H, s, COOCH₃), 3.57 – 3.33 (1H, m, NHCH₂CHCO), 3.24 – 3.19 (1H, m, NHCH₂CHCO), 3.01 – 2.93 (1H, m, NHCH₂CHCO), 2.77 (1H, dd, *J* = 5.8, 14.2 Hz, N(DMB)CHCH₂CO), 2.57 (1H, dd, *J* = 6.0 Hz, 15.8 Hz), 2.43 – 2.33 (3H, m, N(DMB)CHCH₂CHCH₂),

NHCH₂CHCH₂CHCH₂), 2.21 – 2.16 (1H, m, NHCH₂CHCH₂CHCH₂), 1.44 (9H, s, (CH₃)₃).

¹³C NMR (75 MHz, CDCl₃) δ 175.5, 172.3, 160.6, 157.9, 156.0, 135.2, 133.8, 118.8, 117.6, 117.2, 103.8, 98.5, 79.0, 55.4, 55.3, 54.3, 51.6, 45.8, 42.2, 41.9, 37.2, 36.8, 34.7, 28.4.

HRMS (ES⁺) calc. for C₂₂H₃₂N₂O₅ (M+H⁺) 505.2889, found 505.2902

Preparation of methyl (2*R*)-2-[[[(2*R*)-2-[(tert-butoxycarbonylamino)methyl]pent-4-enoyl]-[(2,4-dimethoxyphenyl)methyl]amino]methyl]pent-4-enoate (2.54)



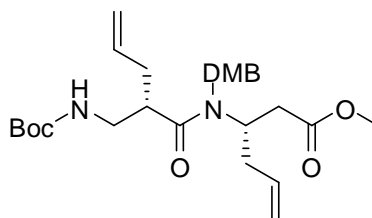
To a solution of **2.32** (164 mg, 0.7 mmol), **2.35** (175 mg, 0.6 mmol) and HATU (340 mg, 0.9 mmol) in anhydrous DCM (2 mL) was added DIPEA (0.5 mL, 2.4 mmol) dropwise. The reaction was stirred at room temperature for 16 h. The solvents were removed *in vacuo* and the reaction was diluted with ethyl acetate (5 mL) and washed with aqueous HCl (1 M, 2 x 5 mL), saturated aqueous NaHCO₃ (5 mL) and brine (5 mL). The organic phase was separated and dried over MgSO₄. The solvent was removed *in vacuo* and the residue purified by flash chromatography on silica gel (eluting with 1/3 ethyl acetate/petroleum ether) to give **2.54** (220 mg, 74 %) as a yellow oil.

^1H NMR (600 MHz, CDCl_3) δ 6.91 (1H, d, $J = 7.8$ Hz, ArH), 6.47 – 6.39 (2H, m, 2 x ArH), 5.75 – 5.68 (2H, m, 2 x CHCH₂), 5.31 (1H, bs, NH), 5.08 – 5.01 (4H, m, 2 x CHCH₂), 4.51 (1H, d, $J = 16.8$ Hz, CH₂DMB), 4.37 (1H, d, $J = 16.8$ Hz, CH₂Ar), 3.80 (3H, s, ArOCH₃), 3.79 (3H, s, ArOCH₃), 3.69 (3H, s, COOCH₃), 3.53 – 3.48 (1H, m, NHCH₂CHCO), 3.77 – 3.33 (1H, m, NHCH₂CHCO), 3.44 – 3.40 (1H, m, N(DMB)CH₂CHCO), 3.25 – 3.20 (1H, m, N(DMB)CH₂CHCO), 3.06 – 2.97 (1H, m, N(DMB)CH₂CHCO), 2.92 – 2.87 (1H, m, NHCH₂CHCO), 2.36 – 2.26 (2H, m, NHCH₂CHCH₂CHCH₂, N(DMB)CH₂CHCH₂CHCH₂), 2.21 – 2.15 (2H, m, NHCH₂CHCH₂CHCH₂, N(DMB)CH₂CHCH₂CHCH₂), 1.42 (9H, s, (CH₃)₃).

^{13}C NMR (75 MHz, CDCl_3) δ 175.3, 174.8, 160.6, 158.2, 156.0, 134.9, 130.7, 128.3, 117.3, 103.9, 98.5, 79.1, 55.4, 55.3, 51.9, 48.1, 47.6, 43.1, 42.0, 41.1, 34.8, 34.4, 28.4, 38.3

HRMS (ES^+) calc. for $\text{C}_{22}\text{H}_{32}\text{N}_2\text{O}_5$ ($\text{M}+\text{H}^+$) 505.2889, found 505.2908

Preparation of methyl (3*S*)-3-[[*(2S)*-2-[(*tert*-butoxycarbonylamino)methyl]pent-4-enoyl]-[(2,4-dimethoxyphenyl)methyl]amino]hex-5-enoate (2.55)



To a solution of **2.33** (94 mg, 0.4 mmol), **2.34** (100 mg, 0.3 mmol) and HATU (194 mg, 0.5 mmol) in anhydrous DCM (1 mL) was added DIPEA (0.3 mL, 1.6 mmol) dropwise. The reaction was stirred at room temperature for 16 h. The solvents were

removed *in vacuo* and the reaction was diluted with ethyl acetate (5 mL) and washed with aqueous HCl (1 M, 2 x 5 mL), saturated aqueous NaHCO₃ (5 mL) and brine (5 mL). The organic phase was separated and dried over MgSO₄. The solvent was removed *in vacuo* and the residue purified by flash chromatography on silica gel (eluting with 1/3 ethyl acetate/petroleum ether) to give **2.55** (110 mg, 65 %) as a yellow oil.

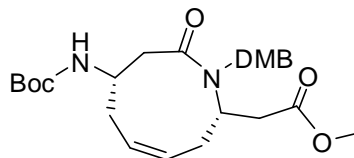
¹H NMR (600 MHz, CDCl₃) δ 7.05 (1H, d, *J* = 7.8 Hz, ArH), 6.44 – 6.42 (2H, m, 2 x ArH), 5.73 – 5.66 (1H, m, CHCH₂), 5.54 – 5.47 (1H, m, CHCH₂), 5.33 (1H, bs, NH), 5.10 – 4.95 (4H, m, 2 x CHCH₂), 4.45 (1H, d, *J* = 16.6 Hz, CH₂Ar), 4.42 – 4.34 (1H, m, N(DMB)CHCH₂CO), 4.34 (1H, d, *J* = 16.8 Hz, CH₂Ar), 3.80 (6H, s, 2 x ArOCH₃), 3.63 (3H, s, COOCH₃), 3.42 – 3.30 (1H, m, NHCH₂CHCO), 3.28 – 3.23 (1H, m, NHCH₂CHCO), 3.01 – 2.94 (1H, m, NHCH₂CHCO), 2.73 (1H, dd, *J* = 8.2, 15.8 Hz, N(DMB)CHCH₂CO), 2.55 (1H, dd, *J* = 4.8, 15.2 Hz, N(DMB)CHCH₂CO), 2.38 – 2.28 (3H, m, N(DMB)CHCH₂CHCH₂, NHCH₂CHCH₂CHCH₂), 2.20 – 2.16 (1H, m, NHCH₂CHCH₂CHCH₂), 1.44 (3H, s, (CH₃)₃).

¹³C NMR (75 MHz, CDCl₃) δ 175.5, 172.5, 160.6, 158.1, 156.1, 135.0, 134.9, 129.4, 117.5, 117.3, 104.2, 98.2, 78.9, 55.4, 55.1, 53.6, 51.7, 42.0, 37.2, 36.4, 34.9, 29.7, 28.4.

HRMS (ES⁺) calc. for C₂₂H₃₂N₂O₅ (M+H⁺) 505.2889, found 505.2899

Preparation of methyl 2-[(2*S*,4*Z*,7*S*)-7-(tert-butoxycarbonylamino)-1-[(2,4-dimethoxyphenyl)methyl]-9-oxo-3,6,7,8-tetrahydro-2*H*-azonin-2-yl]acetate

(2.56)



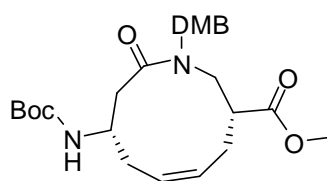
To a solution of **2.50** (100 mg, 0.2 mmol) in refluxing DCM (20 mL) was added Grubbs' second generation catalyst (8 mg, 0.01 mmol). The solution was stirred at reflux for 1 h then cooled to room temperature and activated charcoal was added (160 mg, 20 x w/w charcoal/catalyst). The reaction mixture was stirred at room temperature for 16 h. The solution was filtered through celite and the solvent removed *in vacuo* to give a brown solid. Purification of the residue by flash chromatography on silica gel (eluting with 1/2 ethyl acetate/petroleum ether) gave the alkene **2.56** (50 mg, 53%) as a white solid.

$^1\text{H NMR}$ (600 MHz, CDCl_3) δ 7.01 (1H, d, $J = 7.8$ Hz, ArH), 6.42 (1H, s, ArH), 6.38 (1H, d, $J = 7.8$ Hz, ArH), 6.01 (1H, bs, NH) 5.70 – 5.63 (2H, m, $\text{NHCHCH}_2\text{CHCHCH}_2\text{CH}$, $\text{NHCHCH}_2\text{CHCHCH}_2\text{CH}$), 4.68 (1H, d, $J = 16.0$ Hz, CH_2Ar), 4.20 (1H, bs, NHCHCH_2CO), 3.96 (1H, d, $J = 16.0$ Hz, CH_2Ar), 3.84 (3H, s, ArOCH_3), 3.81 – 3.80 (1H, m, $\text{N(DMB)CHCH}_2\text{CO}$), 3.77 (3H, s, ArOCH_3), 3.56 (3H, s, COOCH_3), 3.32 (1H, dd, $J = 2.8, 13.2$ Hz, NHCHCH_2CO), 2.63 (1H, dd, $J = 8.2, 16.6$ Hz, $\text{NHCHCH}_2\text{CHCHCH}_2\text{CH}$), 2.53 – 2.37 (4H, m, NHCHCH_2CO , $\text{N(DMB)CHCH}_2\text{CO}$, $\text{NHCHCH}_2\text{CHCHCH}_2\text{CH}$), 2.33 – 2.26 (2H, m, $\text{N(DMB)CHCH}_2\text{CHCHCH}_2\text{CH}$), 1.44 (9H, s, $(\text{CH}_3)_3$).

^{13}C NMR (75 MHz, CDCl_3) δ 174.0, 171.4, 159.8, 156.9, 155.2, 130.3, 129.2, 118.4, 104.2, 98.2, 78.9, 55.4, 55.3, 51.7, 49.2, 38.3, 32.3, 29.7, 28.4

HRMS (ES^+) calc. for $\text{C}_{20}\text{H}_{28}\text{N}_2\text{O}_5$ ($\text{M}+\text{H}^+$) 477.2595, found 477.2591

Preparation of methyl (3*R*,5*Z*,8*S*)-8-(tert-butoxycarbonylamino)-1-(2,4-dimethoxyphenyl)-10-oxo-2,3,4,7,8,9-hexahydroazecine-3-carboxylate (2.57)



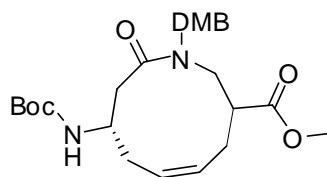
To a solution of **2.51** (280 mg, 0.6 mmol) in refluxing DCM (50 mL) was added Grubbs' second generation catalyst (24 mg, 0.03 mmol). The solution was stirred at reflux for 1 h then cooled to room temperature and activated charcoal was added (480 mg, 20 x w/w charcoal/catalyst). The reaction mixture was stirred at room temperature for 16 h. The solution was filtered through celite and the solvent removed *in vacuo* to give a brown solid. Purification of the residue by flash chromatography on silica gel (eluting with 1/2 ethyl acetate/petroleum ether) gave the alkene **2.57** (155 mg, 59%) as a white solid.

^1H NMR (600 MHz, CDCl_3) δ 7.21 (1H, d, $J = 7.8$ Hz, ArH), 6.87 (1H, d, $J = 7.8$ Hz, NH), 6.46 – 6.43 (2H, m, 2 x ArH), 5.61 (1H, ddd, $J = 3.8, 11.4, 21.8$ Hz, NHCHCH₂CHCHCH₂CH), 5.38 (1H, ddd, $J = 3.8, 11.6, 22.0$ Hz, NHCHCH₂CHCHCH₂CH), 5.20 (1H, d, $J = 15.4$ Hz, CH₂Ar), 3.96 (1H, d, $J = 15.4$ Hz, CH₂Ar), 3.91 – 3.85 (1H, m, NHCHCH₂CO), 3.79 (3H, s, ArOCH₃), 3.78 (3H, s,

ArOCH₃), 3.72 (3H, s, COOCH₃), 3.70 – 3.65 (1H, m, N(DMB)CH₂CHCO), 3.31 (1H, dd, *J* = 3.8, 14.6 Hz, N(DMB)CH₂CHCO), 3.20 – 3.17 (1H, m, N(DMB)CH₂CHCO), 3.08 (1H, dd, *J* = 3.8, 13.8 Hz, NHCHCH₂CO), 2.44 – 2.40 (1H, m, NHCHCH₂CHCHCH₂CH), 2.33 – 2.30 (2H, m, NHCHCH₂CHCHCH₂CH, NHCHCH₂CHCHCH₂CH), 2.24 – 2.18 (1H, m, NHCHCH₂CHCHCH₂CH), 2.17 – 2.14 (1H, m, NHCHCH₂CO), 1.44 (9H, s, (CH₃)₃).

HRMS (ES⁺) calc. for C₂₀H₂₈N₂O₅ (M+H⁺) 477.2595, found 477.2596

Preparation of methyl (3*S*,5*Z*,8*S*)-8-(tert-butoxycarbonylamino)-1-(2,4-dimethoxyphenyl)-10-oxo-2,3,4,7,8,9-hexahydroazecine-3-carboxylate (2.58)



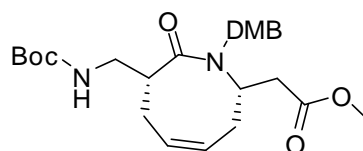
To a solution of **2.52** (250 mg, 0.5 mmol) in refluxing DCM (50 mL) was added Grubbs' second generation catalyst (21 mg, 0.02 mmol). The solution was stirred at reflux for 1 h then cooled to room temperature and activated charcoal was added (400 mg, 20 x w/w charcoal/catalyst). The reaction mixture was stirred at room temperature for 16 h. The solution was filtered through celite and the solvent removed *in vacuo* to give a brown solid. Purification of the residue by flash chromatography on silica gel (eluting with 1/2 ethyl acetate/petroleum ether) gave the alkene **2.58** (66 mg, 29%) as a white solid.

^1H NMR (600 MHz, CDCl_3) δ 7.21 (1H, d, $J = 7.8$ Hz, ArH), 6.87 (1H, d, $J = 7.8$ Hz, NH), 6.46 – 6.43 (2H, m, 2 x ArH), 6.62 (1H, ddd, $J = 3.8, 11.2, 22.8$ Hz, NHCHCH₂CHCHCH₂CH), 5.38 (1H, ddd, $J = 3.8, 11.8, 23.0$ Hz, NHCHCH₂CHCHCH₂CH), 5.20 (1H, d, $J = 15.4$ Hz, CH₂Ar), 3.96 (1H, d, $J = 15.4$ Hz, CH₂Ar), 3.91 – 3.86 (1H, m, NHCHCH₂CO), 3.79 (3H, s, ArOCH₃), 3.78 (3H, s, ArOCH₃), 3.72 (3H, s, COOCH₃), 3.69 – 3.67 (1H, m, N(DMB)CH₂CHCO), 3.31 (1H, dd, $J = 3.8, 14.2$ Hz, N(DMB)CH₂CHCO), 3.20 – 3.17 (1H, m, N(DMB)CH₂CHCO), 3.07 (1H, dd, $J = 3.8, 14.0$ Hz, NHCHCH₂CO), 2.49 – 2.44 (2H, m, NHCHCH₂CHCHCH₂CH), 2.33 – 2.31 (1H, m, NHCHCH₂CO), 2.24 – 2.14 (2H, m, NHCHCH₂CHCHCH₂CH), 1.44 (9H, s, (CH₃)₃).

^{13}C NMR (75 MHz, CDCl_3) δ 173.1, 172.9, 160.4, 158.5, 155.4, 130.9, 130.7, 126.4, 117.1, 104.6, 98.4, 78.8, 55.4, 55.3, 51.9, 48.3, 45.6, 40.6, 39.8, 32.2, 31.7, 28.5, 28.4, 24.4.

HRMS (ES^+) calc. for $\text{C}_{20}\text{H}_{28}\text{N}_2\text{O}_5$ ($\text{M}+\text{H}^+$) 477.2595, found 477.2603

Preparation of methyl 2-[(2*S*,4*Z*,7*R*)-7-[(*tert*-butoxycarbonylamino)methyl]-1-[(2,4-dimethoxyphenyl)methyl]-8-oxo-2,3,6,7-tetrahydroazocin-2-yl]acetate (2.59)



To a solution of **2.53** (160 mg, 0.4 mmol) in refluxing DCM (30 mL) was added Grubbs' second generation catalyst (14 mg, 0.02 mmol). The solution was stirred at

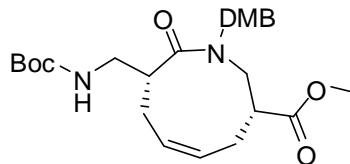
reflux for 1 h then cooled to room temperature and activated charcoal was added (280 mg, 20 x w/w charcoal/catalyst). The reaction mixture was stirred at room temperature for 16 h. The solution was filtered through celite and the solvent removed *in vacuo* to give a brown solid. Purification of the residue by flash chromatography on silica gel (eluting with 1/2 ethyl acetate/petroleum ether) gave the alkene **2.59** (70 mg, 49%) as a white solid.

^1H NMR (600 MHz, CDCl_3) δ 7.10 (1H, d, $J = 7.8$ Hz, ArH), 6.41 – 6.38 (2H, m, 2 x ArH), 5.70 (1H, ddd, $J = 2.6, 7.8, 18.8$ Hz, $\text{NHCH}_2\text{CHCH}_2\text{CHCHCH}_2\text{CH}$), 5.50 (1H, bs, NH) 5.42 (1H, ddd, $J = 1.4, 9.2, 18.6$ Hz, $\text{NHCH}_2\text{CHCH}_2\text{CHCHCH}_2\text{CH}$), 4.96 – 4.91 (1H, m, $\text{N(DMB)CHCH}_2\text{CO}$), 4.61 (1H, d, $J = 16.2$ Hz, CH_2Ar), 4.01 (1H, d, $J = 16.2$ Hz, CH_2Ar), 3.83 (3H, s, ArOCH_3), 3.77 (3H, s, ArOCH_3), 3.51 – 3.40 (2H, m, NHCH_2CHCO), 3.47 (3H, s, COOCH_3), 2.90 – 2.84 (1H, m, NHCH_2CHCO), 2.60 (1H, dd, $J = 8.2, 16.8$ Hz, $\text{N(DMB)CHCH}_2\text{CO}$), 2.46 – 2.40 (1H, m, $\text{N(DMB)CHCH}_2\text{CHCHCH}_2\text{CH}$), 2.34 (1H, dd, $J = 4.8, 16.8$ Hz, $\text{N(DMB)CHCH}_2\text{CO}$), 2.33 – 2.16 (2H, m, $\text{N(DMB)CHCH}_2\text{CHCHCH}_2\text{CH}$, $\text{NHCH}_2\text{CHCH}_2\text{CHCHCH}_2\text{CH}$), 2.14 – 2.10 (1H, m, $\text{NHCH}_2\text{CHCH}_2\text{CHCHCH}_2\text{CH}$), 1.45 (9H, s, CH_3)₃.

^{13}C NMR (75 MHz, CDCl_3) δ 176.1, 171.2, 159.7, 156.9, 156.7, 130.6, 129.6, 127.1, 118.9, 104.3, 98.1, 77.6, 55.3, 55.2, 51.9, 49.5, 43.6, 43.1, 37.1, 36.8, 32.1, 30.0, 28.5, 22.7.

HRMS (ES^+) calc. for $\text{C}_{20}\text{H}_{28}\text{N}_2\text{O}_5$ ($\text{M}+\text{H}^+$) 477.2595, found 477.2593

Preparation of methyl (3*R*,5*Z*,8*R*)-8-[(*tert*-butoxycarbonylamino)methyl]-1-(2,4-dimethoxyphenyl)-9-oxo-3,4,7,8-tetrahydro-2*H*-azonine-3-carboxylate (2.60)



Method A

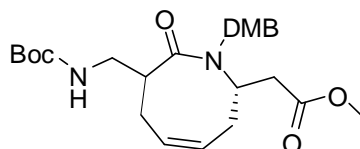
To a solution of **2.54** (50 mg, 0.1 mmol) in refluxing DCM (10 mL) was added Grubbs' second generation catalyst (4 mg, 0.005 mmol). The solution was stirred at reflux for 1 h then cooled to room temperature and activated charcoal was added (80 mg, 20 x w/w charcoal/catalyst). The reaction mixture was stirred at room temperature for 16 h. The solution was filtered through celite and the solvent removed *in vacuo* to give a brown solid. Purification of the residue by flash chromatography on silica gel (eluting with 1/2 ethyl acetate/petroleum ether) gave the starting material **2.54** (16%) and the dimer side product (9%) with no **2.60** observed.

Method B

To a solution of **2.54** (50 mg, 0.1 mmol) in refluxing DCM (10 mL) was added Grubbs' second generation catalyst (16 mg, 0.02 mmol). The solution was stirred at reflux for 72 h then cooled to room temperature and activated charcoal was added (320 mg, 20 x w/w charcoal/catalyst). The reaction mixture was stirred at room temperature for 16 h. The solution was filtered through celite and the solvent removed *in vacuo* to give a brown solid. Purification of the residue by flash chromatography on silica gel (eluting with 1/2 ethyl acetate/petroleum ether) gave the starting material **2.54** (12%) and the dimer side product (11%) with no **2.60** observed.

Preparation of methyl 2-[(2*S*,4*Z*,7*S*)-7-[(*tert*-butoxycarbonylamino)methyl]-1-[(2,4-dimethoxyphenyl)methyl]-8-oxo-2,3,6,7-tetrahydroazocin-2-yl]acetate

(2.61)



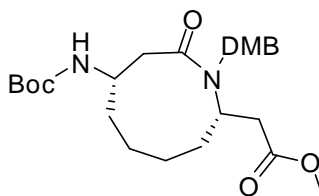
To a solution of **2.55** (160 mg, 0.4 mmol) in refluxing DCM (30 mL) was added Grubbs' second generation catalyst (14 mg, 0.02 mmol). The solution was stirred at reflux for 1 h then cooled to room temperature and activated charcoal was added (280 mg, 20 x w/w charcoal/catalyst). The reaction mixture was stirred at room temperature for 16 h. The solution was filtered through celite and the solvent removed *in vacuo* to give a brown solid. Purification of the residue by flash chromatography on silica gel (eluting with 1/2 ethyl acetate/petroleum ether) gave the alkene **2.61** (66 mg, 44%) as a white solid.

$^1\text{H NMR}$ (600 MHz, CDCl_3) δ 7.20 (1H, d, $J = 7.8$ Hz, ArH), 6.42 – 6.40 (2H, m, 2 x ArH), 5.65 – 5.62 (1H, m, $\text{NHCH}_2\text{CHCH}_2\text{CHCH}_2\text{CH}$), 5.27 (1H, ddd, $J = 2.8, 11.2, 27.6$ Hz, $\text{NHCH}_2\text{CHCH}_2\text{CHCH}_2\text{CH}$), 5.09 (1H, bs, NH), 4.70 (1H, d, $J = 15.4$ Hz, CH_2Ar), 4.38 (1H, d, $J = 15.6$ Hz, CH_2Ar), 4.03 – 3.94 (1H, m, $\text{N(DMB)CHCH}_2\text{CO}$), 3.80 (3H, s, ArOCH_3), 3.79 (3H, s, ArOCH_3), 3.47 (3H, s, COOCH_3), 3.45 – 3.30 (2H, m, NHCH_2CHCO), 3.28 – 3.18 (1H, m, NHCH_2CHCO), 2.63 – 2.51 (3H, m, $\text{N(DMB)CHCH}_2\text{CO}$, $\text{N(DMB)CHCH}_2\text{CHCH}_2\text{CH}$), 2.43 – 2.51 (2H, m, $\text{N(DMB)CHCH}_2\text{CHCH}_2\text{CH}$, $\text{NHCH}_2\text{CHCH}_2\text{CHCH}_2\text{CH}$), 2.09 – 1.98 (1H, m, $\text{NHCH}_2\text{CHCH}_2\text{CHCH}_2\text{CH}$), 1.43 (9H, s, $(\text{CH}_3)_3$).

^{13}C NMR (75 MHz, CDCl_3) δ 174.7, 171.3, 160.1, 158.4, 156.2, 131.8, 130.3, 125.9, 117.9, 115.1, 104.1, 98.0, 79.1, 55.3, 55.2, 54.1, 51.7, 45.8, 43.0, 40.4, 33.8, 29.8, 29.8, 29.7, 28.4

HRMS (ES^+) calc. for $\text{C}_{20}\text{H}_{28}\text{N}_2\text{O}_5$ ($\text{M}+\text{H}^+$) 477.2595, found 477.2595

Preparation of methyl 2-[(2*S*,7*S*)-7-(tert-butoxycarbonylamino)-1-[(2,4-dimethoxyphenyl)methyl]-9-oxo-azonan-2-yl]acetate (2.62**)**



To a solution of **2.56** (50 mg, 0.1 mmol) in ethyl acetate (20 mL) was added palladium on carbon (25 mg, 50% w/w catalyst/alkene). The reaction mixture was stirred at room temperature for 16 h under an H_2 atmosphere at atmospheric pressure then filtered through celite. Removal of the solvent *in vacuo* gave **2.62** (45 mg, 89%) as a white solid.

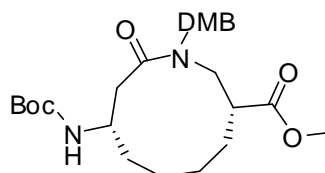
^1H NMR (600 MHz, CDCl_3) δ 7.01 (1H, d, $J = 7.8$ Hz, ArH), 6.42 (1H, s, ArH), 6.38 (1H, d, $J = 8$ Hz, ArH), 5.76 (1H, d, $J = 8.2$ Hz, NH), 4.83 (1H, d, $J = 16.4$ Hz, CH_2Ar), 4.76 – 4.71 (1H, m, N(DMB)CHCH $_2$ CO), 4.10 – 4.03 (1H, m, NHCHCH $_2$ CO), 3.92 (1H, d, $J = 16.4$ Hz, CH_2Ar), 3.83 (3H, s, ArOCH $_3$), 3.77 (3H, s, ArOCH $_3$), 3.47 (3H, s, COOCH $_3$), 3.49 – 3.44 (1H, m, NHCHCH $_2$ CO), 2.60 – 2.52 (2H, m, NHCHCH $_2$ CO, N(DMB)CHCH $_2$ CO), 2.29 (1H, dd, $J = 4.8, 17.0$ Hz,

N(DMB)CHCH₂CO), 2.02 – 1.97 (1H, m, NHCHCH₂CH₂CH₂CH₂CH), 1.86 – 1.71 (2H, m, NHCHCH₂CH₂CH₂CH₂CH), 1.68 – 1.63 (1H, m, NHCHCH₂CH₂CH₂CH₂CH), 1.52 – 1.37 (4H, m, NHCHCH₂CH₂CH₂CH₂CH, NHCHCH₂CH₂CH₂CH₂CH), 1.42 (9H, s, CH₃)₃).

¹³C NMR (75 MHz, CDCl₃) δ 174.0, 171.5, 159.8, 156.9, 155.4, 129.1, 118.5, 104.2, 98.2, 78.8, 55.4, 55.2, 53.4, 51.6, 48.1, 38.1, 37.0, 33.1, 32.2, 29.7, 28.4, 24.8, 22.7, 21.7

HRMS (ES⁺) calc. for C₂₀H₃₀N₂O₅ (M+H⁺) 479.2752, found 479.2747

Preparation of methyl (3*R*,8*S*)-8-(tert-butoxycarbonylamino)-1-(2,4-dimethoxyphenyl)-10-oxo-azecane-3-carboxylate (2.63)



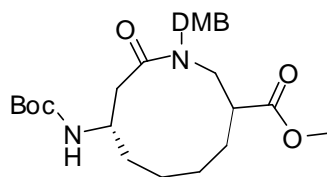
To a solution of **2.57** (150 mg, 0.3 mmol) in ethyl acetate (20 mL) was added palladium on carbon (75 mg, 50% w/w catalyst/alkene). The reaction mixture was stirred at room temperature for 16 h under an H₂ atmosphere at atmospheric pressure then filtered through celite. Removal of the solvent *in vacuo* gave **2.63** (129 mg, 83%) as a white solid.

¹H NMR (600 MHz, CDCl₃) δ 7.20 (1H, d, *J* = 7.8 Hz, ArH), 6.71 (1H, d, *J* = 7.8 Hz, NH), 5.14 (1H, d, *J* = 15.4 Hz, CH₂Ar), 3.96 – 3.92 (2H, m, CH₂Ar, NHCHCH₂CO),

3.82 – 3.74 (1H, m, N(DMB)CH₂CHCO) 3.79 (3H, s, ArOCH₃), 3.78 (3H, s, ArOCH₃), 3.46 (3H, s, COOCH₃), 3.35 (1H, dd, $J = 4.8, 16.0$ Hz, N(DMB)CH₂CHCO), 3.27 (1H, dd, $J = 4.8, 15.6$ Hz, NHCHCH₂CO), 3.08 – 3.03 (1H, m, N(DMB)CH₂CHCO), 2.34 – 2.29 (1H, m, NHCHCH₂CO), 1.81 – 1.69 (2H, m, NHCHCH₂CH₂CH₂CH₂CH, NHCHCH₂CH₂CH₂CH₂CH), 1.61 – 1.53 (2H, m, NHCHCH₂CH₂CH₂CH₂CH, NHCHCH₂CH₂CH₂CH₂CH), 1.43 (9H, s, (CH₃)₃), 1.35 – 1.11 (4H, m, NHCHCH₂CH₂CH₂CH₂CH, NHCHCH₂CH₂CH₂CH₂CH).

HRMS (ES⁺) calc. for C₂₀H₃₀N₂O₅ (M+H⁺) 479.2752, found 479.2754

Preparation of methyl (3*S*,8*S*)-8-(tert-butoxycarbonylamino)-1-(2,4-dimethoxyphenyl)-10-oxo-azecane-3-carboxylate (2.64)



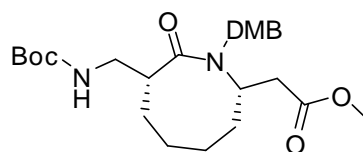
To a solution of **2.58** (60 mg, 0.1 mmol) in ethyl acetate (20 mL) was added palladium on carbon (30 mg, 50% w/w catalyst/alkene). The reaction mixture was stirred at room temperature for 16 h under an H₂ atmosphere at atmospheric pressure then filtered through celite. Removal of the solvent *in vacuo* gave **2.64** (30 mg, 54%) as a white solid.

¹H NMR (600 MHz, CDCl₃) δ 7.20 (1H, d, $J = 7.8$ Hz, ArH), 6.71 (1H, d, $J = 5.6$ Hz, NH), 6.46 – 6.43 (2H, m, 2 x ArH), 5.14 (1H, d, $J = 13.8$ Hz, CH₂Ar), 3.97 – 3.89 (2H, m, CH₂Ar, NHCHCH₂CO), 3.79 (3H, s, ArOCH₃), 3.78 (3H, s, ArOCH₃), 3.68

(3H, s, COOCH₃), 3.49 (1H, d, $J = 5.4$ Hz, NHCHCH₂CO), 3.35 (1H, dd, $J = 5.2$, 15.4 Hz, N(DMB)CH₂CHCO), 3.27 (1H, dd, $J = 5.2$, 15.2 Hz, N(DMB)CH₂CHCO), 3.07 – 3.05 (1H, m, N(DMB)CH₂CHCO), 2.32 (1H, d, $J = 15.6$ Hz, NHCHCH₂CO), 1.86 – 1.82 (1H, m, NHCHCH₂CH₂CH₂CH₂CH), 1.78 – 1.70 (1H, m, NHCHCH₂CH₂CH₂CH₂CH), 1.60 – 1.55 (2H, m, NHCHCH₂CH₂CH₂CH₂CH, NHCHCH₂CH₂CH₂CH₂CH), 1.43 (9H, s, (CH₃)₃), 1.23 – 1.09 (4H, m, NHCHCH₂CH₂CH₂CH₂CH, NHCHCH₂CH₂CH₂CH₂CH).

HRMS (ES⁺) calc. for C₂₀H₃₀N₂O₅ (M+H⁺) 479.2752, found 479.2751

Preparation of methyl 2-[(2*S*,7*R*)-7-[(*tert*-butoxycarbonylamino)methyl]-1-[(2,4-dimethoxyphenyl)methyl]-8-oxo-azocan-2-yl]acetate (2.65**)**



To a solution of **2.59** (70 mg, 0.1 mmol) in ethyl acetate (20 mL) was added palladium on carbon (35 mg, 50% w/w catalyst/alkene). The reaction mixture was stirred at room temperature for 16 h under an H₂ atmosphere at atmospheric pressure then filtered through celite. Removal of the solvent *in vacuo* gave **2.65** (51 mg, 73%) as a white solid.

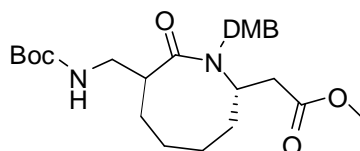
¹H NMR (600 MHz, CDCl₃) δ 7.20 (1H, d, $J = 7.8$ Hz, ArH), 6.71 (1H, d, $J = 8.6$ Hz, NH), 6.46 – 6.43 (2H, m, 2 x ArH), 5.14 (1H, d, $J = 15.4$ Hz, CH₂Ar), 3.96 – 3.92 (2H, m, CH₂Ar, NHCH₂CHCO), 3.79 (3H, s, ArOCH₃), 3.78 (3H, s, ArOCH₃), 3.78 – 3.74 (1H, m, NHCH₂CHCO), 3.67 (3H, s, COOCH₃), 3.35 (1H, dd, $J = 5.2$, 15.4

Hz, N(DMB)CHCH₂CO), 3.26 (1H, dd, $J = 5.4, 15.4$ Hz, N(DMB)CHCH₂CO), 3.08 – 3.04 (1H, m, NHCH₂CHCO), 2.33 (1H, d, $J = 15.2$ Hz, N(DMB)CHCH₂CO), 1.78 – 1.67 (2H, m, NHCH₂CHCH₂CH₂CH₂CH₂CH, NHCH₂CHCH₂CH₂CH₂CH₂CH), 1.59 – 1.51 (2H, m, NHCH₂CHCH₂CH₂CH₂CH₂CH, NHCH₂CHCH₂CH₂CH₂CH₂CH), 1.42 (9H, s, (CH₃)₃), 1.36 – 1.05 (4H, m, NHCH₂CHCH₂CH₂CH₂CH₂CH, NHCH₂CHCH₂CH₂CH₂CH₂CH).

¹³C NMR (75 MHz, CDCl₃) δ 174.0, 171.4, 159.8, 156.9, 155.2, 129.2, 118.4, 104.2, 98.2, 79.0, 55.3, 55.2, 51.7, 51.6, 38.3, 28.5, 28.3

HRMS (ES⁺) calc. for C₂₀H₃₀N₂O₅ (M+H⁺) 479.2752, found 479.2753

Preparation of methyl 2-[(2*S*,7*S*)-7-[(tert-butoxycarbonylamino)methyl]-1-[(2,4-dimethoxyphenyl)methyl]-8-oxo-azocan-2-yl]acetate (2.66**)**



To a solution of **2.61** (66 mg, 0.1 mmol) in ethyl acetate (20 mL) was added palladium on carbon (33 mg, 50% w/w catalyst/alkene). The reaction mixture was stirred at room temperature for 16 h under an H₂ atmosphere at atmospheric pressure then filtered through celite. Removal of the solvent *in vacuo* gave **2.66** (54 mg, 82%) as a white solid.

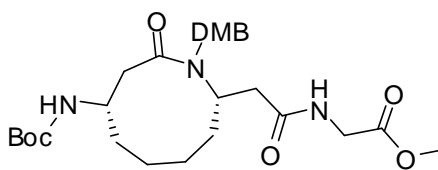
¹H NMR (600 MHz, CDCl₃) δ 7.31 (1H, d, $J = 7.8$ Hz, ArH), 6.45 – 6.43 (2H, m, 2 x ArH), 5.11 (1H, bs, NH), 4.85 (1H, d, $J = 14.6$ Hz, CH₂Ar), 4.33 (1H, d, $J = 14.4$ Hz,

CH_2Ar), 4.19 – 4.09 (1H, m, $\text{N}(\text{DMB})\text{CHCH}_2\text{CO}$), 3.81 (3H, s, ArOCH_3), 3.80 (3H, s, ArOCH_3), 3.62 (3H, s, COOCH_3), 3.34 – 3.22 (2H, m, NHCH_2CHCO), 3.10 – 3.02 (1H, m, NHCH_2CHCO), 2.71 (1H, m, $\text{N}(\text{DMB})\text{CHCH}_2\text{CO}$), 2.54 (1H, dd, $J = 5.4$, 15.8 Hz, $\text{N}(\text{DMB})\text{CHCH}_2\text{CO}$), 1.88 – 1.77 (2H, m $\text{NHCH}_2\text{CHCH}_2\text{CH}_2\text{CH}_2\text{CH}_2\text{CH}$, $\text{NHCH}_2\text{CHCH}_2\text{CH}_2\text{CH}_2\text{CH}_2\text{CH}$), 1.66 – 1.49 (2H, m $\text{NHCH}_2\text{CHCH}_2\text{CH}_2\text{CH}_2\text{CH}_2\text{CH}$, $\text{NHCH}_2\text{CHCH}_2\text{CH}_2\text{CH}_2\text{CH}_2\text{CH}$), 1.43 (9H, s, $(\text{CH}_3)_3$), 1.39 – 1.26 (2H, m $\text{NHCH}_2\text{CHCH}_2\text{CH}_2\text{CH}_2\text{CH}_2\text{CH}$, $\text{NHCH}_2\text{CHCH}_2\text{CH}_2\text{CH}_2\text{CH}_2\text{CH}$).

^{13}C NMR (75 MHz, CDCl_3) δ 175.3, 171.6, 160.3, 156.2, 118.3, 104.2, 98.2, 79.0, 55.3, 55.2, 53.4, 51.7, 43.2, 33.9, 29.7, 29.5, 28.4, 24.1, 22.7

HRMS (ES^+) calc. for $\text{C}_{20}\text{H}_{30}\text{N}_2\text{O}_5$ ($\text{M}+\text{H}^+$) 479.2752, found 479.2748

Preparation of methyl 2-[[2-[(2*S*,7*S*)-7-(tert-butoxycarbonylamino)-1-[(2,4-dimethoxyphenyl)methyl]-9-oxo-azonan-2-yl]acetyl]amino]acetate (2.68)



To a solution of **2.62** (45 mg, 0.1 mmol) in THF (2.5 mL) was added NaOH (10 mg, 0.2 mmol) in water (0.5 mL). The reaction was stirred at room temperature for 16 h, and then solvents were removed *in vacuo*. The residue was acidified to pH 1 with aqueous HCl (1M, 2mL) and the aqueous phase was extracted with ethyl acetate (2 x

5 mL). The combined organic layers were dried over MgSO_4 and solvents were removed *in vacuo* to give the acid (30 mg, 69%) as a colourless oil.

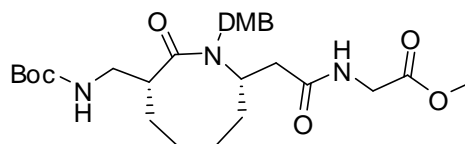
To a solution of this acid (30 mg, 0.06 mmol), glycine-OMe.HCl (25 mg, 0.2 mmol) and HATU (50 mg, 0.1 mmol) in DCM (1 mL) was added DIPEA (0.1 mL, 0.6 mmol). The mixture was stirred at room temperature for 16 h. The organic phase was diluted with DCM (5 mL) and washed with aqueous HCl (1 M, 2 x 5 mL), saturated aqueous NaHCO_3 (5 mL) and brine (5 mL). The organic phase was separated and dried over MgSO_4 . The solvent was removed *in vacuo* and the residue purified by HPLC to give **2.68** (6 mg, 17%) as a white solid.

^1H NMR (600 MHz, CDCl_3) δ 7.11 (1H, d, $J = 7.8$ Hz, ArH), 6.43 (1H, s, ArH), 6.36 (1H, d, $J = 7.8$ Hz, ArH), 5.74 (1H, d, $J = 8.2$ Hz, NHCHCH₂CO), 5.10 (1H, t, $J = 5.4$ Hz, NHCH₂CO), 4.89 (1H, d, $J = 15.6$ Hz, CH₂Ar), 4.86 – 4.81 (1H, m, N(DMB)CHCH₂CO), 4.07 – 4.03 (1H, m, NHCHCH₂CO), 3.94 – 3.93 (1H, m, NHCH₂CO), 3.90 (1H, d, $J = 15.8$ Hz, CH₂Ar) 3.86 (3H, s, COOCH₃), 3.75 (3H, s, ArOCH₃), 3.73 (3H, s, ArOCH₃), 3.53 (1H, dd, $J = 5.2, 17.8$ Hz, NHCH₂O), 3.45 (1H, dd, $J = 4.4, 14.2$ Hz, NHCHCH₂CO), 2.56 (1H, dd, $J = 4.4, 14.4$ Hz, NHCHCH₂CO), 2.36 (1H, dd, $J = 10.2, 15.8$ Hz, N(DMB)CHCH₂CO), 2.21 (1H, dd, $J = 4.0, 16.0$ Hz, N(DMB)CHCH₂CO), 2.04 – 1.99 (1H, m, NHCHCH₂CH₂CH₂CH₂CH), 1.91 – 1.85 (1H, m, NHCHCH₂CH₂CH₂CH₂CH), 1.80 – 1.74 (1H, m, NHCHCH₂CH₂CH₂CH₂CH), 1.66 – 1.61 (1H, m, NHCHCH₂CH₂CH₂CH₂CH), 1.42 (9H, s, (CH₃)₃), 1.30 – 1.17 (4H, m, NHCHCH₂CH₂CH₂CH₂CH, NHCHCH₂CH₂CH₂CH₂CH).

^{13}C NMR (75 MHz, CDCl_3) δ 174., 169.9, 169.8, 159.8, 156.7, 130.0, 119.2, 104.4, 98.1, 78.8, 55.5, 55.3, 53.8, 53.4, 52.3, 48.1, 41.3, 40.2, 36.9, 36.4, 32.9, 32.2, 29.7, 28.4, 24.7, 21.6.

HRMS (ES^+) calc. for $\text{C}_{22}\text{H}_{33}\text{N}_3\text{O}_6$ ($\text{M}+\text{H}^+$) 536.2966, found 536.2961

Preparation of methyl 2-[[2-[(2*S*,7*R*)-7-[(tert-butoxycarbonylamino)methyl]-1-[(2,4-dimethoxyphenyl)methyl]-8-oxo-azocan-2-yl]acetyl]amino]acetate (2.69**)**



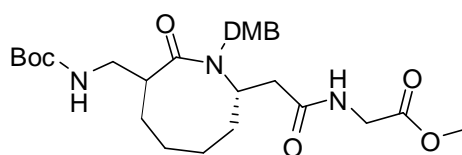
To a solution of **2.65** (60 mg, 0.1 mmol) in THF (2.5 mL) was added NaOH (12 mg, 0.2 mmol) in water (0.5 mL). The reaction was stirred at room temperature for 16 h, and then solvents were removed *in vacuo*. The residue was acidified to pH 1 with aqueous HCl (1M, 2mL) and the aqueous phase was extracted with ethyl acetate (2 x 5 mL). The combined organic layers were dried over MgSO_4 and solvents were removed *in vacuo* to give the acid (40 mg, 72%) as a colourless oil.

To a solution of this acid (40 mg, 0.09 mmol), glycine-OMe.HCl (25 mg, 0.2 mmol) and HATU (65 mg, 0.2 mmol) in DCM (1 mL) was added DIPEA (0.1 mL, 0.6 mmol). The mixture was stirred at room temperature for 16 h. The organic phase was diluted with DCM (5 mL) and washed with aqueous HCl (1 M, 2 x 5 mL), saturated aqueous NaHCO_3 (5 mL) and brine (5 mL). The organic phase was separated and dried over MgSO_4 . The solvent was removed *in vacuo* and the residue purified by HPLC to give **2.69** (5 mg, 10%) as a white solid.

^1H NMR (600 MHz, CDCl_3) δ 7.37 – 7.32 (1H, m, ArH), 6.73 (1H, bs, NHCH_2CHCO), 6.44 – 6.42 (2H, m, 2 x ArH), 5.19 – 5.16 (1H, m, CH_2Ar), 4.98 (1H, d, $J = 12.8$ Hz, NHCH_2CO), 4.26 – 4.20 (2H, NHCH_2CO), 4.06 – 4.01 (1H, m, NHCH_2CHCO), 3.98 – 3.92 (1H, m, NHCH_2CHCO), 3.81 (3H, s, ArOCH_3), 3.80 – 3.78 (1H, m, CH_2Ar), 3.79 (3H, s, ArOCH_3), 3.75 (3H, s, COOCH_3), 3.40 – 3.27 (1H, m, $\text{N(DMB)CHCH}_2\text{CO}$), 3.26 – 3.19 (1H, m, $\text{N(DMB)CHCH}_2\text{CO}$), 3.16 – 3.12 (1H, m, $\text{N(DMB)CHCH}_2\text{CO}$), 3.69 – 3.62 (1H, m, NHCH_2CHCO), 1.76 – 1.55 (4H, m, $\text{NHCH}_2\text{CHCH}_2\text{CH}_2\text{CH}_2\text{CH}_2\text{CH}$, $\text{NHCH}_2\text{CHCH}_2\text{CH}_2\text{CH}_2\text{CH}_2\text{CH}$), 1.44 (9H, s, $(\text{CH}_3)_3$), 1.33 – 1.17 (4H, m, $\text{NHCH}_2\text{CHCH}_2\text{CH}_2\text{CH}_2\text{CH}_2\text{CH}$, $\text{NHCH}_2\text{CHCH}_2\text{CH}_2\text{CH}_2\text{CH}_2\text{CH}$).

HRMS (ES^+) calc. for $\text{C}_{22}\text{H}_{33}\text{N}_3\text{O}_6$ ($\text{M}+\text{H}^+$) 536.2966, found 536.2966

Preparation of methyl 2-[[2-[(2*S*,7*S*)-7-[(*tert*-butoxycarbonylamino)methyl]-1-[(2,4-dimethoxyphenyl)methyl]-8-oxo-azocan-2-yl]acetyl]amino]acetate (2.70)



To a solution of **2.66** (60 mg, 0.1 mmol) in THF (2.5 mL) was added NaOH (12 mg, 0.2 mmol) in water (0.5 mL). The reaction was stirred at room temperature for 16 h, and then solvents were removed *in vacuo*. The residue was acidified to pH 1 with aqueous HCl (1M, 2mL) and the aqueous phase was extracted with ethyl acetate (2 x 5 mL). The combined organic layers were dried over MgSO_4 and solvents were removed *in vacuo* to give the acid (37 mg, 64%) as a colourless oil.

To a solution of this acid (37 mg, 0.08 mmol), glycine-OMe.HCl (25 mg, 0.2 mmol) and HATU (60 mg, 0.1 mmol) in DCM (1 mL) was added DIPEA (0.1 mL, 0.6 mmol). The mixture was stirred at room temperature for 16 h. The organic phase was diluted with DCM (5 mL) and washed with aqueous HCl (1 M, 2 x 5 mL), saturated aqueous NaHCO₃ (5 mL) and brine (5 mL). The organic phase was separated and dried over MgSO₄. The solvent was removed *in vacuo* and the residue purified by HPLC to give **2.70** (5 mg, 12%) as a white solid.

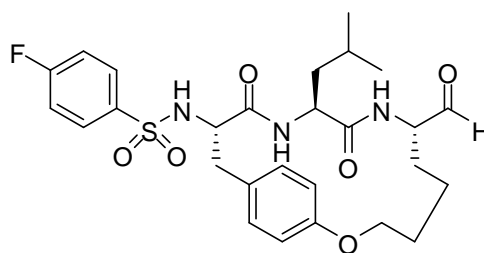
¹H NMR (600 MHz, CDCl₃) δ 7.04 (1H, d, *J* = 8.6 Hz, ArH), 6.36 (1H, s, ArH), 6.29 (1H, d, *J* = 8.8 Hz, ArH), 5.65 (1H, d, *J* = 7.2 Hz, NHCH₂CHCO), 5.06 (1H, bs, NHCH₂CO), 4.82 (d, *J* = 16.6 Hz, CH₂Ar), 4.79 – 4.74 (1H, m, N(DMB)CHCH₂CO), 4.03 – 3.95 (1H, m, NHCH₂CHCO), 3.87 (1H, d, *J* = 16.4 Hz, CH₂Ar), 3.87 – 3.73 (2H, m, NHCH₂CO, NHCH₂CHCO), 3.79 (3H, s, COOCH₃), 3.68 (3H, s, ArOCH₃), 3.66 (3H, s, ArOCH₃), 3.47 (1H, dd, *J* = 4.2, 18.8 Hz, NHCH₂CO), 3.39 (1H, dd, *J* = 4.0, 14.4 Hz, N(DMB)CHCH₂CO), 2.51 (1H, dd, *J* = 4.2, 14.4 Hz, N(DMB)CHCH₂CO), 2.29 (1H, dd, *J* = 10.2, 16.0 Hz, NHCH₂CHCH₂CH₂CH₂CH₂CH), 2.15 (1H, dd, *J* = 4.4, 15.8 Hz, NHCH₂CHCH₂CH₂CH₂CH₂CH), 1.96 – 1.92 (1H, m, NHCH₂CHCO), 1.84 – 1.79 (1H, m, NHCH₂CHCH₂CH₂CH₂CH₂CH), 1.73 – 1.66 (1H, m, NHCH₂CHCH₂CH₂CH₂CH₂CH), 1.62 – 1.55 (1H, m, NHCH₂CHCH₂CH₂CH₂CH₂CH), 1.48 – 1.44 (1H, m, NHCH₂CHCH₂CH₂CH₂CH₂CH), 1.40 – 1.32 (1H, m, NHCH₂CHCH₂CH₂CH₂CH₂CH), 1.35 (9H, s, (CH₃)₃), 1.16 – 1.09 (1H, m, NHCH₂CHCH₂CH₂CH₂CH₂CH).

^{13}C NMR (75 MHz, CDCl_3) δ 173.5, 168.9, 168.8, 158.9, 155.7, 154.3, 128.9, 117.9, 106.9, 103.4, 97.1, 77.9, 54.4, 54.2, 52.9, 51.3, 47.1, 40.3, 39.1, 35.5, 35.4, 31.9, 31.2, 28.7, 27.4, 23.7, 20.7.

HRMS (ES^+) calc. for $\text{C}_{22}\text{H}_{33}\text{N}_3\text{O}_6$ ($\text{M}+\text{H}^+$) 536.2966, found 536.2963

6.3 Experimental for Chapter 3

Preparation of 4-fluoro-N-[(3*S*,6*S*,9*S*)-9-formyl-6-isobutyl-4,7-dioxo-14-oxa-5,8-diazabicyclo[13.2.2]nonadeca-1(17),15,18-trien-3-yl]benzenesulfonamide (**3.02**)



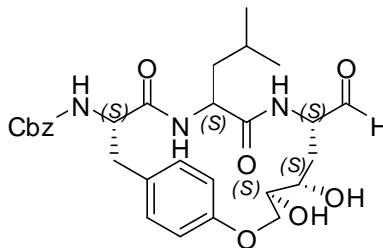
To a solution of **3.06** (50 mg, 0.09 mmol) in dry THF (1 mL) was added LiBH_4 (0.31 mL, 1 M in THF) dropwise. The reaction mixture was stirred at room temperature for 16 h then solvent was removed *in vacuo*. The resultant residue was dissolved in ethyl acetate (5 mL) and washed with water (5 mL). The organic phase was dried over MgSO_4 and solvent was removed *in vacuo* to give alcohol **3.23** (42 mg, 87 %) that was not purified further.

To a solution of **3.23** (42 mg, 0.08 mmol) in DCM (5 mL) under inert atmosphere was added Dess-Martin periodinane (97 mg). The reaction mixture was stirred vigorously for 1.5 h under inert atmosphere at room temperature then quenched with saturated aqueous NaHCO_3 (5 mL) containing $\text{Na}_2\text{S}_2\text{O}_5$ (2 mmol). The aqueous layer was extracted with DCM (2 x 10 mL) then the combined organic layers were washed with water (5 mL). The organic phase was dried over MgSO_4 and the solvents were removed *in vacuo*. The residue was purified by flash chromatography on silica gel (eluting with 2/1 ethyl acetate/petroleum ether) to give **3.02** (26 mg, 79 %) as a white solid.

^1H NMR (600 MHz, CDCl_3) δ 9.48 (1H, s, **CHO**), 7.88 - 7.86 (2H, m, **ArH** FBS), 7.14 - 7.11 (2H, **ArH** FBS), 6.97 (2H, d, $J = 7.2$ Hz, **ArH** Tyr), 6.75 (2H, d, $J = 7.2$ Hz, **ArH** Tyr), 5.77 - 5.75 (2H, m, 2 x **NH**), 5.52 (1H, d, $J = 9.6$ Hz, **NHCHCH**₂Ar), 4.52 (1H, ddd, $J = 4.8, 9.0, 16.2$ Hz, **NHCHCH**₂CH₂CH₂CH₂OAr), 4.24 - 4.20 (1H, m, **NHCHCH**₂CH₂CH₂**CH**₂OAr), 4.14 - 4.10 (1H, m, **NHCHCH**₂CH₂CH₂**CH**₂OAr), 3.86-3.82 (1H, m, **NHCHCH**₂Ar), 3.74 (1H, dd, $J = 6.6, 13.8$ Hz, **NHCHCH**₂CH(CH₃)₂), 3.11 (1H, dd, $J = 6.0, 12.0$ Hz, **NHCHCH**₂Ar), 2.66 (1H, t, $J = 12.0$ Hz, **NHCHCH**₂Ar), 2.04 - 1.96 (1H, m, **NHCHCH**₂CH₂CH₂CH₂OAr), 1.82 - 1.74 (1H, m, **NHCHCH**₂CH₂**CH**₂CH₂OAr), 1.60 - 1.44 (2H, m, **NHCHCH**₂CH₂CH₂CH₂OAr, **NHCHCH**₂CH₂**CH**₂CH₂OAr), 1.38 - 1.20 (2H, m, **NHCHCH**₂**CH**₂CH₂CH₂O, **NHCHCH**₂**CH**(CH₃)₂), 1.16 - 1.10 (1H, m, **NHCHCH**₂CH(CH₃)₂), 1.00 - 0.94 (1H, m, **NHCHCH**₂CH(CH₃)₂), 0.88 - 0.83 (1H, m, **NHCHCH**₂**CH**₂CH₂CH₂O), 0.81 (3H, d, $J = 6.0$ Hz, **NHCHCH**₂(CH₃)₂), 0.79 (3H, d, $J = 6.0$ Hz, **NHCHCH**₂(CH₃)₂).

^{13}C NMR (75 MHz, CDCl_3) δ 197.7, 170.8, 168.7, 165.9, 164.2, 157.5, 136.6, 129.8, 129.7, 116.4, 116.3, 115.9, 66.5, 58.8, 58.2, 51.8, 43.2, 40.4, 29.7, 27.9, 24.5, 22.9, 22.0, 20.1.

Preparation of benzyl N-[(3*S*,6*S*,9*S*,11*S*,12*S*)-9-formyl-11,12-dihydroxy-6-isobutyl-4,7-dioxo-14-oxa-5,8-diazabicyclo[13.2.2]nonadeca-1(17),15,18-trien-3-yl]carbamate (3.03)



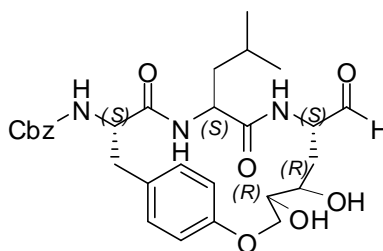
To a solution of **3.25** (1.29 mg, 0.22 mmol) in dry DCM (5 mL) under N₂ at -78 °C was added DIBAL (0.5 mL, 1M in THF). The reaction was stirred at -78 °C for 1 h. Methanol (2 mL) was added to quench the reaction and solvents were removed *in vacuo*. The resulting solid was dissolved in ethyl acetate (10 mL) and washed with water (5 mL). The organic phase was extracted, dried with MgSO₄, and solvents were removed *in vacuo*. Purification by flash chromatography on silica gel (eluting with 9/1 ethyl acetate/petroleum ether) gave **3.03** (11 mg, 9%) as a white solid.

¹H NMR (500 MHz, CD₃OD) δ 7.45 - 7.19 (5H, m, ArH Cbz), 7.05 - 6.93 (2H, m, ArH Tyr), 6.85 - 6.80 (2H, m, ArH Tyr), 5.16 (1H, s, CHOHCH₃), 5.13 (1H, d, *J* = 12.6 Hz, CH₂Ar Cbz), 5.07 (1H, d, *J* = 12.6 Hz, CH₂Ar Cbz), 4.35 (1H, dd, *J* = 5.8, 11.8 Hz, NHCHCH₂Ar), 4.25 (1H, dd, *J* = 3.9, 12.7 Hz, NHCHCH₂CHOHCHOHCH₂OAr), 4.12 (1H, ddd, *J* = 3.0, 8.2, 9.0 Hz, NHCHCH₂CHOHCHOHCH₂OAr), 4.00 - 3.94 (2H, m, NHCHCH₂CH(CH₃)₂), 3.88 (1H, d, *J* = 6.3 Hz, NHCHCH₂CHOHCHOHCH₂OAr), 3.81 (1H, dt, *J* = 3.8, 8.6 Hz, NHCHCH₂CHOHCHOHCH₂OAr), 3.06 (1H, dd, *J* = 5.7, 12.2 Hz, NHCHCH₂Ar),

2.68 (1H, t, $J = 12.3$ Hz, NHCHCH₂Ar), 2.39 (1H, ddd, $J = 6.3, 9.0, 14.2$ Hz, NHCHCH₂CHOHCHOHCH₂OAr), 1.75 (1H, dd, $J = 2.9, 14.0$ Hz, NHCHCH₂CHOHCHOHCH₂OAr), 1.53 - 1.34 (3H, m, NHCHCH₂CH(CH₃)₂), 0.87 - 0.83 (6H, m, (NHCHCH₂CH(CH₃)₂)).

HRMS (ES⁺) calc. for C₂₉H₃₇N₃O₈ (M+H⁺) 556.2659, found 556.2667

Preparation of benzyl N-[(3*S*,6*S*,9*S*,11*R*,12*R*)-9-formyl-11,12-dihydroxy-6-isobutyl-4,7-dioxo-14-oxa-5,8-diazabicyclo[13.2.2]nonadeca-1(17),15,18-trien-3-yl]carbamate (3.04)



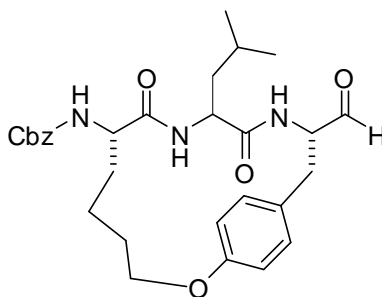
To a solution of **3.26** (as a mixture with **3.25** in an 85:15 ratio) (84 mg, 0.2 mmol) in dry DCM (5 mL) under N₂ at -78 °C was added DIBAL (0.5 mL, 1M in THF). The reaction was stirred at -78 °C for 1 h. Methanol (2 mL) was added to quench the reaction and solvents were removed *in vacuo*. The resulting solid was dissolved in ethyl acetate (10 mL) and washed with water (5 mL). The organic phase was extracted, dried with MgSO₄, and solvents were removed *in vacuo*. Purification by flash chromatography on silica gel (eluting with 9/1 ethyl acetate/petroleum ether) gave **3.04** (as a mixture with **3.03** in an 85:15 ratio) (6 mg, 7%) as a white solid.

¹H NMR (Major isomer) (500 MHz, CD₃OD) δ 7.43 - 7.17 (5H, m, ArH Cbz), 7.03 - 6.93 (2H, m, ArH Tyr), 6.85 - 6.80 (2H, m, ArH Tyr), 5.20 (1H, s, CHOHOCH₃),

5.15 – 5.11 (1H, m, CH_2Ar Cbz), 5.07 – 5.02 (1H, m, CH_2Ar Cbz), 4.33 – 4.27 (1H, m, NHCHCH_2Ar), 4.30 – 4.25 (1H, m, $\text{NHCHCH}_2\text{CHOHCHOHCH}_2\text{OAr}$), 4.10 – 4.05 (2H, m, $\text{NHCHCH}_2\text{CHOHCHOHCH}_2\text{OAr}$, $\text{NHCHCH}_2\text{CHOHCHOHCH}_2\text{OAr}$), 4.02 - 3.94 (2H, m, $\text{NHCHCH}_2\text{CH}(\text{CH}_3)_2$, $\text{NHCHCH}_2\text{CHOHCHOHCH}_2\text{OAr}$), 3.86 – 3.82 (1H, m, $\text{NHCHCH}_2\text{CHOHCHOHCH}_2\text{OAr}$), 3.06 – 3.02 (1H, m, NHCHCH_2Ar), 2.66 – 2.62 (1H, m, NHCHCH_2Ar), 2.39 – 2.29 (1H, m, $\text{NHCHCH}_2\text{CHOHCHOHCH}_2\text{OAr}$), 1.72 – 1.68 (1H, m, $\text{NHCHCH}_2\text{CHOHCHOHCH}_2\text{OAr}$), 1.53 - 1.34 (3H, m, $\text{NHCHCH}_2\text{CH}(\text{CH}_3)_2$, $\text{NHCHCH}_2\text{CH}(\text{CH}_3)_2$), 0.87 - 0.83 (6H, m, $(\text{NHCHCH}_2\text{CH}(\text{CH}_3)_2)$).

HRMS (ES^+) calc. for $\text{C}_{29}\text{H}_{37}\text{N}_3\text{O}_8$ ($\text{M}+\text{H}^+$) 556.2659, found 556.2663

Preparation of benzyl N-[(3*S*,6*S*,9*S*)-3-formyl-6-isobutyl-5,8-dioxo-14-oxa-4,7-diazabicyclo[13.2.2]nonadeca-1(17),15,18-trien-9-yl]carbamate (3.05)



To a solution of **3.36** (230 mg, 0.4 mmol) in dry THF (1 mL) was added LiBH_4 (1.6 mL, 1 M in THF) dropwise. The reaction mixture was stirred at room temperature for 16 h then solvent was removed *in vacuo*. The resultant residue was dissolved in ethyl acetate (5 mL) and washed with water (5 mL). The organic phase was dried over

MgSO₄ and solvent was removed *in vacuo* to give the alcohol **3.37** (190 mg, 86%) that was used without purification.

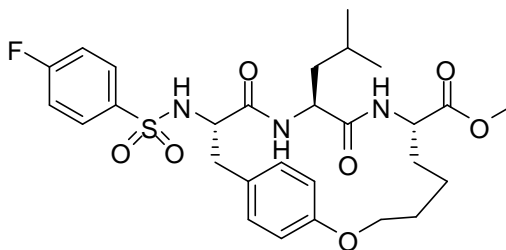
To a solution of **3.37** (190 mg, 0.4 mmol) in DCM (5 mL) under inert atmosphere was added Dess-Martin periodinane (450 mg, 1.1 mmol). The reaction mixture was stirred vigorously for 1.5 h under inert atmosphere at room temperature then quenched with aqueous NaHCO₃ (5 mL) containing Na₂S₂O₅ (2 mmol). The aqueous layer was extracted with DCM then the combined organic layers washed with water (5 mL). The residue was purified by flash chromatography on silica gel (eluting with 2/1 ethyl acetate/petroleum ether) to give **3.05** (110 mg, 62%) as a white solid.

¹H NMR (600 MHz, CDCl₃) δ 9.68 (1H, s, CHO), 7.37 – 7.28 (5H, m, ArH Cbz), 7.14 – 6.95 (2H, m, ArH Tyr), 6.87 (2H, d, *J* = 7.4 Hz, ArH Tyr), 6.13 (1H, d, *J* = 8.4 Hz, NHCHCH₂CH(CH₃)₂), 5.90 (1H, d, *J* = 8.4 Hz, NHCHCH₂Ar), 5.35 (1H, d, *J* = 8.4 Hz, NHCHCH₂CH₂CH₂CH₂OAr), 5.05 (2H, s, CH₂ Cbz), 4.84 – 4.78 (1H, m, NHCHCH₂Ar), 4.28 – 4.22 (2H, m, NHCHCH₂CH(CH₃)₂), NHCHCH₂CH₂CH₂CH₂CH₂OAr, 4.18 – 4.12 (1H, m, NHCHCH₂CH₂CH₂CH₂OAr), 3.92 – 3.86 (1H, m, NHCHCH₂CH₂CH₂CH₂OAr), 3.33 (1H, dd, *J* = 3.8, 14.0 Hz, NHCHCH₂Ar), 2.52 (1H, dd, *J* = 14.0, 24.6 Hz, NHCHCH₂Ar), 1.82 – 1.14 (9H, m, NHCHCH₂CH₂CH₂CH₂OAr, NHCHCH₂CH₂CH₂CH₂OAr, NHCHCH₂CH₂CH₂OAr, NHCHCH₂CH(CH₃)₂, NHCHCH₂CH(CH₃)₂), 0.87 (6H, d, *J* = 6.4 Hz, NHCHCH₂CH(CH₃)₂).

^{13}C NMR (75 MHz, CDCl_3) δ 198.3, 171.4, 170.4, 157.8, 155.9, 136.1, 130.4, 128.5, 128.3, 128.1, 127.2, 67.9, 67.0, 59.4, 54.5, 51.1, 42.1, 34.1, 31.8, 29.2, 24.6, 22.8, 22.1, 21.9.

HRMS (ES^+) calc. for $\text{C}_{29}\text{H}_{37}\text{N}_3\text{O}_6$ ($\text{M}+\text{H}^+$) 524.40, found 524.2755

Preparation of methyl (3*S*,6*S*,9*S*)-3-[(4-fluorophenyl)sulfonylamino]-6-isobutyl-4,7-dioxo-14-oxa-5,8-diazabicyclo[13.2.2]nonadeca-1(17),15,18-triene-9-carboxylate (3.06)



Method A

To a solution of **3.13** (140 mg, 0.2 mmol) in refluxing DCM (20 mL) was added Grubbs' second generation catalyst (6 mg, 0.007 mmol). The solution was stirred at reflux for 1 h then cooled to room temperature and activated charcoal was added (120 mg, 20 x w/w charcoal/catalyst). The reaction mixture was stirred at room temperature over night. The solution was filtered through celite and the solvent removed *in vacuo* to give a brown solid. Recrystallisation of the residue from ethyl acetate gave **3.22** (90 mg, 68%) as a white solid.

To a solution **3.22** (84 mg, 0.01 mmol) in ethyl acetate (10 mL) was added palladium on carbon (16 mg, 20% w/w catalyst/alkene). The reaction mixture was stirred at room temperature for 16 h under an H_2 atmosphere at atmospheric pressure then

filtered through celite. Removal of the solvent *in vacuo* gave **3.06** (80 mg, 89%) as a white solid.

^1H NMR (600 MHz, CDCl_3) δ 7.92 - 7.88 (2H, m, ArH FBS), 7.12 - 7.16 (2H, m, ArH FBS), 6.98 (2H, d, $J = 8.4$ Hz, ArH Tyr), 6.77 (2H, d, $J = 8.4$ Hz, ArH Tyr), 5.83 (1H, d, $J = 6.6$ Hz, NHCHCH₂Ar), 5.77 (1H, d, $J = 8.4$ Hz, NHCHCH₂CH(CH₃)₂), 5.59 (1H, d, $J = 10.2$ Hz, NHCHCH₂CH₂CH₂CH₂OAr), 4.51 (1H, ddd, $J = 3.6, 8.6, 16.8$ Hz, NHCHCH₂CH(CH₃)₂), 4.27 - 4.21 (1H, m, NHCHCH₂CH₂CH₂CH₂OAr), 4.14 - 4.07 (1H, m, NHCHCH₂CH₂CH₂CH₂OAr), 3.86 (1H, ddd, $J = 6.2, 6.6, 12.4$ Hz, NHCHCH₂Ar), 3.74 - 3.68 (1H, m, NHCHCH₂CH₂CH₂CH₂OAr), 3.73 (3H, s, COOCH₃), 3.12 (1H, dd, $J = 6.0, 12.8$ Hz, NHCHCH₂Ar), 2.68 (1H, t, $J = 12.6$ Hz, NHCHCH₂Ar), 1.94 - 1.86 (1H, m, NHCHCH₂CH₂CH₂CH₂OAr), 1.78 - 1.72 (1H, m, NHCHCH₂CH₂CH₂CH₂OAr), 1.60 - 1.52 (1H, m, NHCHCH₂CH₂CH₂CH₂OAr), 1.40 - 1.32 (1H, m, NHCHCH₂CH(CH₃)₂), 1.16 - 1.10 (2H, m, NHCHCH₂CH(CH₃)₂), 1.10 - 0.86 (3H, m, NHCHCH₂CH(CH₃)₂), NHCHCH₂CH₂CH₂CH₂OAr, 0.82 (3H, d, $J = 6.6$ Hz, NHCHCH₂CH(CH₃)₂), 0.80 (3H, d, $J = 6.6$ Hz, NHCHCH₂CH(CH₃)₂)

^{13}C NMR (75 MHz, CDCl_3) δ 172.4, 170.4, 168.9, 165.9, 164.2, 157.4, 136.6, 130.1, 127.5, 116.5, 116.3, 66.6, 58.8, 52.7, 51.8, 51.4, 43.1, 40.4, 31.3, 27.8, 24.4, 22.9, 21.9, 21.0.

HRMS (ES⁺) calc. for C₂₈H₃₄FN₃O₇S (M+H⁺) 576.2159, found 576.2174

obtain a homogenous solution. The reaction was stirred at room temperature for 16 h. The solvents were removed *in vacuo* and the resultant oil was partitioned between ethyl acetate (20 mL) and HCl (1 M, 20 mL). The organic layer was separated and washed with HCl (1 M, 20 mL) and brine (20 mL) before being dried over MgSO₄. Removal of the solvent *in vacuo* gave **3.16** (0.57 g, 93%) as a white foam.

To a solution of **3.16** (0.57 g, 1.31 mmol), allyl-Gly-OMe.HCl (0.50 g, 1.5 mmol) and HATU (0.53 g, 1.4 mmol) in anhydrous DMF (10 mL) was added DIPEA (0.9 mL, 5.2 mmol) dropwise. The reaction was stirred at room temperature for 16 h. The reaction was diluted with ethyl acetate (20 mL) and washed with HCl (1 M, 2 x 10 mL), saturated aqueous NaHCO₃ (10 mL) and brine (10 mL). The organic layer was separated and dried over MgSO₄. Removal of the solvent *in vacuo* and purification by flash chromatography on silica gel (eluting with 1/2 ethyl acetate/petroleum ether) gave **3.10** (0.56 g, 79%) as a white solid.

¹H NMR (500 MHz, CDCl₃) δ 7.10 (1H, d, *J* = 6.0 Hz, ArH), 6.84 (1H, d, *J* = 6.0 Hz, ArH), 6.56 (1H, d, *J* = 7.0 Hz, NHCHCH₂CHCH₂), 6.42 (1H, d, *J* = 7.1 Hz, NHCHCH₂CH(CH₃)₂), 6.09 - 6.00 (1H, m, ArOCH₂CHCH₂), 5.71 - 5.62 (1H, m, NHCHCH₂CHCH₂), 5.40 (1H, dd, *J* = 1.2, 17.0 Hz, ArOCH₂CHCH₂), 5.28 (1H, dd, *J* = 1.2, 10.5 Hz, ArOCH₂CHCH₂), 5.15 - 5.09 (2H, m, NHCHCH₂CHCH₂), 4.93 (1H, bs, NHCHCH₂Ar), 4.59 (1H, dd, *J* = 7.1, 14.0 Hz, NHCHCH₂CHCH₂), 4.52 - 4.49 (2H, m, ArOCH₂CHCH₂), 4.42 (1H, dt, *J* = 3.1, 7.3, 8.6 Hz, NHCHCH₂CH(CH₃)₂), 4.34 - 4.27 (1H, m, NHCHCH₂Ar), 3.74 (3H, s, COOCH₃), 3.04 - 2.99 (2H, m, NHCHCH₂Ar), 2.57 (1H, m, NHCHCH₂CHCH₂), 2.48 (1H, m, NHCHCH₂CHCH₂), 1.67 - 1.51 (2H, m, NHCHCH₂CH(CH₃)₂), 1.48 - 1.43 (1H, m,

NHCHCH₂CH(CH₃)₂, 1.41 (9H, s, (CH₃)₃), 0.93 - 0.88 (6H, m, NHCHCH₂CH(CH₃)₂).

¹³C NMR (75 MHz, CDCl₃) δ 171.9, 171.8, 171.6, 171.4, 133.5, 132.2, 130.5, 119.6, 117.9, 115.2, 69.0, 52.6, 52.1, 52.0, 51.9, 41.1, 36.5, 28.5, 24.7, 23.1, 22.2

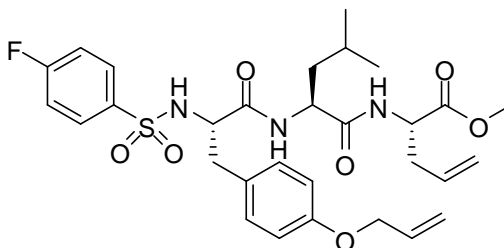
HRMS (ES⁺) calc. for C₂₉H₄₃N₃O₇ (M+H⁺) 546.3180, found 546.3179

Method B

To a solution of methyl ester **3.15** (2.59 g, 5.77 mmol) in THF (70 mL) was added NaOH (3.46 g, 8.65 mmol) in H₂O (23 mL). Methanol (1 mL/mmol) was added to obtain a homogenous solution. The reaction was stirred at room temperature for 16 h. The solvents were removed *in vacuo* and the resultant oil was partitioned between ethyl acetate (100 mL) and HCl (1 M, 100 mL). The organic layer was separated and washed with HCl (1 M, 100 mL) and brine (100 mL) before being dried over MgSO₄. Removal of the solvent *in vacuo* gave **3.16** (2.25 g, 90%) as a white foam.

To **3.16** (2.25 g, 5.15 mmol), allyl-Gly-OMe.HCl (1.02 g, 6.16 mmol) and HATU (2.15 g, 5.65 mmol) in anhydrous DMF (50 mL) was added DIPEA (3.60 mL, 20.7 mmol) drop wise. The reaction was stirred at room temperature for 16 h. The reaction was diluted with ethyl acetate (100 mL) and washed with HCl (1 M, 2 x 50 mL), saturated aqueous NaHCO₃ (50 mL) and brine (50 mL). The organic layer was separated and dried over MgSO₄. Removal of the solvent *in vacuo* and purification by flash chromatography on silica gel (eluting with 1/2 ethyl acetate/petroleum ether) gave **3.10** (2.38 g, 85%) as a white solid.

Preparation of methyl (2S)-2-[[[2S)-2-[[[2S)-3-(4-allyloxyphenyl)-2-[(4-fluorophenyl)sulfonylamino]propanoyl]amino]-4-methyl-pentanoyl]amino]pent-4-enoate (3.13)



To a solution of methyl ester **3.21**¹ (0.15 g, 0.3 mmol) in THF (3 mL) was added NaOH (0.02 g, 0.5 mmol) in H₂O (0.5 mL). Methanol (1 mL/mmol) was added to obtain a homogenous solution. The reaction was stirred at room temperature for 16 h. The solvents were removed *in vacuo* and the resultant oil was partitioned between ethyl acetate (10 mL) and HCl (1 M, 10 mL). The organic layer was washed with aqueous HCl (1 M, 100 mL) and brine (100 mL) before being dried over MgSO₄. Removal of the solvent *in vacuo* gave **3.11** (0.13 g, 90%) as a white foam that was not purified further.

To a solution of **3.11** (0.13 g, 0.3 mmol), allyl-gly-OMe.HCl (0.66 g, 0.4 mmol) and HATU (0.15 g, 0.4 mmol) in anhydrous DMF (2 mL) was added DIPEA (0.2 mL, 1.2 mmol) dropwise. The reaction was stirred at room temperature for 16 h, diluted with ethyl acetate (10 mL) and washed with aqueous HCl (1 M, 2 x 10 mL), saturated aqueous NaHCO₃ (10 mL) and brine (10 mL). The organic layer was dried over MgSO₄ and the solvent removed *in vacuo*. Purification of the residue by flash

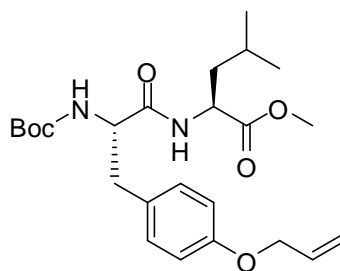
chromatography on silica gel (eluting with 1/2 ethyl acetate/petroleum ether) gave **3.13** (0.15 g, 94%) as a white solid.

^1H NMR (600 MHz, CDCl_3) δ 7.64 - 7.58 (2H, m, ArH FBS), 7.12 - 7.02 (2H, m, ArH FBS), 6.82 (2H, d, $J = 9.2$ Hz, ArH Tyr), 6.72 (2H, d, $J = 9.2$ Hz, ArH Tyr), 6.68 (1H, d, $J = 8.0$ Hz, NHCHCH₂CHCH₂), 6.56 (1H, d, $J = 7.8$ Hz, NHCHCH₂CH(CH₃)₂), 6.10 - 6.02 (1H, m, ArOCH₂CHCH₂), 5.76 - 5.62 (1H, m, NHCHCH₂CHCH₂), 5.94 (1H, dd, $J = 3.8, 16.2$ Hz, ArOCH₂CHCH₂), 5.32 (1H, dd, $J = 3.8, 10.2$ Hz, ArOCH₂CHCH₂), 5.15 - 5.11 (2H, m, NHCHCH₂CHCH₂), 4.83 (1H, d, $J = 5.0$ Hz, NHCHCH₂Ar), 4.66 - 4.60 (1H, m, NHCHCH₂CHCH₂), 4.51 (2H, d, $J = 5.1$ Hz, ArOCH₂CHCH₂), 4.45 (1H, ddd, $J = 5.0, 7.8, 17.8$ Hz, NHCHCH₂CH(CH₃)₂), 3.75 (3H, s, COOCH₃), 3.70 - 3.74 (1H, m, NHCHCH₂Ar), 3.06 (1H, dd, $J = 4.6, 13.6$ Hz, NHCHCH₂Ar), 2.72 (1H, dd, $J = 8.0, 13.4$ Hz, NHCHCH₂Ar), 2.61 - 2.57 (1H, m, NHCHCH₂CHCH₂), 2.58 - 2.47 (1H, m, NHCHCH₂CHCH₂), 1.76 (1H, ddd, $J = 5.2, 7.8, 19.2$ Hz, NHCHCH₂CH(CH₃)₂), 1.44 - 1.56 (2H, m, NHCHCH₂CH(CH₃)₂, NHCHCH₂CH(CH₃)₂), 0.94 (3H, d, $J = 6.6$ Hz, (NHCHCH₂CH(CH₃)₂), 0.92 (3H, $J = 6.6$ Hz, (NHCHCH₂CH(CH₃)₂))

^{13}C NMR (75 MHz, CDCl_3) δ 171.8, 171.1, 169.8, 166.2, 164.5, 158.1, 133.5, 133.0, 132.5, 129.4, 119.0, 117.9, 116.6, 115.1, 68.8, 58.2, 52.5, 51.7, 40.9, 37.8, 36.9, 29.6, 24.5, 22.9, 21.9

HRMS (ES^+) calc. for $\text{C}_{30}\text{H}_{38}\text{FN}_3\text{O}_7\text{S}$ ($\text{M}+\text{H}^+$) 604.2487, found 604.2478

Preparation of methyl (2S)-2-[[[(2S)-3-(4-allyloxyphenyl)-2-(tert-butoxycarbonylamino)propanoyl]amino]-4-methyl-pentanoate (3.15)



Method A

To a solution of **3.14** (0.50 g, 1.6 mmol), L-Leu-OMe.HCl (0.31 g, 1.7 mmol) and HATU (0.65 g, 1.7 mmol) in anhydrous DMF (10 mL) was added DIPEA (1.10 mL, 8.0 mmol) dropwise. The reaction was stirred at room temperature for 16 h. The reaction was diluted with ethyl acetate (20 mL) and washed with aqueous HCl (1 M, 2 x 10 mL), saturated aqueous NaHCO₃ (10 mL) and brine (10 mL). The organic phase was separated and dried over MgSO₄. The solvent was removed *in vacuo* and the residue purified by flash chromatography on silica gel (eluting with 1/2 ethyl acetate/petroleum ether) to give **3.15** (0.64 g, 92%) as a white solid.

¹H NMR (500 MHz, CDCl₃) δ 7.11 (2H, d, *J* = 8.5 Hz, ArH), 6.83 (2H, d, *J* = 8.5 Hz, ArH), 6.29 (1H, d, *J* = 8.6 Hz, NHCHCH₂CH(CH₃)₂), 6.08 - 5.99 (1H, m ArOCH₂CHCH₂), 5.40 (1H, dd, *J* = 1.6, 17.3 Hz, ArOCH₂CHCH₂), 5.27 (1H, dd, *J* = 1.6, 10.5 Hz, ArOCH₂CHCH₂), 5.03 (1H, bs, NHCHCH₂Ar), 4.56 (1H, td, *J* = 5.1, 8.6 Hz, NHCHCH₂CH(CH₃)₂), 4.51 (1H, t, *J* = 1.4 Hz, ArOCH₂CHCH₂), 4.50 (1H, t, *J* = 1.4 Hz, ArOCH₂CHCH₂), 4.30 (1H, m, NHCHCH₂Ar), 3.69 (3H, s, COOCH₃), 3.00 (2H, m, NHCHCH₂Ar), 1.62 - 1.51 (2H, m, NHCHCH₂CH(CH₃)₂), 1.50 - 1.44

(1H, m, NHCHCH₂CH(CH₃)₂), 1.41 (9H, s, (CH₃)₃), 0.90 (3H, d, *J* = 6.2 Hz NHCHCH₂CH(CH₃)₂), 0.88 (3 H, d, *J* = 6.4 Hz, NHCHCH₂CH(CH₃)₂)

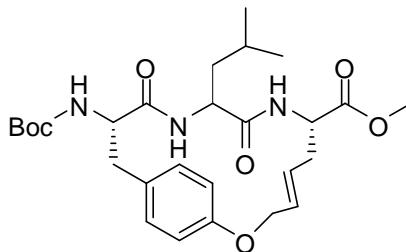
¹³C NMR (75 MHz, CDCl₃) δ 173.1, 171.3, 157.8, 155.6, 133.5, 130.6, 128.9, 117.8, 115.1, 69.0, 56.0, 52.5, 50.9, 41.8, 37.4, 28.5, 24.9, 23.0, 22.1

HRMS (ES⁺) calc. for C₂₄H₃₆N₂O₆ (M+H⁺) 449.2651, found 449.2662

Method B

To a solution of **3.14** (2.00 g, 6.2 mmol), L-Leu-OMe.HCl (1.24 g, 6.8 mmol) and HATU (2.59 g, 6.8 mmol) in anhydrous DMF (50 mL) was added DIPEA (4.44 mL, 24.88 mmol) dropwise. The reaction was stirred at room temperature for 16 h. The reaction was diluted with ethyl acetate (100 mL) and washed with aqueous HCl (1 M, 2 x 50 mL), aqueous NaHCO₃ (50 mL) and brine (50 mL). The organic phase was separated and dried over MgSO₄. The solvent was removed *in vacuo* and the residue purified by flash chromatography on silica gel (eluting with 1/2 ethyl acetate/petroleum ether) to give **3.15** (2.59 g, 93%) as a white solid.

Preparation of methyl (3*S*,6*S*,9*S*,11*E*)-3-(tert-butoxycarbonylamino)-6-isobutyl-4,7-dioxo-14-oxa-5,8-diazabicyclo[13.2.2]nonadeca-1(17),11,15,18-tetraene-9-carboxylate (3.17)



Method A

To a solution of **3.10** (0.55 g, 1.0 mmol) in TCE (100 mL) was added one portion of Grubbs' second generation catalyst (87 mg, 0.1 mmol). The reaction mixture was irradiated with microwave radiation for 10 minutes. The solution was allowed to cool to room temperature. A second portion of Grubbs' catalyst (87 mg, 0.1 mmol) was added and the reaction mixture was irradiated for 10 minutes. The final portion of Grubbs' catalyst (87 mg, 0.1 mmol) was added and the reaction mixture was irradiated for a further 10 minutes. The reaction mixture was cooled to room temperature and activated charcoal was added (5.22 g, 20 x w/w charcoal/catalyst). The reaction mixture was stirred at room temperature for 16 h. The solution was filtered through celite and the solvent removed *in vacuo* to yield a brown solid. Purification by flash chromatography on silica gel (eluting with 1/1 ethyl acetate/petroleum ether) gave **3.17** (0.12 g, 22 %) as a white solid.

^1H NMR (500 MHz, CDCl_3) δ 7.07 (2H, bs, ArH), 6.73 (2H, bs, ArH), 6.00 (1H, d, $J = 8.2$ Hz, NHCHCH₂CHCHCH₂OAr), 5.88 (1H, d, $J = 6.5$ Hz, NH), 5.53 - 5.43 (2H, m, NHCHCH₂CHCHCH₂OAr, NHCHCH₂CHCHCH₂OAr), 5.39 (1H, d, $J = 8.2$ Hz,

NH), 4.73 (1H, t, $J = 8.6$ Hz, NHCHCH₂CHCHCH₂OAr), 4.64 (1H, d, $J = 15.5$ Hz NHCHCH₂CHCHCH₂OAr), 4.57 (1H, d, $J = 15.6$ Hz, NHCHCH₂CHCHCH₂OAr), 4.24 - 4.15 (2H, m, NHCHCH₂Ar, NHCHCH₂CH(CH₃)₂), 3.74 (3H, s, OOCCH₃), 3.06 (1H, dd, $J = 3.2, 12.4$ Hz, NHCHCH₂Ar), 2.73 (1H, d, $J = 12.3$ Hz, NHCHCH₂Ar), 2.70 - 2.63 (1H, m, NHCHCH₂CHCHCH₂OAr), 2.34 - 2.25 (1H, m, NHCHCH₂CHCHCH₂OAr), 1.60 - 1.44 (3H, m, NHCHCH₂CH(CH₃)₂, NHCHCH₂CH(CH₃)₂), 1.44 (9H, s, (CH₃)₃), 0.89 - 0.83 (6H, m, (NHCHCH₂CH(CH₃)₂)).

¹³C NMR (75 MHz, CDCl₃) δ 172.2, 171.3, 170.9, 156.3, 155.3, 130.0, 128.7, 128.4, 127.7, 80.1, 66.6, 57.3, 52.8, 51.9, 43.1, 39.1, 35.1, 28.6, 24.6, 23.0, 22.7.

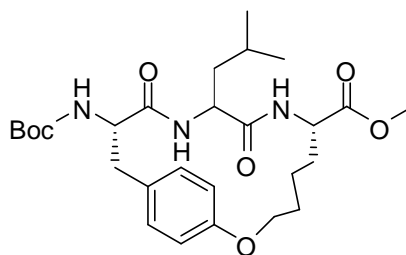
HRMS (ES⁺) calc. for C₂₇H₃₉N₃O₇ (M+H⁺) 518.2866, found 518.2891

Method B

To a solution of **3.10** (2.38 g, 4.36 mmol) in DCM (220 mL) was added one portion of Grubbs' second generation catalyst (37 mg, 0.04 mmol). The reaction mixture was irradiated with microwave radiation for 10 minutes. The solution was allowed to cool to room temperature. A second portion of Grubbs' catalyst (37 mg, 0.04 mmol) was added and the reaction mixture was irradiated for 10 minutes. The final portion of Grubbs' catalyst (37 mg, 0.04 mmol) was added and the reaction mixture was irradiated for a further 10 minutes. The reaction mixture was cooled to room temperature and activated charcoal was added (2.22 g, 20 x w/w charcoal/catalyst). The reaction mixture was stirred at room temperature for 16 h. The solution was

filtered through celite and the solvent removed *in vacuo* to yield a brown solid. Recrystallisation from ethyl acetate gave **3.17** (1.40 g, 62 %) as a white solid.

Preparation of methyl (3*S*,6*S*,9*S*)-3-(tert-butoxycarbonylamino)-6-isobutyl-4,7-dioxo-14-oxa-5,8-diazabicyclo[13.2.2]nonadeca-1(17),15,18-triene-9-carboxylate (3.18)



To a solution of alkene **3.17** (100 mg, 0.2 mmol) in ethyl acetate (20 mL) was added palladium on carbon (10 mg, 10% w/w catalyst/alkene). The reaction mixture was stirred at room temperature for 16 h under an H₂ atmosphere at atmospheric pressure then filtered through celite. Removal of the solvent *in vacuo* gave **3.18** (88 mg, 87%) as a white solid.

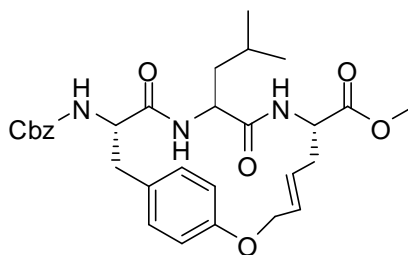
¹H NMR (500 MHz, CDCl₃) δ 7.09 – 7.02 (2H, m, ArH), 6.81- 6.78 (2H, m, ArH), 6.08 (1H, d, *J* = 5.8 Hz, NHCHCH₂CH₂CH₂CH₂OAr), 5.74 (1H, d, *J* = 9.1 Hz, NHCHCH₂CH(CH₃)₂), 5.22 (1H, d, *J* = 9.1 Hz, NHCHCH₂Ar), 4.42 – 4.38 (1H, m, NHCHCH₂CH₂CH₂CH₂OAr), 4.30 – 4.25 (1H, m, NHCHCH₂CH₂CH₂CH₂OAr), 4.22 – 4.17 (1H, m, NHCHCH₂Ar), 4.14 – 4.10 (1H, m, NHCHCH₂CH₂CH₂CH₂O), 4.06 – 3.96 (1H, m, NHCHCH₂CH(CH₃)₂), 3.73 (3H, s, COOCH₃), 3.11 (1H, dd, *J* = 6.4, 12.1 Hz, NHCHCH₂Ar), 2.65 (1H, t, *J* = 12.2 Hz, NHCHCH₂Ar), 1.74 – 1.68 (2H, m, NHCHCH₂CH₂CH₂CH₂OAr), 1.63 – 1.49 (5H, m, NHCHCH₂CH₂CH₂CH₂OAr, NHCHCH₂CH(CH₃)₂, NHCHCH₂CH(CH₃)₂), 1.45

(9H, s, (CH₃)₃), 1.40 – 1.20 (2H, m, NHCHCH₂CH₂CH₂CH₂OAr), 0.85 – 0.82 (6H, m, NHCHCH₂CH(CH₃)₂).

¹³C NMR (75 MHz, CDCl₃) δ 172.6, 170.8, 170.1, 157.0, 155.6, 155.1, 130.3, 130.1, 128.4, 115.9, 115.7, 79.7, 66.8, 56.9, 52.4, 51.6, 51.1, 43.1, 38.7, 31.5, 28.2, 24.4, 22.7, 22.5, 21.4.

HRMS (ES⁺) calc. for C₂₇H₄₂N₃O₇ (M+H⁺) 520.3031, found 520.3023

Preparation of methyl (3*S*,6*S*,9*S*,11*E*)-3-benzyloxycarbonylamino-6-isobutyl-4,7-dioxo-14-oxa-5,8-diazabicyclo[13.2.2]nonadeca-1(17),11,15,18-tetraene-9-carboxylate (3.24)



To a solution of **3.17** (1.38 g, 2.67 mmol) in MeOH (270 mL) at 0°C was added SOCl₂ (0.387 mL, 5.35 mmol) drop wise. The solution was warmed to room temperature and stirred for 16 h. Removal of solvents *in vacuo* gave **3.27** (1.21 g, >99 %) which was used without purification.

To a solution of **3.27** (1.21 g, 2.67 mmol) and benzyl chloroformate (1.17 mL, 8 mmol) in DMF (27 mL) was added DIPEA (2.01 mL, 10.7 mmol) dropwise. The solution was stirred at room temperature for 16 h. The solvent was removed *in vacuo*

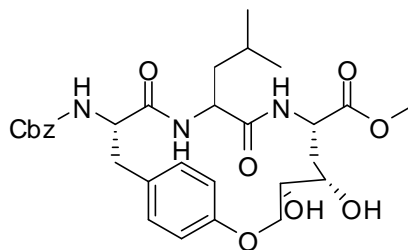
and the reaction mixture was partitioned between ethyl acetate (100 mL) and aqueous HCl (1 M, 100 mL). The organic layer was separated, dried over MgSO₄, and the solvent removed *in vacuo*. Recrystallisation from ethyl acetate gave **3.24** (1.18 g, 80%) as an off white solid.

¹H NMR (500 MHz, CDCl₃) δ 7.42 - 7.30 (5H, m, ArH Cbz), 7.14 - 7.02 (2H, m, ArH Tyr), 6.81 - 6.68 (2H, m, ArH Tyr), 6.08 - 5.90 (2H, m, NHCH₂CHCHCH₂CH₂OAr, NHCHCH₂CH(CH₃)₂), 5.77 - 5.71 (1H, m, NHCHCH₂Ar), 5.59 - 5.42 (2H, m, NHCH₂CHCHCH₂CH₂OAr, NHCH₂CHCHCH₂CH₂OAr), 5.13 (2H, s, CH₂Ar Cbz), 4.76 - 4.70 (1H, m, NHCHCH₂Ar), 4.64 (1H, d, *J* = 15.5 Hz, NHCH₂CHCHCH₂CH₂OAr), 4.57 (1H, d, *J* = 15.4 Hz, NHCH₂CHCHCH₂CH₂OAr), 4.39 - 4.29 (1H, m, NHCHCH₂(CH₃)₂), 4.21 - 4.14 (1H, m, NHCHCH₂CHCHCH₂O), 3.74 (3H, s, COOCH₃), 3.12 (1H, d, *J* = 9.7 Hz, NHCHCH₂Ar), 2.82 - 2.63 (2H, m, NHCHCH₂Ar, NHCHCH₂CHCHCH₂OAr), 2.36 - 2.21 (1H, m, NHCHCH₂CHCHCH₂OAr), 1.59 - 1.39 (3H, m, NHCHCH₂CH(CH₃)₂), 0.94 - 0.80 (6H, m, NHCHCH₂CH(CH₃)₂).

¹³C NMR (75 MHz, CDCl₃) δ 172.20, 171.17, 170.47, 156.42, 155.80, 136.53, 130.01, 128.76, 128.38, 128.23, 127.69, 67.14, 66.57, 57.56, 52.87, 52.13, 51.87, 43.33, 39.29, 35.12, 24.68, 22.91, 22.82.

HRMS (ES⁺) calc. for C₃₀H₃₇N₃O₇ (M+H⁺) 552.2710, found 552.2714

Preparation of methyl (3*S*,6*S*,9*S*,11*S*,12*S*)-3-benzyloxycarbonylamino-11,12-dihydroxy-6-isobutyl-4,7-dioxo-14-oxa-5,8-diazabicyclo[13.2.2]nonadeca-1(17),15,18-triene-9-carboxylate (3.25)



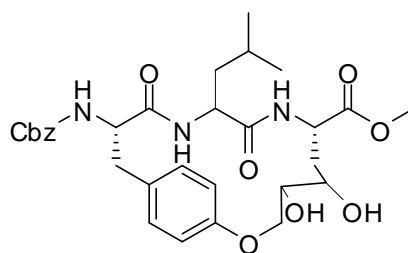
To a solution of **3.24** (510 mg, 0.9 mmol) and potassium osmate (27 mg, 0.07 mmol) in acetone (20 mL) was added *N*-methyl-morpholine-*N*-oxide (209 mg, 1.6 mmol) in H₂O (0.2 mL). The reaction was stirred at room temperature for 72 h. Solvents were removed *in vacuo* and the resultant white solid was dissolved in ethyl acetate and washed with HCl (1 M, 25 mL). The aqueous phase was extracted with EtOAc (2 x 25 mL). The combined organic layers were dried with MgSO₄, and solvents were removed *in vacuo*. Purification by flash chromatography on silica gel (eluting with 3/1 ethyl acetate/petroleum ether) gave **3.25** (134 mg, 25%) as a white solid.

¹H NMR (500 MHz, CD₃OD) δ 7.40 – 7.28 (5H, m, ArH Cbz), 7.09 - 6.87 (2H, m, ArH Tyr), 6.77 - 6.58 (2H, m, ArH Tyr), 5.13 (1H, d, *J* = 12.6 Hz, CH₂Ar Cbz), 5.08 (1 H, d, *J* = 12.4 Hz, CH₂Ar Cbz), 4.63 (1H, dd, *J* = 3.2, 12.2 Hz, NHCHCH₂CH(CH₃)₃), 4.51 (1H, dd, *J* = 9.2 11.8 Hz, NHCHCH₂CHOHCHOHCH₂OAr), 4.38 (1H, dd, *J* = 5.7, 11.8 Hz, NHCHCH₂Ar), 4.15 (1H, t, *J* = 6.5 Hz, NHCHCH₂CHOHCHOHCH₂OAr), 3.97 (1 H, dd, *J* = 3.8, 11.9 Hz, NHCHCH₂CHOHCHOHCH₂OAr), 3.70 (3H, s, COOCH₃), 3.56 (1H, ddd, *J* = 1.3, 3.7, 9.3 Hz, NHCHCH₂CHOHCHOHCH₂OAr), 3.22 (1 H, ddd, *J* = 1.4, 2.6,

3.5 Hz, NHCHCH₂CHOHCHOHCH₂O), 3.00 (1H, dd, $J = 5.8, 13.1$ Hz, NHCHCH₂Ar), 2.71 (1H, t, $J = 13.0$ Hz, NHCHCH₂Ar), 2.26 (1H, ddd, $J = 2.5, 10.5, 13.5$ Hz, NHCHCH₂CHOHCHOHCH₂OAr), 1.67 - 1.30 (4H, m, NHCHCH₂CHOHCHOHCH₂OAr, NHCHCH₂CH(CH₃)₂, NHCHCH₂CH(CH₃)₂), 0.90 - 0.85 (6H, m, NHCHCH₂CH(CH₃)₂).

HRMS (ES⁺) calc. for C₃₀H₃₉N₃O₉ (M+H⁺) 586.2764, found 586.2750

Preparation of methyl (3*S*,6*S*,9*S*,11*R*,12*R*)-3-benzyloxycarbonylamino-11,12-dihydroxy-6-isobutyl-4,7-dioxo-14-oxa-5,8-diazabicyclo[13.2.2]nonadeca-1(17),15,18-triene-9-carboxylate (3.26)

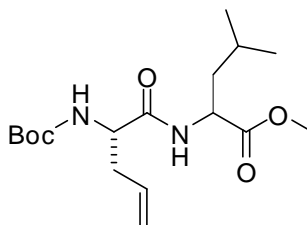


To a solution of **3.24** (500 mg, 0.9 mmol) and potassium osmate (26 mg, 0.07 mmol) in acetone (20 mL) was added *N*-methyl-morpholine-*N*-oxide (204 mg, 1.6 mmol) in H₂O (0.2 mL). The reaction was stirred at room temperature for 72 h. Solvents were removed *in vacuo* and the resultant white solid was dissolved in ethyl acetate and washed with HCl (1 M, 25 mL). The aqueous phase was extracted with EtOAc (2 x 25 mL). The combined organic layers were dried with MgSO₄, and solvents were removed *in vacuo*. Purification by flash chromatography on silica gel (eluting with 3/1 ethyl acetate/petroleum ether) gave **3.26** (as a mixture with **3.25** in an 85:15 ratio) (134 mg, 25%) as a white solid.

^1H NMR (major isomer) (500 MHz, CD_3OD) δ 7.21 (s, ArH Cbz), 7.17 – 6.97 (2H, m, ArH Tyr), 6.94 – 6.73 (2H, m, ArH Tyr), 5.13 – 5.20 (2H, m, CH_2 Cbz), 4.59 – 4.51 (1H, m, $\text{NHCHCH}_2\text{CH}(\text{CH}_3)_2$), 4.31 – 4.23 (2H, m, NHCHCH_2Ar , $\text{NHCHCH}_2\text{CHOHCHOHCH}_2\text{OAr}$), 4.19 (1H, dd, $J = 5.5, 12$ Hz, $\text{NHCHCH}_2\text{CHOHCHOHCH}_2\text{OAr}$), 3.99 – 3.92 (1H, m, $\text{NHCHCH}_2\text{CHOHCHOHCH}_2\text{OAr}$), 3.78 – 3.63 (2H, m, $\text{NHCHCH}_2\text{CHOHCHOHCH}_2\text{OAr}$, $\text{NHCHCH}_2\text{CHOHCHOHCH}_2\text{OAr}$), 3.63 (3H, s, COOCH_3), 3.02 (1H, dd, $J = 5.6, 13.0$ Hz, NHCHCH_2Ar), 2.63 (1H, dd, $J = 13.0$ Hz, NHCHCH_2Ar), 2.24 (1H, ddd, $J = 2.5, 10.5, 13.0$ Hz, $\text{NHCHCH}_2\text{CHOHCHOHCH}_2\text{OAr}$), 1.87 (1H, ddd, $J = 5.5, 13, 13$ Hz, $\text{NHCHCH}_2\text{CHOHCHOHCH}_2\text{OAr}$), 1.62 – 1.33 (3H, m, $\text{NHCHCH}_2\text{CH}(\text{CH}_3)_2$), $\text{NHCHCH}_2\text{CH}(\text{CH}_3)_2$), 0.90 – 0.84 (6H, m, $\text{NHCHCH}_2\text{CH}(\text{CH}_3)_2$).

HRMS (ES^+) calc. for $\text{C}_{30}\text{H}_{39}\text{N}_3\text{O}_9$ ($\text{M}+\text{H}^+$) 586.2764, found 586.2768

Preparation of methyl (2*S*)-2-[[*(2S)*-2-(tert-butoxycarbonylamino)pent-4-enoyl]amino]-4-methyl-pentanoate (3.29)



To a solution of **3.28** (1.00 g, 4.6 mmol), L-Leu-OMe.HCl (0.93 g, 5.1 mmol) and HATU (2.30 g, 6.0 mmol) in anhydrous DMF (20 mL) was added DIPEA (3.50 mL, 20.0 mmol) dropwise. The reaction was stirred at room temperature for 16 h. The reaction was diluted with ethyl acetate (50 mL) and washed with aqueous HCl (1 M,

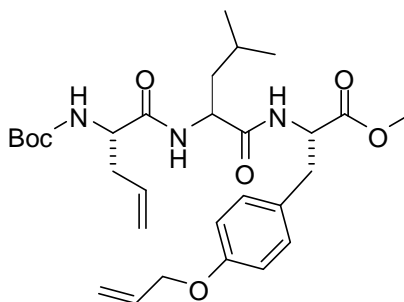
2 x 50 mL), saturated aqueous NaHCO₃ (50 mL) and brine (50 mL). The organic phase was separated and dried over MgSO₄. The solvent was removed *in vacuo* and the residue purified by flash chromatography on silica gel (eluting with 1/2 ethyl acetate/petroleum ether) to give **3.29** (1.49 g, 95%) as a white solid.

¹H NMR (600 MHz, CDCl₃) δ 6.47 (1H, d, *J* = 7.1 Hz, NHCHCH₂CH(CH₃)₂), 5.84 – 5.65 (1H, m, NHCHCH₂CHCH₂), 5.17 – 5.13 (2H, m, NHCHCH₂CHCH₂), 4.97 (1H, bs, NHCHCH₂CHCH₂), 4.60 (1H, ddd, *J* = 4.6, 7.4, 22.0 Hz, NHCHCH₂CH(CH₃)₂), 4.18– 4.08 (1H, m, NHCHCH₂CHCH₂), 3.71 (3H, s, COOCH₃), 2.54 – 2.55 (2H, m, NHCHCH₂CHCH₂), 1.68 – 1.56 (2H, m, NHCHCH₂CH(CH₃)₂), 1.57 – 1.49 (1H, m, NHCHCH₂CH(CH₃)₂), 1.43 (9H, s, (CH₃)₃), 0.92 (6H, d, *J* = 5.6 Hz, NHCHCH₂CH(CH₃)₂).

¹³C NMR (75 MHz, CDCl₃) δ 173.1, 171.1, 133.0, 119.1, 53.7, 52.3, 50.7, 41.6, 36.3, 28.2, 24.8, 22.8, 21.9.

HRMS (ES⁺) calc. for C₁₇H₃₀N₂O₅ (M+H⁺) 343.2227, found 343.2224

Preparation of methyl (2S)-3-(4-allyloxyphenyl)-2-[[[(2S)-2-[[[(2S)-2-(tert-butoxycarbonylamino)pent-4-enoyl]amino]-4-methylpentanoyl]amino]propanoate (3.32)



To a solution of methyl ester **3.29** (1.40 g, 4.1 mmol) in THF (24 mL) was added NaOH (0.25 g, 6.1 mmol) in H₂O (6 mL). Methanol (1 mL/mmol ester) was added to obtain a homogenous solution. The reaction was stirred at room temperature for 16 h. The solvents were removed *in vacuo* and the resultant oil was partitioned between ethyl acetate (50 mL) and aqueous HCl (1 M, 50 mL). The organic layer was separated and washed with aqueous HCl (1 M, 100 mL) and brine (100 mL) before being dried over MgSO₄. Removal of the solvent *in vacuo* gave **3.30** (1.18 g, 90%) as a white foam.

To a solution of **3.30** (1.18 g, 3.6 mmol), O-allyl-Tyr-OMe.HCl (1.47 g, 5.4 mmol) and HATU (2.05 g, 5.4 mmol) in anhydrous DMF (20 mL) was added DIPEA (2.50 mL, 14.4 mmol) drop wise. The reaction was stirred at room temperature for 16 h. The reaction was diluted with ethyl acetate (100 mL) and washed with aqueous HCl (1 M, 2 x 50 mL), saturated aqueous NaHCO₃ (50 mL) and brine (50 mL). The organic layer was separated and dried over MgSO₄. Removal of the solvent *in vacuo*

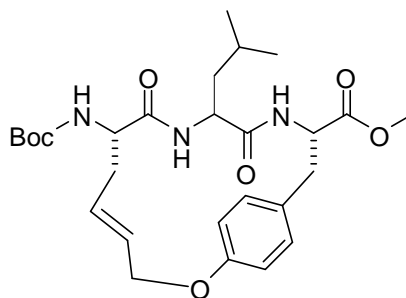
and purification by flash chromatography on silica gel (eluting with 1/2 ethyl acetate/petroleum ether) gave **3.32** (1.43 g, 73%) as a white solid.

^1H NMR (600 MHz, CDCl_3) δ 6.99 (2H, d, $J = 8.4$ Hz, ArH), 6.82 (2H, d, $J = 8.4$ Hz, ArH), 6.52 – 6.44 (2H, m, NHCHCH₂CH(CH₃)₂, NHCHCH₂Ar), 5.75 – 5.68 (1H, m, ArOCH₂CHCH₂), 5.75 – 5.68 (1H, m, NHCHCH₂CHCH₂), 5.39 (1H, dd, $J = 1.0, 17.3$ Hz, ArOCH₂CHCH₂), 5.26 (1H, dd, $J = 1.0, 10.5$ Hz, ArOCHCH₂CHCH₂), 5.15 – 5.11 (2H, m, NHCHCH₂CHCH₂), 4.99- 4.89 (1H, m, NHCHCH₂CHCH₂), 4.76 (1H, dd, $J = 6.0, 13.6$ Hz, NHCHCH₂Ar), 4.49 (2H, d, $J = 5.3$ Hz, ArOCH₂CHCH₂), 4.39 – 4.36 (1H, m, NHCHCH₂CH(CH₃)₂), 4.13 – 4.04 (1H, m, NHCHCH₂CHCH₂), 3.68 (3H, s, COOCH₃), 3.07 – 2.99 (2H, m, NHCHCH₂Ar), 2.51 – 2.41 (2H, m, NHCHCH₂CHCH₂), 1.63 – 1.57 (2H, m, NHCHCH₂CH(CH₃)₂), 1.51 – 1.47 (1H, m, NHCHCH₂CH(CH₃)₂), 1.42 (9H, s, (CH₃)₃), 0.88 (3H, d, $J = 5.6$ Hz, NHCHCH₂CH(CH₃)₂), 0.86 (3H, d, $J = 5.6$ Hz, NHCHCH₂CH(CH₃)₂).

^{13}C NMR (75 MHz, CDCl_3) δ 171.7, 171.4, 171.2, 157.8, 133.3, 132.9, 130.3, 127.8, 119.2, 117.6, 114.8, 68.8, 53.8, 53.4, 52.3, 51.7, 40.9, 36.9, 36.1, 28.2, 24.6, 22.9, 21.9.

HRMS (ES^+) calc. for $\text{C}_{29}\text{H}_{43}\text{N}_3\text{O}_7$ ($\text{M}+\text{Na}^+$) 568.2993, found 568.2992

Preparation of methyl (3*S*,6*S*,9*S*,11*E*)-9-(tert-butoxycarbonylamino)-6-isobutyl-5,8-dioxo-14-oxa-4,7-diazabicyclo[13.2.2]nonadeca-1(17),11,15,18-tetraene-3-carboxylate (3.33)



To a solution of **3.32** (1.39 g, 2.5 mmol) in refluxing DCM (300 mL) was added Grubbs' second generation catalyst (63 mg, 0.08 mmol). The solution was stirred at reflux for 1 h then cooled to room temperature and activated charcoal was added (1.20 g, 20 x w/w charcoal/catalyst). The reaction mixture was stirred at room temperature for 16 h. The solution was filtered through celite and the solvent removed *in vacuo* to yield a brown solid. Purification by flash chromatography on silica gel (eluting with 1/1 ethyl acetate/petroleum ether) gave **3.33** (1.41 g, 63%) as a white solid.

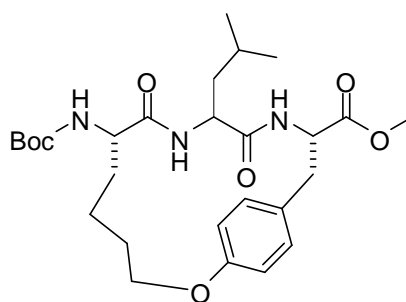
^1H NMR (600 MHz, CDCl_3) δ 7.00 – 6.91 (2H, m, ArH), 6.74 (2H, d, $J = 8.4$ Hz, ArH), 6.39 (1H, d, $J = 8.6$ Hz, NHCHCH₂CH(CH₃)₂), 5.95 (1H, d, $J = 8.6$ Hz, NHCHCH₂Ar), 5.96 – 5.56 (1H, m, NHCHCH₂CHCHCH₂OAr), 5.39 – 5.32 (1H, m, NHCHCH₂CHCHCH₂OAr), 4.95 (1H, d, $J = 8.3$ Hz, NHCHCH₂CHCHCH₂OAr), 4.83 – 4.80 (1H, m, NHCHCH₂Ar), 4.61 (1H, dd, $J = 3.6, 15.4$ Hz, NHCHCH₂CHCHCH₂OAr), 4.58 (1H, dd, $J = 3.6, 15.4$ Hz, NHCHCH₂CHCHCH₂OAr), 4.28 – 4.24 (1H, m, NHCHCH₂CH(CH₃)₂), 3.95 – 3.92

(1H, m, NHCHCH₂CHCHCH₂OAr), 3.79 (3H, s, COOCH₃), 3.30 (1H, dd, $J = 4.8$, 14.0 Hz, NHCHCH₂Ar), 2.71 (1H, dd, $J = 10.0$, 13.8 Hz, NHCHCH₂Ar), 2.58 (1H, dd, $J = 11.8$, 19.6 Hz, NHCHCH₂CHCHCH₂OAr), 2.22 – 2.16 (1H, m, NHCHCH₂CHCHCH₂OAr), 1.56 – 1.43 (3H, m, NHCHCH₂CH(CH₃)₂, NHCHCH₂CH(CH₃)₂), 1.42 (9H, s, (CH₃)₃), 0.86 (3H, d, $J = 5.6$ Hz, NHCHCH₂CH(CH₃)₂), 0.85 (3H, d, $J = 5.6$ Hz, NHCHCH₂CH(CH₃)₂).

¹³C NMR (75 MHz, CDCl₃) δ 172.2, 170.7, 169.9, 156.4, 155.4, 129.9, 128.2, 128.1, 127.8, 116.6, 80.3, 67.5, 54.2, 52.6, 52.5, 51.0, 42.2, 37.4, 33.7, 28.3, 24.4, 22.9, 22.1.

HRMS (ES⁺) calc. for C₂₇H₃₉N₃O₇ (M+Na⁺) 540.2662, found 540.2677

Preparation of methyl (3*S*,6*S*,9*S*)-9-(tert-butoxycarbonylamino)-6-isobutyl-5,8-dioxo-14-oxa-4,7-diazabicyclo[13.2.2]nonadeca-1(17),15,18-triene-3-carboxylate (3.34)



Method A

To a solution **3.33** (500 mg, 0.1 mmol) in ethyl acetate (20 mL) was added 10% palladium on carbon (250 mg, 50% w/w catalyst/alkene). The reaction mixture was stirred at room temperature for 2 h under an H₂ atmosphere at atmospheric pressure

then filtered through celite. Removal of the solvent *in vacuo* gave **3.34** (400 mg, 89%) as a white solid.

^1H NMR (600 MHz, CDCl_3) δ 7.03 – 6.93 (2H, m, ArH), 6.76 (2H, d, $J = 8.2$ Hz, ArH), 6.07 (1H, d, $J = 8.2$ Hz, NHCHCH₂CH(CH₃)₂), 5.80 (1H, d, $J = 8.8$ Hz, NHCHCH₂Ar), 4.96 (1H, d, $J = 8.4$ Hz, NHCHCH₂CH₂CH₂CH₂OAr), 4.86 – 4.82 (1H, m, NHCHCH₂Ar), 4.22 – 4.14 (2H, m, NHCHCH₂CH₂CH₂CH₂OAr, NHCHCH₂CH(CH₃)₂), 4.12 – 4.14 (1H, m, NHCHCH₂CH₂CH₂CH₂OAr), 3.78 – 3.75 (1H, m, NHCHCH₂CH₂CH₂CH₂OAr), 3.74 (3H, s, COOCH₃), 3.27 (1H, dd, $J = 5.0, 13.2$ Hz, NHCHCH₂Ar), 2.55 (1H, dd, $J = 11.8, 13.2$ Hz, NHCHCH₂Ar), 1.75 – 1.65 (1H, m, NHCHCH₂CH₂CH₂CH₂OAr), 1.63 – 1.57 (1H, m, NHCHCH₂CH₂CH₂CH₂OAr), 1.50 – 1.36 (3H, m, NHCHCH₂CH(CH₃)₂, NHCHCH₂CH(CH₃)₂), 1.34 (9H, s, (CH₃)₃), 1.32 – 1.26 (2H, m, NHCHCH₂CH₂CH₂CH₂OAr, NHCHCH₂CH₂CH₂CH₂OAr), 1.16 – 1.08 (2H, m, NHCHCH₂CH₂CH₂CH₂OAr, NHCHCH₂CH₂CH₂CH₂OAr), 0.82 (3H, d, $J = 6.6$ Hz, NHCHCH₂CH(CH₃)₂), 0.81 (3H, d, $J = 6.6$ Hz, NHCHCH₂CH(CH₃)₂).

^{13}C NMR (75 MHz, CDCl_3) δ 172.1, 170.8, 170.6, 157.7, 155.4, 130.3, 127.9, 116.7, 114.6, 79.9, 67.9, 54.1, 52.6, 52.6, 50.9, 42.4, 37.9, 32.0, 29.4, 28.3, 24.4, 22.8, 22.1, 22.0.

HRMS (ES^+) calc. for $\text{C}_{27}\text{H}_{41}\text{N}_3\text{O}_7$ ($\text{M}+\text{Na}^+$) 542.2824, found 542.2837

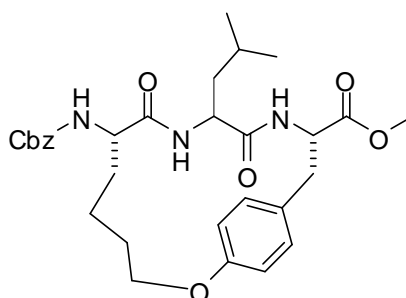
Method B

To a solution **3.33** (100 mg, 0.1 mmol) in methanol (10 mL) was added 10% palladium on carbon (20 mg, 20% w/w catalyst/alkene). The reaction mixture was stirred at room temperature for 16 h under an H₂ atmosphere at atmospheric pressure then filtered through celite. The solvent was removed *in vacuo* to give **3.34** and two unidentified side products as an inseparable mixture.

Method C

To a solution **3.33** (100 mg, 0.1 mmol) in ethyl acetate (10 mL) was added 5 % palladium on carbon (20 mg, 20% w/w catalyst/alkene). The reaction mixture was stirred at room temperature for 2 h under an H₂ atmosphere at atmospheric pressure then filtered through celite. The solvent was removed *in vacuo* to give **3.34** (20 mg, 20 %) and starting material **3.33** (40 mg, 40%) as an inseparable mixture.

Preparation of methyl (3*S*,6*S*,9*S*)-9-benzyloxycarbonylamino-6-isobutyl-5,8-dioxo-14-oxa-4,7-diazabicyclo[13.2.2]nonadeca-1(17),15,18-triene-3-carboxylate (3.36)



To a solution of **3.34** (390 mg, 0.8 mmol) in MeOH (3 mL) at 0 °C was added SOCl₂ (0.3mL, 5.35 4.0 mmol) drop wise. The solution was stirred at room temperature for

16 h. Removal of solvents *in vacuo* gave **3.35** (340 mg, >99%) which was used without purification.

To a solution of **3.35** (340 mg, 0.8 mmol) and benzyl chloroformate (0.34 mL, 2.4 mmol) in CHCl_3 (10 mL) was added DIPEA (0.5 mL, 2.8 mmol) drop wise. The solution was stirred at room temperature for 16 h. The solvent was removed *in vacuo* and the reaction mixture was partitioned between ethyl acetate (10 mL) and aqueous HCl (1 M, 10 mL). The organic layer was separated, dried over MgSO_4 , and the solvent removed *in vacuo*. Purification by flash chromatography on silica gel (eluting with 1/1 ethyl acetate/petroleum ether) gave **3.36** (287 mg, 65%) as an off white solid.

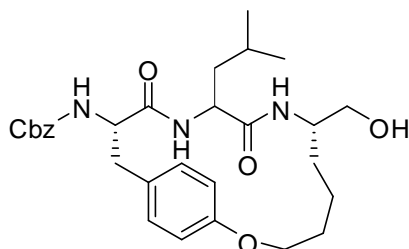
^1H NMR (600 MHz, CDCl_3) δ 7.29 – 7.23 (5H, m, ArH Cbz), 7.01 – 6.92 (2H, m, ArH), 6.75 (2H, d, $J = 7.4$ Hz, ArH), 6.05 (1H, d, $J = 8.2$ Hz, NHCHCH₂CH(CH₃)₂), 5.79 (1H, d, $J = 8.8$ Hz, NHCHCH₂Ar), 5.32 (1H, d, $J = 8.2$ Hz, NHCHCH₂CH₂CH₂CH₂OAr), 5.00 (2H, s, CH₂Ar Cbz), 4.88 – 4.84 (1H, m, NHCHCH₂Ar), 4.19 – 4.12 (2H, m, NHCHCH₂CH(CH₃)₂, NHCHCH₂CH₂CH₂CH₂OAr), 4.10 – 4.06 (1H, m, NHCHCH₂CH₂CH₂CH₂OAr), 3.91 – 3.88 (1H, m, NHCHCH₂CH₂CH₂CH₂OAr), 3.79 (3H, s, COOCH₃), 3.28 (1H, dd, $J = 4.8, 14.2$ Hz, NHCHCH₂Ar), 2.50 (1H, t, $J = 14.2$ Hz, NHCHCH₂Ar), 1.70 – 1.39 (5H, m, 2 x (CH₂), NHCHCH₂CH(CH₃)₂), 1.36 – 1.30 (2H, m, NHCHCH₂CH(CH₃)₂), 1.26 – 1.05 (4H, 2 x CH₂), 0.82 (3H, d, $J = 6.6$ Hz, NHCHCH₂CH(CH₃)₂), 0.81 (3H, d, $J = 6.6$ Hz, NHCHCH₂CH(CH₃)₂).

^{13}C NMR (75 MHz, CDCl_3) δ 172.1, 170.6, 170.1, 157.6, 155.7, 136.3, 128.5, 128.6, 128.0, 127.9, 67.7, 66.9, 54.6, 52.7, 52.5, 51.1, 42.7, 38.1, 32.5, 29.4, 24.5, 22.7, 22.3, 21.7.

HRMS (ES^+) calc. for $\text{C}_{30}\text{H}_{39}\text{N}_3\text{O}_7$ ($\text{M}+\text{H}^+$) 554.2851, found 554.2861

6.4 Experimental for Chapter 5

Preparation of benzyl N-[(3*S*,6*S*,9*S*)-9-(hydroxymethyl)-6-isobutyl-4,7-dioxo-14-oxa-5,8-diazabicyclo[13.2.2]nonadeca-1(17),15,18-trien-3-yl]carbamate (**4.04**)



To a solution of **5.11** (200 mg, 0.4 mmol) in dry THF (1 mL) was added LiBH₄ (1.6 mL, 1 M in THF) dropwise. The reaction mixture was stirred at room temperature for 16 h then solvent was removed *in vacuo*. The resultant residue was dissolved in ethyl acetate (5 mL) and washed with water (5 mL). The organic phase was dried over MgSO₄ and solvent was removed *in vacuo* to give the alcohol **4.04** (160 mg, 83%) that was used without purification.

¹H NMR (500 MHz, C₅D₅N) δ 7.68 (2H, m, ArH, Cbz), 7.36 - 7.27 (3H, m, ArH, Cbz), 7.08 - 7.04 (2H, m, ArH), 6.79 - 6.75 (2H, m, ArH), 5.04 (1H, d, *J* = 13.0 Hz, CH₂ Cbz), 4.99 (1H, d, *J* = 13.1 Hz, CH₂ Cbz), 4.34 - 4.26 (2H, m, NHCHCH₂Ar and NHCHCH₂CH₂CH₂CH₂OAr), 4.12 - 4.06 (1H, m, NHCHCH₂CH₂CH₂CH₂OAr), 4.02 - 3.96 (1H, m, NHCHCH₂CH(CH₃)₂), 3.86 - 3.74 (1H, m, NHCHCH₂OH), 3.33 - 3.30 (2H, m, NHCHCH₂OH), 2.98 (1H, dd, *J* = 5.8, 13.2 Hz, NHCHCH₂Ar), 2.67 (1H, t, *J* = 13.2 Hz, NHCHCH₂Ar), 1.84 - 1.75 (2H, m, NHCHCH₂CH₂CH₂CH₂OAr), 1.56 - 1.46 (3H, m, NHCHCH₂CH(CH₃)₂), 1.44 - 1.22 (4H, m, NHCHCH₂CH₂CH₂CH₂OAr,

NHCHCH₂CH₂CH₂CH₂OAr), 0.84 (3H, d, $J = 6.4$ Hz, NHCHCH₂CH(CH₃)₂), 0.83 (3H, d, $J = 6.4$ Hz, NHCHCH₂CH(CH₃)₂)

¹³C NMR (75 MHz, C₅D₅N) δ 170.6, 169.6, 156.3, 155.5, 137.3, 130.2, 129.3, 128.4, 127.8, 115.6, 109.1, 104.4, 66.6, 65.3, 64.3, 56.3, 50.9, 49.4, 48.1, 43.5, 37.3, 33.5, 30.1, 28.1, 24.0, 23.0 22.9, 22.2 20.7

Method B

To a solution of **CAT0811** (20 mg, 0.4 mmol) in THF (1 mL) and water (1 mL), was added NaBH₄. The reaction was stirred at room temperature for 24 h. The solvents were removed *in vacuo* and the residue was partitioned between ethyl acetate (2 mL) and aqueous HCl (1M, 2 mL). The organic phase was washed with brine (2 mL) and dried over MgSO₄. The solvents were removed *in vacuo* to yield **4.04** (17 mg, 85%) as a white solid.

Method C

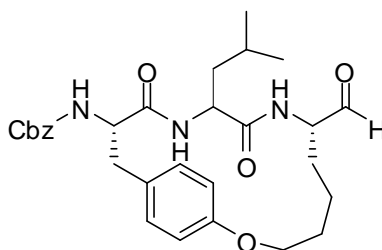
To a solution of **CAT0811** (20 mg, 0.4 mmol) in THF (1 mL) and water (1 mL), was added NaBH₄. The reaction was stirred at room temperature for 48 h. The solvents were removed *in vacuo* and the residue was partitioned between ethyl acetate (2 mL) and aqueous HCl (1M, 2 mL). The organic phase was washed with brine (2 mL) and dried over MgSO₄. The solvents were removed *in vacuo* to yield **4.04** (18 mg, 93%) as a white solid.

Method D

To a solution of **CAT0811** (20 mg, 0.4 mmol) in THF (1 mL) and water (1 mL), was added NaBH₄. The reaction was stirred at room temperature for 72 h. The solvents were removed *in vacuo* and the residue was partitioned between ethyl acetate (2 mL) and aqueous HCl (1M, 2 mL). The organic phase was washed with brine (2 mL) and dried over MgSO₄. The solvents were removed *in vacuo* to yield **4.04** (20 mg, >95%) as a white solid.

Method E

To a solution of **CAT0811** (20 mg, 0.4 mmol) in THF (1 mL) and water (1 mL), was added NaBH₄. The reaction was stirred at room temperature for 14 days. The solvents were removed *in vacuo* and the residue was partitioned between ethyl acetate (2 mL) and aqueous HCl (1M, 2 mL). The organic phase was washed with brine (2 mL) and dried over MgSO₄. The solvents were removed *in vacuo* to yield **4.04** (20 mg, >95%) as a white solid.

Preparation of benzyl N-[(3*S*,6*S*,9*S*)-9-formyl-6-isobutyl-4,7-dioxo-14-oxa-5,8-diazabicyclo[13.2.2]nonadeca-1(17),15,18-trien-3-yl]carbamate (CAT0811**)**

To a solution of **4.04** (200 mg, 0.4 mmol) in DCM (6 mL) and DMSO (6 mL) under inert atmosphere at 0 °C was added DIPEA (0.28 mL, 1.5 mmol) and sulfur trioxide

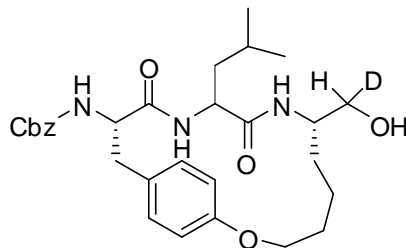
pyridine complex (240 mg, 1.5 mmol) in DMSO (25 mL). The reaction mixture was stirred at 0 °C for 2 h under inert atmosphere then diluted with ethyl acetate (100 mL). The organic phase was washed with aqueous HCl (1M, 50 mL), saturated aqueous NaHCO₃ (50 mL) and brine (50 mL). The organic phase was dried over MgSO₄ and the solvents were removed *in vacuo*. The residue was purified by flash chromatography on silica gel (eluting with 2/1 ethyl acetate/petroleum ether) to give **CAT0811** (160 mg, 80 %) as a white solid.

¹H NMR (600 MHz, (CD₃)₂SO) δ 9.33 (1H, s, CHO), 8.05 (1H, d, *J* = 8.2 Hz, NH), 7.55 (1H, d, *J* = 7.4 Hz, NH), 7.37 - 7.30 (5H, m, ArH, Cbz), 7.18 - 7.14 (1H, m, NH), 7.03 - 6.98 (2H, m, ArH Tyr), 6.77 (2H, d, *J* = 8.0 Hz, ArH Tyr), 5.04 (1H, d, *J* = 13.2 Hz, CH₂ Cbz), 5.00 (1H, d, *J* = 13.2 Hz, CH₂ Cbz), 4.36 - 4.31 (3H, m, NHCHCH₂Ar, NHCHCH₂CH₂CH₂CH₂OAr), 4.25 - 4.18 (1H, m, NHCHCH₂CH(CH₃)₂), 4.07 - 4.00 (2H, m, NHCHCH₂CH₂CH₂CH₂OAr, NHCHCH₂CH₂CH₂CH₂OAr), 2.86 (1H, dd, *J* = 5.0, 12.2 Hz, NHCHCH₂CH₂CH₂CH₂OAr), 2.63 (1H, t, *J* = 12.8 Hz, NHCHCH₂Ar), 1.77 - 1.70 (1H, m, NHCHCH₂CH₂CH₂CH₂OAr), 1.52 - 1.46 (1H, m, NHCHCH₂CH(CH₃)₂), 1.39 - 1.22 (5H, m, NHCHCH₂CH(CH₃)₂, NHCHCH₂CH₂CH₂CH₂OAr, NHCHCH₂CH₂CH₂CH₂OAr), 0.83 - 0.80 (6H, m, NHCHCH₂CH(CH₃)₃).

¹³C NMR (75 MHz, (CD₃)₂SO) δ 201.8, 172.1, 170.3, 156.6, 156.1, 137.9, 130.1, 129.0, 128.4, 116.2, 66.8, 65.9, 57.2, 56.8, 51.4, 44.1, 31.0, 27.6, 27.1, 24.6, 23.6, 22.2.

HRMS (ES⁺) calc. for C₂₉H₃₇N₃O₆ (MH⁺) 524.2740 found 524.2750;

Preparation of benzyl N-[(3*S*,6*S*,9*S*)-9-[deuterio(hydroxy)methyl]-6-isobutyl-4,7-dioxo-14-oxa-5,8-diazabicyclo[13.2.2]nonadeca-1(17),15,18-trien-3-yl]carbamate (5.01)

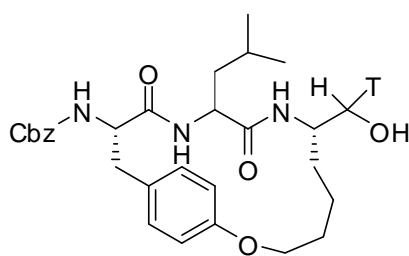


To a solution of **CAT0811** (20 mg, 0.4 mmol) in THF (1 mL) and water (1 mL), was added NaBD₄. The reaction was stirred at room temperature for 72 h. The solvents were removed *in vacuo* and the residue was partitioned between ethyl acetate (2 mL) and aqueous HCl (1M, 2 mL). The organic phase was washed with brine (2 mL) and dried over MgSO₄. The solvents were removed *in vacuo* to yield **5.01** (20 mg, >95%) as a white solid.

¹H NMR (500 MHz, C₅D₅N) δ 7.68 (2H, m, ArH, Cbz), 7.36 - 7.22 (3H, m, ArH, Cbz), 7.08 - 7.04 (2H, m, ArH Tyr), 6.79 - 6.75 (2H, m, ArH Try), 5.04 (1H, d, *J* = 13.2 Hz, CH₂ Cbz), 4.99 (1H, d, *J* = 13.2 Hz, CH₂ Cbz), 4.34 - 4.26 (2H, m, NHCHCH₂Ar, NHCHCH₂CH₂CH₂CH₂OAr), 4.12 - 4.06 (1H, m, NHCHCH₂CH₂CH₂CH₂OAr), 4.02 - 3.96 (1H, m, NHCHCH₂CH(CH₃)₂), 3.86 - 3.74 (1H, m, NHCHCHDOH), 3.33 - 3.30 (1H, m, NHCHCHDOH), 2.98 (1H, dd, *J* = 6.0, 13.4 Hz, NHCHCH₂Ar), 2.67 (1H, t, *J* = 13.4 Hz, NHCHCH₂Ar), 1.84 - 1.75 (2H, m, NHCHCH₂CH₂CH₂CH₂O), 1.56 - 1.46 (3H, m, NHCHCH₂CH(CH₃)₂), 1.44-1.22 (4H, m, NHCHCH₂CH₂CH₂CH₂OAr,

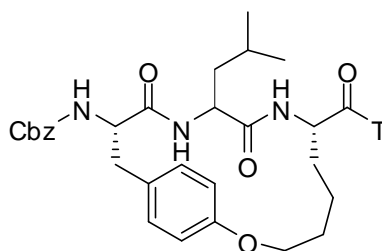
NHCHCH₂CH₂CH₂CH₂OAr), 0.84 (3H, d, $J = 6.2$ Hz, NHCHCH₂CH(CH₃)₂), 0.83 (3H, d, $J = 6.2$ Hz, NHCHCH₂CH(CH₃)₂).

Preparation of benzyl N-[(3*S*,6*S*,9*S*)-9-[hydroxy(tritio)methyl]-6-isobutyl-4,7-dioxo-14-oxa-5,8-diazabicyclo[13.2.2]nonadeca-1(17),15,18-trien-3-yl]carbamate (5.02)



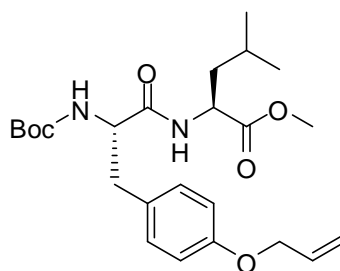
To a solution of **CAT0811** (16 mg, 0.4 mmol) in THF (1 mL) and water (1 mL), was added NaBT₄. The reaction was stirred at room temperature for 72 h. The solvents were removed *in vacuo* and the residue was partitioned between ethyl acetate (2 mL) and aqueous HCl (1M, 2 mL). The organic phase was washed with brine (2 mL) and dried over MgSO₄. The solvents were removed *in vacuo* to yield **5.02** (15 mg, >95%) as a white solid.

Preparation of benzyl N-[(3S,6S,9S)-6-isobutyl-4,7-dioxo-9-tritiocarbonyl-14-oxa-5,8-diazabicyclo[13.2.2]nonadeca-1(17),15,18-trien-3-yl]carbamate (5.03)



To a solution of **5.02** (13 mg, 0.02 mmol) **4.04** (187 mg, 0.4 mmol) in DCM (6 mL) and DMSO (6 mL) under inert atmosphere at 0 °C was added DIPEA (0.28 mL, 1.5 mmol) and sulfur trioxide pyridine complex (240 mg, 1.5 mmol) in DMSO (25 mL). The reaction mixture was stirred at 0 °C for 2 h under inert atmosphere then diluted with ethyl acetate (100 mL). The organic phase was washed with aqueous HCl (1M, 50 mL), saturated aqueous NaHCO₃ (50 mL) and brine (50 mL). The organic phase was dried over MgSO₄. Removal of the solvents *in vacuo* gave **5.03** as a white solid.

Preparation of methyl (2S)-2-[[[(2S)-3-(4-allyloxyphenyl)-2-(tert-butoxycarbonylamino)propanoyl]amino]-4-methyl-pentanoate (5.05)



To a solution of **5.04** (1.0 g, 3.2 mmol), L-Leu-OMe.HCl (0.62 g, 3.4 mmol) and HATU (1.30 g, 3.4 mmol) in anhydrous DMF (20 mL) was added DIPEA (2.20 mL, 16.0 mmol) dropwise. The reaction was stirred at room temperature for 16 h. The

reaction was diluted with ethyl acetate (40 mL) and washed with aqueous HCl (1 M, 2 x 20 mL), saturated aqueous NaHCO₃ (20 mL) and brine (20 mL). The organic phase was separated and dried over MgSO₄. The solvent was removed *in vacuo* and the residue purified by flash chromatography on silica gel (eluting with 1/2 ethyl acetate/petroleum ether) to give **5.05** (1.24 g, 89%) as a white solid.

¹H NMR (500 MHz, CDCl₃) δ 7.11 (2H, d, *J* = 8.5 Hz, ArH), 6.83 (2H, d, *J* = 8.5 Hz, ArH), 6.29 (1H, d, *J* = 8.6 Hz, NHCHCH₂CH(CH₃)₂), 6.08 - 5.99 (1H, m, ArOCH₂CHCH₂), 5.40 (1H, dd, *J* = 1.6, 17.3 Hz, ArOCH₂CHCH₂), 5.27 (1H, dd, *J* = 1.6, 10.5 Hz, ArOCH₂CHCH₂), 5.03 (1H, bs, NHCHCH₂Ar), 4.56 (1H, td, *J* = 5.1, 8.6 Hz, NHCHCH₂CH(CH₃)₂), 4.51 (1H, t, *J* = 1.4 Hz, ArOCH₂CHCH₂), 4.50 (1H, t, *J* = 1.4 Hz, ArOCH₂CHCH₂), 4.30 (1H, m, NHCHCH₂Ar), 3.69 (3H, s, COOCH₃), 3.00 (2H, m, NHCHCH₂Ar), 1.62 - 1.51 (2H, m, NHCHCH₂CH(CH₃)₂), 1.50 - 1.44 (1H, m, NHCHCH₂CH(CH₃)₂), 1.41 (9H, s, (CH₃)₃), 0.90 (3H, d, *J* = 6.2 Hz, NHCHCH₂CH(CH₃)₂), 0.88 (3 H, d, *J* = 6.4 Hz, NHCHCH₂CH(CH₃)₂)

¹³C NMR (75 MHz, CDCl₃) δ 173.1, 171.3, 157.8, 155.6, 133.5, 130.6, 128.9, 117.8, 115.1, 69.0, 56.0, 52.5, 50.9, 41.8, 37.4, 28.5, 24.9, 23.0, 22.1

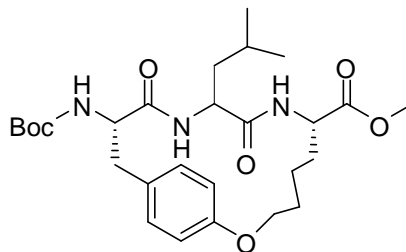
HRMS (ES⁺) calc. for C₂₄H₃₆N₂O₆ (M+H⁺) 449.2651, found 449.2662

^1H NMR (500 MHz, CDCl_3) δ 7.10 (1H, d, $J = 6.0$ Hz, ArH), 6.84 (1H, d, $J = 6.0$ Hz, ArH), 6.56 (1H, d, $J = 7.0$ Hz, NHCHCH₂CHCH₂), 6.42 (1H, d, $J = 7.1$ Hz, NHCHCH₂CH(CH₃)₂), 6.09 - 6.00 (1H, m, ArOCH₂CHCH₂), 5.71 - 5.62 (1H, m, NHCHCH₂CHCH₂), 5.40 (1H, dd, $J = 1.2, 17.0$ Hz, ArOCH₂CHCH₂), 5.28 (1H, dd, $J = 1.2, 10.5$ Hz, ArOCH₂CHCH₂), 5.15 - 5.09 (2H, m, NHCHCH₂CHCH₂), 4.93 (1H, bs, NHCHCH₂Ar), 4.59 (1H, dd, $J = 7.1, 14.0$ Hz, NHCHCH₂CHCH₂), 4.52 - 4.49 (2H, m, ArOCH₂CHCH₂), 4.42 (1H, dt, $J = 3.1, 7.3, 8.6$ Hz, NHCHCH₂CH(CH₃)₂), 4.34 - 4.27 (1H, m, NHCHCH₂Ar), 3.74 (3H, s, COOCH₃), 3.04 - 2.99 (2H, m, NHCHCH₂Ar), 2.57 (1H, m, NHCHCH₂CHCH₂), 2.48 (1H, m, NHCHCH₂CHCH₂), 1.67 - 1.51 (2H, m, NHCHCH₂CH(CH₃)₂), 1.48 - 1.43 (1H, m, NHCHCH₂CH(CH₃)₂), 1.41 (9H, s, (CH₃)₃), 0.93 - 0.88 (6H, m, NHCHCH₂CH(CH₃)₂).

^{13}C NMR (75 MHz, CDCl_3) δ 171.9, 171.8, 171.6, 171.4, 133.5, 132.2, 130.5, 119.6, 117.9, 115.2, 69.0, 52.6, 52.1, 52.0, 51.9, 41.1, 36.5, 28.5, 24.7, 23.1, 22.2

HRMS (ES^+) calc. for $\text{C}_{29}\text{H}_{43}\text{N}_3\text{O}_7$ ($\text{M}+\text{H}^+$) 546.3180, found 546.3179

Preparation of methyl (3*S*,6*S*,9*S*)-3-(tert-butoxycarbonylamino)-6-isobutyl-4,7-dioxo-14-oxa-5,8-diazabicyclo[13.2.2]nonadeca-1(17),15,18-triene-9-carboxylate (5.09)



To a solution of **5.07** (1.10 g, 2.0 mmol) in TCE (200 mL) was added one portion of Grubbs' second generation catalyst (60 mg, 0.2 mmol). The reaction mixture was irradiated with microwave radiation for 10 minutes. The solution was allowed to cool to room temperature. A second portion of Grubbs' catalyst (60 mg, 0.2 mmol) was added and the reaction mixture was irradiated for 10 minutes. The final portion of Grubbs' catalyst (60 mg, 0.2 mmol) was added and the reaction mixture was irradiated for a further 10 minutes. The reaction mixture was cooled to room temperature and activated charcoal was added (1.20 g, 20 x w/w charcoal/catalyst). The reaction mixture was stirred at room temperature for 16 h. The solution was filtered through celite and the solvent removed *in vacuo* to yield a brown solid. Purification by flash chromatography on silica gel (eluting with 1/1 ethyl acetate/petroleum ether) gave **5.08** (0.21 g, 20 %) as a white solid.

To a solution of alkene **5.08** (200 mg, 0.4 mmol) in ethyl acetate (40 mL) was added palladium on carbon (20 mg, 10% w/w catalyst/alkene). The reaction mixture was stirred at room temperature for 16 h under an H₂ atmosphere at atmospheric pressure

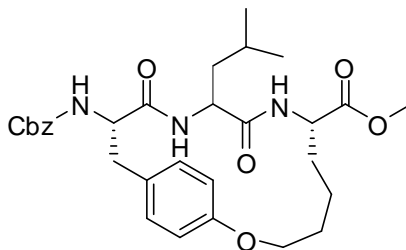
then filtered through celite and solvent was removed *in vacuo* to give **5.09** (170 mg, 85%) as a white solid.

^1H NMR (500 MHz, CDCl_3) δ 7.09 – 7.02 (2H, m, ArH), 6.81– 6.78 (2H, m, ArH), 6.08 (1H, d, $J = 5.8$ Hz, NHCHCH₂CH₂CH₂CH₂OAr), 5.74 (1H, d, $J = 9.1$ Hz, NHCHCH₂CH(CH₃)₂), 5.22 (1H, d, $J = 9.1$ Hz, NHCHCH₂Ar), 4.42 – 4.38 (1H, m, NHCHCH₂CH₂CH₂CH₂OAr), 4.30 – 4.25 (1H, m, NHCHCH₂CH₂CH₂CH₂OAr), 4.22 – 4.17 (1H, m, NHCHCH₂Ar), 4.14 – 4.10 (1H, m, NHCHCH₂CH₂CH₂CH₂OAr), 4.06 – 3.96 (1H, m, NHCHCH₂CH(CH₃)₂), 3.73 (3H, s, COOCH₃), 3.11 (1H, dd, $J = 6.4, 12.1$ Hz, NHCHCH₂Ar), 2.65 (1H, t, $J = 12.2$ Hz, NHCHCH₂Ar), 1.74 – 1.68 (2H, m, NHCHCH₂CH₂CH₂CH₂OAr), 1.63 – 1.49 (5H, m, NHCHCH₂CH₂CH₂CH₂OAr, NHCHCH₂CH(CH₃)₂, NHCHCH₂CH(CH₃)₂), 1.45 (9H, s, (CH₃)₃), 1.40 – 1.20 (2H, m, NHCHCH₂CH₂CH₂CH₂OAr), 0.85 – 0.82 (6H, m, NHCHCH₂CH(CH₃)₂).

^{13}C NMR (75 MHz, CDCl_3) δ 172.6, 170.8, 170.1, 157.0, 155.6, 155.1, 130.3, 130.1, 128.4, 115.9, 115.7, 79.7, 66.8, 56.9, 52.4, 51.6, 51.1, 43.1, 38.7, 31.5, 28.2, 24.4, 22.7, 22.5, 21.4.

HRMS (ES^+) calc. for $\text{C}_{27}\text{H}_{42}\text{N}_3\text{O}_7$ ($\text{M}+\text{H}^+$) 520.3031, found 520.3023

Preparation of methyl (3*S*,6*S*,9*S*)-3-benzyloxycarbonylamino-6-isobutyl-4,7-dioxo-14-oxa-5,8-diazabicyclo[13.2.2]nonadeca-1(17),15,18-triene-9-carboxylate (5.11)



To a solution of **5.09** (150 mg, 0.3 mmol) in MeOH (3 mL) at 0 °C was added SOCl₂ (0.15 mL, 1.5 mmol) drop wise. The solution was stirred at room temperature for 16 h. Removal of solvents *in vacuo* gave **5.10** (130 mg, >99%) which was used without purification.

To a solution of **5.10** (130 mg, 0.3 mmol) and benzyl chloroformate (0.13 mL, 0.9 mmol) in CHCl₃ (10 mL) was added DIPEA (0.19 mL, 1.1 mmol) drop wise. The solution was stirred at room temperature for 16 h. The solvent was removed *in vacuo* and the reaction mixture was partitioned between ethyl acetate (10 mL) and aqueous HCl (1 M, 10 mL). The organic layer was separated, dried over MgSO₄, and the solvent removed *in vacuo*. Purification by flash chromatography on silica gel (eluting with 1/1 ethyl acetate/petroleum ether) gave **5.11** (77 mg, 49%) as an off white solid.

¹H NMR (600 MHz, CDCl₃) δ 7.18 – 7.23 (5H, m, ArH, Cbz), 7.10 – 7.00 (2H, m, ArH Tyr), 6.80 – 6.67 (2H, m, ArH Tyr), 6.09 – 5.95 (2H, m, NHCHCH₂CH₂CH₂CH₂OAr, NHCHCH₂CH(CH₃)₂), 5.90 – 5.84 (1H, d, *J* = 8.4 Hz, NHCHCH₂Ar), 5.20 (2H, s, CH₂ Cbz), 4.70 – 4.68 (1H, m, NHCHCH₂Ar), 4.62 –

4.57 (2H, m, NHCHCH₂CH₂CH₂CH₂CH₂OAr), 4.42 – 4.36 (1H, m, NHCHCH₂CH₂CH₂CH₂CH₂OAr), 4.21 – 4.14 (1H, m, NHCHCH₂CH₂CH₂CH₂CH₂OAr), 3.72 (3H, s, COOCH₃), 3.17 – 3.12 (1H, m, NHCHCH₂Ar), 2.87 – 2.67 (2H, m, NHCHCH₂Ar, NHCHCH₂CH₂CH₂CH₂OAr), 2.56 – 2.21 (m, 5H, NHCHCH₂CH₂CH₂CH₂OAr, NHCHCH₂CH₂CH₂CH₂O, NHCHCH₂CH₂CH₂CH₂OAr), 1.59 – 1.39 (3H, m, NHCHCH₂CH₂CH₂CH₂O, NHCHCH₂CH₂CH₂CH₂OAr), 1.59 – 1.39 (3H, m, NHCHCH₂CH₂CH₂CH₂O, NHCHCH₂CH₂CH₂CH₂OAr), 0.83 – 0.80 (6H, m, NHCHCH₂CH₂CH₂CH₂O, NHCHCH₂CH₂CH₂CH₂OAr).

¹³C NMR (75 MHz, CDCl₃) δ 172.5, 170.8, 169.7, 157.1, 155.5, 136.3, 130.1, 128.5, 128.2, 128.1, 127.9, 115.7, 66.8, 66.6, 57.0, 52.5, 51.7, 51.2, 43.3, 39.0, 31.5, 28.1, 24.5, 22.9, 22.3, 21.2

HRMS (ES⁺) calc. for C₃₀H₄₀N₃O₇ (M+H⁺) 554.2859, found 554.2866

(1) Jones, S. A., University of Adelaide, **2011**.

A1 Liquid scintillation counting

A1.1 Theory

Liquid scintillation counting is used to measure levels of β emitters such as tritium.

A tritiated sample is dissolved in a scintillation cocktail (Optiphase) comprising an aromatic solvent and an aromatic fluorophore. The tritium emits a β -particle that dissipates energy into the solvent and this energy is transferred to the aromatic fluor. The excited fluor returns to the ground state with emission of a photon. The photon is detected by the scintillation counter and reported as the number of counts per minute (CPM).ⁱ

The CPM gives the radioactivity of the sample (disintegrations per minute or DPM) in the absence of chemical quenching from impurities or colour quenching.ⁱⁱ When chemical quenching occurs, the fluorescence quantum yield of the sample is decreased by non-fluorescent molecules competing with the fluor molecules for the excitation energy of the solvent.ⁱⁱⁱ

The measured CPM can be corrected to DPM using the external standard ratios method. In this method, the Spectral Quench Parameter using an external Eu^{152} standard (SQP(E)) is determined for each measurement. The SQP(E) parameter is a relative number used to compare the amount of quenching between different samples. This information, in conjunction with a calibration curve, is used to convert the CPM to the absolute radioactivity DPM.

A1.2 Determination of a calibration curve

Tritiated tyrosine of known DPM was used for determination of the calibration curve. CHCl_3 acts as a quenching agent, and was added in 50 μL increments to the tritiated tyrosine standard. The SQP(E) was calculated by the liquid scintillation counter, and plotted against the ratio of measured CPM/known DPM (efficiency) to give a quench curve (**Figure 4**). This quench curve then allows the corrected DPM to be calculated from the sample CPM measurements.

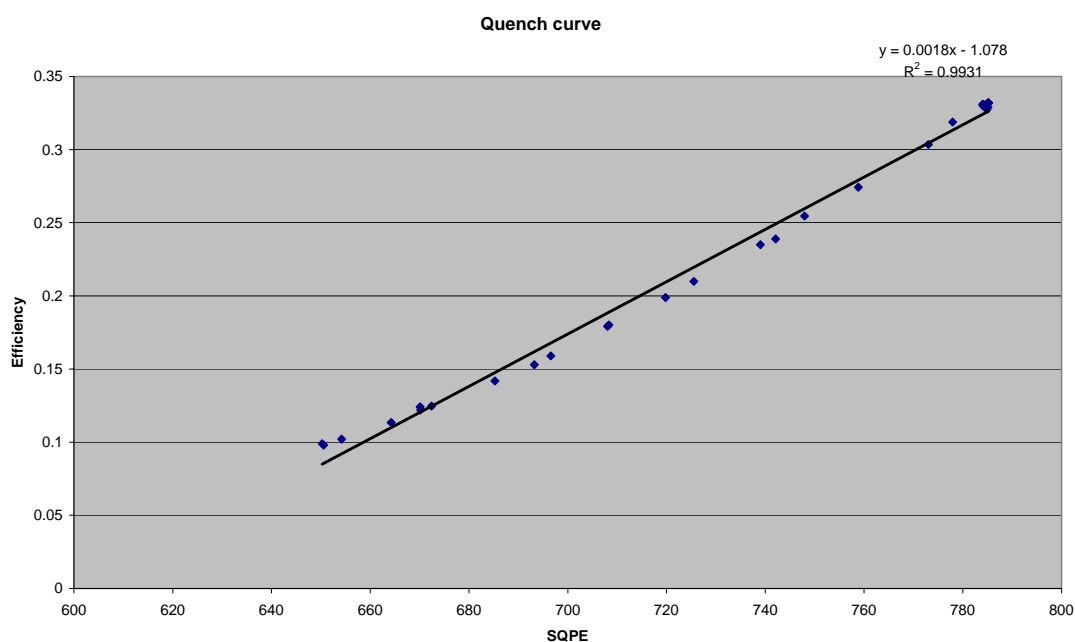


Figure 4. Quench curve with efficiency of the sample plotted against SQP(E) parameter.

ⁱ Bell, C.; Hayes, F. N., *Liquid Scintillation Counting*. 2nd ed.; Peramon Press Ltd: Oxford, 1958; p 292.

ⁱⁱ Fox, B. W., *Techniques of Sample Preparation for Liquid Scintillation Counting*. North Holland Publishing Company: Amsterdam, 1976; p 333.

A2 Chymotrypsin Assay

A2.1 Assay Method and data

The activity of **3.05** against bovine chymotrypsin was assayed spectrophotometrically with a Varian Cary 5000 UV-VIS-NIR spectrophotometer equipped with a thermostated multicell holder at 25.0 ± 0.1 °C. Assay buffer was: Tris-HCl (77 mM), CaCl₂ (20 mM), pH 7.8 (pH optimum of achymotrypsin⁶⁸). A solution of bovine chymotrypsin (21.9 mg/mL) in aq HCl (1 mM) was prepared daily by a 1:40 dilution of a stock solution (874 mg/ mL) in aq HCl (1 mM) and kept at 0 °C. A 1:100 dilution in ice-cold aq HCl (1 mM) was prepared immediately before starting each measurement. Stock solutions of the substrate Suc-Ala-Ala-Pro-Phe-pNA (10 mM) and **3.05** (10–50 mM) were freshly prepared in DMSO and stored at room temperature. Progress curves were monitored at 405 nm over 6 min and characterized by a linear steadystate turnover of the substrate. Inhibition studies were performed in the presence of 6% v/v DMSO in a volume of 1 mL containing 0.011 mg/mL bovine chymotrypsin, different concentrations of Suc-Ala-Ala-Pro-Phe-pNA (5 mM and 10 mM) and inhibitor (2.5 mM, 1.25 mM, 0.625 mM, 0.3125 mM, 0.15 mM). Into a cuvette containing 890 mL assay buffer, 10 mL of substrate solution (5 or 10 mM), inhibitor stock, and DMSO were added to give a total volume of 950 mL. After thoroughly mixing the contents of the cuvette, the enzymatic reaction was initiated by adding 50 μ L of bovine chymotrypsin solution. Uninhibited enzyme activity was determined by adding DMSO instead of inhibitor solution. Non-enzymatic hydrolysis of Suc-Ala-Ala-Pro-Phe-pNA was analyzed by adding DMSO and 1 mM aqueous HCl instead of inhibitor and enzyme solution, respectively, and found to be negligible. The rate of enzyme-catalyzed hydrolysis of 10 mM substrate was determined without inhibitor in each experiment and was set to 100%. The K_i value

of **3.05** was determined graphically according to Dixon¹ using mean values of percentage rates obtained in three or four separate experiments at two different substrate concentrations, [S]. The K_i value of **3.05** was calculated as the negative X-intercept in the Dixon plot.

A2.2 Dixon plot for 3.05

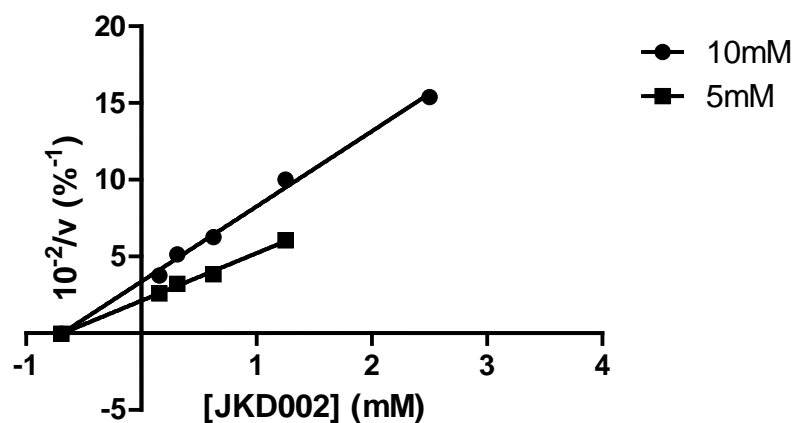


Figure A2.1. Dixon plot for **3.05** at substrate concentrations of 10 mM and 5 mM

Slope	4.898 ± 0.1491	3.101 ± 0.1059
Y-intercept when X=0.0	3.362 ± 0.1807	2.115 ± 0.07574
X-intercept when Y=0.0	-0.6863	-0.6820
1/slope	0.2042	0.3225
Goodness of Fit		
R square	0.9963	0.9965
Sy.x	0.3634	0.1502

Table A2.1 Data from Dixon plot

1. Dixon, M., *Biochemistry Journal* **1953**, 137, 143.